#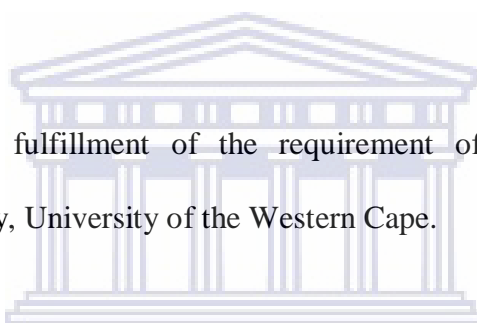 ELECTROPOLYMERIZATION AND ELECTROCHROMISM OF POLY(4,7-DITHIEN-2-YL-2,1,3-BENZOTHIADIAZOLE) AND ITS COPOLYMER WITH 3-METHOXYTHIOPHENE IN IONIC LIQUIDS

ABEBAW ADGO TSEGAYE

A thesis submitted in fulfillment of the requirement of Philosophiae Doctor in the Department of Chemistry, University of the Western Cape.

Supervisor: Prof. Emmanuel I. Iwuoha

Co supervisor: Dr. Tesfaye T. Waryo

May 2013

ELECTROPOLYMERIZATION AND ELECTROCHROMISM OF POLY(4,7-DITHIEN-2-YL-2,1,3-BENZOTHIADIAZOLE) AND ITS COPOLYMER WITH 3-METHOXYTHIOPHENE IN IONIC LIQUIDS

Abebaw Adgo Tsegaye

KEYWORDS

4,7-Dithien-2-yl-2,1,3-benzothiadiazole

Diffusion coefficient

Standard heterogeneous rate constant

Electropolymerization

Poly(4,7-dithien-2-yl-2,1,3-benzothiadiazole)

Donor-acceptor polymers

p-and n-dopable

Ionic liquids

Poly(3-methoxythiophene)

Copolymerization

Electrochromic properties

ABSTRACT

ELECTROPOLYMERIZATION AND ELECTROCHROMISM OF POLY(4,7-DITHIEN-2-YL-2,1,3-BENZOTHIADIAZOLE) AND ITS COPOLYMER WITH 3-METHOXYTHIOPHENE IN IONIC LIQUIDS

A. A. Tsegaye

This thesis is based on the study of electropolymerization and electrochromism of poly(4,7-dithien-2-yl-2,1,3-benzothiadiazole) (P(DTBT) and its copolymer with 3-methoxythiophene (MOT) in imidazolium ionic liquids (ILs) 1-butyl-3-methylimidazolium tetrafluoroborate (bmimbf$_4$) hydrophilic, 1-butyl-3-methylimidazolium hexafluorophosphate (bmimpf$_6$) and 1-butyl-3-methylimidazolium bis(trifluoromethylsulfonyl)imide (bmimtnf$_2$) hydrophobic ILs. Traditional organic solvents acetonitrile and dichloromethane in the presence of 0.1 M tetrabutylammonium perchlorate (n-Bu$_4$NClO$_4$) as a supportive electrolyte was also used as a medium for comparison. Besides, a more hydrophobic ionic liquid, 1-octyl-3-methylimidazolium bis(trifluoromethylsulfonyl)imide (octmimtnf$_2$) was also used for the electrodeposition of poly(3-methoxythiophene) (PMOT). The techniques employed are cyclic voltammetry (CV), electrochemical impedance spectroscopy (EIS), uv-visible spectroelectrochemistry and scanning electron microscopy (SEM).

4,7-Dithien-2-yl-2,1,3-benzothiadiazole (DTBT) a type of donor –acceptor monomer and 3-methoxythiophene (MOT) has been electropolymerized using ionic liquids as growth and supportive electrolytes. Imidazolium based ionic liquids with different anions were used to assess the influence of the nature of ionic liquids have on the morphology, electrochemical

activity and optical properties of the polymers. The hydrophobic ILs based on bis(trifluoromethylsulfonyl)imide anion produced slightly smoother and more electrochemically active film for both thiophenes containing species studied. P(DTBT) polymer film showed p-and n-doping processes unlike poly(3-methoxythiophene). The redox potential of the polymer film during n-doping occurred in a lower negative potential region (-1.02 to -1.40 V versus ferrocene/ferrocenium redox couple) in comparsion to -1.56 V exhibited by the monomer. Cyclic voltammetry suggested narrow bandgap P(DTBT) film was electrochemically deposited in ILs ranges from 0.1 to 1.29 eV whereas its monomer bandgap was found to be 2.45 eV. Impedance spectroscopy analysis of P(DTBT) film on glassy carbon electrode (GCE) exhibited a semicircle in higher frequency region and a Warburg line in the lower frequency region showing a quasi reversible process. Variation of electrical parameters obtained by fitting the impedance spectra of GEC/P(DTBT)/ionic liquid interface to the proposed model attributes to the difference in electroactive surface area of P(DTBT) film and size of the anions of ILs.

Thin films of P(DTBT) polymer deposited on indium tin oxide (ITO)-glass substrate in ILs revealed two absorption bands in the neutral state both due to $\pi \rightarrow \pi^*$ transitions. The maximum absorbance bands appeared around 540 nm and 579 nm for the polymer obtained from hydrophilic and hydrophobic ILs. Upon doping, the colour of the polymer turned from dark blue to transparent with red-purple residue colour while bands in the visible region depleted bipolaron bands appeared in the near infrared region. Narrow bandgap determined from optical absorption spectra of P(DTBT) ranges from 1.39 to 1.54 eV compared to (3-methoxythiophene) bandgap 1.63 to 1.86 eV. P(DTBT) film formed in bmimtnf$_2$ ionic liquid exhibited the lowest bandgap (1.39 eV). From simultaneous double potential step chronoamperometry and fixed-wavelength transmittance (*T*) measurements, moderate optical contrast (ΔT%=17-34) and rapid response time (1.0 to 1.4 s) at 95% of optical contrast was

estimated as the film turns from bleached to coloured state and 3.3 to 4.2 s for the reverse process in contrary to this a slower response time for P(DTBT) film deposited from 0.1 M n-Bu$_4$NClO$_4$/dichloromethane (2.3 s, 5 s) recorded whereas the colouration efficiency of the polymer varied in between 91 to 187 mC/cm^2 at 1000 nm. The fast response time of P(DTBT) film in Ils is possibly due to the formation of smoother and highly doped film in ILs that may enhance the movement of counter ions compared to the rough imaged scanning electron microscope reaveled for P(DTBT) film obtained in organic media.

On the other hand, a new composite were produced by electrocopolymerization of DTBT and MOT in the two ionic liquids bmimpf$_6$ and bmimtnf$_2$. Cyclic volatammograms, uv-visible spectroelectrochemistry spectra and scanning electron microscope image of P(DTBT)-co-PMOT film revealed copolymerization. Colour of P(DTBT)-co-PMOT copolymer film was modulated in the ILs between dark blue to blue in fully reduced and oxidized states which indicates that the copolymer is electrochromic. Compared with P(DTBT) the copolymer bandgap was lower and 1.32 eV was estimated from uv-vis spectra. These gives a clue that PMOT unit incorporated into P(DTBT) system act as a π- spacer and hence increase conjugation length of the copolymer.

Poly(4,7-dithen-2-yl-2,1,3-benzothiadiazole) has become an interesting materials because of its potential applications for electrochromic, solar cell, charge storage and biosensors applications. The polymer film electrochemically deposited in ionic liquids on ITO−glass substrate showed moderate optical contrast, fast response time, high stability and smoother morphology. In addition to this, electrochromic properties of P(DTBT) have been also improved by copolymerization. These behaviours demonstrates the potential application of poly(4,7-dithien-2-yl-2,1,3-benzothiadiazole) for electrochromic devices or displays that change colour in the near infrared region.

DECLARATION

I declare that "*Electropolymerization and Electrochromism of poly(4,7-dithien-2-yl-2,1,3-benzothiadiazole) and its copolymer with 3-methoxythiophene in ionic liquids*" is my own work, that it has not been submitted for any degree or examination in any other university, and that all sources I have used or quoted have been indicated and acknowledged by means of complete references**.**

Abebaw Adgo Tsegaye   **May 2013**

Signed

ACKNOWLEDGMENT

I offer my sincere gratitude to my supervisors, Professor Emmanuel I. Iwuoha and Dr. Tesfaye T. Waryo, for their guidance and support at all stages of the work. Their excellence supervision and noble personality have helped me to grow up to this stage. I will not forget how patient Dr. Tesfaye has been during the whole work in fixing those problems whenever I face dispute. He shared his rich experience and knowledge of the electrochemistry everywhere we happen to be together, from working in the lab, to walking around Cape Town.

I would like to express my sincere thanks to National Research Fund (NRF) for funding the project. I am also indebted to my home institution Haramaya University for the grant to the study leave.

Needless to say, I am also grateful to all sensorlab members, Professor Prisilla Baker, Dr. Abdu Almonam Baleg, department of chemistry, University of the Western Cape for making me feel at home and the wonderful times we had and for being there whenever I need assistance. I also pleased thanking Leul Shumye and Enat Tadesse my spouse parents for their love to my kids. A special thanks to my brothers (Enyew, Getachew and Zemene Adgo) their motivation and encouragement has given me comfort and energy to go on. My special thanks also go to Tegegne Sishaw he is really an honest friend and keep writing emails to me during the whole study time.

Last but not certainly least, special words of thank to my daughters Lidiya and Bitaniya for helping me to see a bright future, my wife Alemnesh Leul, for the love and take care of our children. I am greatly indebted to your time during which I was away from home. Thank you very much for your understanding and patient. You gave me your time to do this thesis.

DEDICATION

Lidiya Abebaw

Bitaniya Abebaw and

Alemnesh Leul

LIST OF CONFERENCES ATTENDED AND PUBLICATIONS

1. **Abebaw A. Tsegaye**, Tesfaye T. Waryo, Prisilla Baker and Emmanuel I. Iwuoha Electrochemical studies on 4,7-dithien-2-yl-2,1,3-benzothiadiazole towards electrochromic donor-acceptor polymer applications. *International Symposium of Electrochemistry*, July 2012, University of the Western Cape, 7535 Bellville, Cape Town, South Africa.

2. **Abebaw A. Tsegaye**, Tesfaye T. Waryo, Prisilla Baker and Emmanuel I. Iwuoha Electropolymerization and electrochromism of poly(4,7-dithien-2-yl-2,1,3-benzothiadiazoel) in 1-butyl-3-methylimidazolium ionic liquids. *13th Tropical Meeting of International Electrochemical Society*, April 2013, Pretoria, South Africa.

3. **Abebaw A. Tsegaye**, Tesfaye T. Waryo, Prisilla Baker and Emmanuel I. Iwuoha Electrocopolymerization and electrochromism of poly(4,7-dithien-2-yl-2,1,3-benzothiadiazole) with 3-methoxythiophene in 1-butyl-3-methylimidazolium ionic liquids. *Electrochemistry Communications (in preparation)*

4. **Abebaw A. Tsegaye**, Tesfaye T. Waryo, Prisilla Baker and Emmanuel I. Iwuoha Electropolymerization and electrochromism of poly(4,7-dithien-2-yl-2,1,3-benzothiadiazole) in 1-butyl-3-methylimidazolium ionic liquids. *Chemical Communications (submitted)*

5. **Abebaw A. Tsegaye**, Tesfaye T. Waryo, Prisilla Baker and Emmanuel I. Iwuoha Electrochemical studies of 4,7-dithien-2-yl-benzothiadiazole in nonaqueous solvents. *Journal of The Electrohemical Society (in preparation)*

6. **Abebaw A. Tsegaye**, Tesfaye T. Waryo, Prisilla Baker and Emmanuel I. Iwuoha Electrosynthesis and characterization of poly(3-methoxythiophene) and its copolymer with EDOT in ionic liquids 1-butyl-3-methylimidazolim tetrafluroborate and 1-octyl-3-methylimidazolium bis(trifluoromethylsulfonyl)imide. *Synthetic Metals (in preparation)*
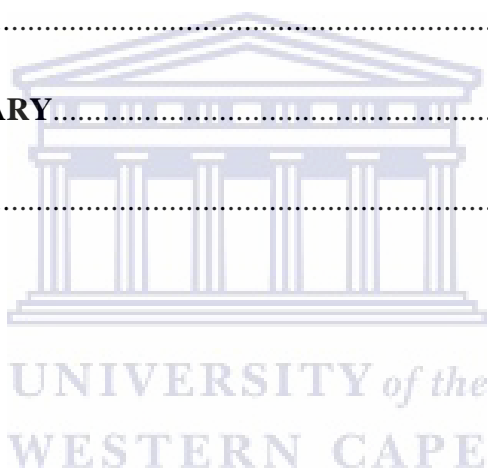
TABLE OF CONTENTS

LIST OF FIGURES

LIST OF TABLES

SCHEMES

LIST OF ABBREVIATIONS

DTBT   4,7-Dithien-2-yl-2,1,3-benzothiadiazole

CV   Cyclic voltammetry

EIS   Electrochemical impedance spectroscopy

AFM   Atomic force microscopy

SEM   Scanning electron microscopy

ATR-FTIR   Attenuated total reflectance Fourier transforms infrared spectroscopy

$LiClO_4$ Lithium perchlorate

$n\text{-}Bu_4NClO_4$ tetrabutylammonium perchlorate

P(DTBT)   Poly(4,7-dithien-2-yl-2,1,3-benzothiadiazole)

ACN   Acetonitrile

DCM   Dichloromethane

Pt   Platinum

Au   Gold

GC   Glassy carbon

GCE   Glassy carbon electrode

ILs   Ionic liquids

RTILS   Room temperature ionic liquids

$bmimbf_4$ 1-Butyl-3-methylimidazolium tetrafluoroborate

$bmimpf_6$ 1-Butyl-3-methylimidazolium hexaflurophosphate

$emimbf_4$ 1-Ethyl-3-methylimidazolium tetrafluoroborate

emimpf$_6$	1-Ethyl-3-methylimidazolium hexafluorophosphate
emimcf$_3$so$_4$	1-Ethyl-3-methylimdazolium trifluoromethanesulfonate
hmimfap	1-Hexyl-3-methylimidazolium tris(pentafluoroethyl)trifluorophosphate
bmimtnf$_2$	1-Butyl-3-methylimidazolium bis(trifluoromethylsulfonyl)imide
octmimtnf$_2$	1-Octyl-3-methylimidazolium bis(trifluoromethylsulfonyl)imide
edmimtnf$_2$	1-Ethyl-2,3-dimethylimidazolium bis(trifluoromethylsulfonyl) imide
eeimtnf$_2$	1-Ethyl-3-ethylimidazolium bis(trifluoromethylsulfonyl)imide
E$_g$	Bandgap
λ	Wavelength
λ$_{max}$	Maximum absorbance
ν	Frequency
c	Speed of light
h	Planck's constant
ω	Angular frequency
a	Anode
c	Cathode
dl	Double layer
p	Peak
C	Capacitance
E$_p$	Peak potential
i$_{pa}$	Anodic peak current

i_{pc}	Cathodic peak current
i_{ox}	Anodic peak oxidation current
i_{red}	Cathodic peak reduction current
D	Diffusion coefficient
D_{ox}	Diffusion coefficient of oxidized species
D_{red}	Diffusion coefficient of reduced species
δ	Diffusion layer thickness
R_{ct}	Charge transfer resistance
C_{dl}	Double layer capacitance
R_s	Solution resistance
Z_w	Warburg diffusion impedance
k^o	Standard heterogeneous rate constant
υ	Scan rate
α	Anodic electron transfer coefficient
β	Cathodic electron transfer coefficient
C_{ox}	Concentration of oxidized species
C_{red}	Concentration of reduced species
n	Number of electrons
η	Over potential
$E^{o'}$	Formal potential
E^o	Standard potential

T	Temperature
$^{\circ}$C	Temperature in degree Celsius
R	General gas constant
$E_{1/2}$	Half wave potential
E_{pa}	Anodic peak potential
E_{pc}	Cathodic peak potential
e	Electron
Q	Charge
η	Viscosity
ϕ	Phase angle
ΔE	Peak separation potential
P(DTBT)1	P(DTBT) electrodeposited in $bmimbf_4$
P(DTBT)2	P(DTBT) electrodeposited in $bmimpf_6$
P(DTBT)3	P(DTBT) electrodeposited in $bmimtnf_2$
P(DTBT)4	P(DTBT) electrodeposited in 0.1M Bu_4NClO_4/dichloromethane
PTs	Polythiophenes
ECD	Electrochromic devices
MOT	3-Methoxythiophene
PMOT	Poly(3-methoxythiophene)
PMOT1	PMOT electrodeposited in $bmimbf_4$
PMOT2	PMOT electrodeposited in $octmimtnf_2$

PMOT3   PMOT electrodeposited in bmimpf$_6$

PMOT4   PMOT electrodeposited in bmimtnf$_2$

EDOT   3,4-ethylenedioxythiophene

PEDOT1   PEDOT electropolymerized in bmimbf$_4$

PEDOT2   PEDOT electropolymerized in octmimtnf$_2$

PMOT-co-PEDOT   Poly(3-methoxythiophene)-co-poly(3,4-ethylenedioxithiophene)

PMOT-co-PEDOT1   PMOT-co-PEDOT electropolymerized in bmimbf$_4$

PMOT-co-PEDOT2   PMOT-co-PEDOT electropolymerized in octmimtnf$_2$

P(DTBT)-co-PMOT   Poly(4,7-dithien-2-yl-2,1,3-benzothiadiazole)-co-poly(3-
                  methoxythiophene)

P(DTBT)2-co-PMOT P(DTBT)-co-PMOT electropolymerized in bmimpf$_6$

P(DTBT)3-co-PMOT P(DTBT)-co-PMOT electropolymerized in bmimtnf$_2$

t   Response time

%T   Percent transmittance

η   Colouration efficiency

ΔT%   Optical contras

Γ   Surface concentration

MO   Molecular orbital

HOMO   Highest occupied molecular orbital

LUMO   Lowest unoccupied molecular orbital

CHAPTER 1

INTRODUCTION

1.1 Background

Ever since the discoveries of the first organic conducting polymer, beginning with poly (acetylene), organic conducting polymers has been subject to intense research for more than the last three decades, both in terms of trying to understand the chemistry and physics of these materials [1]. They have become interesting materials, because of their prospect applications in different types of electrochemical devices such as photovoltaic cells, batteries, sensors, super capacitors, electrochromic devices [2-3] and smart devices [4-5]. Common to all the conducting polymers is the conjugated backbone, hence the name 'conjugated polymers' that is commonly used as a result of an extended π - electron system along the polymer chain. The π - electron on the backbone of organic polymers is responsible for the conduction mechanism and some of the other features found among these polymers. Examples of common monomers of conducting polymers are shown in Fig.1.1.

It has been shown that organic materials such as polyethylene, poly(phenylene vinylene) [6], polythiophene [7], polypyrrole [8] and their derivatives can be utilized as an active component in light emitting diodes, electrochemical cells, solar energy converting and photovoltaic devices, sensors, batteries, super capacitors, conducting textiles, electrochromic devices, to mention a few. For all of these applications all conducting polymers do not possess good environmental stability in the presence of oxygen and water and some of them have poor mechanical properties [9-11]. Poor stability in the presence of oxygen and
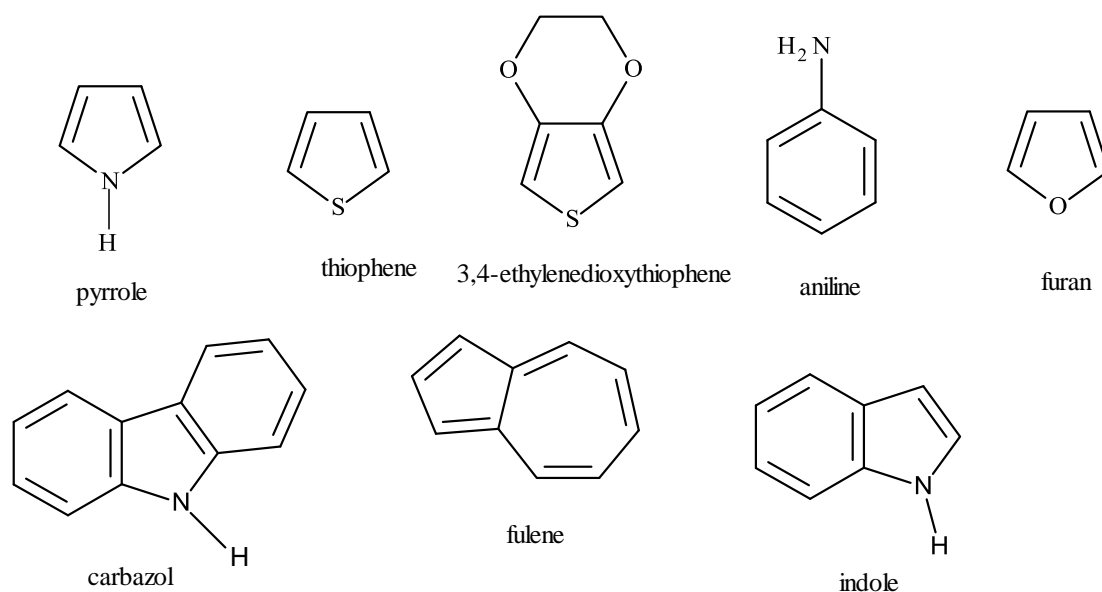
Figure 1.1: Structure of common conjugated monomers.

water and poor mechanical properties of the polymers are reported as limitations for the various applications. Moreover, the use of conventional electrolytes (molecular solvents and supporting salts) has restricted their practical applications. This is because of evaporation of solvent and degradation of the electrolytes. Use of ionic liquids appropriately replaced common organic solvents with the problem of solvent evaporation. Ionic liquids are non-volatile and they posses' excellent intrinsic electrical conductivities in a wider electrochemical potential window. These desirable properties exhibited by ionic liquids rapidly made them very attractive electrolytes and has become a medium for electrosynthesis of conducting polymers [12].

Various kinds of conducting polymers such as polyaniline, polythiophene, and polypyrrole have been synthesized and characterized in various media. Especially, polythiophene and its derivatives are the most important of conjugated polymers due to their superior environmental and thermal stabilities [2, 6-7, 13-14]. Among the families of polythiophene

derivatives, poly(3-methoxythiophene) (PMOT) has drawn many researchers' attention because the monomer 3-methoxythiophene possesses a lower oxidation potential due to the inductive effect of the methoxy group. It has been reported that the monomer with lower oxidation potential gives a quality polymer film since the less side reactions such as α- ß coupling and over oxidation during the electropolymerization of the monomers [15]. Additionally, PMOT possesses excellent physical and chemical stability, high redox potential and high electronic conductivity [16]. Furthermore, PMOT is soluble in organic solvents like acetonitrile, dichloromethane provided an opportunity to study its properties in solution unlike the other polymers which are generally insoluble and infusible [17]. Because of its high solubility in these organic media, PMOT could not be directly electrodeposited as solid film on metallic substrate in organic media. To overcome this challenges, Fall, *et al.* [18-19] electropolymerized PMOT in aqueous micellar solutions medium containing sodium dodecyl sulphate as surfactant and 1-buthanol as co surfactant to succeed in depositing PMOT films on platinum electrode surface. According to the authors, their approach yielded a film of oligomer of PMOT mainly hexamers and pentamers. Recently Dong e*t al* [15] reported electrochemical synthesis of PMOT in the presence of 1-buthyl-3-methylimidazolium hexafluorophosphate ionic liquid in an aqueous micro emulsion the non-ionic surfactant Tween 20. In this medium, onset oxidation potential of MOT 1.08 V vs SCE at scan rate of 20 mV/s reported and it was the most suitable medium for the electropolymerization of MOT. For comparison, its onset oxidation potential in other solvents such as 0.1 M $LiClO_4$ in acetonitrile, aqueous micellar medium (0.03 M sodium dodecyl sulphate and 0.1 M $LiClO_4$ aqueous solution) [18] and 0.1 M $NaClO_4$ in distilled water/acetonitrile (3:1) by volume [20] at the same scan rate are 1.39, 1.2 and 1.1 V vs. SCE respectively.

Copolymerization has been used as one of the strategies to modify the structures and properties of polymers such as bandgap and redox potential [9-10]. During electrochemical

copolymerization two monomers simultaneously copolymerize to form a material which exhibits properties in between the corresponding homopolymers. Electrochemical and optical properties of various copolymers varied based on the synthesis condition, type of monomers used and extent of π-conjugation in the copolymers structure [10, 21-22]. Electrochemical copolymerization is mainly performed with 3, 4-ethylenedioxythiophene (EDOT) due to its desired properties such as environmental stability and low band gab [21, 23-24]. There is little report available in the literature about the electropolymerization of MOT with other monomers. Recently, copolymerization of 3-methoxythiophene with 3-thiophene methanol, 3-thiophene ethanol, and 3-thiophene carboxylic acid monomers has been reported using 0.1 M NaClO$_4$ electrolyte in water/acetonitrile (3:1) medium [20]. MOT copolymerized with these monomers and the resulting copolymers varies its colour between blue and orange in oxidized and reduced state demonstrating its potential for electrochromic applications. It has been also reported that the homopolymer PMOT is a promising active material for batteries [25], solar cells [26] and sensor [27-28] and catalysis [29].

Research has shown that the use of a room temperature ionic liquid (RTIL) as a source of dopant ions and as a medium for variety of electrochemical synthesis has given a polymer with improved electrochemical stability and in some cases smoother and denser or similar films when compared to electrochemical synthesis in the traditional organic solvents and supporting electrolytes [12, 30-32]. RTILs are room temperature molten salts composed of organic cations and organic or inorganic anions[33]. They show excellent intrinsic electrical conductivities and higher viscosities. The electrical conductivities at wide electrochemical potential window a RTIL exhibits are highly desirable properties for applying it as two in one solvent and supporting electrolyte. Besides, RTILs are non-volatile and this makes them appropriate replacements for common organic solvents with the problem of solvent evaporation. Exploiting these advantages, electrochemical synthesis of polypyrrole [34],

4

poly(3-(4-fluorophenyl)thiophene) [35], poly(3,4-ethylenedioxythiophene) [35-38], poly(para)phenylene [39], poly(3-chlorothiophene) [40] and polythiophene [41] and various other polymers has been successfully synthesized in ionic liquids.

The nature of one or both of the anion and cation of the ionic liquid strongly control the doping processes in the conducting polymer, determining the kinetics, morphology and the properties of the resulting polymers [12, 31]. For example, the electropolymerization of pyrrole was found to be more efficient in 1-ethyl-3-methylimidazolium methanesulphonate (conductivity (σ) = 1.36 S/m, viscosity (η) = 42.7 cP at 25 $^\circ$C) than 1-ethyl-3-methylimidazolium hexafluorophosphate (σ = 0.52 S/m, η = 15.0 cP at 25 $^\circ$C) and 1-ethyl-3-methylimidazolium tetrafluoroborate (σ = 0.92 S/m, η = 31.8 cP at 25 $^\circ$C), with a formation of smoother and more highly doped polymer than those from the latter ionic liquids [42]. Since anions remain incorporated as dopants in the resulting polymer, the higher viscosity of the former ionic liquid affect favourably the insertion of anions thereby smoother and highly doped polymers can be produced. Furthermore, electrochemical oxidation of pyrrole; the resulting polymer is more electrochemical active (large oxidation and reduction peak currents) in ionic liquid compare with that of traditional acetonitrile and aqueous solvents. On the other hand, electropolymerization of EDOT in N, N - butylmethylpyrrolidium bis(trifloromethanesulfonyl)imide proceeds more slowly than in (N – ethyl-N-methylimidazolium bis (trifluromethanesulfonyl)imide [31]. This phenomenon is attributed to the more viscous and lower conductivity of the former (η = 85 cP, σ = 2.2 mS/cm at 25 $^\circ$C) in comparison to the later ionic liquid (η = 34 cP, σ = 8.8 mS/cm at 20 $^\circ$C) less viscous and relatively highly conductive. The decrease in transport of reactants and ions to the electrode surface decrease significantly in the pyrrolidinium cation based ionic liquid indicating the role of cation during electrochemical polymerization of EDOT.
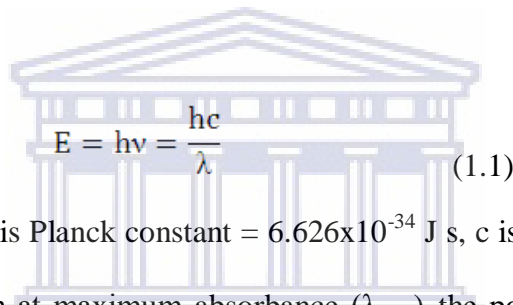
One of the potential applications of conducting polymers is in electrochemical devices due to their electrochromic properties upon doping and dedoping process. Electrochromism is the reversible change of the colour of a substance associated with an electrochemical induced oxidation – reduction reaction or by an electron transfer (redox) process [43-44]. Electrochromism which broadly defined as reversible change in the reflected or transmitted light upon electrochemical oxidation or reduction of electrochromic materials has attracted researchers in the last three decades [9, 24]. The first electrochromic materials in the visible region studied were inorganic materials such as tungsten trioxide (WO_3), iridium dioxide (IrO_2) then followed by small organic molecules such as viologen and metallophthaocyanines [45-47]. Oxides of the following transition metals cerium, chromium, cobalt, copper, iridium, iron, manganese, molybdenum, nickel, niobium, palladium, rhodium, ruthenium, tantalum, titanium, tungsten and vanadium are electrochromic. The electrochromic performance of WO_3 improved in the presence of carbon – nanotubes (0.1 % w) [48], hybrid with polyaniline [49].

Organic electrochromic materials such as conducting organic polymers has received researchers attention to be used for electrochromic applications [46]. The fact that conjugated polymers can repeatedly undergo electrochemical doping/undoping processes; make them the most promising class of materials to be used in electrochromic devices. Electrochromic devices has been employed for the construction of mirrors, displays, and windows [46]. Electrochromic polymers research is mostly focused on the synthesis and electronic characterization to obtain a polymer with high optical contrast, colouration efficiency, switching speed and stability, which are decisive properties for commercial applications.

Electrochromism in conjugated polymers occurs through change in the conjugated polymer's π – electronic character accompanied by reversible insertion and extraction of ions through

the polymer film upon electrochemical oxidation and reduction [27]. Electrochemical oxidation (removal of electron accompanied with insertion of the anion of the electrolyte) and reduction (addition of electron/exclusion of cation of the electrolyte) modify the electronic structure of a polymer and hence its electrochromic properties. Example: poly(3, 4-ethylenedioxythiophene) colour changes blue on reduction and transmissive during oxidation. It results from the generation of different visible region electrochromic absorption bands upon switching between redox states [9, 24].

The wavelength of light absorbed is related to the energy gap

$$E = h\nu = \frac{hc}{\lambda}$$ (1.1)

Where ν is frequency, h is Planck constant = 6.626×10^{-34} J s, c is the speed of light = 3.0×10^{8} m/s, λ is the wavelength at maximum absorbance (λ_{max}), the position of it on the spectrum governs the observed colour.

In white light, the perceived colour of a material is the complementary colour of the light it absorbs. In the electromagnetic radiation, visible light wavelength ranges from 420 nm (violet) to 700 nm (red).

Red 635…………………750 nm

Orange 596………………635 nm

Yellow 580………………596 nm

Green 520………………..580 nm

Blue 470…………………520 nm

Indigo 440………………...470 nm

Violet 400…………………440 nm

Fundamental properties of electrochromic materials to be considered are optical contrast, switching speed, stability and colouration efficiency. These properties are defined as: Optical contrast is the percent transmittance change ($\Delta\%T$) at a specified wavelength where the electrochromic material has the highest absorption. Switching speed is the time required for the colouring – bleaching process of an electrochromic material. Cycle life/stability is the number of full switches that can be performed for an electrochromic film before measurable degradation occurs. A workable minimum of about 10^5 is often stipulated. This is an important indicating factor of the electrochromic durability which also depends on switching potential and electrolyte.

Switching speed is the time required for an electrochromic material to change colour from one to the other, commonly from colouring to bleaching state and vice versa. There are few reliable resources for switching speed also called switching time or more colloquially response time of electrochromic devices in the literature because of lack of standard in reporting and determination of data Monk *et al* [44] and it has become difficult to compare the switching speeds of materials. The lack of inconstancy originated from the different kinetic criteria involved during the experimental investigation of switching speed. On one hand, researchers define switching speed is the time required some fraction of the colour formed. On the other hand, it is may be related to the time required for 90 or 95 present of the charge consumed in forming the expected colour as the potential steps for oxidation and reduction at the electrode modified by an electrochromic material. It has been also reported, unlikely no equality on the time required from coloured to bleaching ($t_{coloured}$) and from bleaching to coloured (t_{bleach}) states for an electrochromic material. For example, stacked

structure WO_3 nanosheet on fluorine doped trioxide (FTO) glass electrode produced layer by layer showed slow colouration process but fast bleaching process [50]. Electrochromic devices for display applications require a more rapid switching time. Inorganic electrochromic materials such as iridium oxide a fast response time of 50 ms reported, thin film 100 nm $WO_3.2H_2O$ at activated FTO glass showed a fast colouration (t_c, 90% 3.2 s, t_b, 90 % = 1.2 s), high optical contrast 53.8% and colouration efficiency of 107.8 cm^2/C [51].

Research for the utilization of conducting polymers in electrochromic devices has been intensively performed in the last three decades to synthesis an organic material with a fast switching speed. Welsh *et al* [52] prepared a series of polymers based on PEDOT thickness of about 300 nm required (0.8 − 2.2) s with a modest transmittance change (44 − 63)% to switch between reduced and oxidized states. Multiple electrochromism with a response time of 2.6 s and optical contrast 29 % at 767 nm achieved by copolymerization of thiophene/EDOT feed ratio of 2/1 in boron trifluoride diethyl ethanoate. Applications such as electrochromic office windows actually require a very slow response. For display application fast response is required. Ultra fast switching times (0.74 s and 0.88 s) with a very good stability at a maximum colouration efficiency of 250 cm^2/C by electrodepositing followed by an oxidation of air nanostructured nickel oxide (NiO) thin film for 10 s in ionic liquid reported [53].
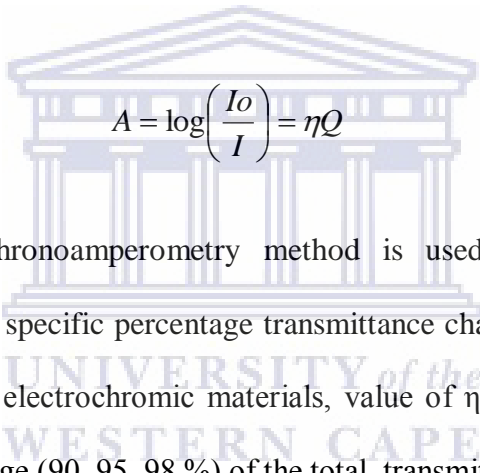
Another important property of electrochromic materials to be considered is colouration efficiency (η) which determines the amount of optical density change indicated as a function of the injected/ejected electrochromic charge. It is the amount of charge necessary to produce optical change. It is more similar in concept to the extinction coefficient of Beer–Lambert Law.

Beer – Lambert Law

$$A = \varepsilon l c \qquad (1.2)$$

$$\Delta A = \varepsilon l \Delta c \qquad (1.3)$$

A stands for is absorbance, ε molar absorptivity coefficient, l length of the cell and c concentration. The optical absorption (A) of an electrochromic film is related to the injected charge per unit area Q by an expression in transmissive mode (I_o) intensity of incident light and (I) intensity of transmitted light.

$$A = \log\left(\frac{I_o}{I}\right) = \eta Q \qquad (1.4)$$

Chronocoloumetry – chronoamperometry method is used to measure and calculated colouration efficiency at specific percentage transmittance change at λ_{max}. To provide points of reference for various electrochromic materials, value of η is calculated at fixed specific wavelength as a percentage (90, 95, 98 %) of the total transmittance change (Δ%T).

$$\eta = \frac{\Delta A}{Q} = \frac{\Delta(OD)}{Q} = \frac{\log \frac{T_b}{T_c}}{Q} \qquad (1.5)$$

T_c: colour transmittance, T_b: bleached transmittance, ΔOD: change in optical density and Q change in charge density.

Change density (Q) is the charge consumed per unit electrode area for the change in the optical density, which can be determined by integrating current density versus time graph. Graph of A versus Q accurately gives η as the gradient. Organic electrochromes exhibit a

greater η than do inorganic species because the molar absorptive of the former are usually higher.

Spectroelectrochemical data from the literature indicates that a number of organic conjugated polymers investigated were absorbing/reflecting blue and red in the neutral states [30]. However, conjugated polymers synthesized and characterized in an attempt to make saturated green polymers chemically or electrochemically have limited success due to their requirement that at least two absorption bands must exist. Challenges like this seems to be addressed after Havinga *et a*l [54] in 1993 introduced the 'donor – acceptor' concept for tuning the bandgap (as narrow as 0.5 eV) between highest occupied molecular orbital (HOMO) and lowest unoccupied molecular orbital (LUMO) based on alternating electron rich and poor moieties in conjugated polymers. The combination of electron rich and electron deficient moieties has been used effectively to lower the bandgap of conjugated polymers. Electron rich units such as 2,7-carbazole, indole[3,2,b]carbazole, benzo[1,2-b:4,5-b']dithiophene, cyclopenta[2,1-b:3,4-b']dithiophene, dithieno[3,2-b:2',3'-d]silole and quite a few electron deficient units 2,1,3-benzothiadiazole, diketopyrrolo[3,4-c]-pyrrol-1,4-dione, ester or ketone substituted thieno[3,4-b]thiophene and thieno[3,4-c]pyrrol-4,6-dione has been mostly used for the synthesis of donor – acceptor polymers [55]. Although the discovery of this theory has contributed for the development of electrochemically driven device applications such as field – effect transistors, Light- emitting diodes, and photovoltaic, it is only recently has the use donor – acceptor based polymers attracted the attention of researchers with an interest in the investigation of their electrochromic properties[56-60].

Neutral state green coloured polymer material Sonmez et al [45] reported the first electrochemically prepared 2,3-di(thien-3-yl)-5,7-di(thien-2-yl)thieno[3,4-b]pyrazine polymer. In recent works in which 4,7-di(2, 3-dihydro-thieno[3,4-b][1,4]dioxin-5-

y)benzo[1,2,5]thiadiazole, was electropolymerized and its polymer was reinvestigated as a possible candidate for electrochromic applications because its neutral state green, switching rapidly and reversibly to a transmissive light blue oxidized state. In another work, Wu *et al* [61] synthesized cyclopentadithiophene–benzothiadiazol polymer using cyclopentadithiopene as a donor. This polymer is green in the neutral and transmissive in oxidized state and gave maximum optical contrast of 38%. Replacing benzothiadiazole sub unit with the stronger acceptor benzoselenadiazole as has been proven with other polymers, changed electronic structure and hence the absorption bands [62]. Koyuncu *et al* synthesized a donor - acceptor electrochromic material containing carbazole and 1, 8-naphtalimide as a sub unit with a bandgap of 2.44 eV with multi- electrochromic behaviour [55]. And a number of other green coloured polymers have been reported by many research groups [1, 45, 61, 63-66].

Donor - acceptor monomers are synthesized by combining electron donating and accepting units' usually using Stille coupling reactions The Stille reaction involves the coupling of an organic halide, triflate, or carbonyl chloride with an organotin compounds catalyzed by a palladium (II) catalyst and detail mechanism are found in reference [67-71]. A proposed mechanism is shown in scheme 2 a palladium (II) or palladium (o) couple is generally introduced as a catalyst. When a palladium (II) compound is used in the first step palladium (II) complex reduced to palladium (0) species by the organotin compounds. The resulting palladium (0) reacts with the organic halide to form the organopalladium halide intermediate by oxidative addition. The intermediate formed then undergoes transmetalation. Reduction elimination affords the product and palladium (0) species in the final step to complete the catalytic cycle.

Scheme 1: General scheme for the Stille coupling reaction.

$$RX \ + \ R'SnBu_3 \xrightarrow{\ \ Pd(O)\ \ } R\!\!-\!\!R'$$
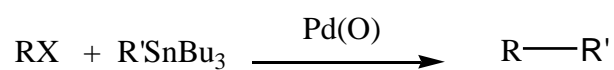
Where X = I, Br and etc and R and R': aromatic, vinyl, hydrocyclic and etc.

Electron donating units

Thiophene   3,4-Dioxyethylenethiophne   Carbazole

4,4-Di-octyl-cyclopentadithiophene

Electron accepting units

2,1,3-Benzothiadiazole   2,1,3-Benzoselenathiadiazole   Benzobisthiadiazole
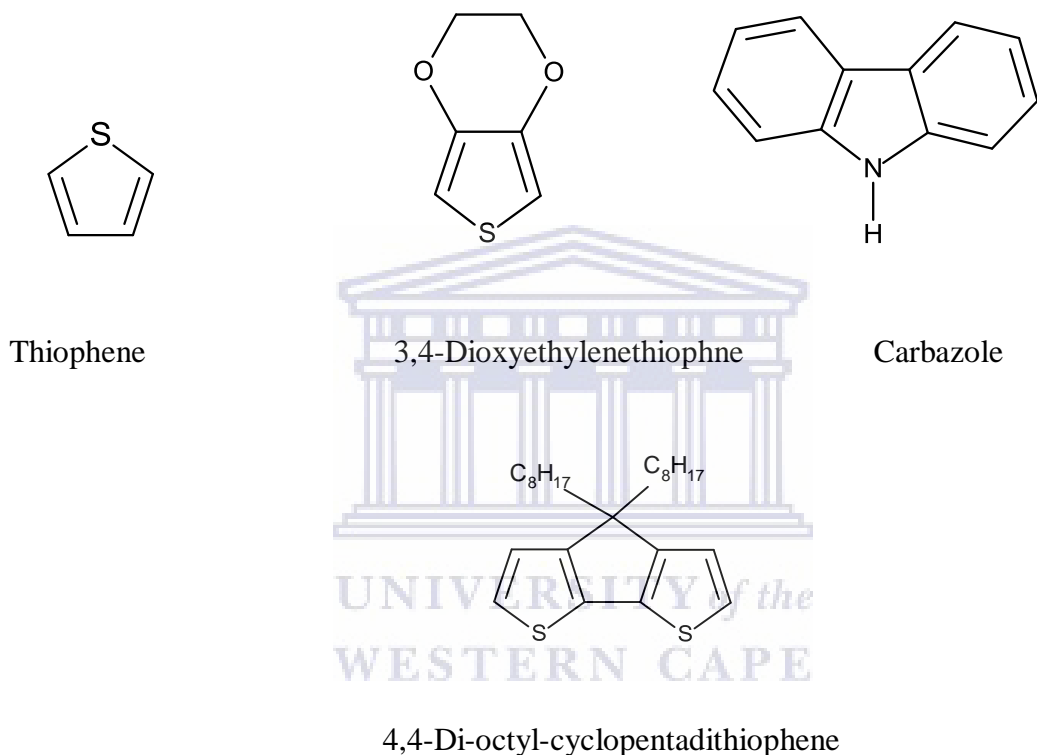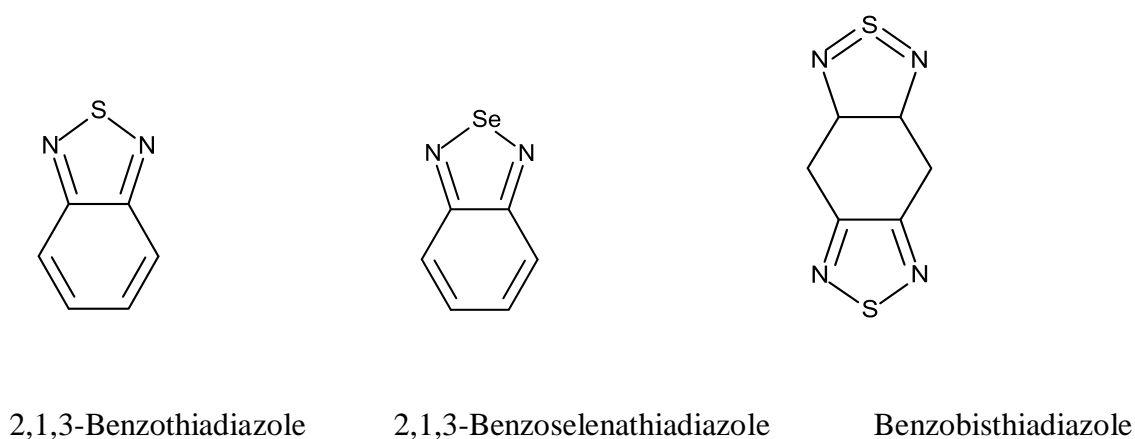
Figure 1.2: Commonly used electron donor and acceptor groups.

Among donor– cceptor polymers, poly(4,7-dithien-2-yl-2,1,3-benzothiadiazole) P(DTBT) have received considerable attention because these materials have a bandgap of $E_g = 1.1$–1.2 eV when polymerized electrochemically. Besides this interesting property, P(DTBT) thin polymer film possesses high stability during both p-and n-doping. It has been also shown that 4,7-dithien-2-yl-2,1,3-benzothiadiazole (DTBT) monomer act as a course bandgap tuning and copolymerized with many kind of electron rich segments for broad range optical absorption in the near infrared region [68, 75-76].

There are also a number of reports that showed poly(4,7-dithien-2-yl-2,1,3-benzothiadiazole) derivative polymers has been synthesized for electrochromic and photovoltaic applications. However, as far as our knowledge is concerned there are only few reports about electrochemical and electrochromic properties about poly(4,7-dithien-2-yl-2,1,3-benzothiadiazole) though, used intensively as a unit for copolymerization with other electron donating groups or as a core of functionalized donor–acceptor polymers. Obviously there is a demand about its property such as optical contrast, stability and reversibly for electrochromic applications.

1.2 Motivation of the study

Poly(4,7-dithien-2yl-2,1,3-benzothiadiazole), P(DTBT) has been reported as promising material for electrochromic, photovoltaic, batteries, biosensor devices. Reported electrochromism of P(DTBT) showed two absorptions bands in the visible region (neutral) with dark blue colour. The colour of the polymer in its oxidized state has not been clearly indicated in the literature. Low bandgap (E_g) P(DTBT) insoluble polymer and its derivatives more soluble one has been investigated by different research groups particularly for photovoltaic and solar cell applications. Most synthesis and studies has been performed in organic media.

14

Our literature review shows that previous studies on the electrochemical properties of P(DTBT) in organic media were not exhaustive. In addition to this, there is little or no studies found in the literature employing ionic liquids as a solvent and electrolyte for the electrochemical synthesis of P(DTBT). The monomer DTBT is well known to possess two redox systems (I) irreversible oxidation that initiates polymerization and (II) reversible reduction which can be exploited. The reversible redox system, which characteristics behaviours of DTBT is also exhibited by its corresponding polymer, P(DTBT). Electrochemistry of DTBT monomer has not been well known and detail investigation of the reversible redox pair of DTBT may be useful for post-polymerization diagnostics of P(DTBT) film, to compare n-doping behaviour of P(DTBT) with the monomer and evaluation of the electron affinity of P(DTBT). Hence DTBT detailed electrode kinetics study is interesting. Furthermore, copolymerization of DTBT with MOT and its electrochemical and optical properties have not been reported so far in both organic and ionic liquids. Poly(3-methoxythiophene) is a promising material for electrochromic, supercapacitor and photovoltaic devices and sensor applications. Only a couple of papers found about its electropolymerization in ionic liquids. There is a need more about its behaviour in ionic liquids. In this project, homopolymers PMOT and P(DTBT) properties were compared with that electrochemically synthesized novel composite P(DTBT)-co-PMOT.

As far as our knowledge is concerned, there are only a couple of articles reported on electropolymerization of DTBT in organic solvents. By contrast, electropolymerization of DTBT monomer which contains thiophene as donor and benzothiadiazole as acceptor, electrodeposition of PMOT and copolymerization of DTBT with MOT in Ils is lacking. It has been reported that the nature of the ionic liquids employed during electropolymerization of conjugated organic polymers affects both the rate of polymer growth as well as their properties. These interesting aspects of the ionic liquids together with the promising

applications of P(DTBT) and PMOT motivated us to utilize them as a medium in study of the electrochemical polymerization of DTBT and MOT and their mixtures (which we expect copolymerized similar to other polythiophene derivatives). We choose 1,3-dialkylimidazolium ionic liquids compounds of tetrafluoroborate, hexafluorophosphate and bis(trfluoromethanesulfonyl)imide; 1-butyl-3-methylimidazolium tetrafluoroborate (bmimbf$_4$), 1-buthyl-3-methylimidazolium hexafluorophosphate (bmimpf$_6$), 1-buthyl-3-methylimidazolium bis(trifluoromethylsulfonyl)imide (bmimtnf$_2$) and 1-octyl-3-methylimidazolium bis(trifluoromethylsulfonyl)imide (octmimtnf$_2$) ionic liquids having a range of physical properties such as polarity, viscosity and conductivity for the electrochemical synthesis of P(DTBT) and PMOT and their copolymer. In this work we assess, the influence of ionic liquids on the rate of polymerization, electrochemical activity, impedance, optical and electrochromic of the resulting polymer films. PMOT characterization and its electrochemical activities were examined in the respective ionic liquids and aqueous solution of LiClO$_4$ (0.1 M).

Thus there is certainly a need for more electrochemical and optical data for P(DTBT), PMOT, and PMOT-co-PMOT in ionic liquids. In particular we seek to gain an understanding of how the physical properties of imidazolium based ILs; bmimbf$_4$, bmimpf$_6$, bmimtnf$_2$ and octmimtnf$_2$ affect polymerization rate, peak potentials (E$_p$), maximum absorbance λ_{max}, electrochemical and optical bandgap (E$_g$), electrochemical activity, optical contrast (%ΔT), response time (t), colouration efficiency (η), stability of P(DTBT) and its copolymer P(DTBT)-co-PMOT, diffusion coefficient of DTBT, standard heterogeneous rate constant on DTBT/DTBT$^-$ redox couple have been investigated.

1.3 Research questions

Investigation of electrochemical and electrochromic properties of poly(4,7-dithien-2-yl-2,1,3-benzothiadizole) (P(DTBT) and its copolymer with poly(3-methoxythiophene) in imidazolium based ionic liquids (bmimbf$_4$, bmipf$_6$ and bmimtnf$_2$) and 0.1 M n-Bu$_4$NClO$_4$/ dichloromethane and acetonitrile has been conducted to address the following research question. Preliminary electrochemical properties of the monomer 4,7-dithien-2-yl-2,1,3-benzothiadizole (DTBT) have been also related to its corresponding polymer.

1. The effect of the nature of ionic liquid on the oxidation and half wave potential of the monomer (DTBT) and the corresponding polymer P(DTBT).

2. Reversibility and kinetics (dependence on basecity of solvent and type of electrode) of DTBT/DTBT$^-$ redox pair in nonaqueous solvents and ionic liquids.

3. The influence of ionic liquids on morphology and electrochemical activity of electrodeposited P(DTBT) and PMOT.

4. Impedance of GCE/P(DTBT) film /ionic liquid interface.

5. The bandgap of P(DTBT), PMOT and P(DTBT)-co-PMOT polymers difference and dependence on the physicochemical properties of ionic liquids.

6. Comparison of electrochemical and optical bandgap of P(DTBT) and its monomer DTBT.

7. Uv-visible absorption band difference between P(DTBT), PMOT and P(DTBT)-co-PMOT electrochemically coated on ITO-coated glass electrode.

8   Dependence of homopolymers (P(DTBT) and PMOT) and copolymers P(DTBT)-co-PMOT optical properties with the nature of growth medium.

9   Variation of the diffusion coefficient of DTBT across nonaqueous solvents and ionic liquids.

10. The influence of the growth medium on electrochromic properties (tuning of bandgab, colour reversibility, switching times, redox stability, optical contrast and colouration efficiency) of P(DTBT) thin film deposited on ITO-glass substrate in bmimbf$_4$, bmimpf$_6$ and bmimtnf$_2$ ionic liquids and in 0.1 tetrabutylammonim perchlorate/dichloromethane.

11. Variation of morphology of P(DTBT), PMOT and P(DTBT)-co-PMOT grown in the ionic liquids and 0.1 M n-Bu$_4$NClO$_4$/dichloromethane.

12. Correlate the electrochemical and electrochromic properties of P(DTBT) and its copolymer with PMOT to the homopolymers as well as to the physical properties of ionic liquids.

CHAPTER 2

THEORY OF ELECTOCHEMISTRY AND ELECTROCHROMISM OF CONDUCTING POLYMERS

In this section, basic mechanisms of the electrochemical polymerization of conducting polymers are described using as an example thiophene electrochemical oxidation. It helps to understand the growth of conductive material on the surface of the electrode in solution containing the monomer. Since our interest was on the electrochromism of poly(3-methoxythiophene) and poly(4,7-dithien-2-yl-2,1,3-benzothiadiazole), the basic theory for colour modulation and the formation of inner band states polaron and bipolaron upon doping are briefly stated.

2.1 Electrochemical polymerization

Electrochemical polymerization has been used to synthesize conducting polymers such as polythiophene, polypyrrole and polyaniline from their corresponding monomers. The main requirement in the electropolymerization of the monomer is that the monomer oxidation potential is accessible through a suitable solvent. In addition to this, the monomer should produce a radical cation which reacts more quickly with other monomer to form oligomers and then polymers than it will react with other nucleophiles in the electrolyte solution [77]. The electropolymerization of conducting polymers is easily carried out with a classical thee electrode cell arrangement. Most of the time polymers are electrodeposited at platinum, gold, glassy carbon and indium tine oxide (ITO) electrodes which usually serve as working electrodes. A monomer is dissolved in traditional organic solvents and anodically polymerized on the electrode surface from the solution containing the monomer and a

supportive electrolyte. Since the last decade, electropolymerization has been performed in ionic liquids which serve simultaneously as a solvent and electrolyte [78-79].

It is supposed that the electropolymerization of thiophene involves coupling of a monomer radical cation through (α, α') position [80]. The coupling of a monomer radical cation occurs at the carbon atom which is known to be the most reactive towards addition and substitution reactions. The general reaction steps are as shown in Fig.2.1 for thiophene polymerization. The first step in the polymerization is assumed to be the irreversible electrochemical oxidation of the neutral monomer [81] to form radical cations (1 to 3 in Fig. 2.1a). In the next stage, two radical cations combine to form a dimmer. The other possibility is that the radical cation could react like an electrophile and add to a neutral monomer (Fig. 2.1b). This reaction is expected to occur since there is repulsion between two like charges when they come closer. Then, the dimmer loses two protons to become electrically neutral. This dimmer which is more easily oxidized to a radical cation can react with other radical cations or monomers. Chain growth proceeds between the radical of the monomer and those of continuously formed oligomers. In order to sustain film growth at the electrode surface, the electrode potential has to be maintained at the oxidation potential of the monomer. The electrochemical reaction proceeds through successive electrochemical and chemical steps, until the oligomer becomes insoluble in the electrolyte medium and precipitates onto the electrode surface.
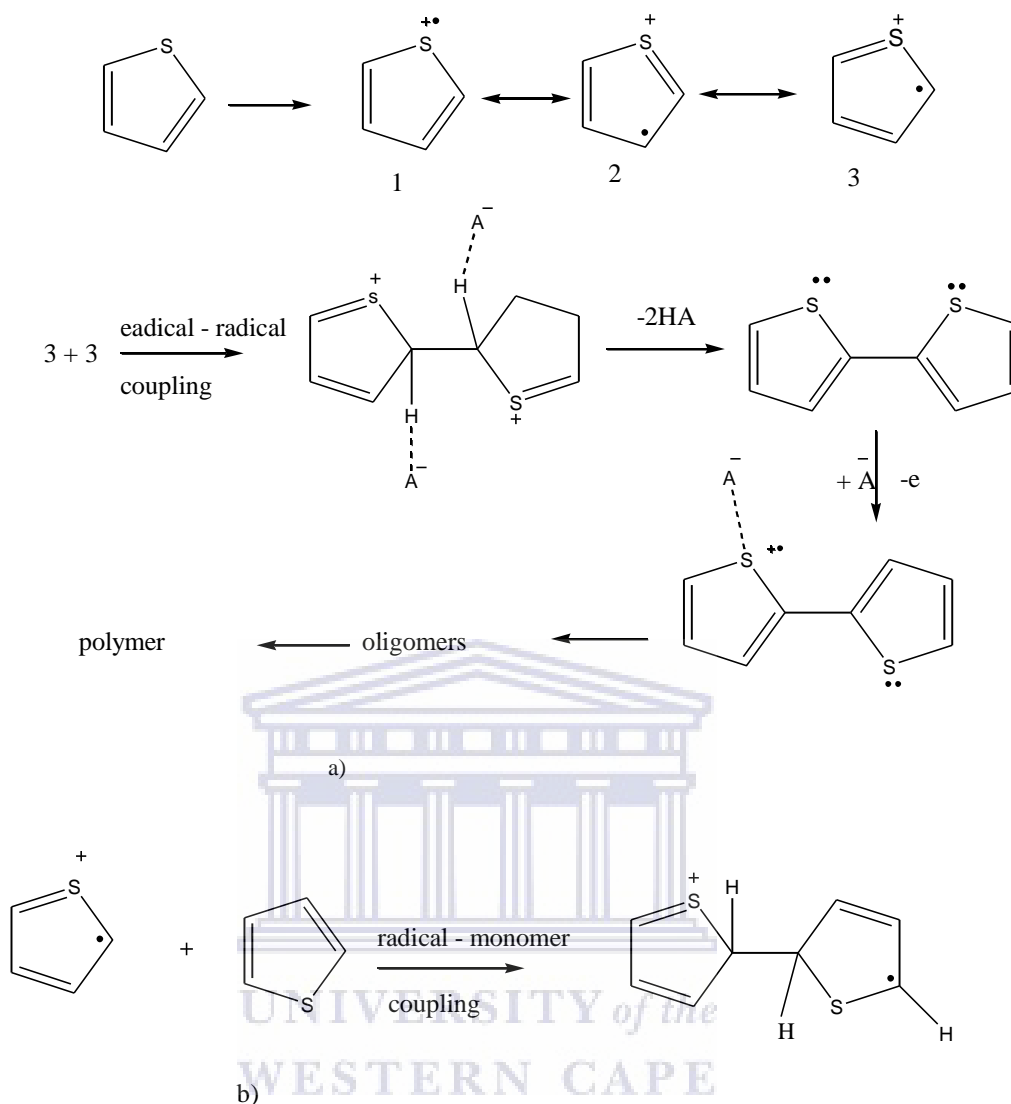
Scheme 2: Possible polymerization mechanisms for the thiophene monomers [81].

Since the polymerization reaction proceeds only when the potential is sufficiently high to oxidize the monomer, the coupling reaction must involve the coupling of two radicals. Because at this potential, the concentration of thiophene is zero on the electrode surface and negligible in the region of the electrode [82].

2.1.1 Mechanisms of the deposition of a polymer on the electrode surface

Initially, Downward and Pletcher [83] studied the oxidation of 10 mM thiophene and bithiophem in 0.1 M tetrabutylammonium tetrafluoroborate as a supportive electrolyte in acetonitrile using Pt disk electrode. The authors found that the deposition of polythiophene occurs via a nucleation growth mechanism (NGM) similar to the deposition of a metal onto a foreign substrate. A linear I vs. $t^{1/2}$ relationship for the early portion of the current transient obtained response to a potential step. It was almost consistent with an instantaneous nucleation/three –dimensional growth mechanism.

Hillman and Mallene [84] have carried out a more detail potentiostatic study on the deposition of polythiophene on Au electrode. The authors proposed a model for the nucleation growth mechanism (NGM) of polythiophene films and estimated some of the kinetic parameters as a function of polymerization potential. This indicates that the formation of a bulk film occurs by instantaneous/three dimensional growth mechanism. Later the same authors studied the deposition of polythiophene on Au electrode using potential step and time resolved spectroscopic measurements [85]. The study indicates different stages in the polymerization process of polythiophene. At short times, small quantities of intermediates were observed. It has been suggested that there may be short chain oligomers consists of 5 to 7 monomer units. At slightly longer times, where the current time transient shows the expansion of growing sites, the optical absorbance shifted to longer wavelengths which was attributed to the formation of longer oligomer chains (15 to 17 monomeric units), a situation that occurs together with the predominance of metallic character of the polymer. On the other hand, Hamnett and Hillman [86], using ellipsometry studies, indicated that the previous analysis of current – time data is more complex, suggesting three dimensional growth process. As they suggested, the standard nucleation and growth theory does not explain the

thickness versus the square of time (t^2) relationship found from ellipsometry data. Furthermore, another contradiction for three - dimensional (3D) growth mechanism reported [87] from the investigation of the kinetics and mechanisms of electrochemically deposited polythiophene-3-acetic acid. The experiments were done in 0.2 to 0.6 M solution of thiophene-3-acetic acid in 0.1 M $LiClO_4/CH_3CN$ on Pt disc electrode. It is proved that deposition undergo in prevailed two - dimensional (2D) layer to layer growth mechanism during polymer formation.

Schrebler *et al* [87] described the effect of potential, monomer concentration and nature of electrolyte on the NGM of polythiophene on Pt electrode in dichloromethane. The current–time transient obtained were fitted using a mathematical equation (2.1).The equation contains three contributions, 2D and 3D instantaneous nucleation both of which are charge transfer controlled whereas 3D progressive nucleation as diffusion controlled. The weight of each contribution was dependent on time. The author found that at any condition the principal contribution is 3D instantaneous nucleation. The contribution of 2D instantaneous nucleation is important in the first stage of the nucleation process. The contribution of 3D progressive nucleation appears at longer times and it is favoured with increasing monomer concentration.

$$j = at[\exp(-bt^2)] + c[1 - \exp(-dt^2)] + et^{-0.5}[1 - \exp(-ft^2)] \tag{2.1}$$

The first two terms in equation (2.1) correspond to 2D and 3D dimensional instantaneous growth respectively. The last term corresponds to progressive nucleation and 3D growth mechanism. The constants a, b, c, d, e and f are described through the following equations (equations 2.2-2.4).

$$a = 2\pi n MhFN_{2D}K_2^2 \qquad b = \frac{\pi N_2 DM^2 K_2^2}{\rho} \tag{2.2}$$

$$c = NFK_3'$$

$$d = \frac{\pi M^2 K_3^2 N_{3D}}{\rho^2}$$

(2.3)

$$e = \frac{\pi F D^{1/2} C^b}{\rho^{1/2}}$$

$$f = \frac{A' K \pi D}{2}$$

(2.4)

$$A' = AN_{Dif}$$

$$K = \frac{4}{3}\left(\frac{8\pi C^b M}{\rho}\right)^{1/2}$$

(2.5)

Where n is the number of electrons transferred, F is Faraday's constant, ρ is density of the monomer, M is molecular mass of the molecules on the surface of the electrode, h is the height of nuclei, K_2 is the growth rate of the 2D nuclei, N_{2D} and N_{3D} are the instantaneous nuclei number formed at t= 0 in 2D and 3D form, K_3' are the rate constants of the 3D nucleus growth parallel and perpendicular to the surface, D and C^b are diffusion coefficients and bulk concentrations of the monomer, A' is the rate constant of a nucleus formation and N_{dif} is the number of nuclei formed at t= 0 under diffusion control.

Film thickness estimated using equation (2.6)

$$h = \frac{K_3' V_m c d t^2}{k}$$

(2.6)

Where

$$k = aeexp(-bt^2) + cdt + eft^{1/2}$$

(2.7)

V_m = the molar volume of polythiophene that is deposited

24

2.2 Electrochromism of conducting polymers

Since the last two decades electrochromism of conducting polymers has been investigated to utilize them in electrochromic devices. It is widely accepted that conducting polymers will play an important role as anodic and cathodic colouring materials in the future electrochromic derives. However, due to lack of long term switching ability, stability, processability, design, and mechanical and thermal stability, various research groups conducting mutidisplinary enormous research activities is going ahead. In this respect understanding the origin of colour change and its correlation with molecular structure is highly important.

Various research groups reported the synthesis of conjugated conducting polymers with fast switching time, high optical contrast, stable and solution processable polymers. In addition to this, donor – acceptor polymers has become an active area of research for the synthesis of green neutral polymers. Syntheses of green conjugated polymers were the most challenging aspects because of the requirement of two saturation absorption in the visible region (red and blue).

2.2.1 Molecular orbitals and hybridization

Quantum mechanics based on Heisenberg uncertainty principle and the Pauli Exclusion Principle is the base for Schrödinger equation. Atomic and molecular orbitals are wave function and they are solutions of Schrodinger equation. Solving Schrödinger equation for the hydrogen atom gives atomic orbitals which are the base for molecular orbital formation. For example molecular orbital (MO) of hydrogen molecule can be formed when two 1s orbitals of hydrogen atom comes closer enough and hence overlap. That is the electron moving at a given time around one of the hydrogen atom may move to another nucleus of the other atom and the same probability for the other electron. As a result, two molecular orbitals are formed

one with lower and another one at higher energy higher. The molecular orbital with lower energy than the original atomic orbitals is known as bonding MO whereas the other with a higher energy than the atomic orbitals is known as anti-bonding MO. The energy level diagram is shown Fig. 2.1
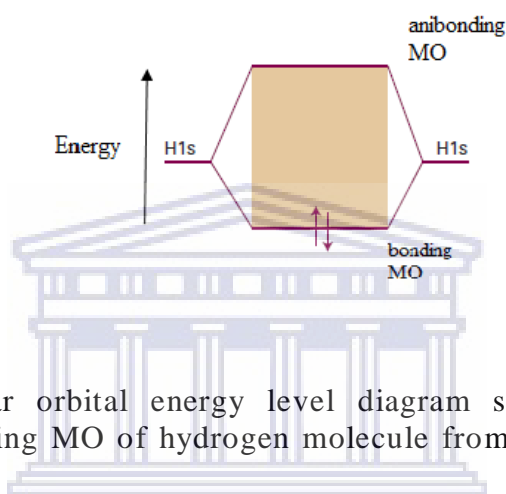
Figure 2.1: Molecular orbital energy level diagram showing the formation of bonding and antibonding MO of hydrogen molecule from two 1s atomic orbitals of hydrogen atom.

Molecular orbitals like that of atomic orbitals can hold a maximum of two electrons only. When bond is formed (covalent) the two electrons from the atomic orbital's of the separate hydrogen atom will occupy the lower energy of bonding MO. Covalent bond formation involves the sharing of two electrons which is paired in bonding MO. The essence of bond formation is when an electron move around a nucleus of given atom may have a chance to move into another nucleus of the other atom and similarly the electron from the other atom may move around to the nucleus of another atom as a result electron cloud build up in between the two atoms that can simultaneously attracted by both nuclei and bind the atom together. The bonding MOs that results in a geometry of cylindrical symmetrical about a line joining the two nuclei involved are called sigma (σ) sigma orbital and the bond formed called σ bond.
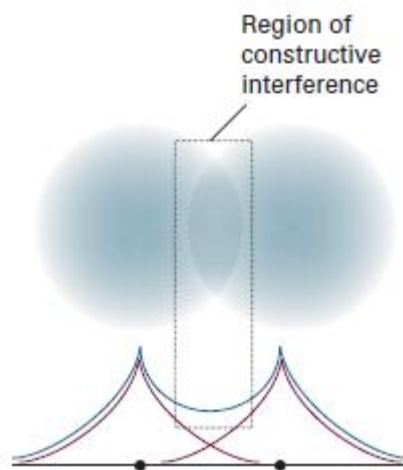
Figure 2.2: Constructive interference when two 1s orbital's of hydrogen atoms forms a σ- bonding of a hydrogen molecule [88].
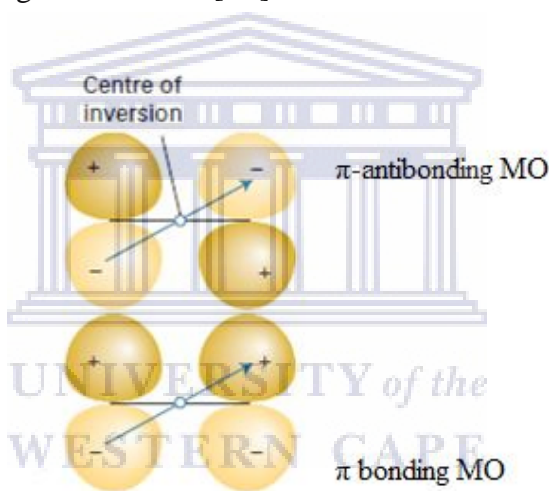
Figure 2.3: A Schematics representation of overlap of two p atomic orbitals to give a π-bonding and antibonding π MO [88].

On the other hand, pi (π) bonding molecular orbitals; the bond called a π- bond is formed from the side overlap of two 2p atomic orbitals as shown in Fig.2.3 The energy of π-MO orbital is lower than σ-bonding MO since its geometry is not cylindrical symmetrical a line join the two atoms.

27

Hybridization of atomic orbitals is an important concept to be taken into consideration for describing covalent bonds in molecules and compounds. Let us take methane (CH₄) since the four C-H bonds posses identical energy as proved from experiment, the overlap orbitals leading to bond formation in the molecule should be equivalent to each other [89]. A stable covalent bond is formed when one 2s and three 2p orbital combine to form four hybrid orbitals known as sp3 hybrid orbitals of carbon rather than individual 2s and 2p orbital to combine with the hydrogen atomic orbitals. These four hybrid orbitals overlap with the 1s orbital of hydrogen atom at the corner of the tetrahedron to from σ MO of C-H covalent bond. The phenomena of the formation of hybridized atomic orbitals are referred as hybridization.
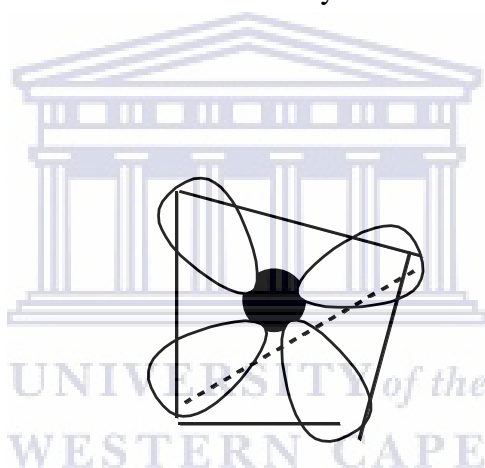
Figure 2.4: The Sp3 hybridized carbon atoms in methane.

In contrast to this molecule which contains double bond such as ethylene follows a different pattern of bonding Fig. 2.5. Ethylene is sp2 hydride orbital as a result of 2s and 2p orbital hybridization. But the fourth orbital is 2p orbital which is perpendicular to the plane of the three sp2 hybridized orbitals. In this kind of compound there are two C-H σ bond (overlap of two of the sp2 orbital's with the 1s orbitals of the hydrogen atom, one σ bond C- C bond formed between the remaining sp2 orbital's with another carbon atom and 1 π bond (C=C) comes from the overlap of the 2p orbital of carbon with another p orbital's of carbon. It is interesting to look the scheme of π bonding in conjugated organic polymers since its

conductivity and properties arise as a result of its π electron delocalization in the π orbitals of the molecule.

The type of orbital hybridization has a significant impact on the structure of the polymer. Sp3 hybrid molecules form only σ bond. As a result of this the separation between bonding also known as highest occupied molecular orbital (HOMO or valance band) and anti-bonding also known as lowest unoccupied molecular orbitals or conduction band) is large. The energy difference between the two is known as bandgap (E_g). In contrast, organic polymers with sp2 hybridization which consists of σ and π bond, produces smaller separation between bonding
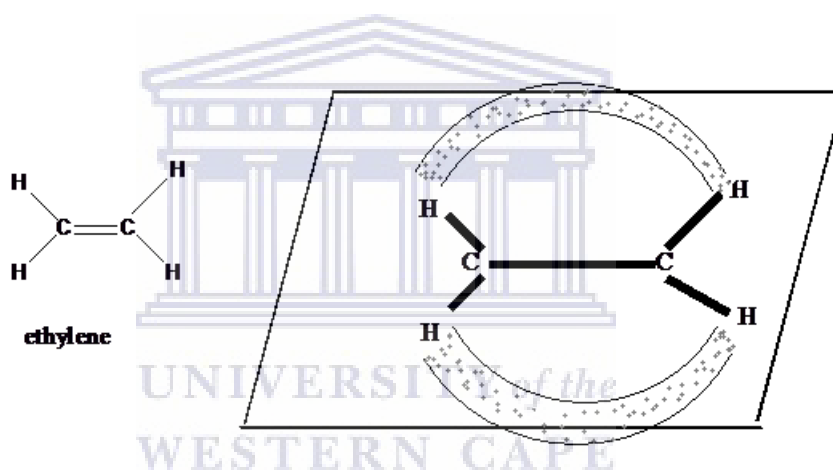
Figure 2.5: Overlap of 2p orbital of carbon atoms in ethylene to form a π bond.

(π) and anti-bonding (π^*) states. For this kind of systems the E_g is smaller. Furthermore, Sp^2 hybridized polymers with σ and π bond classified into two that is localized and delocalized states. Conjugated polymers with delocalized states can be doped to high electrical conductivity.

2.2.2 Electronic structure of conjugated polymers

The electronic structure of conjugated polymers is conveniently described using poly(acetylene). One thing, poly(acetylene), (CH)n or PA, has the simplest, most regular with strictly alternating single and double bonds, and simplest symmetric structure of a prototype of conjugated polymers. The other think is the historically discovery of poly(acetylene) doping triggered extensive research on conductive polymers by the wider research community [1]. Therefore, poly(acetylene) is the base for theoretical background, modelling and electronic properties of conjugated polymers.
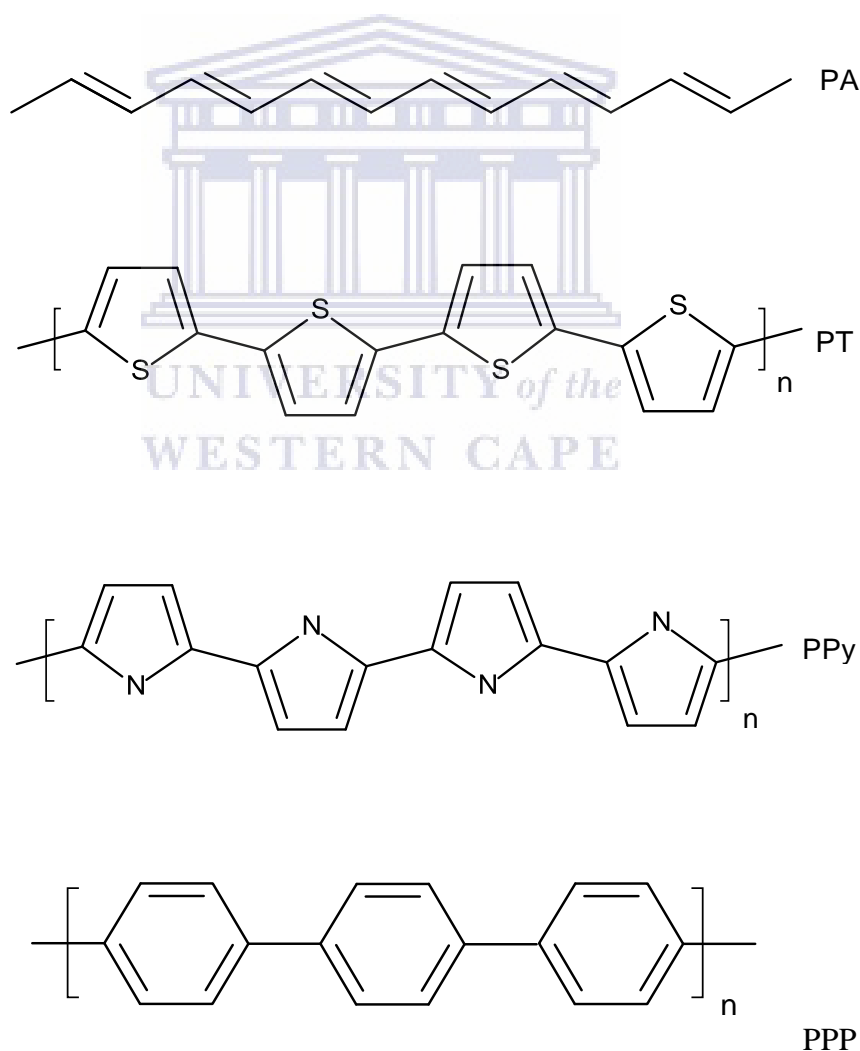
Figure 2.6: Representative of conjugated polymers.

Each carbon atoms of poly(acythelene) is sp2 hybridized with a bond angle of 180 degree instead of 120 degree so that the polymer is treated as one dimensional solid. The double bond is stronger than from that of a single bond and hence C-C bond length in poly(acetylene) is not equivalent. They are alternatively slightly shorter and slightly longer. This is because of Peierl's distortion.

There are four electrons at each carbon atom. Among this four electron two of them form bonding with the nearby CH radical the other one is overlap with a hydrogen atom and the fourth one is non – bonding and delocalized it can move freely along the backbone of the polymer chain. So, linear poly(acetylene) and other conjugated polymers can be considered as a one dimensional solid (metal).

Because of Peierl's distortion in poly(acetylene) the "metallic state" (undimerized state) all bonds have equal length and the spare electron out (delocalized) over the whole system and the non – bonding state (dimerized state) all bonds do not have equal length as presence of single and double bonds.

2.2.3 Soliton, polarons and bipolarons

There are two types of soliton generation, the first one is intrinsically formed solitons during synthesis or dimerization and the second one is doping induced solitons. Let us first discuss intrinsically how solitons are formed by taking polyacetylene as an example. Trans-polyacytlene has two degenerate states as shown in Fig. 2.7. They are idealized structures means that no misfits or domain walls appear.
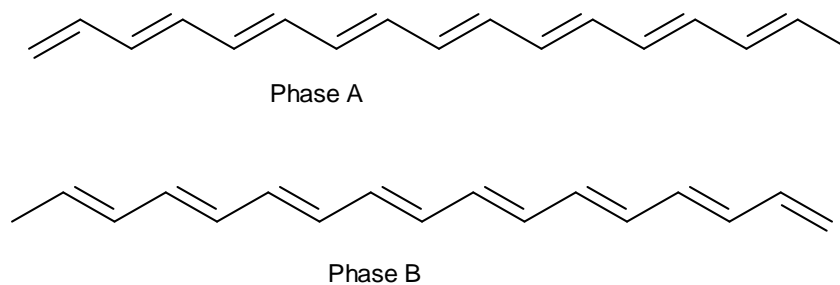
Phase A

Phase B

Figure 2.7: The ground state energy dimerized trans-polyacetylene of phase A is equal to phase B.

There will be 50 % probability of misfit when the transition from undimerized to dimerized (Peierls) transition starts at the same time at ends of the polymer chain assumed. The misfit which is also called "domain" wall divided domains into phase A and phase B, which are termed as "domain". Therefore a Peierls transition results domain separated by domain walls. These domain walls are conjugated defects called "solitons".

The cause of energy gap formation is regular double bond and single bond alteration in the chain of the polymer. However, at the misfit (soliton) position bond alteration in the chain is interrupted, this means that no energy gap. At the misfit position it is "unknown" whether atomic orbitals overlap to form π-bonding and π^{*} (antibonding) states. Instead, the atomic orbitals form non-bonding states in the energy gap, as a result of symmetry reasons they form a mid-gap state [90].

Doping of conjugated polymers is another means that changes its structure and electronic properties [1]. It changes the band structure of polymers and form mid gap states. There are two types of redox doping known as p-doping and n-doping. Doping can be performed either chemically or electrochemically. For example during anodic oxidation of polyacetylene, a radical cation (Fig. 2.8) is formed with simultaneous insertion of an appropriate number of anions of the electrolyte between the polymer chains to neutralize the charge of polycarbonium cations. Removal of a second electron give rise to a second radical cation and the combination of the two radicals gives a spineless dictation called positive solitons [1]. In polyacetylene, doping –induced states are related to the misfit to solitons [91].

In heterocyclic conjugated polymers, different charge configurations are formed. Doping in heterocyclic systems can be explained taking polythiophene. The removal of one electron during electrochemical doping results in the formation of a radical cation called polaron (Fig. 2.8b). It results a non –degenerate ground states. The higher energy part called aromatic which contains two double bonds in a ring and a single bond between rings and a lower energy a quinoid state with a structure of only one double bond in a ring and a double bond separating the rings. Polaron formation is considered as solitons creation. These two defects are pushed by the lattice force and migrate to each other; to minimizing the energy i.e. minimizing the length of a quinodal state into two aromatic states to reduce its length.
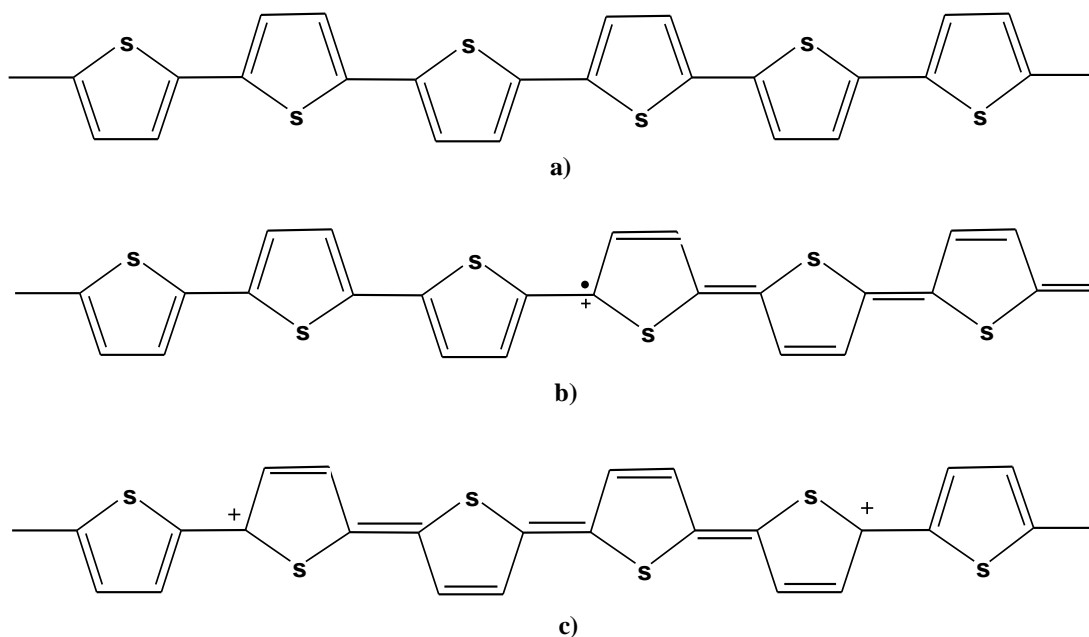
Figure 2.8: a) Neutral, b) polaron and c) biolaron of polythiophenes.

The removal of another electron leads to the formation of another polarons. Spineless radical dictation called bipolaron (Fig. 2.8c).Two polarons attract each other while two bipolaron repel each other, whereas one polaron and one bipolaron can coexist, freely passing each other.
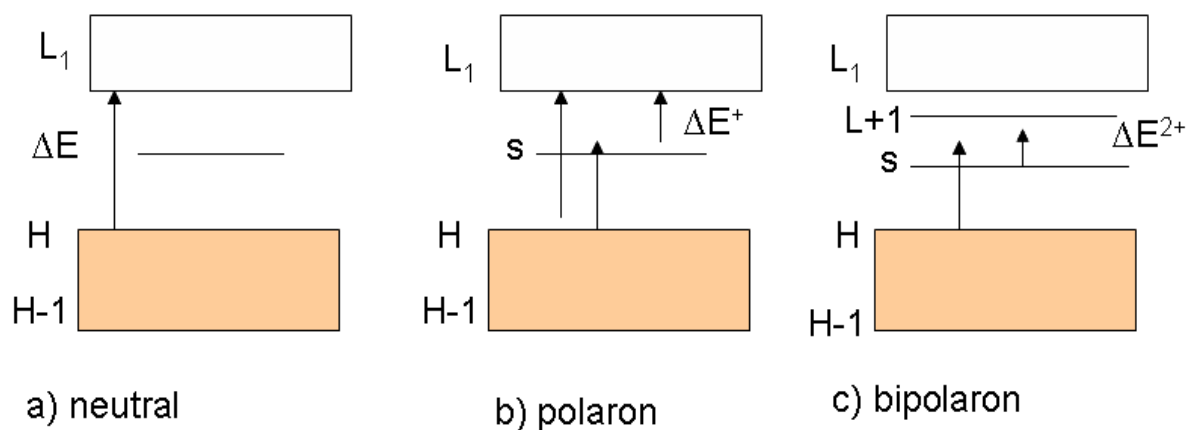
Figure 2.9: Bandgap of polaron and bipolaron and possible optical transitions.

2.3 Donor–accepter polymers

The interaction between the molecular orbital of a strong electron donor (D) unit and strong electron acceptor (A) unit give rise to an increased double bond character between the units, since each unit can accommodate the charges that are associated with such a mesomersism ($D–A \leftrightarrow D^+ = A^-$). For this reason a conjugated polymer which consists of an alternative part of electron releasing – electron taking units in the main chain shows a small bandgap [92]. Quantum chemical calculations of the energy of hybridization of the donor and the acceptor energy level, particularly the HOMO of the donor fragment (higher lying) and LUMO of the acceptor fragment (low lying) produce a D-A monomer with unusual small HOMO-LUMO separation [93-94] (Fig. 2.10). Further hybridization upon increase the chain length and yield D-A monomer with a further narrower bandgap.
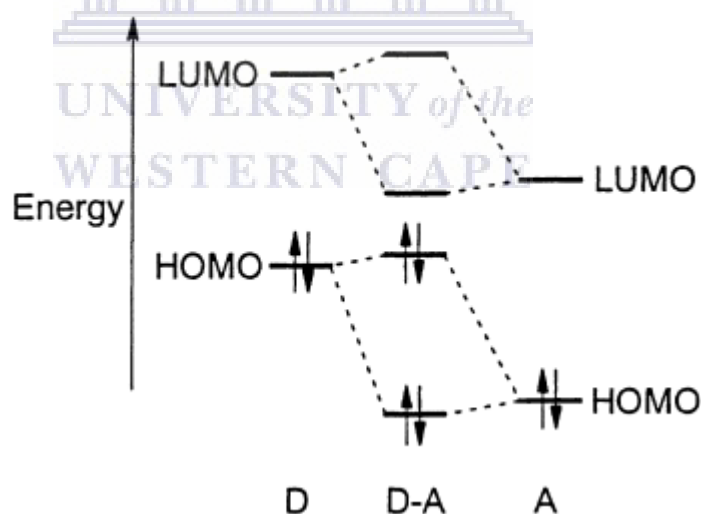
Figure 2.10: Hybridization of the energy levels of a donor (D) and acceptor (A) fragments leads to a D-A monomer with a small narrow HOMO–LUMO energy separation.

For conjugated polymer the dispersion of the HOMO and LUMO units in to a new band continues until a broad valance and conduction band have emerged. It is from these conjugated polymers lend their semiconductor properties. Bandgap is lowered by donor-acceptor strategy. For instance, DTBT (thiophene and 2, 1, 3-benzothiadiazole containing oligomer) λmax 447 nm (E_g = 2.77 eV) and for its oligomer containing two units of DTBT λ_{max} 521 nm (E_g = 2.37 eV). DTBT oligomer is bathochromic shift in the absorption maxima upon excitation of the conjugates. The less red shift, for the donor–acceptor oligomer should therefore be caused by a diminished dispersion of the HOMO and /or LUMO levels upon extension of these systems compared with oligothiophenes and oligopyrrols [92].

This strategy has been employed particularly to synthesis green polymers. The requirement of two absorption bands in the visible region (red and blue) to have a saturated green neutral polymer and simultaneously depleted as it oxidized to give a transparent polymer have been addressed.

2.4 Brief description of calorimetric theory

The colour change of conjugated organic polymers driven by redox process is referred by the position of maximum wavelength of absorbance λ_{max} in the spectrum. Since colour perception is dependent on individuals, describing a colour based on λmax is not satisfactory. To avoid discrepancy of variation of colour; it is defined by three attributers commonly called hue related to wavelength, saturation (relative level of white or black) and Luminance (brightness of colour) [95-96].

Using the three attributes of colour (hue, saturation and luminance) any colour can be quantified. The Commission International de I' Eclairage (CIE) has developed the first one CIE 1931, and then CIE 1976. CIE has been developed based on how the "average" person

subjectively sees colour and thus simulates mathematically how people perceive colour. Basically, CIE system expressed colour in terms of 'tristsmulus' (X,Y,Z), since the theory of colour vision, eye has three types of photoreceptors for the three primary colours (red, green and blue) and all other colours perceived by human eye is a mixture of these colours. The X, Y, Z defines the CIE system of colorimetric whereas the values of x, y, z defines the CIE colour space methods of describing the colour in terms of numbers. Where x is the sum of X, Y and Z divided by X and y is the sum of X, Y, and Z divided by Y. In   this case X, Y, Z tristimulus represented all possible colours graphically. It is shown commonly in two dimensional spaces that are luminance and chromaticity (hue and chroma).
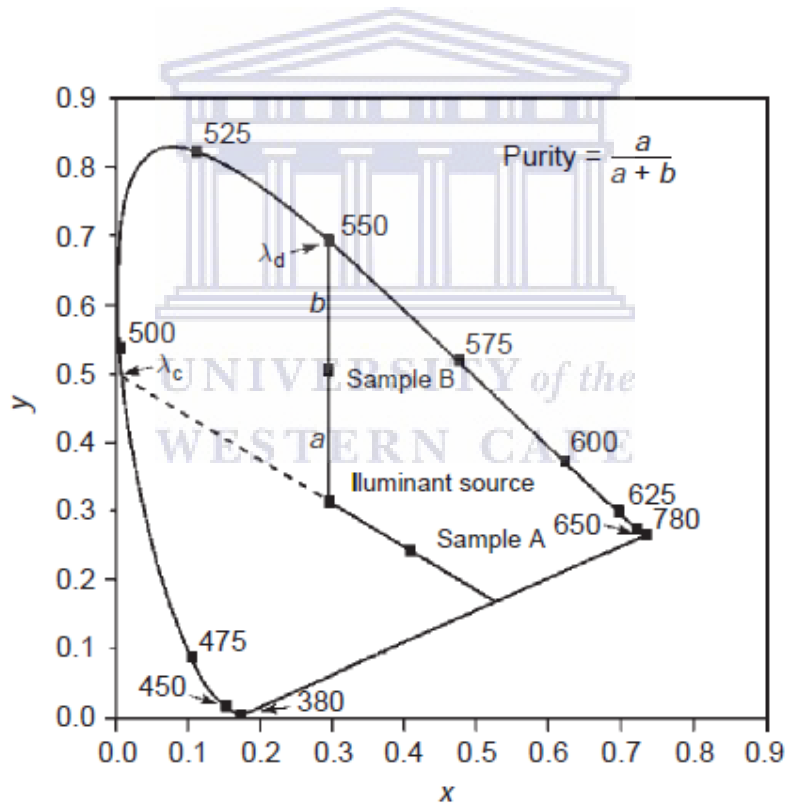
Figure 2.11: CIE 1971 xy chromatic diagram with a labeled illuminant source [44]. The above xy chromatic diagram shows the determination of complementary wavelength of a sample with xy coordinates of arbitrary sample A, and the dominant wavelength and a sample with xy coordinates of arbitrary sample B. In this case x represenbts the hue and y represents the chroma.

CHAPTER 3

LITERATURE SURVEY

3.1 Imidazolium ionic liquids and electropolymerization

Room temperature ionic liquids (RTILs) or ionic liquids (ILs) are organic salts in the liquid state. In some contexts, the term has been restricted to salts having low meting point usually below 100 ^{o}C or including room temperature [97-98]. This arbitrary temperature limit identifies the difference from inorganic molten salts often characterized by their high melting temperature. Ils are liquid over a wide temperature range including room temperature and are composed of solely bulk heterocyclic delocalized cations and weekly coordinated symmetrical small inorganic or organic anions. The most common organic cations are the 1, 3-dialkylimidazolium, N, N-dialkylpyrrolidium, N, N, N, N-tetraalkylammonium, or N-alkylpyridinium cations (Fig.3.1). On the other hand, the typical popular inorganic anions are tetrafluroborate (bf_4^-) and hexafluorophosphate (pf_6^-) whereas bis(trifluoromethylsulfonyl)imide (tnf_2^-) and triflate (otf^-) are organic anions (Fig.3.2) [12, 30, 32]. The big difference in size between cations and anions makes ionic liquids to have poor lattice structure. Consequently, Ils structures are disorder and hence the reason ILs being in the liquid state at room temperature [99]. Of course, there are ionic liquids synthesized from a small cation and highly symmetrical larger anions (ammonium diacetate) which have higher conductivity (9.8 mS/cm) and lower viscosity (64 mPas at 45 ^{o}C) [100]. The term "ionic liquid" in general sense was used as early as 1943 [101]. However, in the literature ILs are also called liquid electrolytes, ionic melts, ionic fluids, fused salts, liquid salts or ionic glasses.

Since the discovery of nonhaloaluminate (air and water stable) ILs in 1992 [102], research for the application of these materials has grown at ever accelerating rate [103] because of their unique chemical and physical properties. Air and moisture stable ILs display excellent intrinsic ionic conductivities and thermally stable over a wide temperature range, with a decomposition temperature around $300 - 500$ $^\circ$C. Ionic liquids are now widely used in various research areas as solvent for organic and inorganic synthesis since they are good solvent for organic and inorganic compounds, either polar or nonpolar [104-105]. Ionic liquids have negligible vapour pressure and they are non-flammable and non-volatile [103]. ILs generally exhibits a wide potential window in some cases, enlarged electrochemical windows $4.5 - 7$ V have been reported [12]. These are highly desirable property for applying the ILs as electrochemical solvents [12, 30-32, 37, 42]. Because of these important properties, ILs has become a novel solution for the short coming of traditional organic solvents. Thus, ILs is promising mediums for a variety of electrochemical synthesis and applications [106-107]. Since the electrolyte used for the preparation of the conducting polymers has also key influence on the properties of the resulting polymer including conductivity, electrochemical stability and efficiency and mechanical properties, ILs have become much more widespread to perform the electrochemical synthesis of conducting polymers. They serve simultaneously as a solvent and electrolyte. ILs are also used as conducting fluids (electrolytes) in electrochromic [108] devices, Li ion batteries [109], solar cells [110]. Moreover, they become useful in organic synthesis [104-105, 111], catalysis [112] and adsorbents of pollutants [113]

Ionic liquids of different class have been studied. The most common once includes imidazolium, pyrrolidinium, phosphonium, quaternary ammonium, pyridinium and triazolium salts [97]. The combination of the choice of anion and the alky substituent's of cation in any of these classes can produce a number of diverse ILs. The literature survey in this work focuses on the popular imidazolium based salts shown in Table 3.1.

Common cations
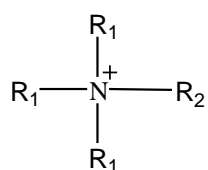
teraalkyl ammonium
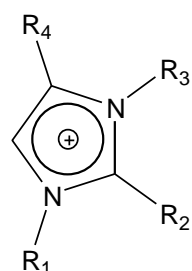
di, tri, and terraalkylimidazolium
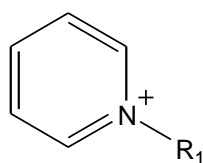
alkylpyridinium
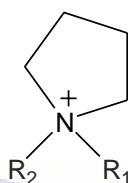
dialkylpyrrolidinium
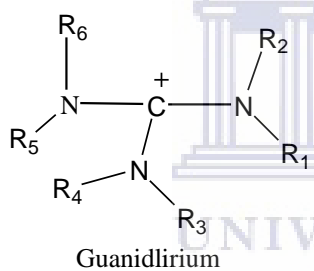
Guanidlirium
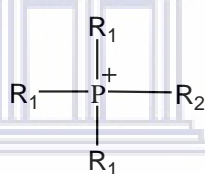
tetraalkylphosphate
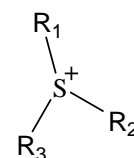
trialkylsulfonium
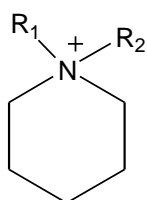
Dialkylpiperidinium
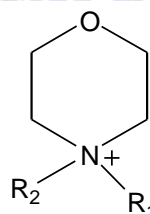
Morpholinium

Figure 3 1: Common cations of ionic liquids.

Common anions

The most popular inorganic anions are tetrafluroborate water miscible and hexafluorophosphate water immiscible while organic cations are bis(triflate), bis(triflyl)imide, triflate, heptaflurobutanoate and trifloroacetate
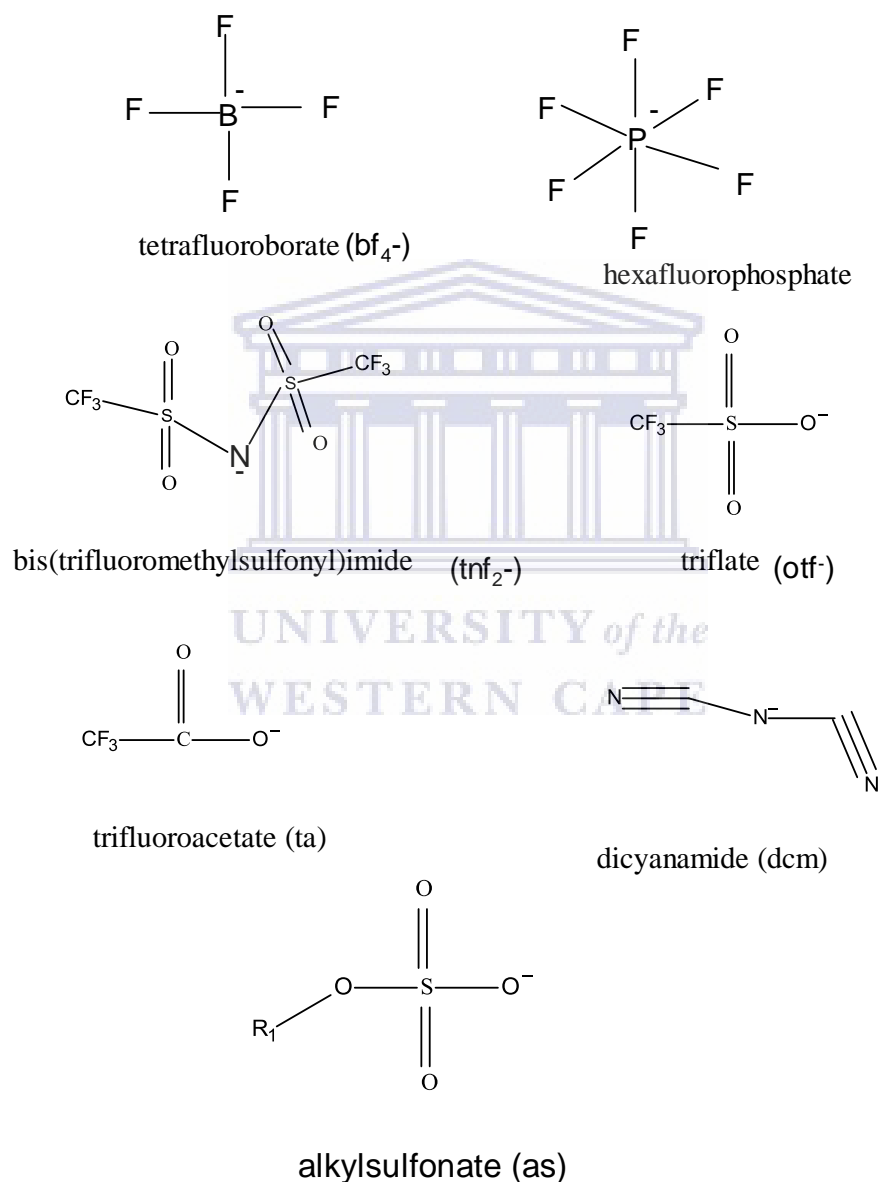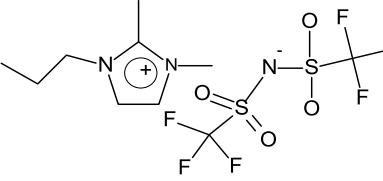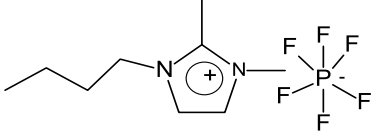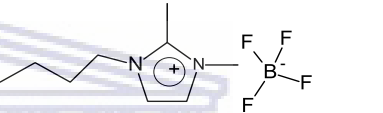
Figure 3.2: Common anions of ionic liquids.

Table 3.1: List of most popular imidazolium based ionic liquids.

Compound	Structure	Abbreviation
1-buthyl-3-methylimidazolium Tetrafluoroborate		bmimbf$_4$
1-buthyl-3-methylimidazolium Hexafluorophosphate		bmimpf$_6$
1-buthyl-3-methylimidazolium Chloride		bmimCl
1-buthyl-3-methylimidazolium Bromide		bmimBr
1-buthyl-3-methylimidazolium Dicyanimide		bmimdca

Compound	Structure	Abbreviation
1-buthyl-3-methylimidazolium Trifluoromethanesulfonate		bmimotf
1-buthyl-3-methylimidazolium tris(trifluoromethylsulfonyl) Methide		bmimmethide
1-buthyl-3-methylimidazolium bis(trifluoromethylsulfonyl)imide		bmimtnf$_2$
1-ethyl-3-methylimidazolium bis(trifluoromethylsulfonyl)imide		emimtnf$_2$
2,3-dimethyl-ethylimidazolium bis(trifluoromethylsulfonyl)imide		emmimtnf$_2$

Compound	Structure	Abbreviation
2,3-dimethyl-propylimidazolium bis(trifluoromethylsulfonyl)imide		pmmimtnf$_2$
1-buthyl-2,3-dimethylimidazolium Hexaflurophosphate		bmmimpf$_6$
1-buthyl-2,3-dimethylimidazolium Tetrafluroborate		bmmimbf$_4$

3.1.1 Physical properties of imidazolium ionic liquids

An important property of the imidazolium salts is the variation of physical properties such as conductivity, viscosity and melting point could be adjusted by changing the alkyl substituents and imidazolium and halide ratios. Physicochemical properties of imidazolium based ionic liquids with anions bf$_4^-$, Br$^-$, Cl$^-$, pf$_6^-$, tnf$_2^-$, otf$^-$ and dca$^-$ presented in Table 3.1 has been reported by many research groups. Both the cations and the anions of ILs plays their role in determine the physical properties of ionic liquids [114-115].

Understanding basic physicochemical properties of ILs is vital for evaluation of electrochemical, optical and morphological properties of electrochemically synthesised polymers in ionic liquids. For instance, conductivity (σ), viscosity (η) at a given temperature helps to know how fast the electroactive species reach on the surface of electrode, electrochemical potential window is required to know the potential range in which the

background current of the ionic liquid is minimum, density (ρ) as a function of temperature is needed for apparatus sizing, m_p (melting point)), T_{ag} (glass transition temperature), T_d (thermal decomposition temperature) are required to set the feasible temperature range a particular fluid can operate and heat capacitance are needed to estimate heat storage capacity of a particular ILs.

Table 3.2: Static properties of imidazolium ionic liquids at 25 $^{\circ}$C.

Ionic liquids	c_{water} ppm	d/g/cm	V_m/cm^3 mol	molecular weight g/mol	$\gamma/10^{-3}$ N/m	molar Concentration (mol/L)
bmimbf$_4$	61[a]	1.19[a]	190[a]	226.01	44.0[a]	5.575
bmimpf$_6$	45[a]	1.37[a]	208[a]	284.18	40.9[a]	4.75
bmimotf	-	1.29[b]	-	288.29	-	4.48
bmimtnf$_2$	12[a]	1.42[a]	295[a]	419.37	33.0[a]	3.41
bmimtf$_3$c	27[a]	1.56[a]	352[a]	-	35.1[a]	-
emimtnf$_2$	-	1.50[c]	-	391.32[c]	-	3.84[c]

[a] data taken from reference [103], [b] data taken from reference [116] an [c] from [117].

Table 3:3: Viscosity, conductivity and polarity of some of the common of ionic liquids.

Ionic liquids	water content (Wt %)	viscosity mPa s	conductivity mS/cm	polarity $E_T(30)$ kJ/mol
bmimbf$_4$	-	154, 114	3.5	217[c]
bmimpf$_6$	-	308	1.46	218.5[c]
bmimtnf$_2$	1.4[a]	52[a]	3.9[a]	218.5[c]
Bmimotf	5.01	90	3.7	-
emimbf$_4$	-	154	0.35	-
emimtnf$_2$	-	28-34	0.91	-
octmimtnf$_2$	-	96[d]	7.5[d]	-
octmimpf$_6$	-	-	9.996[b]	217.6[c]

[a] [118] at 20 ^{o}C , [b] [119]; [c] [120], [121] and [d] [12, 122]. Smaller E_T shows high polarity.

3.1.1.1 Conductivity, viscosity, density and potential window of ionic liquids

Conductivity of ionic liquids is an important criterion for the evaluation and ground work application of ILs in electrochemistry. The conductivity of ionic liquids reviewed in several papers [123]. Generally, conductivity of ILs at room temperature ranges from (0.1–20 mS/cm) [123-124]. Therefore, ionic liquids conductivities are sufficient to use them as simultaneously both as solvent and electrolyte in electrochemistry. Their intrinsic conductivity without the addition of supportive electrolyte makes them advantageous over traditional organic solvents. Based on the fact that ILs is composed of solely asymmetrical cations and anions, it would be expected high conductivities. This is not the case found in ionic liquids since conductivity related to viscosity, molecular weights and the size of the ions. Bigger size of cation and the anion constituents of ILs reduce the mobility of ions and

then their conductivity though the numbers of charge carriers are so large in these systems. Furthermore, ion pair formation between oppositely charged species reduces conductivity. In fact, the change in conductivity between ionic liquids is directly related with their viscosity [125]. It is reported by different research groups, ILs with higher viscosity exhibited lower conductivity.

The viscosity of ILs are large be about 10 to 100 times than that of water and conventional organic solvents. This is attributed to the presence of strong interactions between oppositely charges ions and other interactions [118]. Both cation and the anion part of the ILs play a role in determining their viscosities. Longer alkyl substituents on the cation favours stronger van deer Waals force between the cation leads to higher viscosity. On the other hand, the nature of basecity of the anions and their ability to involve in hydrogen bonding affect the viscosity of the ILs. For example, ILs containing pf_6^- and bf_4^- as anions are more viscous than that of tnf_2^- due to stronger H….F interaction in the former ionic liquids than the weekly basic anion in the later one in which the negative charge is quite delocalized over the two sulfoxide groups [126]. Besides, the size, shape, and molecular mass of anion affect the viscosity of ILs. Smaller and more symmetric anions lead to more viscous ILs.

Imidazolium cation with longer alkyl substituents exhibits lower density [127]. The density of aromatic onium salts is higher than that of aliphatic ammonium salts. In similar fashion the density of ILs decrease by increasing the chain length of the alkyl substituents on the anion. The introduction of heavy chain such as fluoroalkyl increases the density of ILs. For example emim with different anions its density increase with $CH_3SO_3^- < BF_4^- < CF_3COO^- < CF_4SO_3^-$ $(CF_3SO_2)N^- < (C_2F_5SO)_2N^-$ [128].

Generally ILs shows insignificant background current in a wider potential window a key criterion to be considered when they are use one in two in electrochemical measurement. This

is because of the fact that ILs are inherently redox robustness, because of the robustness of cations and anions used for their preparation. Typical range of potential window 4.5-5 V (slightly wider than that observed in molecular organic electrolytes but exceeds much that of aqueous electrolytes) have been reported [129] and even wider potential window up to 7 V was reported for some ILs such as bmimbf$_4$ [130].

3.1.1.2 Thermal stability and decomposition temperature

The decomposition temperatures of ILs are in the range of 300 to 500 $^\circ$C. The strength of heteroatom –carbon and heteroatom-hydrogen bond determines the thermal stability of ILs. Thermal stability of ILs decrease with increase in anion hydrophobicity. Huddleston *et al* [131] studied the thermal stability of bmim with the various anions. They suggest their thermal stability decrease in the order pf$_6^-$ > tnf$_2^-$ ≈ bf$_4^-$ >halides. Halides reduce the thermal stability of ILs at least by 20 $^\circ$C compare to nonhalide anions [132]. ILs with halide anion posse's high melting point compare to inorganic anions such as bf$_4^-$ and pf$_6^-$ and a larger organic anion tnf$_2^-$, triflate or tosylate.

3.1.1.3 Miscibility and solubility of ionic liquids

Miscibility of ionic liquids with water various depends on the chain length on the cation part as well as the nature of anion. Halide anions are moisture sensitive and acidic. The anions bf$_4^-$ and pf$_6^-$ are neutral and less toxic whereas tnf$_2^-$ is moisture stable.

The solubility of different species in imidazolium ILs depends mainly on the polar and hydrogen bonding ability. Saturated aliphatic compounds are generally only sparingly soluble in ILs where as olefins somewhat show greater solubility and aldehyde can be completely miscible. Gas solubility follows the same trend, carbon dioxide exceptionally showing higher solubility in many ILs.

3.2 Polythiophene and its derivatives

Polythiophenes and its derivatives are the most important of conjugated polymers. With their environmental and thermal stabilities, they can be used as electrical conductors, none linear optical devices, polymer light emitting diodes, sensors, batteries, organic transistors, and electrochromic devices [2, 6-7, 13-14, 21, 133]. For thiophene monomers substituted with electron – withdrawing groups, such as 3 – halide thiophene, which is prepared from easily accessible or commercially available monomers, the decrease electronic density of the thiophene and its derivatives, are of particular interest for use as electrochromic materials.

The electrochemical synthesis of polythiophenes was first reported in 1981 [134] using tetraethylammonium tetrafluoroborate supporting electrolyte under galvanostatic conditions, in a method similar to that employed for the polymerization of polypyrrole. The conductivity of the product was found to be in the range of 10^{-3} to 10^{-1} S/cm. Ever since then, other workers have polymerized thiophene onto platinum coated glass electrode to produce thin film using acetonitrile solution containing small amounts of water and a variety of supporting electrolytes. Similar results were achieved by Kaneto *et al* [135] using monomer solutions in oxygen free anhydrous solvent (acetonitrile) and benzonitrile) at ITO-glass substrate.

Ayeiyach *et al* [136] studied the electropolymerization of thiophene on oxidizable metals (Fe, Al and Zn) in acidic, neutral or basic media. They reported out of several salts, pf_6^- alone could hinder the anodic dissolution of iron and allow the galvanostatic electropolymerization of thiophene on this metal in propylene carbonate. Propylene carbonate is considered as a good neutral solvent for the electropolymerization of thiophene on noble metals. In a basic solution, such as tetrahydrofuran, electropolymerization of thiophene could not achieve, due to passivating of the metal making the electrode surface highly insulating. The best result was obtained in dichloromethane, which allow the deposition of homogeneous polythiophene

films on Fe and Zn in both potentiostatic in the galvanostatic conditions. On Zn the best film was obtained in the galvanostatic mode only. This is because Zn is believed to be dissolving even at a low potential.

Adding substituents to the thiophene affects the oxidation potential by either increasing or decreasing the electron density in the thiophene ring. Increasing the electrophilic character of the substituents, such as CN^- and NO_2 shifts the oxidation potential to more positive values, whilst the presence of electron donation groups such as methyl (CH_3) have the opposite effect, shifting the peak potential of the monomer in the cathodic direction compare to the unsubstituted materials [137]. On the other hand, the substitution effect on the oxidation of potential explained through radical cation intermediates. The oxidation potential of the monomer decrease as the chain length of the substituent increased again implying the greater stability of the intermediates. It has been noted that with 3-methylthiophene, colouration of the monomer solution occurs in the anodic region during the polymerization process due to the presence of low molecular weight oligomers which are soluble or due to higher concentration of more long lived radicals [81].

With large β- substituents the polymerization is less successful, an evidence of large quantities of short– chain oligomers being formed. In plotting peak potential of the monomer versus that of the peak potential of the polymer a linear relationship has been found. It indicates that the substituents affect both the monomer and the polymer in similar ways, although to a greater extent for the later [137]. The use of lower current densities during polymerization results in higher quality film than when high current densities are employed. The use of oxygen and water free conditions gives films with higher conductivities. Kobel *et al* [138] found that the use of propylene carbonate as a solvent during electrochemical oxidation of 3-methylthiophene gives highest quality film of poly(3-methylthiophene). The

50

polymerisation of 3-methylthiophene has also been achieved in aqueous media, although significant quantities of the solvent was incorporated into the polymer during the polymerization process.

Polythiophene and derivatives were commonly prepared by the direct anodic oxidation of the corresponding monomers in conventional organic solvents. The problems related to structure and properties can be modified by using three main strategies, i.e. derivation of the monomer structure before polymerization, synthesis of copolymers and association of the conducting polymer with other materials [139]. Many key properties like oxidation potential of the monomer and the polymer, solubility, bandgap, morphology, and miscibility with other substances depend on the type and position of the side chains in the polymer structure. Introducing electron donating alkoxy substituents on the conjugated polymers' backbone produces a remarkable influence on its electrical and optical properties. Substituted polythiophenes with improved properties has been employed as active electrode in several electrochemical/electronic devices. 3,4–ethylenedioxythiophene (EDOT) is commercially available monomer, and since 1990, after its synthesis poly(3,4-ethylenedioxy thiophene), PEDOT, occupies a prominent position among the conducting polymers owing among other things, to the multiple well – established technological applications of its various conducting forms [31, 34-37]. PEDOT displays many interesting properties including low half – wave potential and bandgap, high environmental stability, high conductivity, and excellent transparency in its doped state. In addition, this polymer exhibits outstanding, electrochemical stability upon cycling, as well as superior air, thermal and electrical properties compared to other polythiophenes. It is crucial to organic electrochromic materials such as rapid switching and lower oxidation states [9].

3.3 Copolymerization

Copolymerization by introducing new groups alters the existing structure and bandgap, leading to absorption at different wavelengths and colours, which offers a means of controlling the electrochromic properties of conjugated polymers [9].

Synthesizing copolymers has been used to have the desired properties of polymers. Two monomers could be polymerized into a conducting polymer having different properties than that of their corresponding homopolymers. Synthesis of copolymers is mainly performed with EDOT due to its desired properties. In this way, the resultant copolymer could reveal better electrochemical and optical properties [24, 40]. 1- (Phenyl) 2-, 5-di(2 – thienyl)-1H– pyrrole copolymer with 3,4–ethylenedioxythiophene(EDTO), this copolymer shows an electronic bandgap 1.9 eV at 480 nm with red in the full reduced form and blue colour in the fully oxidized form. Besides, copolymerization of derivative of polypyrrole, 4-((1H)-pyrrole-1-yl)phenyl-4-(1H-pyrrole-1-yl)butanoate with EDOT results well defined cyclic voltammograms and spectroelectrochemistry result showed multicolour electrochromism and a fast switching of 0.8 s at 367 nm and optical contrast of 17% at 1100 nm . Electrochemical homopolymerization of 3–chlorothiophene (CIT) and copolymerization of with 3 – methylthiophene (MeT) was synthesized via potentiodynamic and galvanostatic methods by using air and moisture stable ionic liquid 1-buthyl-3-methylimidazolium hexafluorophosphate (bmimpf$_6$) as the growth medium and supporting electrolyte [40]. Compared with PCIT (580 times), the copolymer CIT-co-MeT) exhibited a long – term switching stability up to 23000 double switches. The result implied that copolymerization is a valuable approach to achieve the desired electrochromic properties.

Furthermore, copolymerization of 1,4-dithiophene-3-yl)benzene and pyrene shows various colour and improve switching time (1.5 s at 750 nm, 1.0 s at 11000nm). A new polythiophene

derivative, poly(2,3-bis(4–tert-butylphenyl)-5,8-bis(4–hexylthiophen-2-yl) quinoxaline synthesized electrochemically in convectional media, revealed three distinctive colours upon doping which indicated that the polymer is multichromic [9]. Copolymer of 5-cyanoindol and 3,4–ethylenedioxythiophene synthesized electrochemically by direct oxidation of the monomer mixtures in traditional organic solvents, has shown good redox activity, good thermal stability and high conductivity and own the properties of poly(5-cyanoindol) and poly(3,4– ethylenedioxythiophene). The fluorescent spectra indicate that the copolymer is a good blue light emitter [24]. There is increased interest in the synthesis of rapid switching electrochromic polymers. New polythiophene derivatives have been synthesized in convectional media electrochemically that show rapid switching ability and reported by many groups. The development of electrochromic devices that show rapid switching ability is still required and not fully investigated.

3.4 Ionic liquids as medium of electropolymerization of conjugated polymers

The properties of conducting polymers are highly influenced by the nature of the dopants and the electrolytes used in the electrochemical preparation and cycling of the polymer [41]. Room temperature ionic liquids (RTILs) have attracted increasing interest during the last decade because of their unique chemical and physical properties [12, 15, 30-32, 42, 140]. Ionic liquids are salts that are fluids over a wide temperature, including room temperature, with moderate to low intrinsic electrical conductivities, higher viscosities about 1-3 orders of magnitude higher than those of aqueous and organic electrolytes at room temperature. RTILs generally exhibit enlarged electrochemical windows (4.5–7 V) a highly desirable property for applying RTILs as electrolytes or solvents in electrochemical experiments. Because of these important properties, RTILs are becoming a promising medium for a variety of electrochemical synthesis and application [12, 30-32]. For example electrochemical synthesis

of polypyrrole [30], poly(3-(4-fluorophenyl)thiophene [42], poly(3,4-ethylenedioxythiophene), polyparaphenylene [30], poly(3-chlorothiophene) [40] and polythiophene in RTILs, the formation of electroactive and stable polymer similar to those obtained in conventional organic media has been synthesized. The disadvantage of using RTILs as a medium for electropolymerization is that they are relatively expensive and require a slightly higher concentration of monomers (10^{-1} to 5×10^{-1} mol/L) than conventional organic concentrations (10^{-2} to 10^{-1} mol/L) [27, 30].

Various experimental works have been conducted to understand the influence of the nature of the RTILs towards, the preparation, the morphology, and the electrochemical properties of the polymers. The electropolymerization of pyrrole was found to be more efficient in 1-ethyl-3-methylimidazolium triflate than in 1-buthyl-3-methylimidazoliumtetrafloroborate and 1-ethyl-3-methylimidazolium hexaflurophosphate with a formation of smoother and more highly doped polymer compare to those of the latter ionic liquids [12]. Since anions are dopants in electropolymerization, the investigator ascribed the increased growth of the polypyrrole to the higher viscosity of the triflate. This shows a considerable influence of the anion. Thiophene, bithiophene, and tetrathiophene have been polymerized in imidazolium and pyrrolidinium based bis(trifluromethylsulfonyl)imide in room temperature ionic liquids [31]. It was demonstrated that the use of the pyrrolidium salt led to the formation of polythiophene film with smoother and denser but with a lower electroactive surface than those obtained from the imidazolium salts [12, 15, 42]. Electropolymerization of EDOT in N, N - butylmethylpyrrolidium bis(trifloromethanesulfonyl)imide proceeds more slowly than in (N–ethyl-N-methylimidazolium bis (trifluromethanesulfonyl)imide [42]. This phenomenon is attributed to the higher viscosity and lower conductivity of N, N-butylmethylpyrrolidium bis(trifluoromethylsulfonyl)imide compared to N–ethyl-N-methylimidazolium bis (trifluoromethylsulfonyl)imide. Similar difference was also observed in the electrochemical

activities of the polymer, signifying the cation played a useful role in the charging process of PEDOT films. Thus the nature of both anion and cation of the RTILs strongly control the doping processes in the conducting polymer, determining the morphology and the properties of the polymers [12, 42].

Many research groups have been investigated electrochemical polymerizations of conducting polymers in RTILs. Electrochemical synthesis of polypyrrole in 1-buthyl-3-methylimidazolium hexaflurophosphate (bmimpf$_6$) on iron and platinum electrode and in 1-ethyl-3-methylimidazoliom triflate, 1-ethyl-3-methylimidazoliom tetrafluoroborate (emimbf$_4$), and 1-ethyl-3-methylimidazolium hexafluorophosphate (emimpf$_6$) on Pt resulted in the formation of polymer film resembled to those obtained in conventional media. Sekiguchi *et al* [42] also electropolymerized pyrrole in 1-ethyl-3-methylimidazolium trifluoromethanesulfate (emicf$_3$so$_3$). The morphological structure of polypyrrole film formed on the anode and the polymerization rate, electrochemical capacity and electron conductivity were significantly improved. It was also investigated that emicf$_3$so$_3$ as recyclable medium. 90 % of emicf$_3$so$_3$ after polymerization was easily recovered by a simple removal (extraction) of the remaining pyrrole monomer from the ionic liquid with chloroform and then reused without significant loss of reactivity for the polymerization.

Electrosynthesis of polyphenylene in 1–hexyl-3-methylimidazolium tris(pentafluoroethyl)trifluorophosphate (hmimfap) on Pt, polythiophene, poly(3-chlorothiophene) [12]), Poly (3-(4-fluorophenyl)thiophene in pure 1-ethyl-2,3-dimethyimidazolium bis (trifluoromethyl)sulfonyl)imide (edmimtnf$_2$), and 1,3-diethyl-3-methyimidazolium bis(trifluoromethyl)sulfonyl)imide (demimtnf$_2$) at Pt [35] have been reported. It was found that these polymers can be grown and cycled in pure ionic liquids. For example poly (3-(4-fluorophenyl)thiophene electrochemical behaviour reported was very

similar to that prepared from common nonaqueous media such as tetraethylammonium salt in acetonitrile. However, it was characterized by slower redox kinetic processes. The polymer is less stable upon repeated potential cycling. This difference was attributed to gradual deswelling of the polymer in ionic liquids.

Poly(3,4-etheylenedioxythiophene) in emimtnf$_2$ and eeimtnf$_2$ ionic liquids [38, 141] poly(paraphenylene) in 1–hexyl-3-methylimidazolium tris(pentafluroethyl)triphosphate, poly(3-chlorothiophene) in bmimpf$_6$ and polythiophene in emimtnf$_2$ on pt, benzene in hmimfap to give polyphenylene have been also reported. All of these works found the formation of electroactive and stable polymer similar to those obtained in conventional organic media. It has been indicated that electrosynthesized PEDOT in bmimbf$_4$ or bmimpf$_6$ showed the same behaviour as PEDOT film prepared in common organic media [12, 36]. Uv– visible analysis showed that the average conjugation length was nearly the same for both media.

There was some investigations that strengths the idea that ionic liquids as powerful media for the preparation of conducting polymers. Electropolymerization of pyrrole in neat emimotf and emimotf diluted in CH$_3$CN or H$_2$O (0.1 M), indicated that the electropolymerization is more efficient in the neat ionic liquid. The electropolymerization of benzene performed more efficiently with milder conditions in RTILs than in commonly used concentrated sulphuric acid or liquid sulpherdioxide. It was reported employing ionic liquids as a media would enable further studies on the nanoscale with in situ scanning tunnelling microscope that would totally prohibited in aggressive media like 18 M sulphuric acid or liquid SO$_2$.

Research has been undertaken to understand further the doping (insertion of anion)/undoping (exclusion of anions). The cyclic voltammetry and the electrochemical impedance spectroscopy of PEDOT film was studied in emimtnf$_2$[141-142]. The polymer grown in

acetonitrile medium, the cyclic voltammograms displayed two distinct anodic peaks indicating at least two redox reaction mechanisms. The result indicated that for one of these mechanisms emim cation was the exchanged species (exclusion) during the oxidation, and at the same time bis(trifluoromethylsulfonyl)imide anion could be viewed as immobile ions trapped in the polymer film. Randriamahazaka *et al* [37] studied the electrochemical responses of PEDOT formed in acetonitrile then cycled in emimtnf$_2$ and PEDOT formed and cycled in emimtnf$_2$ by cyclic voltammetry and potential step experiments. The outcome showed PEDOT films grown in emimtnf$_2$ exhibited only one anodic and cathodic peak. PEDOT grown in acetonitrile showed different shape of cyclic voltammogram; two anodic and two cathodic peaks. The authors explained these patterns by two types of coexisting zones: a compact layer consisting of highly conjugated and rigid chains whose oxidation was located to the lowest potential and a more open zone with oxidation potential at a more positive value.

PEDOT film electrosynthesized in an extremely hydrophobic ionic liquid, 1-ethyl-3-methylimidazolium bis(perfluoroethylsulfonyl)imide without the use of any additional dopant. The incorporation of the imidazolium cation along with the bis(tetrafluoroethylsulfonyl)imide anion in the polymer film matrix, affirmed by X – ray photoelectron spectroscopy and energy dispersive X–rays (EDX) studies provide the information of film with a fibrillar structure. There is small number of reports on hydrophobic medium facilitates deposition of uniform well–adherent thick film unlike highly polar media, which interact weakly with EDOT and are known to cause the polymers flaking off the substrate following growth but all are limited to different ionic liquids. Earlier results confirm the need to devote more research on the elucidation of the structure–property relations in PEDOT grown in RTILs. The relaxation kinetics PEDOT electrodeposited on platinum electrode surface was studied in a room temperature ionic liquid, emimtnf$_2$, by

means of large amplitude potential step experiments. The influence of the applied potential and the film thickness were analyzed. These kinetic constants seemed independent to the applied potential. It was showed that the kinetic constant for the fast process dependent upon the thickness of the polymer film. However, the time constant for the slow process was virtually independent of the film thickness. It was also reported that the kinetics for the oxidation was faster than that of reduction.

Schneider *et al* [30] studied the electropolymerization of benzene in 1–hexyl-3-methylimidazolium tris(pentafluoroethyl)trifluorophosphate with electrochemical quartz – crystal microbalance to deposit poly(para)phenylene. It was found that in the polymer, every third to fourth benzene ring carried a positive charge in the oxidized state. This charge was compensated by the incorporation of anions from the ionic liquid. With increasing scan rate, cation exchange became prevalent over anion exchange, indicating a faster kinetics for the cation exclusion. The PEDOT synthesized and cycled in ionic liquids with bulky organic anion (1- buthyl-3- methylimidazolium octylsulphate) [140] as electrolyte on glassy carbon showed an anionic potentiometric response in KCl(aq) solution, indicating that the dopant anions (1-butyl-3-methylimidazolium octylsulphate) are mobile inside the polymer and are able to exchanged by the chloride ions at the solution- polymer interface. In contrast, only cationic exchanges were observed in the ionic liquids. These works support the importance of the choice of the cation and conclude that oxidation kinetics (exclusion of cations) is facilitated over that of reduction (insertion of cation) in the RTILs.

Improved electrochemical properties of the polymers prepared in the RTILs or when prepared in conventional electrolytes then cycled in RTILs has been reported by many research groups. For example conductivities, electrochemical capacity, electrochromic displays properties enhanced. Lu *et a*l [36] studied commercialization of conducting polymers electrochemical

device by employing the room temperature ionic bmimbf$_4$, in the fabrication of a conducting polymer based electrochromic numeric display. They reported greatly enhanced electrochemical stability with negligible polymer degradation (up to 1 million cycles) and fast switching speeds (100 ms) under ambient conditions without sacrificing the electrochemical performance of the device. Murray *et al* [32] used an ionic liquid as a solvent and enable the successful preparation of films composed of polyterthiophene doped with an anionic dye. Photoelectrochemical cells constructed using these films showed significant improvements in photovoltaic properties when the films were first reduced in the presence of a cationic dye. Absorption spectroscopic studies provided evidence for retention of both dyes in the films, while photocurrent action spectra showed that the increase in photovoltaic performance was due largely to improvements in light harvesting by the polymer. These findings amplified the use of RTILs as electrolyte in electrochemical devices involving conducting polymers. On the other hand it was reported that a clear decrease of the electroactive of poly(3-(4-fluorophenyl)thiophene upon repetitive cycling. This was explained because of gradual deswelling of the polymer in the RTILs.

However, there are major barriers to commercialization of ionic liquid processes. Firstly is their higher viscosity of Ils is much larger than convectional organic solvents as a result their higher resistance hence ohmic potential drop is a major problem. The secondly problem is biodegradability, commonly used Ils such as imidazolium and pyridinium are nonbiodegradable. Therefore, they are toxic especially for aquatic life. To improve their biodegradability, functionalising of ionic liquid has become a good method. Ester functionalized Ils are biodegradable than nonfunctionalized once. For example, pyridinium groups are relatively more biodegradable. Increasing alkyl chains increase biodegradability. On the other hand, the effect of the anion of the ILs on biodegradability is insignificant [143]. The third limitation is toxicity of Ils. The cation is reported to play a major role in the level of

toxicity of ILs. It was also indicated by Wells *et al* cited in [143] showed toxicity increased as the alkyl chain length on the imidazolium cation was increased for an IL containing chloride inions. Ecotoxicity of hydrophobic ionic liquids becomes higher than hydrophilic.

3.5 Electrochromic study of polythiophene and its derivatives in ionic liquids

Beanjuge and Reynolds reviewed electrochromism of organic and fully π- conjugated polymers [144] published in a year from 2006 to 2008. More detail is found in literature. Utilization of polythiophenes (PTs) for electrochromic devices was first reported in 1983 by Garnier and Gazard [145-146] and Druy and Seymour [147]. Electrochemically polymerized polythiophene (PT) (**1**) its electrochromic properties was investigated, showing a colour change red to blue upon p-doping corresponding to $\pi \rightarrow \pi^*$ transition depletion and simultaneous appearance of polaron and bipolaron charge carriers in the infrared region tailing into the red region. Electrochemically n-doped PT also undergo red to black green colour change as described later by Aizawa *et al* [148]. The bandgap of PT generally falls into 2.0–2.2 eV range [144], depending on molecular weight of PT. Larger amount of polybithiophene [149] TiO_2 deposited on TiO_2 layer on fluorine doped tin oxide (FTO) coated glass (at a scale of TiO_2 nanocrystals) at lower oxidation potential compare to PT (based on the idea that oligomers oxidize at a low potential) the polymer film switched its colour red in the neural state to light blue on oxidation and dark blue on reduction (mainly due to metal oxide change its oxidation state).

Polythiophenes has been an attractive electrochromic material for several reasons. Firstly, it's easy of functionalization and has been reported a number of substituted PTs chemically and electrochemically synthesized PT in which their optical properties can be controlled by structural modification of polythiophene. Either electron donating or electron withdrawing substituents induced backbone conformation found in the literature to fine tune the coloured

neutral state. Electrochromism of polythiophene, and analogous synthesized in organic media have been discussed in detail in reference[144].

Poly(3-octylthiophene) (**3**) film electrochemically synthesized in bmimpf$_6$ reversible changes colour between orange red in the neutral to blue in the oxidized state in bmimpf$_6$/CH$_3$CN. Pang *et al* [150] also electrochemically synthesized poly(3-methylthiophene) (**2**) in bmimpf$_6$ changes colour from orange red to blue as it switches between its neutral and oxidized state respectively. Polymer **3** in bmimpf$_6$ changed its colour from orange red to pale blue. Polymers **2**, **3** and **4** exhibited switching time ranging from 1 to 2 s at considerable film thickness whereas their colouration efficiency varies in the range 230 to 250 cm^2/C. A longer term switching stabilities reported in bmimpf$_6$/CH$_3$CN only few transmittances lost after 1000 cycles.

Interestingly the copolymerization of 3-chlorosubstitute thiophene (**5**) with 3-methylthiophene in bmimpf$_6$ [40] resulted high optical contrast, bandgap 1.74 eV and switched its colour from bright red and greenish blue in bmimpf$_6$ compared with the poly(3-chlorothiophene) deep red and deep blue in fully reduced and oxidized state. Furthermore, the copolymer exhibited fast switching rate (0.9 s) and longer stability up to 2300 cycles than the homopolymer (580 cycles) at 2.4 s switching speed. The homopolymer deposited on TiO$_2$ based electrochemical device (ECD) shows less than 2% contrast loss over 1000 cycles. It showed poor redox reversibility onto ITO and lost its switching ability after 580 cycles.

Incorporation of substituents into thiophene ring tunes the colour change as a result of conformational changes induced by the substituents. Besides this, colour tuning effect, substituents at 3 and 4 – position of thiophene prevents the α, β and β, β, cross coupling that can happen during electropolymerization which reduce the quality of the polymer film deposited on the electrode surface (e.g. conductivity and optical properties [151]. Electron

denoting substituents to have also been shown to lower oxidation potential of thiophene monomers, which s an advantage to prevent polymer over oxidation during their synthesis [151]. Electosynthesis of thiophene substituted with methoxy electron donating group at 3-position in bmimpf$_6$ in water ionic liquid microimulsion, poly(3-methoxythiophene) (**6**) film on ITO in acetonitrile as a solvent reversibly switched its colour between orange and blue in the dedoped and neutral state. Recently Song *et a*l [152] electrochemically synthesized in the same polymer **6** in nana scale in bmimbf$_4$ ionic liquid revealed red colour in the neutral and blue in the oxidized form with a moderate optical contrast and switching speed (33.1%, 2.4 s).

Table 3.4: Representative polythiophenes electrochromism synthesized in ILs.

Polymer	λ_{max}(nm)	E_g(eV)	neutral	oxidized	reference
1	480	2.0 - 2.2	red	blue	[144]
2	500	1.97	orange–red	blue	[144]
3	430 – 440	-	red	blue – purple	[150]
4	460	2.00	orange–red	pale blue	[144]
5	520	1.74	deep red	deep blue	
6	-	-	red	blue	
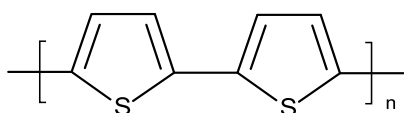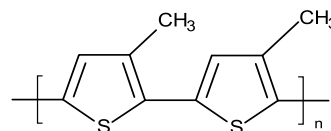
Polythiophene (**1**)   Poly(3-methylthiophene) (**2**)
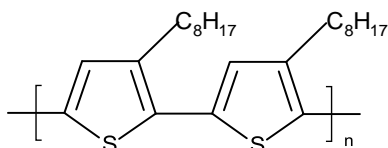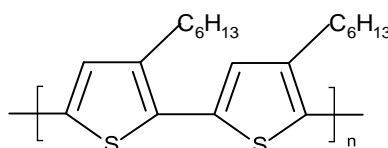
Poly(3-octylthiophene) (**3**)   Poly(3-hexylthiophene) (**4**)
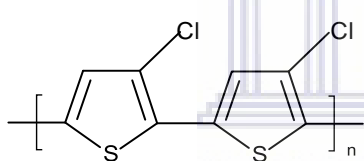
Poly(3-chlorothiophene) (**5**)   Poly(3-methoxythiophene) (**6**)
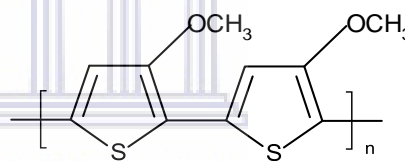
3.6 Donor-acceptor systems

Havinga *et al* [54] in 1993 introduced the 'donor – acceptor' concept for tuning the bandgap (as narrow as 0.5 eV) between highest occupied molecular orbital (HOMO) and lowest unoccupied molecular orbital (LUMO) based on alternating electron rich and poor moieties in conjugated polymers. The combination of electron rich and electron deficient moieties has been used effectively to lower the bandgap of conjugated polymers. Electron rich units such as 2,7-carbazole [55], indole[3,2,b]carbazole, benzo[1,2-b:4,5-b']dithiophene, cyclopenta[2,1-b:3,4-b']dithiophene [153], dithieno[3,2-b:2',3'-d]silole Fig. 1.3 and quite a

few electron deficient units cyanovinylene [154], quinoxaline derivatives [155], benzotriazole [156], pyridine [157], 2,1,3-benzothiadiazole [158], pyridopyrazine [159], diketopyrrolo[3,4-c]-pyrrol-1,4-dione, ester or ketone substituted thieno[3,4-b]thiophene and thieno[3,4-c]pyrrol-4,6-dione (Fig. 1.3) has been mostly used for the synthesis of donor – acceptor polymers [55]. A new strong acceptor moieties dibenzothiophene-S,S-dioxide and its derivatives because of the presence of sulphonyl group in its structure has been recently used as an acceptor unit in the synthesis of donor-acceptor polymers [66]. Although the discovery of this theory has contributed for the development of electrochemically driven device applications such as field –effect transistors, light- emitting diodes, and photovoltaic's, it is only recently has the use donor – acceptor based polymers attracted the attention of researchers with an interest in the investigation of their electrochromic properties. For example, Koyuncu *et al* synthesized a donor - acceptor electrochromic material containing carbazole and 1,8-naphtalimide as a sub unit with a ban gap of 2.44 eV with multi-electrochromic behaviour [15] and number of other green polymers has been reported by many research groups [45, 62-64, 153, 160-161].

Several studies on electrochromic polymers focused on their multicolour nature change upon reduction and oxidation. For example poly(3-alkylthiophenes) switching red to blue, polypyrrole(switching yellow to black) and for many derivatives of polythiophene essentially every colour of the spectrum has been attained [12]. Recently, using donor acceptor system the magnitude of the bandgap for π - π transition of conjugated polymer can be tuned from the ultraviolet, through the entire visible region of the spectrum and well into the near infrared. The lack of green polymers that transmit or reflect green light because of the requirement of a simultaneous two band absorption (red and blue) part of the spectrum has been achieved [61-65, 160-161]. In the literature it is reported that [62] changing the acceptor subunit from benzothiadiazole to benzoselenadiazol in bis(proplynedioxythiophene) (Fig.3.3)

gave change in colour for turquoise to saturated green for the former and the later respectively as the acceptor changes from intermediate benzothiadiazole to the stronger acceptor benzoselenadiazole in the polymer. The polymer with benzoselediazole subunit showed 42% of optical contrast at 732 nm and fast switching speed by shifting the absorption band to red compare with that of benzothiadiazole
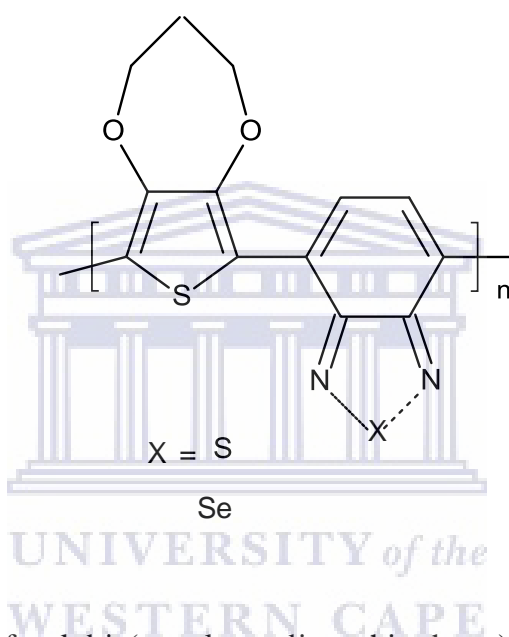
Figure 3.3: Structure of polybis(proplyenedioxythiophene).

The application of organic polymers in non – emissive devices such as smart windows, e-papers, low cost displays and synthesis of transmissive polymers in the oxidized state were a challenge. Hellstrom *et a*l [162] synthesized a high molecular weight poly[2,3-bis-(3-octyloxyphenyl]quinoxaline-5,8-diyl-thiophene-2,5-diyl (Fig. 3.4) soluble donor –acceptor polymer switching from an intense blue colour to transmissive yellow-brown when oxidized with a high contrast ratio of 50% at 623 nm. Besides, the switching time of the polymer was improved (0.5 s) by introducing ethylhexyloxy as side chains.
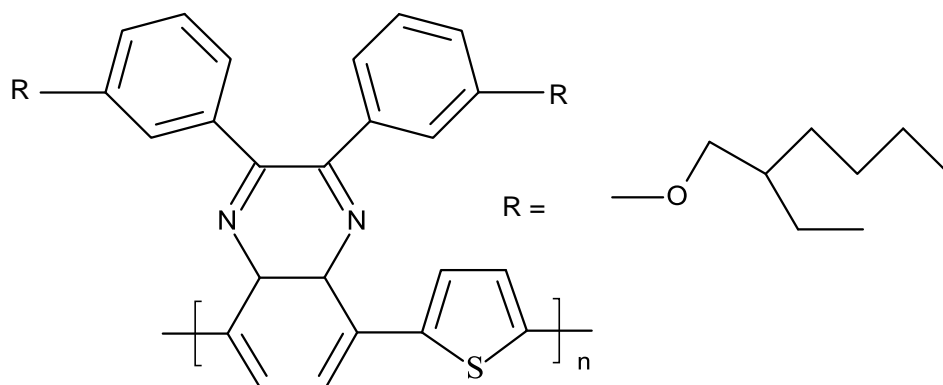
Figure 3.4: Poly[2,3-bis-(3-octyloxyphenyl]quinoxaline-5,8-diyl-thiophene-2,5-diyl].

Spectroelectrochemistry data from the literature indicates that a number of organic conjugated polymers were investigated that absorb/reflect blue and red in their neutral states. However, conjugated polymers synthesis and characterization in an attempt to make saturated green polymers chemically or electrochemically have meet limited success due to its requirement that at least two absorption bands in the neutral state of the material. Sonmez *et al* [45] reported the first electrochemically prepared, neutral, green colour 2,3-di(thien-3-yl)-5,7-di(thien-2-yl)thieno[3,4-b]pyrazine polymer. In recent works an experimental result strongly supporting the utility of the donor – acceptor theory in the design of neutral green electronic polymers reported. For example, 4,7-di(2, 3-dihydro-thieno[3,4-b][1,4]dioxin-5-y)benzo[1,2,5]thiadiazole], was electropolymerized and reinvestigated as a possible candidate for electrochromic applications. Because it was green in the neutral state and switched rapidly and reversibly to a transmissive light blue oxidized state. In another work, Wu *et a*l. [153] synthesized cyclopentadithiophene–benzothiadiazole polymer using cyclopentadithiopene as a donor and 2,1,3-benzothiadiazole. This polymer was green in the neutral and transmissive in oxidized state and gave maximum optical contrast of 38%. Replacing benzothiadiazole

subunit by a stronger acceptor benzoselenadiazole changed electronic structure and electrochromic properties of the resulting polymers [62].

As indicated in the previous sections the optical as well as the electrochemical properties of conjugated organic polymers can be altered by the nature of the substituens to the aromatic ring and by copolymerization of two monomers which have close oxidation potential. It is also reported that bandgap of π-conjugated polymers have been controlled by several parameters such as manipulation of bond length alteration, inter ring torsional angle, resonance energy, inter chain effects and substitution effects [74]. The discovery of poly(isothianaphthene) highly conductive (50 S/cm) and low bandgap polymer (E_g = 1.1 eV) has triggered researchers the synthesis of low bandgap polymers by structural modification [163-164] since the bandgap is one of the most important factor of controlling physical properties the materials. A number of methods have been used for the synthesis of narrow bandgap systems. One method is based on the relaxation of bond length alternation that can be achieved by the appropriate arrangements of aromatic and quinoid units at the back bone of the polymer [165-166]. The second method which has become a common strategy recently is based on intra –chain charge transfer [73] through the alteration of strong electron donating and accepting moieties in the back bond. The bandgap of this material is effectively minimized due to the intrachain charge transfer resulting from the interaction of HOMO of the donor and LUMO of the acceptor segments [75]. Besides, the steric interaction between adjacent units related to coplanarity should be taken into account in order to maximize the effective π-conjugation length along the polymer backbone[167]

3.7 Electrochromism of poly(4,7-dithien-2-yl-2,1,3-benzothiadiazole) P(DTBT)

As far as our knowledge is concerned poly(4,7-dithien-2-yl-2,1,3-benzothiadiazole) P(DTBT) fist synthesized by Yamashita and co-workers [168]. Since then, P(DTBT) have received considerable attention because these materials have a bandgap of E_g = 1.1–1.2 eV when polymerized electrochemically [73-74, 169-170]. Besides this interesting property, P(DTBT) thin polymer film possesses high stability during both p-and n-doping [171].

P(DTBT) is a potential material for light emitting diodes application. Niu *et al* [172] synthesized copolymer of P(DTBT) with 2,7-(9,9-dioctylfluorene that emit high efficient white light emitting diodes. The material was also used for photovoltaic cells [173-176]. For instance, DTBT based conjugated polymer with cyno group in vinylene unit [177] synthesized for photovoltaic applications. Besides these applications the cauliflower–like structure bearing more homogeneity of P(DTBT) polymer film makes it a promising material for biosensor application [171, 178].

Electrochemically polymerized P(DTBT) is insoluble in common organic solvents like acetonitrile and dichloromethane [168]. This was a limitation for the practical application of P(DTBT) and has been improved by synthesizing more soluble alkyl substituted derivatives of 4, 7-di-2-thienyl-2,1,3-benzothiadiazole [179]. Moreover, soluble and processable low bandgap derivatives of DTBT was synthesized by Janssen and co-workers [180]. They synthesized three new alkyl substituted 4, 7-di-2-thienyl-2,1,3-benzothiadiazole monomers and their corresponding electrochemically polymerized polymers were soluble in common organic solvents. The optical properties of both the monomers and their polymers were studied and compared with the unsubstituted analogues.

As stated above, P(DTBT) and its derivatives are potential material for photovoltaic applications. The DTBT monomer was copolymerized with many kind of electron rich segments such as the fluorene [181], silafluorene [182], carbazole [76], dithienosilole [183-185], heteroarylenevinylenes [186], phenylenevinylene [187], cyclopenta[2,1-b:3,4-b]dithiophene [188] and di(p-toly)phenylamine side group (DTBT added to improve the hole transport ability and boarder the absorption spectrum) [189] to serve as a potential donor component for high efficient bulk-hetero junction type solar cell applications. DTBT as a whole has been used extensively as electron deficient unit for the generation of efficient intra-molecular charge transfer moiety to reduce the bandgap. Recently, DTBT copolymerized with cyno(-CN) substituted vinylene, as the electron deficient moiety coupled with carbazole and fullorene [177] by Knoevenagle condition to provide poly(bis -2,7-((Z)-1-cyano-2,-(7-(2-thienyl)-2,1,3-benzothiadiazole-4-yl)-2-thienyl-alt-9-(1-octylnonyl)-9H-carbazol-2-yl-2-butenenitrile (E_g=1.74 eV) a lower bandgap, advantageous for better coverage of longer wavelength region compare with poly(bis-2,7-((Z)-1-cyano-2-(5-7(-(2-thienyl)-2,1,3-benzothiadiazole -4-yl)-2-thienyl)-ethenyl)-alt-9,9-dihexy-9H-fluoren-2-yl) (E_g =1.80 eV). Bulk hetero junction solar cell based on the blends of the former polymer with [6,6]-phenyl-C_{61}-butyric acid methyl ester gave power conversion efficiencies of 0.76%.

Thin films of P(DTBT) electrochemically polymerized potentiostatically at 1.15 V vs Ag/Ag$^+$ in 0.01 M of DTBT in 0.1 M Bu$_4$NClO$_4$ /CH$_3$CN on ITO coated glass electrode by Atwani *et al* [171] showed a bandgap of 1.5 eV. Switching ability and kinetics of the polymer film studied by double potential step (potential steps between 0.1 and 1.5 V) 10 s at each step in n-Bu$_4$NClO$_4$/propylene carbonate experiment simultaneously monitoring its transmittance change. High optical contrast (ΔT% = 65 film thickness not indicated) at 1100 nm was found which ensures the polymer is suitable for near infrared electrochromic applications. P(DTBT) film deposited on ITO electrode was homogeneous and stable (cycled 1000 times

without significant change of anodic and cathodic charges) at 200 mV/s in monomer free 0.1 M Bu$_4$NClO$_4$ /CH$_3$CN between -0.6 to 0.90 V makes P(DTBT) is a potential material for electrochromic applications (for displays or other colour changing surfaces).

3.8 Conclusion and future trends

In the literature survey it can be concluded that the optical and electrochemical properties of conjugated conducting polymers are highly dependent on the growth medium. Ionic liquids serves as one in two as electrolyte and solvent. Their influence on electrochromic, optical, morphological, electrochemical properties and on the stability of the polymers has been shown by different researchers. Both the nature of the cation and anion plays a role in determining the properties of polythiophene derivatives and other conducting polymers.

Another important point that modifies bandgap and tuned the colour of conjugated polymers is copolymerization. By copolymerizing two monomers having nearly similar oxidation potential, multicolour and narrow bandgap composites can be produced. Furthermore, narrower bandgap polymers can also be prepared using donor- acceptor monomers. The intramolecular charge transfer from the HOMO of the donor to the LUMO of the acceptor reduced the bandgap. As a result, using this strategy a green to black polymer can be electrochemically synthesized which has been a challenge in early times.

Poly(4,7-dithien-2-yl-2,1,3-benzothiadiazole) which contains thiophene as a donor and benzothiadiazole as an acceptor and its derivatives is an interesting material because of their various potential application such as in electrochromic devices, solar cells and sensors. DTBT can be easily derivatized and copolymerized with other electron deficient units. However, its electrochromic properties have not been exhaustibly studied and to the best of our knowledge no report found in ionic liquids.

The future trend seems electrosynthesis of conducting polymers in ionic liquids as a medium or as an electrolyte for the various applications in different devices because of their stability in water and oxygen. In addition to this, the physicochemical properties of ionic liquids can be controlled by combining different organic cations and anions during their preparation. Recently, new biodegradable ionic liquids have been prepared which farther motivates researchers to use them as a novel medium for electrosynthesis and for various applications in future research.

CHAPTER 4

EXPERIMENTAL

In this section, the principles of analytical methods employed in this study are briefly described. Materials and instruments used for the synthesis and characterization of 4,7-dithien-2-yl-2,1,3-benzothiadiazole (DTBT) are presented. General procedures for the electrochemical synthesis, electrochemical and optical characterization of poly(3-methoxythiophene) and its copolymer with poly(3,4-ethylenedioxythiophene) are clearly indicated. Electrochemical study of DTBT monomer, methods used in the investigation of poly(4,7-dithen-2-yl-2,1,3-benzothiadiazole) and its copolymer with 3-methoxythiophene in various media are outlined in this part of the thesis.

4.1 Analytical methods

4.1.1 Cyclic voltammetry (CV)

Cyclic voltammetry (CV) is a very versatile electrochemical technique and have been extended in every aspects of chemistry, for instance for the characterization of electroactive species in modern analytical chemistry, electrochemistry, and biochemistry [190]. Cyclic voltammetry provided information about the electroactive species by measuring the faradic current as a function of applied potential. The current response is measured by applying a potential ramp starting from an initial potential to a first switching potential and at this potential the direction of the potential is reversed and the same potential range is scanned in the opposite direction (hence the term "cyclic").This change of the direction of the potential can happen multiple times. On the process, the electro active species formed by oxidation or reduction depending on the direction can be reduced or oxidized on the reverse scan. Cyclic

voltammetry is usually performed in three electrode arrangement (the working usually Pt, Au and GC electrode), counter or auxiliary electrode and reference electrode (in aqueous solution Ag/AgCl and SCE). The potential is applied to the working electrode with respect to a reference electrode and the current is measured between the counter and working electrode [191-192]. The current measured between the working electrode and the counter electrode is plotted against the applied potential relative to the reference electrode to give the cyclic voltammogram. Typical cyclic voltammograms of a reversible processes is shown in (Fig. 4.1)
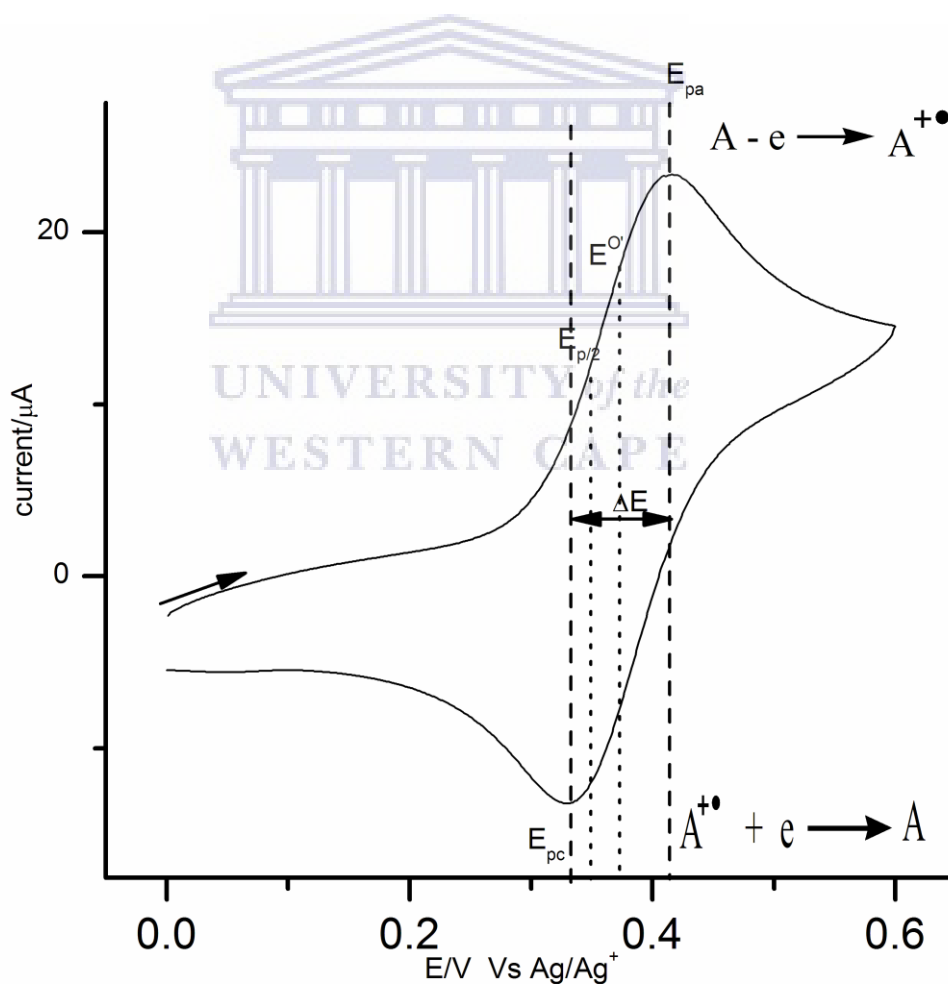
Figure 4.1: Typical cyclic voltammograms of a reversible process.

The following equations can be used for a reversible process to evaluate the electrochemical parameters' from cyclic voltammetry.

$$i_p = 0.4463FA \left[\frac{F}{RT} \right]^{1/2} n^{3/2} D^{1/2} C \, v^{1/2}$$

(4.1)

Randles –Sevcik equation

$$E^{o\prime} = \frac{E_{p,c} + E_{p,a}}{2}$$

(4.2)

$$\Delta E_p = \frac{58}{n} \, mV$$

(4.3)

$$E_{p/2} = E_{\frac{1}{2}} + 28 \, mV \, at \, 25 \, °C$$

(4.4)

Where i_p is peak current/A; F is Faraday constant (96, 487 mol C/mol); D is diffusion coefficient/cm/s of the electroactive species; A is the area of the electrode/cm^2; v is the sweep rate/V/s; R is the general gas constant (8.413 J/mol K) and T is temperature (25 °C); $E^{o\prime}$ is the formal potential which is the average value of the peak potentials; E_{pa} and E_{pc} are anodic and cathodic peak potential/V; $E_{p/2}$ is the half peak potential at half of the peak current; n is number of electrons involved in the reaction; ΔE_p is the peak potential difference (approximately 58 mV for one electron reversible process but for quasi reversible and irreversible processes its magnitude is large) and $E_{1/2}$ is the half wave potential.

Nernst Equation

$$E = E^o + \frac{RT}{nF} lnQ$$

(4.5)

The electrode kinetics is described by Butler-Volmer Equation (eq. 4.6)

$$\frac{i}{nFA} = k^o C_{ox} exp\left[\frac{-\alpha nF}{RT}\left(E - E^{o\prime}\right)\right] - k^o C_{red} exp\left[\frac{(1 - \alpha)nF}{RT}\left(E - E^{o\prime}\right)\right]$$ (4.6)

Where k^o is standard heterogeneous rate constant, α cathodic transfer coefficient and $1 - \alpha$ anodic transfer coefficient and Q at equilibrium becomes the equilibrium constant K is the ratio of concentration of the oxidized form and reduced form.

4.1.2 Electrochemical impedance spectroscopy (EIS)

Impedance spectroscopy is a powerful method of characterizing many of the electrical properties of interfaces of various materials with electrically conducting electrodes. It may be used to investigate the dynamics of bound or mobile charge in the bulk or interface regions of any types of solids or liquid medium (ionic, semiconducting, mixed electronic –ionic) and even insulators [193]. Impedance spectroscopy is also known as electrochemical impedance spectroscopy (EIS) measures electrical properties as a function frequency. Electrochemical impedance spectroscopy is the technique where the cell or electrode impedance is plotted versus frequency [192].

The general impedance which is similar to the classical impedance (Ohm's law) defined by equation 4.7

$$Z(\omega) = \frac{E(t)}{I(t)}$$ (4.7)

With $\phi = \phi(\omega)$ mathematically it is represented by a rotating vector diagram (phaser) in a complex rectangular or polar coordinates. The complex impedance (Z) plot and its magnitude and direction can form the relation (Eq.4.8)

$$Z = Z_{Re} - jZ_{im}$$ (4.8)

Where imaginary component (Z_{im}) (Eq. 4.8)

$$j = \sqrt{-1} = \exp(j\pi 2) \qquad (4.9)$$

The magnitude of real component impedances and phase angle is given by (Eq.4.11) (Eq.4.12) respectively. Complex Impedance

$$Z(f) = \frac{E_o}{I_o} e^{j\varphi} \qquad (4.10)$$

j is the imaginary unit.

The complex number appears as a point, whose x-coordinate correspond to one component and whose y-coordinate to the other component. The first one is called a real part and the second part called imaginary part of the complex number. The impedance Z is the AC-analogous to the Ohm's resistance

$$/Z/ = (Z_{Re}^2 + Z_{im}^2)^{1/2} \qquad (4.11)$$

$$\phi = \arctan\left(\frac{Z_{im}}{Z_{Re}}\right) \qquad (4.12)$$

/Z/ and ϕ varies with ac frequency ($f = \frac{\omega}{2\pi}$)

The general approach in EIS experiment is a system at steady state of dc potential (E_{dc}) is perturbed by applying a voltage with a small amplitude less than 10 mV ac potential (E_{ac}) of frequency, $f = \frac{\omega}{2\pi}$ to the electrical system under test and current is observed as a response. If a sinusoidal excitation potential $E_{ac} = /E_{ac}/\sin(2\pi ft)$ (Eq. 4.13) with a frequency of $\omega = 2\pi f$, imposed to the system the in phase and out phase ac current(i_{ac}) responses are

measured at varies frequency values, $I(t) = /I/\sin(\omega t \pm \phi)$, (Eq. 4.14) where ϕ is the phase shift between the voltage and current and modulus (total impedance $/Z/$ in Ω)are evaluated for each frequency.

$$E_{ac} = /E_{ac}/ \sin(2\pi ft) \tag{4.13}$$

$$I(t) = /I/ \sin(\omega t \pm \phi) \tag{4.14}$$

The plotting of complex impedance (Z_{im} and Z_{re}), log $/Z/$ vs log f and ϕ versus log f plots are generated. Nyquist plot (Fig. 4.2) is a plot of the real component of impedance versus imaginary (Z_{Re} vs Z_{im}) whereas Bode plot is the plot of logarithm of total impedance log $/Z/$ and ϕ versus log (f). A possible best equivalent circuit model is proposed from the impedance spectra. Then from the best model fitting; solution resistance (R_s), double layer capacitance (C_{dl}), charge transfer resistance (R_{ct}) and Warburg impedance (Z_w) etc are analyzed. It is from this parameters standard heterogeneous rate constant (k^o), exchange current density (i_o), diffusion coefficients of oxidized and reduced species are calculated.

Electrochemical impedance spectra of electrode reaction with semi-infinite diffusion for a reaction O + ne→ R, and applying a steady stat direct current (dc) potential usually the formal potential and ac potential E_{ac} (t) = Asin(2πft) frequency between 1 MHz ≥ f ≥ 1mHz. The faradic impedance (Z_f) expressed as a diameter of the semi – circle and/or the 45° line (Fig. 4.3).When the reaction is totally irreversible it will be a perfect semi circle and the circuit model will be C_{dl} and R_{ct} in parallel while Rs in series whereas for a quasi-reversible system the impedance spectra shows a semi circle and Warburg line having slope -1 implies -45° phase angle in the higher and lower frequency region respectively. The diffusion layer thickness (δ) can be estimated using the relation, x- intercept $= R_{\Omega} + R_{ct} - 2\delta^2 C_{dl}$.

$$i = i_o \left(\exp\left(\alpha \frac{nF}{RT} \eta \right) - \exp\left(-(1 - \alpha) \frac{nF}{RT} \eta \right) \right) \tag{4.15}$$

When $C^{surface} = C^{bulk}$

$$R_{ct} = \frac{RT}{nFi_o} \tag{4.16}$$

From an electrode reaction $O + ne \rightarrow R$ and Butler − Volumer equation (Eq.4.15), small signal approximation gives an expression for charge transfer resistance (R_{ct}). Therefore EIS can be used to determine R_{ct} more easily by model fitting.

Diffusion impedance is diffusion limited transport Warburg impedance (Z_W) at high angular frequency means small Z_W and low means high Z_W. Two types of Warburg impedance exist. The first one is infinite Warburg (Z_w) for unbounded diffusion layer and the second one is finite Warburg (Z_o) bound diffusion layer.

$$Z_W = \frac{\sigma}{\sqrt{\omega}} (1 - j) \tag{4.17}$$

$$\sigma = \frac{RT}{n^2 F^2 A \sqrt{2}} \left[\frac{1}{C_O^* \sqrt{D_O}} + \frac{1}{C_R^* \sqrt{D_R}} \right] \tag{4.18}$$

$$Z_O = \frac{\sigma}{\sqrt{\omega}} (1 - j) \tanh\left(\delta \sqrt{\frac{j\omega}{D}} \right) \tag{4.19}$$

Where δ diffusion layer thickness and D is average coefficient of diffusion

Warburg (W_s) component where's' short circuit terminus and a good example is thin electroactive films with thickness L.

$$Z_{ws} = \frac{\sigma}{\sqrt{\omega}}(1-f)ctnh\left(L\sqrt{\frac{j\omega}{D}}\right)$$

(4.20)

$$Z_{wo} = R^*\left[\frac{e^{\sqrt{2I^*L^2\omega/D}}+1}{e^{\sqrt{2I^*L^2\omega/D}}-1}\right]\frac{1}{\sqrt{I^*L^2\omega/D}}$$

(4.21)

$$Z_{Ws} = R^*\left[\frac{e^{\sqrt{2\delta^2\omega/D}}-1}{e^{\sqrt{2\delta^2\omega/D}}+1}\right]\frac{1}{\sqrt{I^*\delta^2\omega/D}}$$

(4.22)
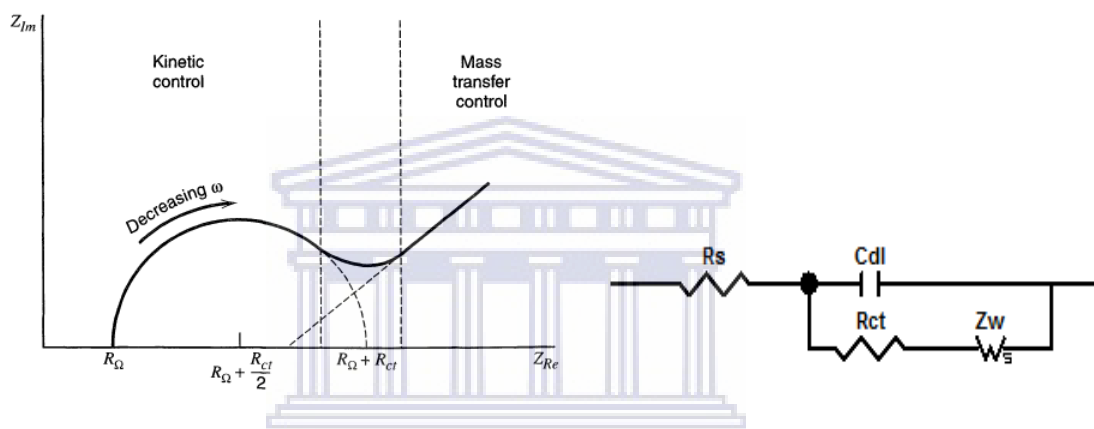
Figure 4.2: Nyquist plot and model in the presence of Warburg impedance.

4.1.3 Uv-visible spectroelectrochemistry

Uv-visible spectroelectrochemistry is an important method in the study of redox reactions especially for reversible systems. It has become an important technique in the investigation of the redox and conformational properties of conducting polymers. Uv-vis spectroelectrochemistry of conducting polymers is used in the attempt to monitor the absorption of the new species; polarons and bipolarons generated up on doping [194].

Chronoabsorptometry is a simultaneous measurement of absorbance change with time and current with time when a potential is switched from completely oxidized state to reduced state and for reverse process. It helps to study the kinetics of doping and dedoping in thin polymers films.

4.2 Chemicals and materials

3-Methoxythiophene (98%), 3, 4-ethylenedioxythiophen (99%), lithium perchlorate (95%), acetonitrile anhydrous (99.8%), ferrocene (98%), were purchased from Aldrich and used as received. Alumina powders (1, 0.3 and 0.05 µm) were purchased from Böchler. The ionic liquids 1-buthyl-3-methylimidazolium tetrafl\uroborate (Aldrich) and 1-octyl-3-methylimidazolium bis(trifluoromethylsulfonyl)imide (Merck) were used without further purification. 4,7-Dibromo-[2,1,3]benzothiadiazole (97%), 2-(tributhylstannyl)thiophene (97%), bis(triphenylphosphate)palladium (II)dichloro, sand, hexane $\geq$ (99.0 %) (GC), acetonitrile anhydrous (99.8%), ethanol and silica gel Merck grade 9385, 60 A^{o} purchased from (sigma −Aldrich). Dichloromethane (99.9 %) biotech grade solvent (Aldrich), tetrabuthylammonium perchlorate (98%) (Fluka), tetrahydrofuran (Merck), toluene, sodium metal lamp and benzophenone obtained from Kimix. Water (Resistivity 18 MΩcm) used in the preparation of 0.1 M $LiClO_4$ was purified with the RiOs 3 reverse osmosis on ion Millipore system.

Beaker, condenser, measuring cylinder, volumetric flask, column, adaptor, tubes, dendirrimite, silicon oil, heater, funnel, dropper, pasture pipette, cotton, rod, funnel, were some of the materials used.

4.3 Instrumentation

All cyclic voltammetry experiments were performed using BASi Epsilon potentiostat. The working electrode was glassy carbon (GC) (diameter 3 mm), platinum wire was used as counter electrode, and platinum wire was used as pseudo reference electrode. The Pt wire pseudo reference electrode in bmimbf$_4$ and octbmimtnf$_2$ ionic liquids was calibrated with respect to the ferrocene/ferrocinium couple (1 mM ferrocene) formed redox potential was

observed at 0.10 V. The pseudo reference electrode in 0.1 M n-Bu$_4$NClO$_4$/dry acetonitrile and in three of the ionic liquids (bmimbf$_4$, bmimpf$_6$ and bmimtnf$_2$) was also calibrated with respect to the ferrocene/ferrocinium couple (5 mM ferrocene) and formed redox potential was observed at 0.16 V in bmimbf$_4$, 0.18 V in bmimpf$_6$ and 0.20 V in bmimtnf$_2$. Uv–visible spectra of the monomer were measured using (3 cm by 3 cm) quartz cuvette cell using UV Thermo Electron Corporation model Nicolet evolution 100 spectrometer. Impedance of DTBT/DTBT anion redox couple and GEC/P(DTBT) thin film was measured using electrochemical impedance spectroscopy (EIS) using utolab frequency response analyzer system (IM6ex ZAHNER elektrik). Melting point of DTBT was measured using Stuart melting point/SMP10/, FTIR spectra were reordered by using ATR-FTIR 100 series spectrophotometer.

Spectroelectrochemistry experiments were performed using a specially design quartz cuvette (1 mm x 10 mm) cell with a UV Thermo Electron Corporation model Nicolet evolution 100 spectrometer. The working electrode was indium tin oxide (ITO) coated glass (7 x 50 x 0.6 mm, R $\leq$ 10 Ω, Delta Technologies Inc USA); the counter electrode was a platinum gauze, and also platinum wire used as pseudo reference electrode.

AFM (atomic force microscopy) analysis of the film on ITO electrode were carried on using a Veeco NanoMan V model with a silicon tip at a spring constant of 1-5 N/m and resonance frequency of 60 – 100 kHz. Scanning electron microscope (SEM) analysis of the film on ITO electrode was carried on ZEISS AURIGA higher SEM.

4.4 Procedures

4.4.1 Distillation of tetrahydrofuran (THF)

About 400 ml of ordinary grade tetrahydrofuran was poured into 500 ml flask. Using the sodium press and 1mm die about 5 g of sodium wire extruded and added into THF. Besides, about 10 g of benzophenone is added as an indicator to the flask. After the solution was refluxed for about 1 hour over nitrogen atmosphere, the light yellowish colour of the THF changed to greenish. Then some more benzophenone added and the THF was refluxed for some times until the content changed to deep blue; indicating that peroxides and water has been removed. Finally, distilled tetrahydrofuran was collected as shown in Fig. 4.3.

Figure 4.3: Distillation setup of tetrahydrofura on sodium wire.

4.4.2: Synthesis of 4,7-dithien-2-yl-2,1,3-benzothiadiazolee (DTBT) monomer

To the solution of 4,7-dibromo-2,1,3-benzithiadiazole (4.05 g, 15.0 mmol) and tributhyl(thien-2-yl)stannane (13.47 g, 36.1 mmol) weighing using weigh bottle on analytical balance Mettler Toledo Model (Maximum 101 g, minimum 10 mg, deviation = 0.1 and error = 1mg) from distilled tetrahydrofuran 100 ml was taken using measuring cylinder, bis(triphenylphosphine)palladium(II)dichloro (PdCl$_2$(PPh$_3$)$_2$) ((213 mg, 2 mol%) was added. The mixture was refluxed for 3 h under nitrogen atmosphere on silicon oil bath using Heidolph MR 3001 K heater. The temperature was set at 82 $^\circ$C and controlled using a thermometer. After removal of the solvent under reduced pressure, the residue was purified by column chromatography on silica gel (eluent dichloromethane/hexane, 1:1). After crystallization from ethanol-toluene mixture, the title compound collected as red needles solid. Finally, the sample was dried at 55 $^\circ$C and pressure of 20 mmHg, using Thermostat Townson and Mercer LTD Altrincham England yield compond 1 (4,7-dithien-2-yl-2,1,3-benzothiadiazole) (1.00 g, 50%) a much lower value compare to the literature yield (3.70 g, 82%).

4,7-Dibromo-[2,1,3]-benzothiadiazol   1
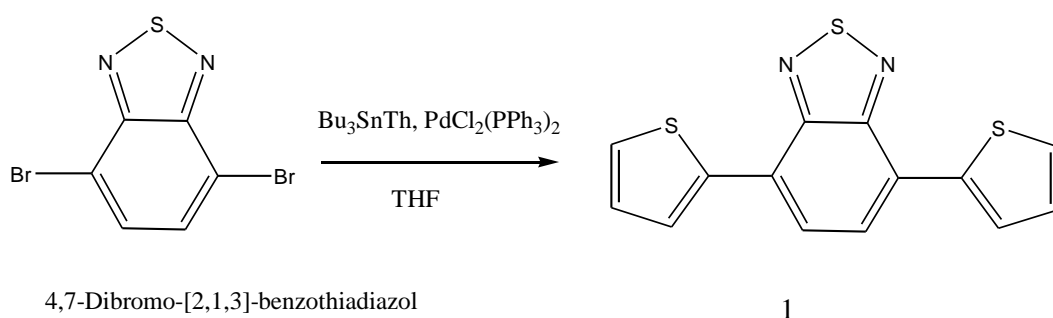
Scheme 3: Synthesis of 4,7-dithien-2-yl,2,1,3-benzothiadiazole by Stille coupling reaction [168].

4.4.3 Column chromatography

Packing of column: about 250 g of silica gel is dissolved in ethanol – toluene solvent (1:2 v/v) for the preparation of slurry about 1: 25 ratio because the mass of the sample was 11.0 g. A piece of cotton was placed at the bottom of the column using a rod to prevent the sand to keep smooth flow of the eluent. The cotton was not pushed strongly to prevent the flow of the eluent. About 3 spatula or 1 cm length of sand is added over the cotton. Then the slurry was added into the column using a funnel at the top. Then silica gel left was rinsed and added into the column. After some times, the eluent flow out was adjusted and then about 2 spatula of sand added over the slurry to support the sample. The sand was leveled by applying pressure in different direction by allowing the eluent to flow. In the next step, the sample was quickly added straight over the sand using a pasture pipette. As the sample started to cross the sand level, the eluent was added over it using a funnel. The eluent was maintained over the sand to prevent dring. The flow out was adjusted in such a way that it should not be too fast or too slow for effective separation of the various components of the sample.

4.4.4 Recrystalization

The residue was dissolved in hot toluene–ethanol (2:1 (v/v)) ratio. About 10 ml of the solution is heated just below its boiling point. After adding about 2 ml of the solvent using a pipette the residue was dissolved and some more added to dissolve the entire residue in the elementary flask and then warm-up. The mixture was allowed to cool to room temperature for half an hour. No crystallization observed. But when it was keep in ice bath, after 15 minutes needle red crystals appeared, the characteristic colour of DTBT. It was keep for another half an hour for completion crystallization. Then the solvent is removed using a pipette and the residue is dried and kept for characterization. Finally, a red product was obtained as shown below.
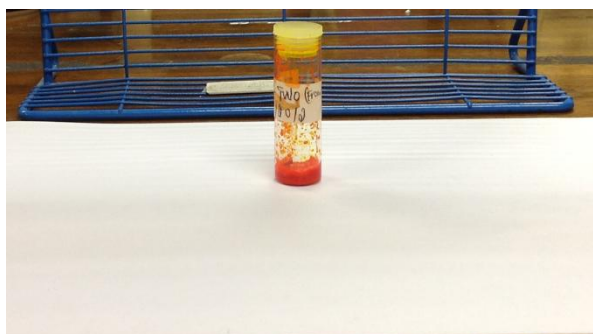
4,7-Dithhien-2-yl-2,3-benzothiadiazole (DTBT)

4.4.5 Characterization of DTBT

The purity of DTBT was checked using thin layer chromatography (TLC). Dichloromethane hexane (1:1) v/v solvent system was used as mobile phase. Small amount of DTBT was dissolved in the solvent. The DTBT solution drop/spot on the thin layer plate using a small rod. The plate was placed in a beaker which contains a solvent and closed to prevent evaporation. A yellow colour appeared for that of DTBT and no other impurities appeared. Moreover, no UV fluorescence material observed and all these proved the purity of DTBT.

Uv-Visible absorption of DTBT dissolved in chloroform was measured using UV Thermmo Electron Corporation model Nicolet evolution 100 spectrometer The ATR-FTIR spectra of the sample were recorded using ATR-FTIR 100 series spectrophotometer. The melting point of DTBT was measured using Stuart melting point (SMP 10). The melting point tube (2-3 mm) filled with dry DTBT and placed in SMP 10. After the instrument set to a plateau 100 $^\circ$C it was heated until it melts.

4.4.6 Electrochemical polymerization and electrochemical characterization of poly(3-methoxythiophene)

The potentiodynamically electrochemical polymerization of MOT (0.1M) and its copolymerization in the presence of EDOT (0.1 M) in 1-buthyl-3-methylimidazolium tetrafluroborate (bmimbf$_4$) and 1-octyl-3-methylimidazolium bis(trifluoromethylsulfonyl)imide (octmimtnf$_2$) were carried out in one compartment cell with glassy carbon (GC) as working electrode, platinum wire counter electrode and platinum wire pseudo reference electrode. Before electrochemical polymerization solutions were purged with nitrogen and overflow of nitrogen was maintained during electrosynthesis. Prior to all the polymerizations the GC working electrodes was polished with 1μm, 0.3 μm and 0.05 μm alumina powder successively to get shiny surface and rinsed first with deionised water and then with acetone. Electropolymerization was performed at the scan rate of 50 mV/s and five cycles were taken for the characterization of the polymers by cyclic voltammetry (CV) first in monomer free bmimbf$_4$ when it is used as medium or octmimtnf$_2$ of electrosynthesis growth medium and secondly in monomer free aqueous LiClO$_4$ (0.1 M). Homopolymer and copolymer as formed was washed with deionised water before characterization by CV. The potential range was from -1.05 V to + 0.85 V at scan rate of 5, 10, 20, 50, and 100 mV/s. All experiments were performed at room temperature (20 $^{\circ}$C).

4.4.7 Uv- vis spectroelectrochemistry of PMOT

Homopolymer and copolymer films were obtained by potentiodynamically depositing upon ITO coated glass, from 0.1 M MOT for the homopolymers and MOT and EDOT mixture each 0.1 M for copolymers at the scan rate 50 mV/s. After deposition, the films were rinsed with distilled water and inserted in electrochemical cell. The electrochemical cell was assembled in a standard quartz cuvette (1 cm x 1 cm) using ITO as working electrode, a Pt

gauze as counter electrode and Pt wire as a quasi– reference. In the spectroelectrochemistry experiment the cuvette was filled with aqueous $LiClO_4$ (0.1 M) as supporting electrolyte.

4.4.8 Electrochemical study of DTBT

Stock solution of 0.05 M DTBT in 0.1 M n-Bu_4NClO_4 in anhydrous acetonitrile as well as in dichloromethane was prepared. 40 μL was used from the stock to prepare 0.85 mM DTBT for electrochemical oxidation in 0.1 M n-Bu_4NClO_4/acetonitrile. Range of the potential oxidation was from -1.38 to 1.2 V vs. Fc/Fc$^+$ couple. Electrochemical oxidation of 0.85 mM DTBT was studied on Pt, Au and GC electrode in three different electrolytes 0.1 M Bu_4NClO_4 in acetonitrile, 0.1 M n-Bu_4NClO_4 in dichloromethane and mixture of 0.1 M n-Bu_4NClO_4-ACN and 0.1 M Bu_4NClO_4 –DCM (2:3 v/v) ratio. The reversibility of DTBT oxidation reduction peak was further investigated in the scan range of 30 – 500 mV/s sweep rates.

Electrochemical impedance spectroscopy (EIS) measurement of 0.85 mM DTBT was performed in 0.1 M n-Bu_4NClO_4 in ACN, DCM- ACN and DCM using an Autolab frequency response analyzer system (IM6ex ZAHNER elektrik) at formal potential of -1.56 V. Before each EIS measurement the electrode held at the stated potential for an equilibrium time of 5 min. The impedance spectra were recorded in the frequency range 100 kHz – 10 MHz using sinusoidal excitation signal with amplitude of 5 and 10 mV. Impedance spectra were fitted to an equivalent electrical circuit by using the Autolab impedance analysis software.

4.4.9 Electrochemical polymerization and electrochemical characterization of P(DTBT)

The electrochemical oxidation of DTBT (1.5 mM) in 0.1 M n-Bu$_4$NClO$_4$ in anhydrous acetonitrile and dichloromethane and 20 mM of DTBT in 1-buthyl-3methylimidazolium tetrafluroborate (bmimbf$_4$) and 1-butyl-3-methylimidazolium bis(trifluoromethylsulfonyl)imide (bmimtnf$_2$), 1-buthyl-3-metylimidazolium hexafluorophosphate (bmimpf$_6$) were carried out in one compartment cell with platinum (Pt), glassy carbon (GC) and Gold (Au) as working electrodes, platinum wire counter electrode and platinum wire pseudo reference electrode. Before electrochemical polymerization solutions were purged with nitrogen and overflow of nitrogen was maintained during electro synthesis. Prior to all the polymerizations the working electrodes was polished with 1 μm, 0.3 μm and 0.05 μm alumina powder successively to get shiny surface and rinsed first with deionised water ethanol and then with acetone. The scan rate was 100 mV/s. All experiments were performed at room temperature (20 $^\circ$C).

4.4.10 Electrochemical impedance spectroscopy (EIS) of P(DTBT)

Impedance of GC electrode/P(DTBT) film was performed using an Autolab frequency response analyzer system (IM6ex ZAHNER elektrik)PDTBT. The measurement was carried out at various applied potential sequenced as follows from 0.45 V to 1.1 V. Before each EIS measurement the electrode hold until for an equilibrium time of 5 min. Impedance spectra were recorded in the frequency range 100 kHz -10 mHz using sinusoidal excitation signal with amplitude of 10 mV. The measurement performed in 0.1 M n-Bu$_4$NClO$_4$/ ACN, pure bmimbf$_4$, bmimpf$_6$ and bmimtnf$_2$. The impedance spectra were fitted to an equivalent electrical circuit by using the Autolab impedance analysis software.

4.4.11 Uv- vis spectroelectrochemistry of P(DTBT) and its copolymer with MOT

The homopolymer and copolymer films were obtained by potentiodynamically depositing upon ITO coated glass, DTBT (20 mM) for homopolymers and DTBT and MOT mixture each 20 mM for the copolymers at the scan rate of 100 mV/s. After deposition, the films were rinsed with monomer free electrolytes. The electrochemical cell was assembled in a standard quartz cuvette (1 cm x1 cm) using ITO as working electrode, a Pt gauze as counter electrode and Pt wire as a quasi – reference. In the spectroelectrochemistry experiment the cuvette was filled with 0.1 M n-Bu4NClO4/dichloromethane, $bmimbf_4$, $bmimpf_6$ and $bmimtnf_2$ depending on the growth medium of the polymer. Furthermore, chronoabsorptometry experiment was performed by applying a double step potential ($E_1 = -0.6$, $E_2 = 1.1$ V) at 10 s for each potential and at fixed wavelength transmittance (T) measurement.
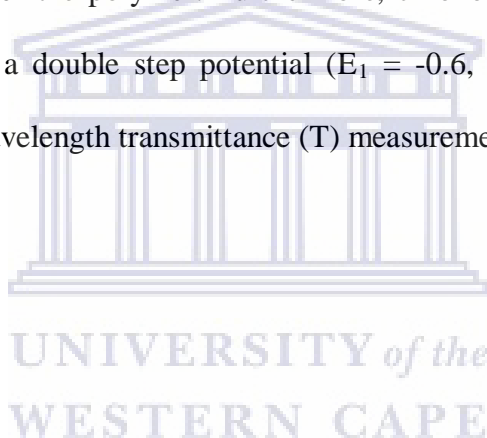
CHAPTER 5

RESULTS AND DISCUSSIONS

5.1 Electrochemical synthesis, voltammetry and uv-vis spectroelectrochemistry of poly(3-methoxythiophene) and its copolymer with EDOT in ionic liquids

Poly(3-methoxythiophene) (PMOT), electrodeposition and characterization were investigated in imidazolium based room temperature ionic liquids. The finding in this section was utilized to compare and contrast the electrochemical and optical behaviours of poly(4,7-dithien-2-yl-2,1-3-benzothiadiazole) with that of PMOT (one of the derivatives of polythiophenes). Moreover, a new composite was produced by electrochemical copolymerization of DTBT with MOT and presented in section 5.4. Therefore, the properties PMOT deposited in ionic liquids are first discussed for easy of comparsion with the properties of P(DTBT)-co-PMOT copolymer.

5.1.1 Electrochemical polymerization of MOT and EDOT

Figure 5.1(a-f) shows the anodic polarization curves of 3-methoxythiophene (MOT), 3,4-ethylenedioxythiophene (EDOT), and their mixtures in 1-butheyl-3-methylimidazolium tetrafluoroborate (bmimbf$_4$) and 1-octyl-3-methylimidazolium bis(trifluoromethylsulfonyl)imide (octmimtnf$_2$) ionic liquids. The onset oxidation potential of MOT in both ionic liquids occurred at about 1.01 V whereas its mixture with EDOT was at about 1.13 and 1.10 V in the former and the later ionic liquids (see Fig. 5.1 and Table 1). There was no significant onset oxidation potential difference observed in both cases for MOT and solution of MOT and EDOT. On the other hand, EDOT oxidation starts around 0.73 V (Table 1) in the hydrophobic octmimtnf$_2$ ionic liquids which was lower by about 200 mV compare with that of EDOT and MOT in bmimbf$_4$. The MOT oxidation potential was low

compare with that of its value reported in the literature (1.39, 1.2, 1.1 and 1.08 V vs. SCE) [15, 17-18, 20]. All the potential indicated here are relative to ferrocene/ferrocenium redox potential unless stated otherwise.
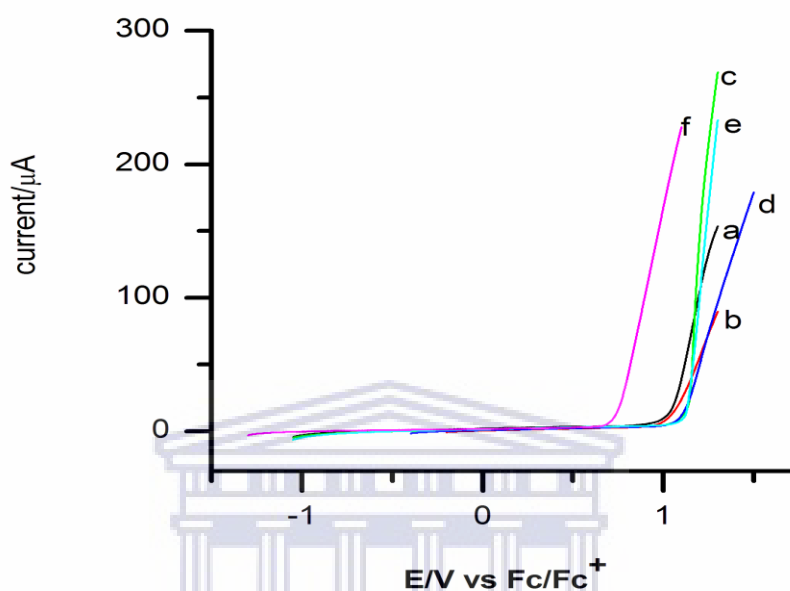
Figure 5.1: Anodic polarization curves showing the onset oxidation potential of MOT (a.b), and their mixture (c, d) each 0.1 M and EDOT (e, f) in the ionic liquids bmimbf$_4$ (a, c, e) and octmimtnf$_2$ (b, d, f).

Cyclic voltammograms recorded in the course of electropolymerization of MOT in bmimbf$_4$ and octmimtnf$_2$ ionic liquids are shown in Fig. 5.2a and b respectively. The first cycle is characterized by an irreversible oxidation of MOT during the forward scan. When the potential is switched in the reverse scan two broad cathodic waves appeared in both of the ionic liquids. The origin of the anodic wave is attributed to the oxidation of methoxy theinyl group to its radical cation and the cathodic wave is as a result of the reduction of the polymer deposited at the electrode surface following the electrogeneration of the radical cations [18].

Broad anodic peaks as a result of reoxidation of the polymer film (PMOT1 and PMOT2) appeared starting from the second cycle in the region -0.07 to 0.02 V bmimbf$_4$ and 0.31 to 0.35 V octmimtnf$_2$. PMOT1 and PMOT2 are PMOT films obtained by the electrodeposited of

PMOT in bmimbf$_4$ and PMOT2 in octmimtnf$_2$ ionic liquids respectively. In the two media one anodic and two cathodic peaks were formed. PMOT1 first cathodic peak was in the region -0.24 to -0.15 V and PMOT2 -0.29 to -0.19 V and the second one between 0.12–0.16 V form CV of PMOT1 and 0.15-0.18 V PMOT2 were noticed during electropolymerization of MOT in bmimbf$_4$ and octmimtnf$_2$. As the number of cycles increased, the anodic peak potential becomes positive and the second reduction potential becomes more negative which probably due to the ionic liquids counter ion mobility and possibly conjugation length increase with successive cycles [195]. Upon scanning repetitively, the increase of anodic and cathodic currents confirmed the growth of the polymer film. Black polymer film well adhered to the electrode surface was observed in both ionic liquids. The rate of polymerization of PMOT2 was faster than PMOT1. This was informed based on the fact that the anodic polymer growth current (i_{ox}) of the last growth cycle and the total charge that passed during all polymerization cycles (Q_P) in the case of octmimtnf$_2$ (i_{ox} = 24.0 μA, Q_p = 0.20 mC) was nearly twice that of bmimbf$_4$ (i_{ox} = 11.0 μA, Q_p = 0.10 mC) (Table 5.1). The peak oxidation current of PMOT2 was the largest indicating that PMOT2 was easily created as a result of highest polymerization rate [42]. Thus, a higher polymer growth rate was observed for the less viscous and more conductive octmimtnf$_2$ (η = 96 cP, σ = 0.75 S/m at 293.1 K) [12, 122] than in bmimbf$_4$ (η = 154 cP, σ = 0.28 S/m at 293.1) [196]. Lower viscosity allows faster diffusion of MOT and radical cation through the solution to the electrode surface and hence facilitates polymerization.

The first cathodic as read from the last polymerization cycle, appeared at about -0.15 V for PMOT1 film grown in bmimbf$_4$ and -0.19 V for PMOT2 produced octmimtnf$_2$ film. The second cathodic peak was observed at about 0.12 V for the former and 0.18 V for the later polymer. Such reduction peaks have been explained for involve of expulsion of cations trapped during polymerization step [18] or the insertion of anions for charge balance

following the change in oxidation state of the polymer upon reduction. Similarly, in the presence case, the peaks involve either the expulsion of cations of the ionic liquid or insertion of their counter ions. PMOT has a high porous morphology [25], as a result of this, during reduction exclusion of negatively charged dopant ion or insertion of a significant amount of cations of the ionic liquid to the polymer matrices may occur at the time of dedoping and incorporation of cation of the electrolyte into the polymer becomes more favourable when the dopant is large and relatively immobile [32]. Terafluoroborate and bis(trifloromethylsulfonyl)imide anions are relatively large ions and this property probably facilitate the insertion of the 1-octyl-3-methylimidazolium cation and 1-butyl-3-methylimidazolium cation into the polymer. Furthermore, much larger amount of the solvent may be incorporate as it has been reported for polythiophenes due to more porous morphology [197].
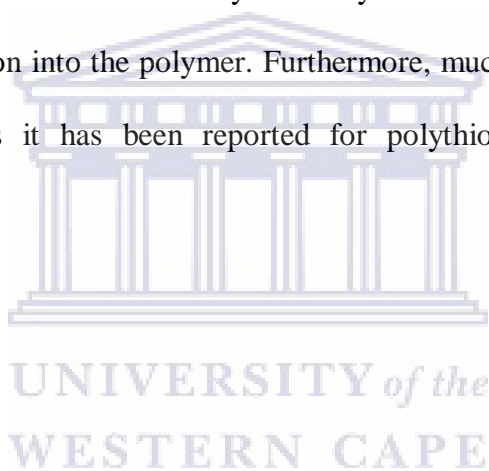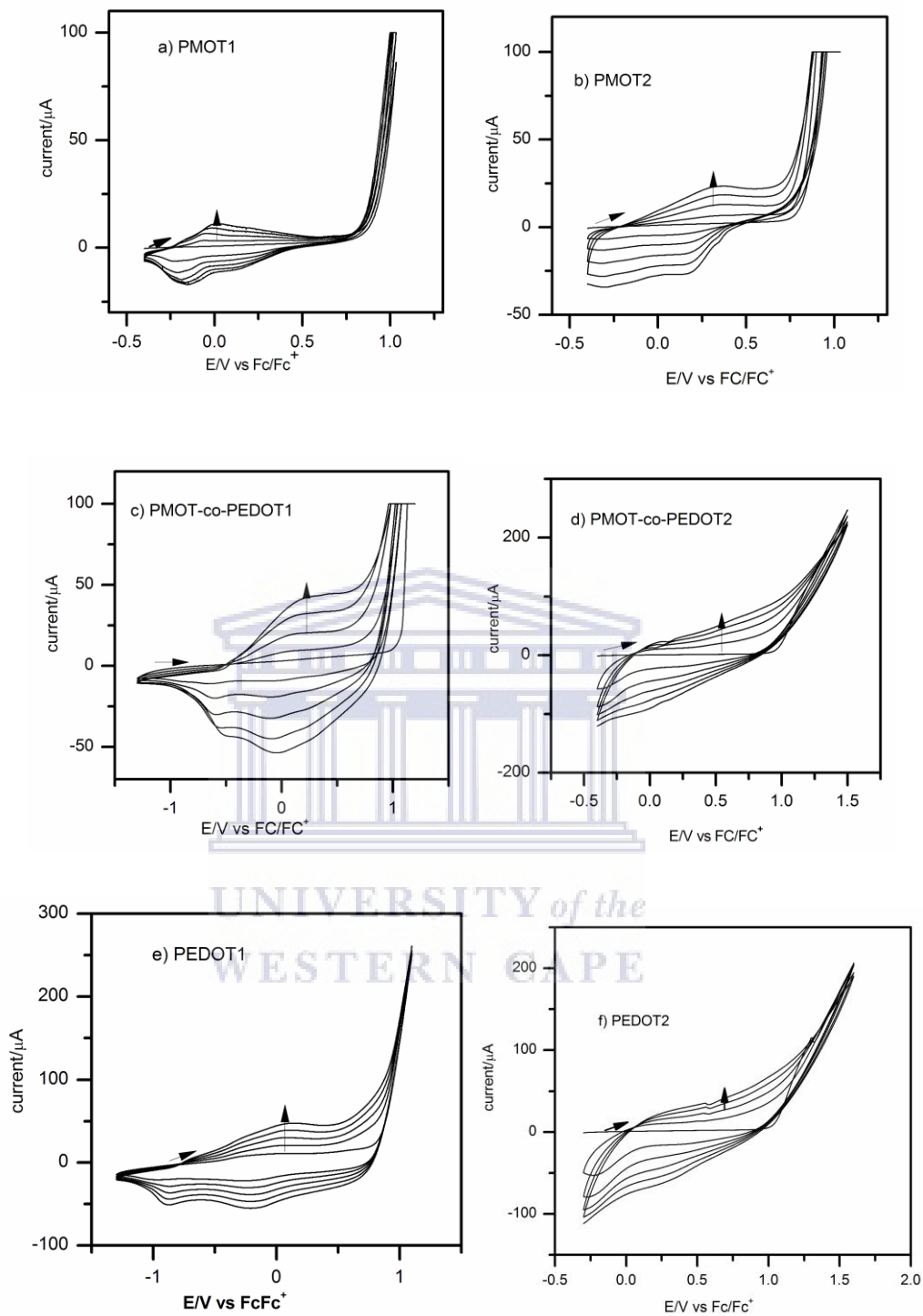
Figure 5.2: Cyclic voltammograms for a) PMOT1, b) PMOT2, c) PMOT-co-PEDOT1, d) PMOT-co-PEDOT2, e) PEDOT1 and f) PEDOT2 in the ionic liquids bmimbf$_4$ (a, c, e) and octmimtnf$_2$ ((b, d, f) at glassy carbon electrode and scan rate of 50 mV/s. Concentrations were 0.1 M for both MOT and EDOT.

Table 5.1: Electrochemical parameters evaluated for the potentiodynamic electrosynthesis of PMOT, PMOT-co-PEDOT and PEDOT.

	PMOT1	PMOT2	PMOT-co-PEDOT1	PMOT-co-PEDOT2	PEDOT1	PEDOT2
Monomer V_{ox}/V	1.01	1.01	1.13	1.10	1.13	0.73
Polymer i_{ox} /μA	11.0	24.0	44.0	-	48.8	-
Polymer V_{ox}/V	0.02	0.35	0.22	-	0.11	-
Qp/mC	0.10	0.20	0.28	0.78	0.17	0.65
Polymer V_{red}/V	-0.15, 0.12	-0.19, 0.18	-0.60, -0.01	-0.33, -0.06	-0.86, -0.20	-0.34, 0.16
Polymer i_{red}/μA	-16.7, -8.9	-33.1, -25.9	-41.9, -52.4	-114.0, -95.7	-51.0, -54.8	-105, -73.9

Onset oxidation potential, monomer V_{ox}, was taken from the anodic polarization curve (Fig.5.1). The peak polymer growth current (growth i_{ox}) was taken after 5 potential cycles and charge of polymerization Q_P /mC was obtained as net sum of appropriate integration of each cyclic voltammogram (Fig.5 2) used as an indication of the amount of polymer formed. The oxidation and reduction potentials of the monomers were taken from the top of the peak rather than the onset. (1) indicates electrodeposited in bmimbf$_4$ and (2) octmimtnf$_2$.

Cyclic voltammograms of PMOT3 electrodeposited in 1-buthyl-3-methylimidazolium hexafluorophosphate (bmimpf$_6$) and PMOT4 in 1-buthyl-3-methylimidazolium bis(trifluoromethylsulfonyl)imide (bmimtnf$_{2)}$ at 0.02 M showed one oxidation and reduction peaks (Fig. 5.3) while during characterization the same behaviour recorded as of PMO1 and PMO2 (Fig. 5.5).
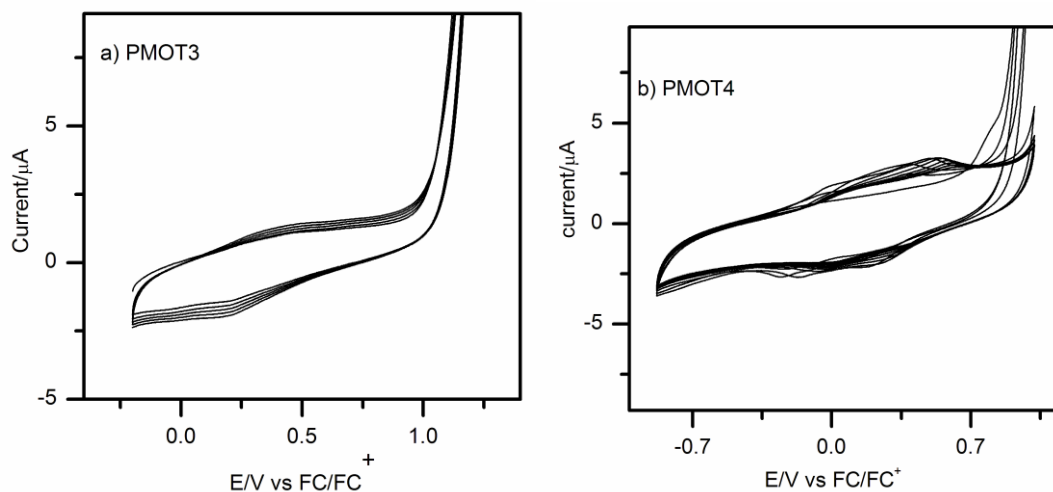
Figure 5.3: Cyclic voltammograms for a) PMOT3 grown in bmimpf$_6$ and b) PMOT4 grown in bmimtnf$_2$ at glassy carbon electrode and scan rateof 50 mV/s. Concentration of MOT was 0.02 M.

5.1.2 Electrochemical copolymerization of MOT with EDOT

Cyclic voltammograms of copolymerization of MOT and EDOT are illustrated in (Fig.5. 2c and D). In bmimbf$_4$ the resulting copolymer (PMOT-co-PEDOT1), cyclic voltammograms similar to PMOT1 and PEDOT1, exhibited one oxidation around 0.12 to 0.22 V and two reduction peaks (the first peak -0.60 to -0.50 V and the second -0.06 to -0.01 V) which appeared after the first anodic scan (Fig.5.2 and Table 5.1). One evidences for copolymerization is the shift in the oxidation potential of the copolymer compared with that of its homopolymer. This as well observed in our experimental result. Besides, peak oxidation current observed from PMOT-co-PEDOT1 (i_{ox} = 44 μA) significantly higher than PMOT1 ((i_{ox} =11.0 μA) and slightly smaller than PEDOT1 (i_{ox} =48 μA) Table 1. In the case of the copolymerization process in octmimtnf$_2$ (PMOT-co-PEDOT2) exhibited a cyclic voltammograms with two reduction peaks around (-0.33 and -0.06 V) but without clear corresponding anodic peak (Fig. 5.2d). The shape of its voltammograms was more similar to

that of PEDOT2 (Fig.5.2e and f). On the other hand, total charge obtained by integrating the polymerization CV PMOT-co-PEDOT1 (Q_p= 0.28 mC) and PMOT-co-PEDOT2 (Q_p = 0.78 mC) were larger compared with the homopolymer 0.10 mC for PMOT1, 0.20 mC PMOT2, 0.17 mC PEDOT1 and 0.65 mC PEDOT2 Table 5.1. That is the amount of total mass of copolymers deposited or its rate of formation was larger than the homopolymer. These could serve as a clue to copolymer formation. It is worthwhile to notice that PMOT-co-PEDOT2 grown in octmimtnf$_2$ resulted larger total polymerization charge compared with that of PMOT-co-PEDOT1 electrodeposited in bmimbf$_4$ in similar fashion as that of PMOT2 and PEDOT2.

5.1.3 Electrochemical characterization PMOT and PMOT-co-PEDOT

The PMOT1 film electrodeposited on GCE (GCE/PMOT1) was first characterized with cyclic voltammetry (5 to 100 mV/s) in a fresh monomer free bmimbf$_4$. The same GCE/PMOT1 was then transferred to aq. LiClO$_4$ (0.1 M) and characterize the same way. In both electrolytes the polymer film was found to be electroactive. PMOT1 exhibited two oxidation (E_{pa}^{I} = -0.18 V, E_{pa}^{II} = +0.06 V) and two reduction peaks (E_{pc}^{I} = -0.18, E_{pc}^{II} = -0.05 V) peaks in bmimbf$_4$ as shown in (Fig. 5.4a). All the peak potentials indicated here are at scan rate of 50 mV/s. The appearance of the second reduction peak (E_{pc}^{II} = -0.05 V) as a shoulder implies the kinetics of insertion of the cation is faster than that of exclusion of the anion [30] specially at high scan rates. In aq. LiClO$_4$ in contrast, one oxidation (E_{pa}^{II} = 0.22 V) and also one reduction ($E_{pc}^{II'}$ = -0.13 V) peaks were observed. It is valuable to notice that in the aqueous media the anodic and cathodic waves were more broader and peak separation (ΔE_P = 0.35 V) were large which is a typically characteristics of thin films [25]. It may also be concluded that the film transformed to a different type of structural changes in aq. LiClO$_4$ in contrast with that in bmimbf$_4$ upon oxidation and reduction. Moreover, the peaks current

were large in bmimbf4 than in LiClO4. This indicates swelling of the polymer in this medium

and faster ion transport [35]. Swelling and flattering of the polymer is caused by the transport

of the ionic species into and out of the polymer during oxidation and reduction and vice

versa. It has been reported that the anion (dopant) movement and hence oxidation and

reduction of the film are facilitated by incorporation of an ionic liquid in to the polymer

[198]. Thus, the observed electrochemical activity reflects the electrochemical accessibility of

the PMOT1 bulk to the bulk ions of bmimbf4, which may suggest the electrochemistry of the

polymer is surface dominated. This observations agreeed with report by Wagner *et al* [31]
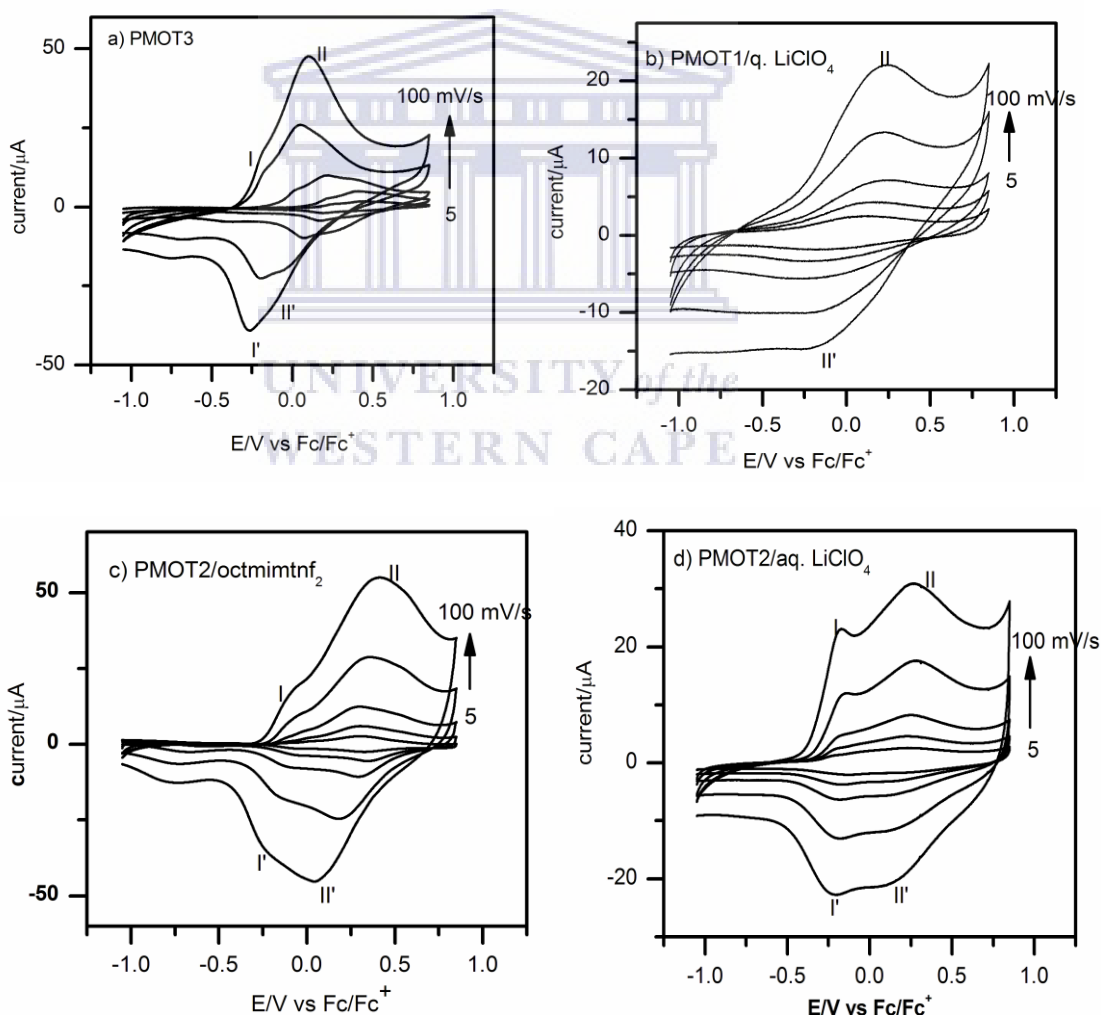
Figure 5.4: PMOT1 electrodeposited on GCE from MOT/bmimbf4 (a, b) and PMOT2
from MOT/octmimtnf2 (c. d) solutions were transferred to fresh monomer free media
and CVs were recorded at various scan rates.

PEDOT in N,N-butylmethylpyrrolidium bis(trifluoromethylsulfonyl)imide and in tetrabuthyl ammonium perchlorate in acetonitrile.

In separate experiments the PMOT2 electrodeposited from the MOT/octmimtnf$_2$ was also characterized the same way in fresh octmimtnf$_2$ and aq. LiClO$_4$. Its cyclic voltammograms in octmimtnf$_2$ (Fig. 5.4c) exhibited two oxidation (E_{pa}^{I} = -0.08 V, E_{pa}^{II} = 0.35 V) and reduction ($E_{pc}^{I'}$ = -0.14 V, $E_{pc}^{II'}$ = 0.20 V) peaks indicating at least two redox reaction mechanisms[42]. This is different from PMOT galvanostatically produced in 0.1 M NaClO$_4$, H$_2$O/CH$_3$CN on GC electrode where only one oxidation peak reported [20]. In aq. LiClO$_4$ (Fig. 5.4d), the first anodic peak increased by about 50 % going from the ionic liquid than to aq. LiClO$_4$ while the second are decreased.

The PMOT2 grown in octmimtnf$_2$ exhibited smaller anodic/cathodic peak separation in aq. LiClO$_4$ (ΔE_p = 0.16 V) compared to PMOT grown in bmimbf$_4$ (ΔE_p = 0.35 V) between Epa II and E_{pc} II' redox pairs. As explained above, this may be due to a higher polymerization rate which resulted in the deposition of a thicker PMOT2 film in octmimtnf$_2$. The second broad anodic peak at about 0.06 V for PMOT1 in bmimbf$_4$ and 0.35 V for PMOT2 in octmimtnf$_2$ is due to oxidation (doping) of the polymer accompanied with insertion of anions. Reduction peak ($E_{pc}^{II'}$ = -0.05 V for PMOT1) which appeared as a shoulder and ($E_{pc}^{II'}$ = 0.20 V for PMOT2) could be due to the reduction of the polymer accompanied by expelling of the inserted anions. The first reduction (dedoping) peak ($E_{pc}^{I'}$ = -0.18 V for PMOT1 and -0.14 V PMOT2) in the ionic liquid may be due to insertion of 1-octyl-3-methyl-imidazolium cation when it was characterized in octmimtnf$_2$ and 1-buthyl-3-methyl-imidazolium cation in that of bmimbf$_4$. In the literature it is generally accepted that
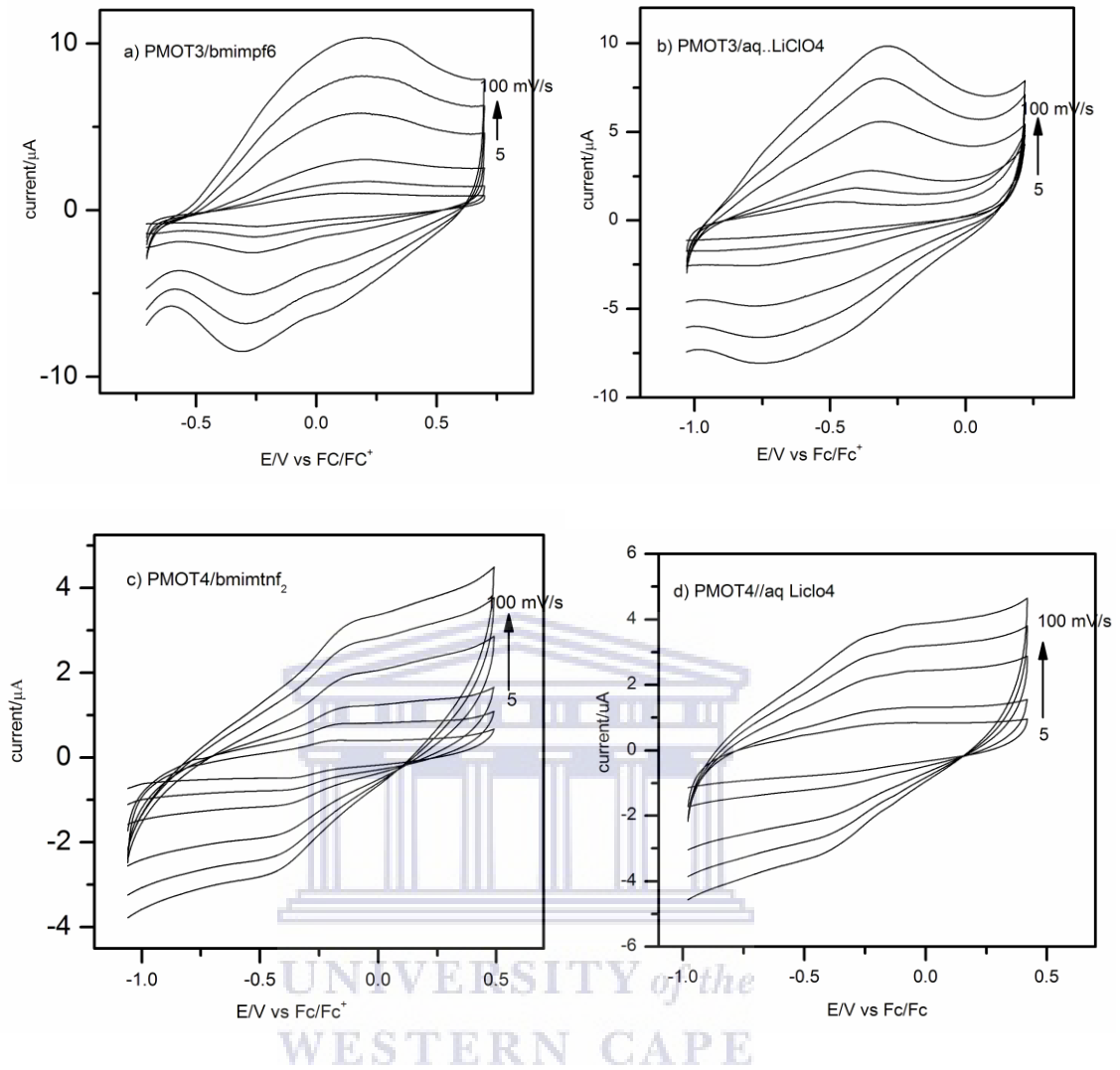
Figure 5.5: The PMOT3 electrodeposited on GCE from MOT/bmimpf$_6$ (a, b) and PMOT4 from MOT/bmimtnf$_2$ (c. d) solutions were transferred to fresh monomer free media and CVs were recorded at various scan rates.
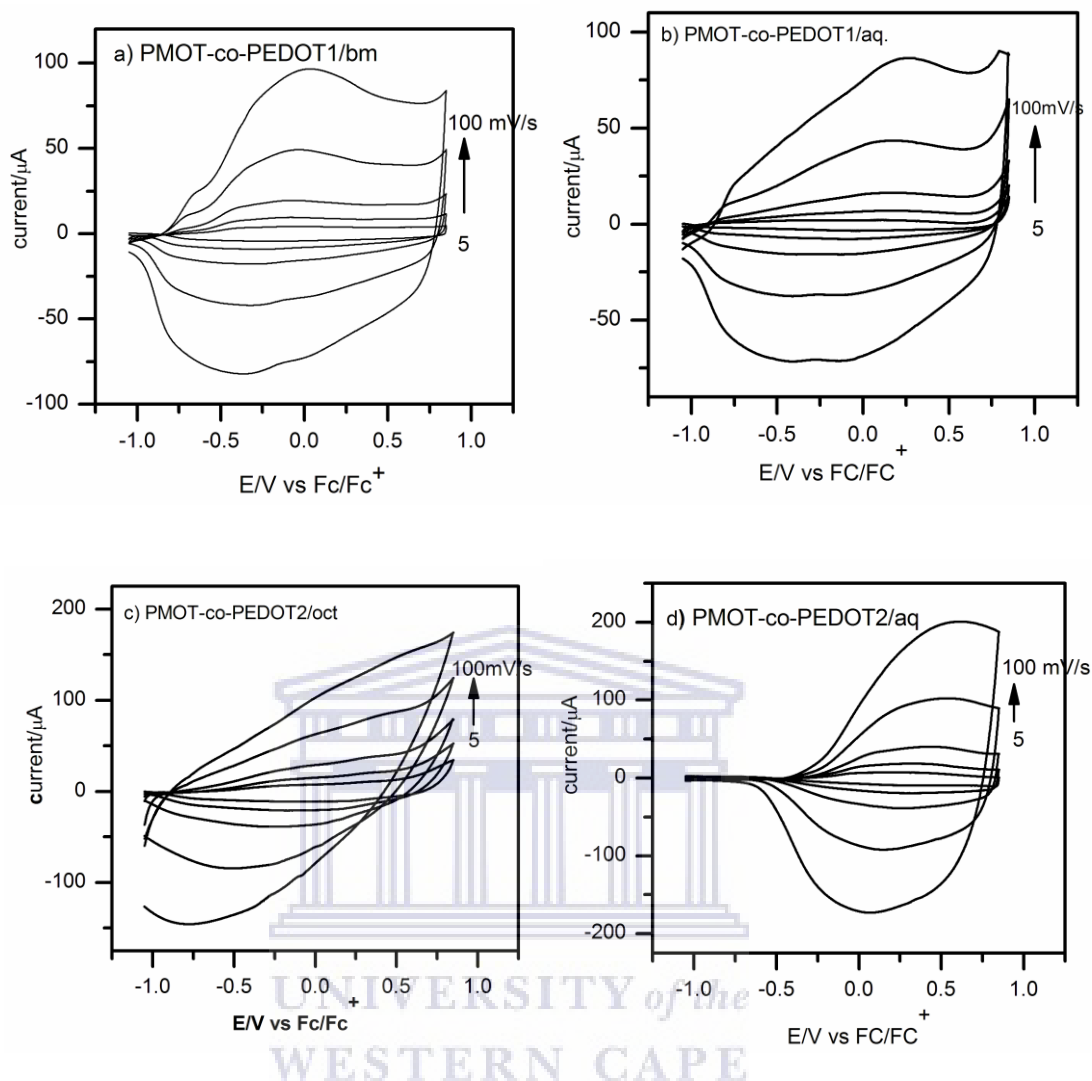
Figure 5.6: Typical cyclic voltammograms of PMOT-co-PEDOT1 copolymer film in bmimbf$_4$ (a, b) and PMOT-co-PEDOT2 in octmimtnf$_2$ (c, d) after transferring to fresh bmimbf$_4$ (a), octmimtnf$_2$ (c) and aq. LiClO$_4$ (b, d).

cations only can incorporate during reduction if space is available [12]. PMOT film at Pt and GCE electrode in aq. LiClO$_4$ and NaClO$_4$ [18, 20] the authors reported the appearance of the first cathodic peak which has no corresponding anodic peaks. Contrary to this, the first oxidation peak appeared as a small shoulder when PMOT1 and PMOT2 cycled in bmimbf$_4$ and octmimtnf$_2$ may be as a result of exclusion of cations of the ionic liquid during oxidation while the anions (tetrafluoroborate and bis(trifluoromethylsulfonyl)imide anions) trapped in

101

the polymer film [42]. PMOT1 and 2 film characterized in the respective monomer free ionic liquid and aq. LiClO$_4$, anodic peak potential becomes more positive with scan rate indicates a quasi– reversible profile. Similar to that of polythiophene [41] the CV of PMOT is dependent on the nature of ionic liquids. In the case of polythiophenes post – polymerization CVs its broadness and number of redox peaks depends on the ionic liquid used.
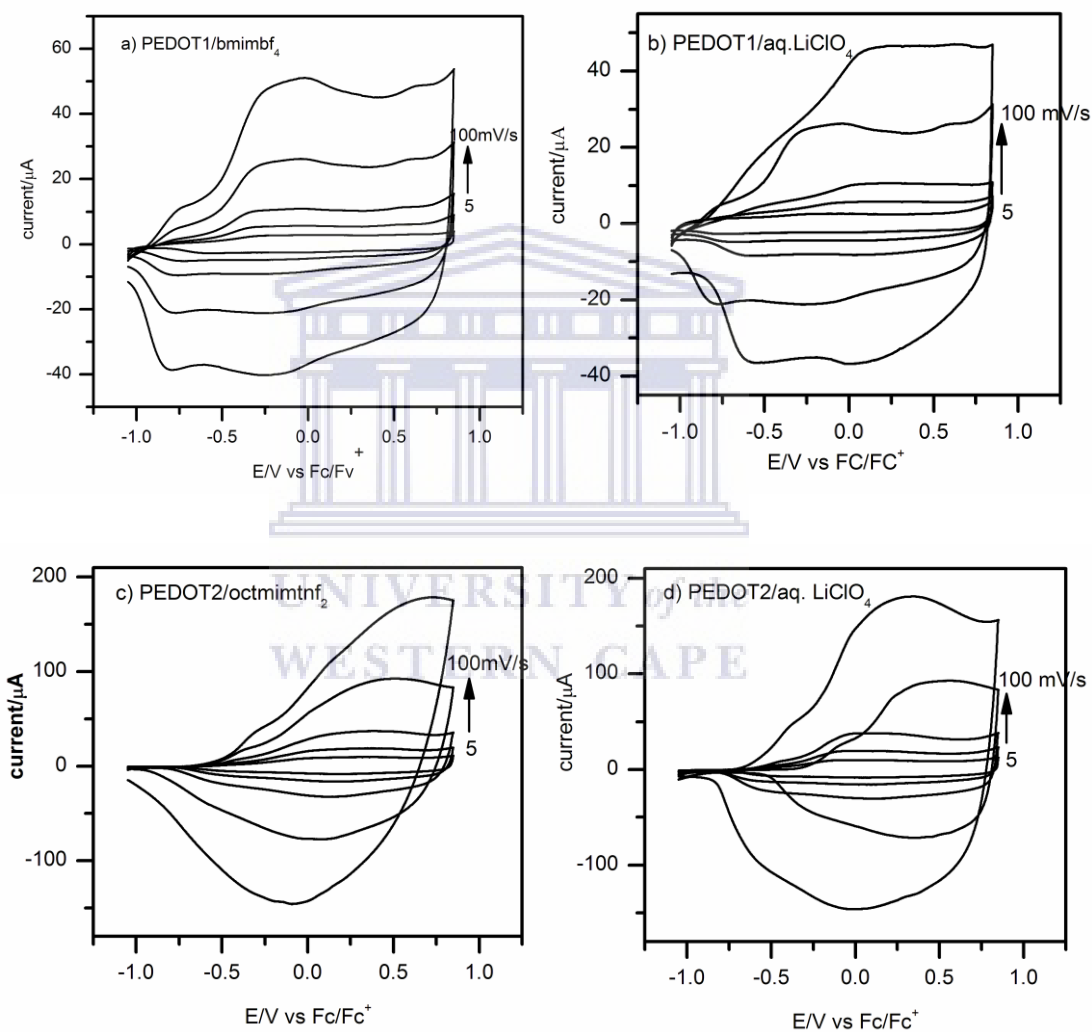
Figure 5.7: Cyclic voltammograms of PEDOT1 film in bmimbf$_4$ (a, b) and PEDOT2 in octmimtnf$_2$ (c, d) after transferring to fresh bmimbf$_4$ (a), octmimtnf$_2$ (c) and aq. LiClO$_4$) (b, d).

The electrochemical activities of the copolymer PMOT-co-EDOT1 and 2 films were evaluated in the same electrolyte as the homopolymer at different scan rates. The PMOT-co-PEDOT1 film electrochemically prepared in bmimbf$_4$ exhibited similar electrochemical activity in both bmimbf$_4$ and aq. LiClO$_4$ (Fig. 5.6a and b) with multiple broad oxidation and reduction peaks. The multiple of the peaks appears consistent with the superposition of the peaks and corresponding to each component (PMOT1 and PEDOT1) or the composite film. Obviously the contribution of the PEDOT1 parts was very dominant (Fig. 5.7a and b). Electropolymerization CV of EDOT in both ionic liquids is also shown in Fig. 5.2 for comparison. Comparison of Fig. 5.4a and Fig. 5.7a-b indicates that PEDOT1 CVs are characterized with broader peaks at larger apparent charging currents than PMOT1. A similar effect of PEDOT2 was noted regarding the PMOT-PEDOT2 composite electrodeposited from the octmimtnf$_2$ solution of the monomer (Fig. 5.4c and d, 5.7c-d). The PEDOT1 which was electrodeposited from EDOT/bmimbf$_4$ was characterized by very broad CV while especially from -1.0 V to +0.85 V in both bmimbf$_4$ and aq. LiClO$_4$. For the PEDOT2 from octmimtnf$_2$ CV was as well broad but especially from -0.5V to +0.75V.
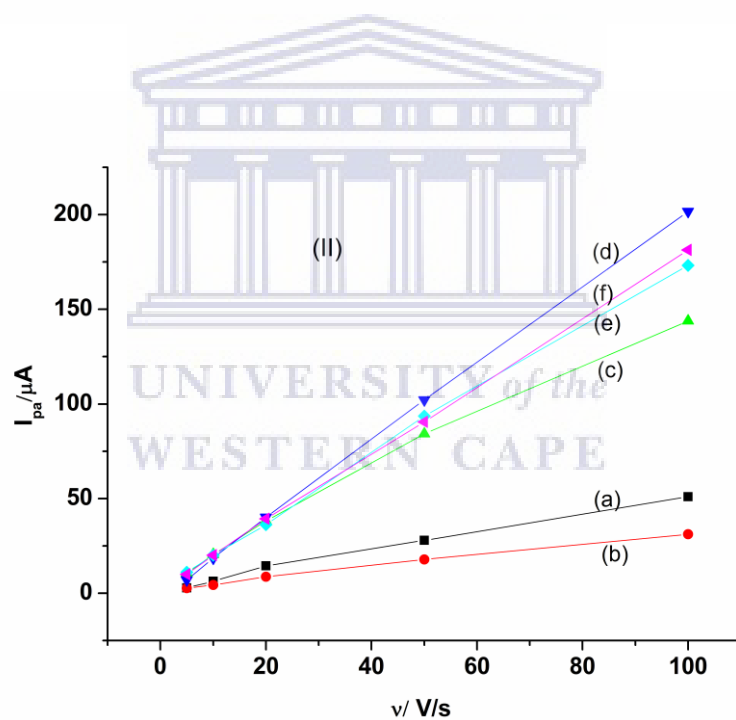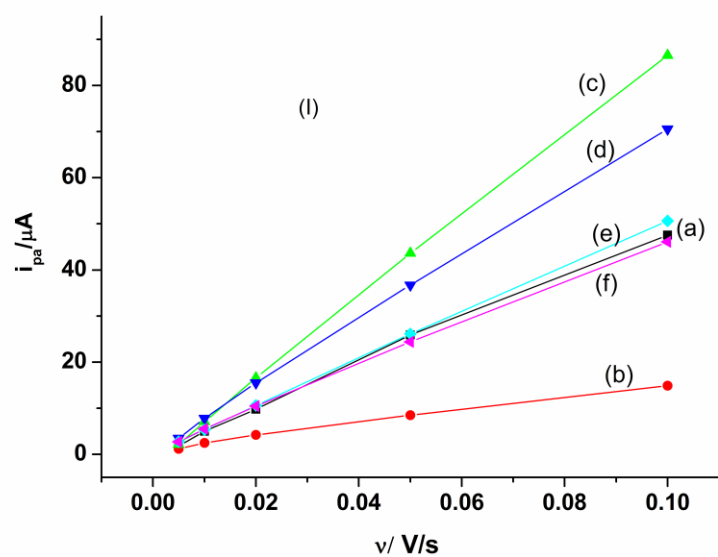
Figure 5.8: Randles - Sevcik plots for polymer films electrosynthesized from bmimbf$_4$ (I) a) PMOT1/bmimbf$_4$, b) PMOT1/aq.LiClO$_4$, c) PMOT-co-PEDOT1/bmimbf$_4$, d) PMOT-co-PEDOT1/aq. LiClO$_4$, e) PEDOT1/bmimbf$_4$ and f) PEDOT1/aq. LiClO$_4$ and octmiimtnf$_2$ (II) a) PMOT2/octmimtnf$_2$, b) PMOT2/aq. LiClO$_4$, c) PMOT-co-PEDOT2/ octmimtnf$_2$, d) PMOT-co-PEDOT2/aq. LiClO$_4$, e) PEDOT2/octmimtnf$_2$ and f) PEDOT2/aq. LiClO$_4$. CV–characterization in various media: (Except (I) b and (II) c (R^2 = 0.997) for all curve R^2 ≥ 0.999).

The second anodic peak currents in all cases followed a linear relationship with the scan rate from 5 to 100 mV/s (Fig. 5.8). This observation indicates the films formed were thin and denoting the associated redox processes are not controlled by mass transport [20].

PMOT-co-PEDO1 film was found to be the most electroactive in all electrolytes when comparing peak to charge per peak per unit concentration based on the CV at 50 mV/s (Fig. 5.9 I) followed by PEDOT1 and PMOT1. Similarly, PMOT-co-PEDO2 (Fig. 5.9 II) the most electroactive compared with PEDOT2 and PMOT2. This could be either due to large mass of polymer deposited or increased surface concentration at the same total mass as indicated in Table 5.2. Surface concentration (Γ) was calculated using [199] equation 5.1. Charge (Q) passed during reduction or oxidation was estimated from the sum of CV area of each cycle during polymerization shown in (Fig. 5.2) at scan rate of (0.050 V/s). As indicated in Table 2 the surface concentration PMOT-co-PEDOT2 (Γ_{ox} = 7.3 x 10^{-7} mol/cm^2) was the largest compare with PMOT-co-PEDOT1 or the homopolymes PEDOT2 and PMOT2 in agreement with their CV shown Fig. 5.9. PMOT-co-PEDOT1 also resulted higher surface concentration (Γ_{ox} = 3.7 x 10^{-7} mol/ cm^2) and then followed by PEDOT1 and PMOT1 electrodeposited and cycled in the same medium.

$$\Gamma = \frac{Q}{nFA}$$

(5.1)

Where Q is charge passed during oxidation or reduction (C), A is the area of GC electrode (cm^2), n is 2 (the number of electron involved during polymerization) and F is the Faraday constant.
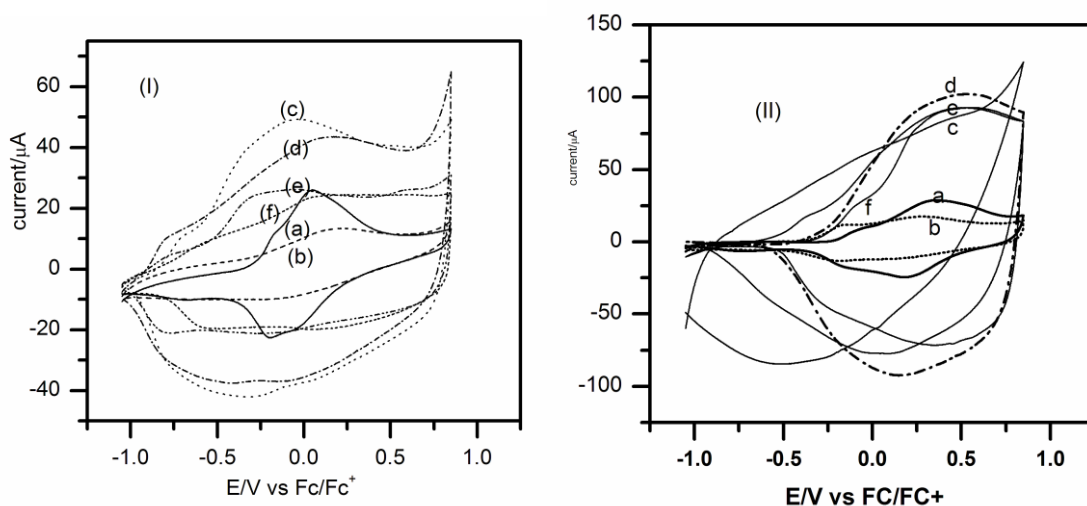
Figure 5.9: Comparison of the cyclic voltammograms of: (I) in monomer free bmimbf$_4$ and aqueous LiClO$_4$ a) PMOT1/bmimbf$_4$, b)PMOT1/aq. LiClO$_4$, c)PMOT-co-PEDOT1/octmimtnf$_2$, d)PMOT-co-PEDOT1/aq. LiClO$_4$, e)PEDOT1/octmimtnf$_2$ and f)PEDOT1/aq. LiClO$_4$; (II) in monomer free octmimtnf$_2$ and aq. LiClO$_4$ a) PMOT2/octmimtnf$_2$, b)PMOT2/aq. LiClO$_4$, c)PMOT-co-PEDOT2/octmimtnf$_2$ d)PMOT-co-PEDOT2/aq. LiClO$_4$, e)PEDOT2/octmimtnf$_2$ and f)PEDOT2/aq. LiClO$_4$. The scan rate was 50 mV/s.

Figure 5.10 shows the plot of E$_p$ versus the logarithm of the scan rates from 10 to 100 mV/s. At lower scan rate (10 mV/s) the difference between redox pairs (E$_{pa}^{II}$, E$_{pc}^{II'}$) were small specially for the polymers electrodeposited in octmimtnf$_2$ medium (Fig. 5.10b, d and f) a characteristics of reversible behaviour. As the scan rate increase (20 mV/s looks a turning point) peak separation becomes large and the potential varies linearly with scan rate indicating a quasi - reversible behaviour (Fig. 5.10a-f). From the linear part of the curve E$_p$ vs log charge transfer coefficient (α) and number of electrons (n) was calculated using [200] equation 5.2 and their values are presented in Table 5.2. Except the PEDOT's other the polymer film showed one electron transfer redox behaviour. Besides this, standard rate constant (k^o) was evaluated using [199] equation 5.3. As depicted in table 2 the magnitude of k^o of PMOT2

106
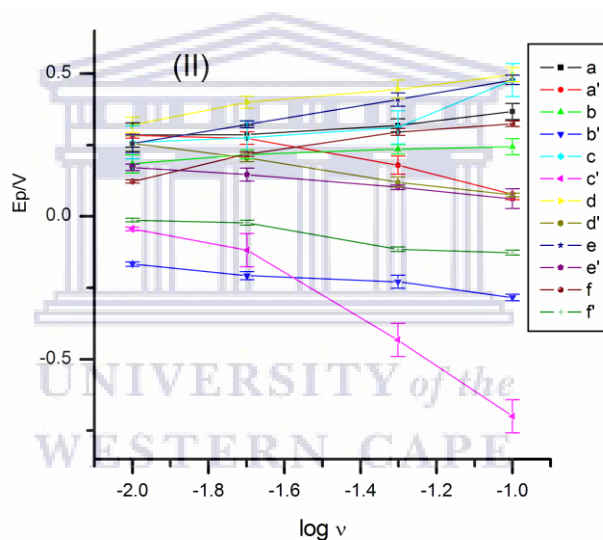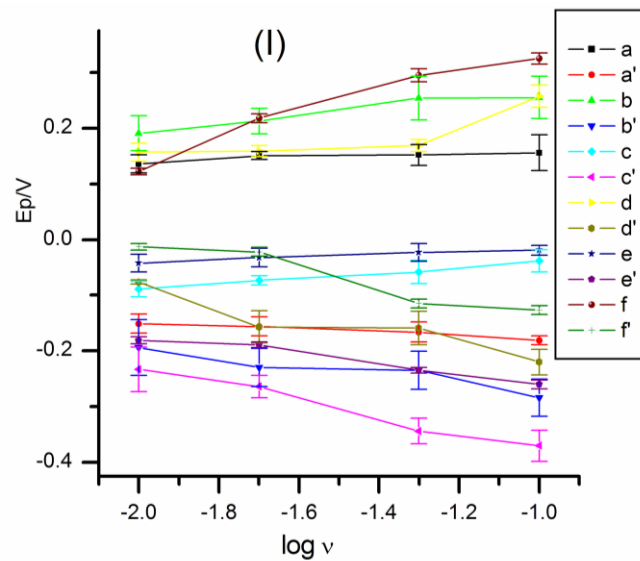
Figure 5.10: Scan rate dependance of peak potential for characterization of PMOT1 & 2 (a,b), PMOT–co-PEDOT1& 2 (c, d) and EDOT1& 2 (e, f) in the ionic liquids bmimbf$_4$ (a, c, e) and octmimtnf$_2$ ((b, d, f) at glassy carbon electrode.The scan rate was 10 to 100 mV/s.

was larger than PMOT1 implies faster kinetic of electron or ion movement in octmimtnf$_2$ compare with that of bmimbf$_4$ in line with that predicted from i_{ox} and Q_p.

$$slop = \frac{2.3RT}{2n\alpha F} \qquad (5.2)$$

$$lnk° = α(ln(1 − α)) + (1 − α)lna − ln\left(\frac{RT}{nFv}\right) − α(1 − α)\frac{nFΔE_p}{RT}$$

(5.3)

Where α is electron transfer coefficient, k^o standard rate constant (/s), ν scan rate (0.05 V/s),

$ΔE_p$ change in peak potential at 0.05 V/s, R, T, n, and F have their usual meaning.

Table 5.2: PMOT1&2 and Its copolymer with PMOT-co-PEDOT1&2 characterized in the growth medium and their surface concentration (Γ), number of electrons (n), electron transfer coefficient (α) and standard rate constant (k^o) at scan rate of 50 mV/s.

Polymer	Γ/ x 10^{-7} mol/cm^2		n	α	k^o/s
	$Γ_{ox}$	$Γ_{red}$			
PMOT1	1.1	0.3	1.03 ± 0.019	0.52	1.74 x 10^{-2}
PMOT2	2.2	0.6	0.71 ± 0.032	0.35	6.39 x 10^{-2}
PMOT-co-PEDOT1	3.7	2.4	1.17 ± 0.016	0.59	1.30 x 10^{-2}
PMOT-co-PEDOT2	7.3	1.5	0.76 ± 0.058	0.38	2.15 x 10^{-3}
PEDOT1	2.4	1.1	2.5 ± 0.015	0.63	3.18 x 10^{-3}
PEDOT2	6.0	1.2	0.27 ± 0.021	0.13	8.70 x 10^{-2}

5.1.4 Uv–vis spectroelectrochemistry of PMOT and PMOT-co-PEDOT

UV-Vis spectroelectrochemistry experiments were done on the polymer films to examine optical properties as a function of applied voltage. It also gives information about the electronic structure of the polymer such as bandgap (E_g) and intergap states that appear upon oxidation (doping) [40]. The films were first electrochemically synthesized on ITO electrode in the two ionic liquids bmimnf$_4$ (PMOT1, PMOT-co-PEDOT1 and PEDOT1) or octmimtnf$_2$ (PMOT2, PMOT-co-PEDOT2 and PEDOT2) and transferred to aq. LiClO$_4$ (0.1 M) for the study.
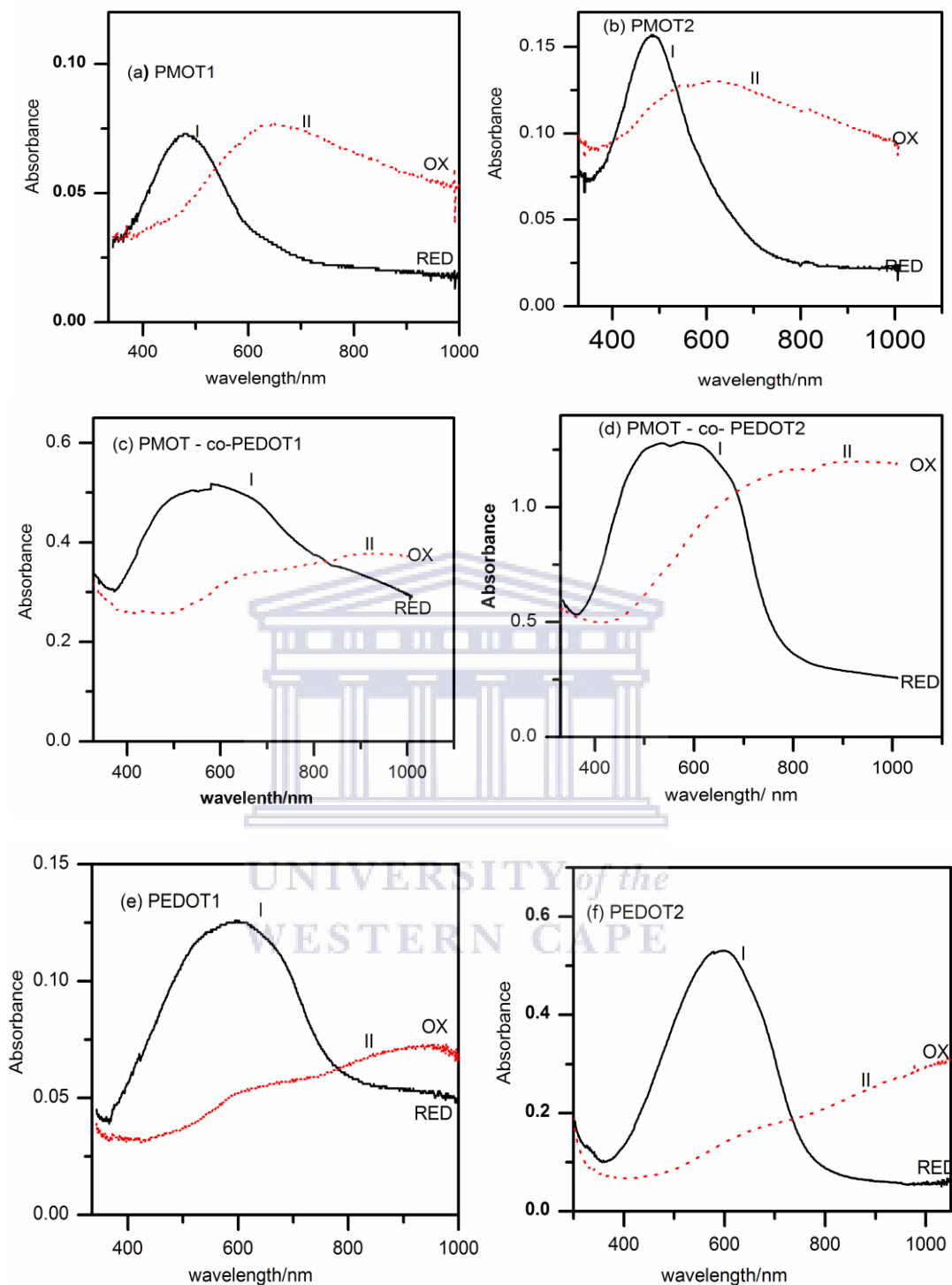
Figure 5.11: Spectroelectrochemical absorption spectra in aq. LiClO$_4$ (0.1 M) of PMOT1, PMOT-co-PEDOT1 and PEDOT1 films which were first electrodeposited on ITO coated glass electrode in bmimbf$_4$ (a, c, & e) and PMOT2, PMOT-co-PEDOT2 and PEDOT2 in octmimtnf$_2$ (b, d & f). Applied potentials: -0.95 V (curve 'I') and +0.95 V (curve 'II').

Table 5.3: Optical properties of PMOT, PEDOT and their copolymer [*] λ_{max} of absorption (nm).

Polymer	reduced	oxidized	E_g
PMOT1	480[*]	608-680, 645[*]	1.86
PMOT2	485[*]	528 – 656, 600[*]	1.63
PMOT-co-PEDOT1	505-618, 560[*]	653, 871 - 970, 915[*]	1.38
PMOT-co-PEDOT2	494-628, 560[*]	780 – 1000, 795[*]	1.38
PEDOT1	540- 636, 600[*]	614, 850-1000, 941[*]	1.58
PEDOT2	618 -562, 598[*]	670, 850–1100, 1021[*]	1.55

Maximum absorption bands were observed at about 480 nm (bandgap, E_g = 1.86) for the reduced PMOT1 and 485 nm (E_g = 1.63 eV) for PMOT2 (Fig. 5.11a – b curve I) and (Table 5.3). These bands are as a result of $\pi \rightarrow \pi^*$ electronic transitions in the thiophene - ring repeat unit namely from the highest occupied molecular orbital (HOMO) to the lowest unoccupied molecular orbital (LUMO) H→ L electronic transition as shown in (Fig. 5.12 top), in accordance with the existence of conjugated segment in the polymer chain [18, 20]. The absorption bands of PMOT1 and PMOT2 are broad and their maximum wavelength of absorption appear at longer wavelengths compare with that of PMOT (λ_{max} = 400 nm) potentiostatically polymerized on ITO electrode in distilled water/acetonitrile (3:1) solvent in the presence of $NaClO_4$ as supportive electrolyte [20]. This implies the formation of a longer chain of PMOT in the ionic liquids.

Upon complete electrochemical doping, the intensity of the $\pi \rightarrow \pi^*$ interband absorption at λ_{max} 480 and 485 nm vanished and replaced with new absorption bands λmax 645 nm (Δλ=72 nm) for oxidized PMOT1 and λmax 600 nm (Δλ = 128 nm) for PMOT2. As shown in figure 5.12, this oxidative doping changes the structure of PMOT from benzenoid to quinoid like

110

structure. The resulting charged five or four 3-methoxythiophene units of the polymer radical cations repeat units (polarons) are characterized by two states in the subgab highest singly occupied orbitals (S) and higher polaronic level (L) (Fig. 5.12 middle). Three possible spectroscopic subgab transitions (H→S, S→L and H→L) expected upon doping [201-202]. For the dictation repeat units (bipolarons) only two optical transitions [202] (H→S and H→L) predicted since the S sates are empty transition from the S→L state is absent (Fig. 5.12 bottom). As seen from Fig. 5.11a-b curve II doped PMOT1 and PMOT2 results a broad absorption band characteristic feature of a single subgap absorption similar to that of longer oligopolythiophenes bipolaron state [202]. The absorption bands at about λ_{max} 645 nm and 600 nm for PMOT1 and PMOT2 are attributed to polaronic transitions from S→L and bipolaron transitions from HOMO to lower bipolaron states (H→L) Fig. 5.12 bottom [203]. Since $\Delta E > \Delta E^+ > \Delta E^{2+}$ the band due to bipolarons appeared at a higher wavelength region of the spectrum. There were no significant difference observed in absorption bands for the as-produced PMOTs grown in the two ionic liquids, but a small absorption - band difference about $\Delta\lambda = 45$ nm between λ_{max} after oxidation was noted.

On the other hand, broader absorption bands around λmax 560 nm ($\Delta\lambda = 93$ nm) was recorded at -0.95 V for PMOT-co-PEDOT1 film and PMOT-co-PEDOT2 (more broader $\Delta\lambda=134$ nm). The bandgap of both films was 1.38 eV. For comparison, the reduced state of PEDOT1 and PEDOT2 spectra is also indicated (Fig. 5.11e – f curve I) and its absorption band appeared at λmax 600 nm ($\Delta\lambda =76$) for PEDOT1 ($E_g = 1.58$ eV) and λ_{max} 600 ($\Delta\lambda= 56$) for PEDOT2 ($E_g = 1.55$ eV) which is assigned as $\pi\rightarrow\pi^*$ transitions. Maximum wavelength of PEDOT1 and PEDOT2 at ca. 600 nm characteristics absorption spectra of PEDOT was in agreement with PEDOT synthesized in 1-ethyl-3-methylimidazolium bis(trifluromethanesulfonyl)imide [31]. PMOT-co-PEDOT1 and PMOT-co-PEDOT2 uv-visible spectra in the reduced state and with center of maximum absorption λ_{max} 560 nm was nearly the average of λ_{max} of PMOT1 and

PEDOT1 and PMOT2 and PEDOT2 respectively. This indicates that PMOT and PEDOT units may cover a certain portion of the area of the electrode surface and each unit not independently absorbs but rather as a whole in the copolymer chains. PMOT-co-PEDOT1 in the doped state (at +0.95 V) the bands as a result of $\pi \rightarrow \pi^*$ transition decrease instead weaker absorption peaks around 653 associated to PEDOT units of the neutral polymer and bands at longer wavelength λ_{max} 915 nm appeared. On the other hand, PMOT-co-PEDOT2 film at a potential of +0.95 V, $\pi \rightarrow \pi^*$ transition bands at 560 nm completely vanished and as can be seen from (Fig. 5.11d curve II) broader bands λ_{max} 795 nm ($\Delta\lambda$ =113 nm) appeared. Bands at about λ_{max} 915nm for PMOT-co-PEDOT1 and 795 nm for PMOT-co-PEDOT2 assigned to be as a result of the formation of two bipolaronic states. Thus, spectral bands of PMOT-co-PEDOT1 Fig. 5.11c curve II is a superposition of PMOT1 (Fig. 5.11a curve II) and PEDOT1 (Fig. 5.11e curve II). Similarly, PMOT-co-PEDOT2 is also a superposition of PMOT2 (Fig. 5.11b curve II) and PEDOT2 (Fig. 5.11f curve II) reveals copolymerization [35]. The generation of reversible absorption bands upon electrochemically doping/dedoping of PMOT and its copolymer with PEDOT films on ITO electrode in the visible region from blue to red to near infrared region makes them the most promising class of materials for potential applications in electrochromic devices.

112
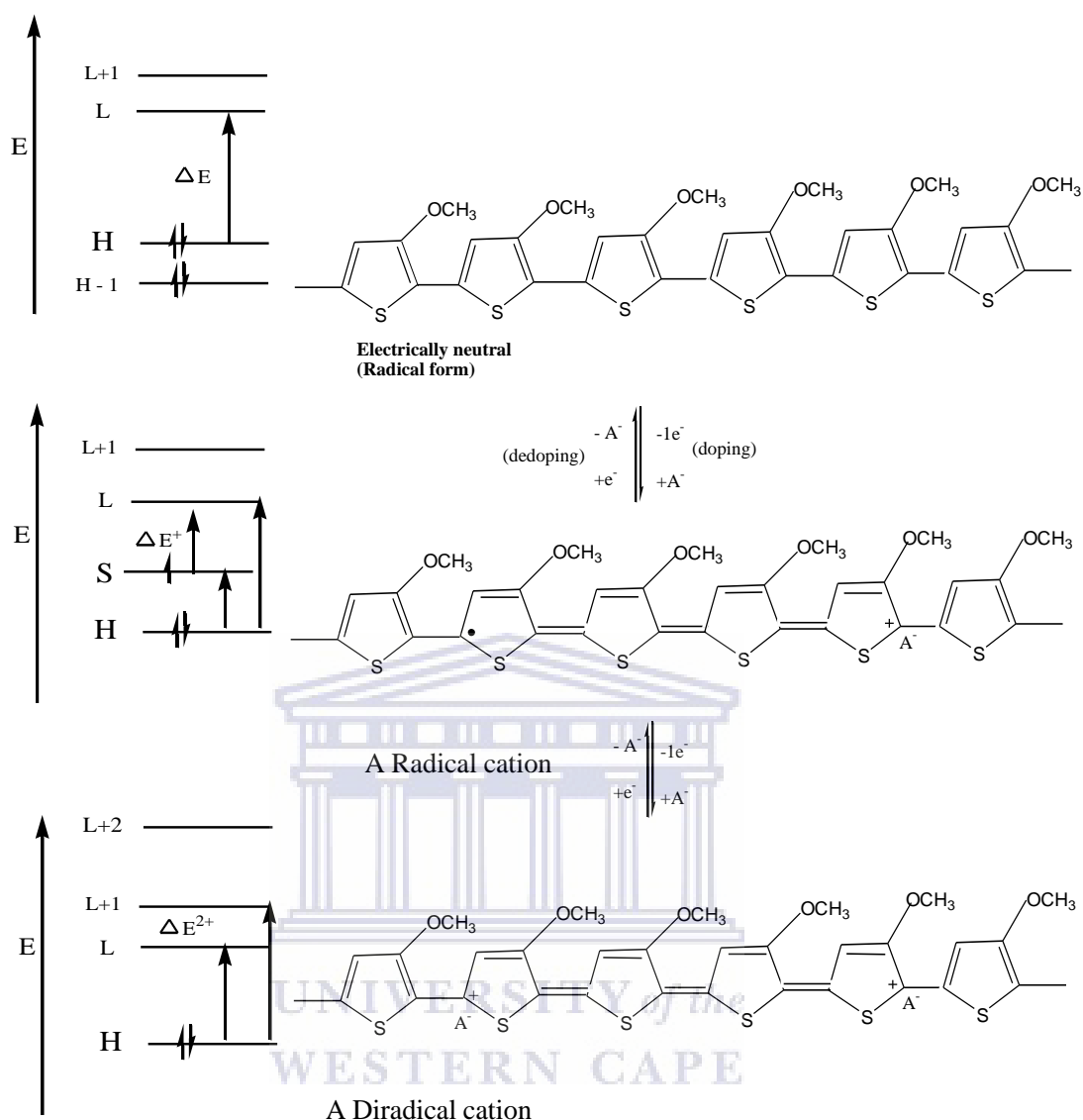
Figure 5.12: Neutral, polaron, bipolaron states of PMOT and its band structure model.

5.1.5 Morphology of PMOT and PMOT-co-PEDOT polymer films

AFM images of PMOT and PMOT-co-PEDOT films on ITO electrode were acquired to assess the effect of the nature of growth medium on the morphology of the conducting polymer films (Fig. 5.13). The oxidized forms of the PMOT-co-PEDOT1 films electrochemically synthesized in bmimbf$_4$ (Fig. 5.13c) and PMOT-co-PEDOT2 in octmimtnf$_2$ (Fig. 5.13) were found to posses morphologies different from image of PMOT1 and PEDOT1
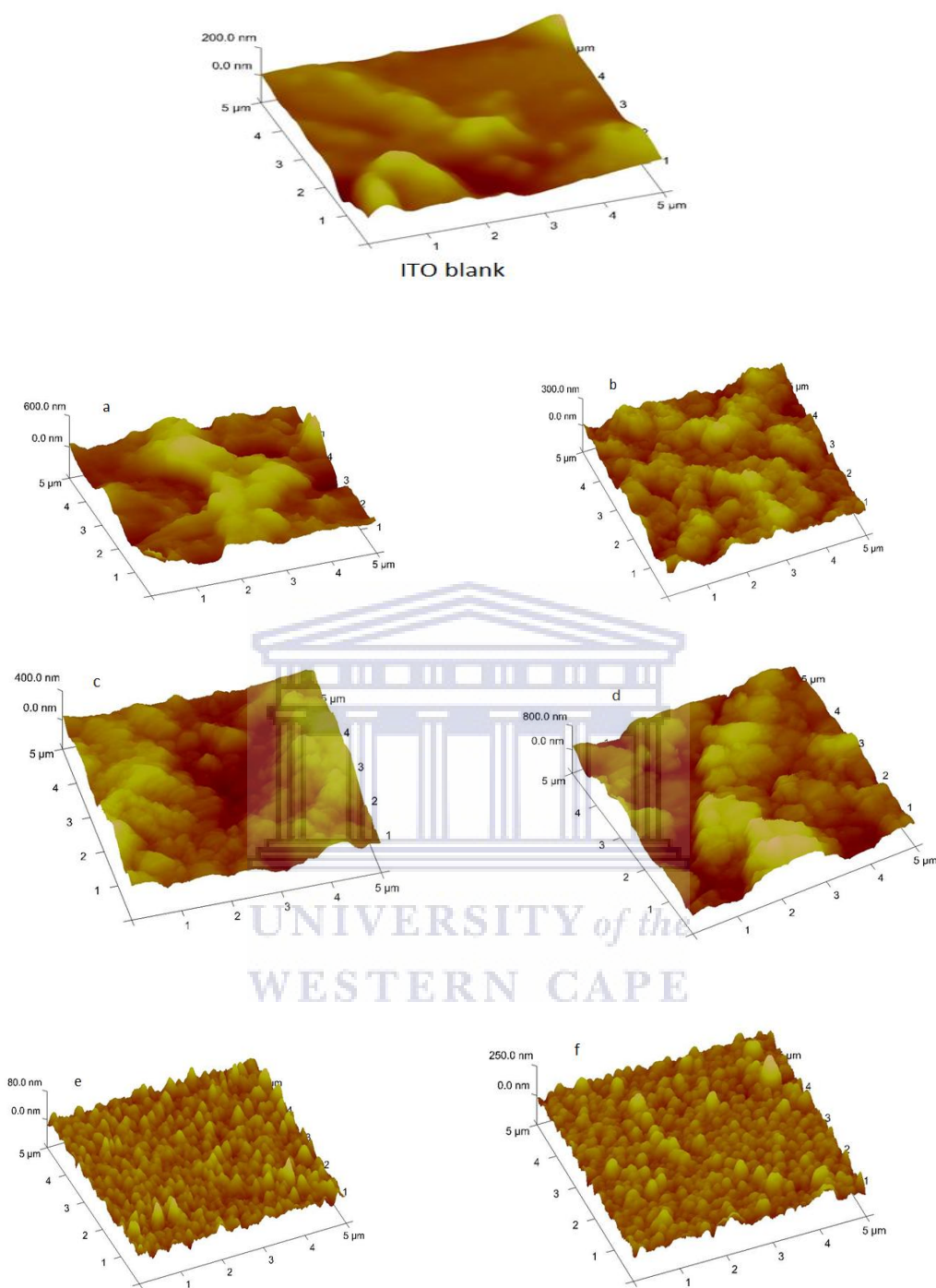
Figure 5.13: AFM image of: ITO electrode blank top, a) PMOT1), b) PMOT-co-PEDOT1, c) PEDOT1 electrochemically synthesized in bmimbf$_4$ and d) PMOT2, e) PMOT-co-PEDOT2 and f) PEDOT2 grown in octmimtnf$_2$. Films were completely oxidized by applying +0.95 V DC voltage in aq. LiClO$_4$.

(Fig. 5.13a & e) and PMOT2 and PEDOT2 (Fig. 5.13b & f) respectively. Thus the copolymerization caused different morphology as it caused different electrochemical or optical properties. The PMOT1 film formed in bmimbf$_4$ appears to possess a more globular topography hence porosity significantly incorporating 1-buthyl-3-methyl imidazolium cation [31, 40-41]. Roughness analysis of PMOT1 image estimated as root mean roughness (Rq) was 129 nm. In contrast, when PMOT2 grown in octmimtnf$_2$ (Fig. 5.13b) the film become smoother (Rq = 46.6 nm), more ordered and denser. In the case the PMOT-co-PEDOT1 finer granular (R$_q$ = 86.0 nm) topography than PMOT-co-PEDOT2 (Rq = 181 nm) observed. Both PEDOT1 (R$_q$ = 9.29 nm) and PEDOT2 (R$_q$ = 29.6 nm) the polymer film has 'grain packed' structure which is a typical characteristic of 3D growth mechanism [31, 41]. Thus the nature of the ionic liquid changes the film morphology.
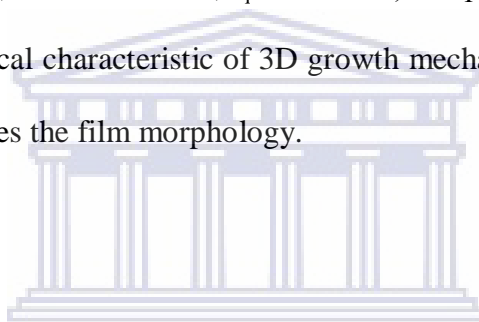
Conclusion

3-Metoxythiophe (MOT) and its mixture with 3,4-ethylenedioxythiophene (EDOT) have been successfully electropolymerized in both bmimbf$_4$ and octmimtnf$_2$ ionic liquids. Film growth was faster in the less viscous and more conductive octmimtnf$_2$ hydrophobic than bmimbf$_4$ hydrophilic ionic liquids as it was jugged from peak current and the total charge of polymerization from its CV. Poly(3-methoxythophene) and its copolymer with PEDOT were electrochemically activity both in ionic liquids and aqueous LiClO$_4$. Plot of anodic peak current versus scan rate shows a quasi reversible electrochemical profile. PMOT-co-PEDOT1 and PMOT-co-PEDOT2 copolymers CVs, uv-visible spectrum and their morphology were quite different from that of the homopolymers (PMOT1 and PEDOT1) and (PMOT2 and PEDOT2) indicating copolymerization. All of the obtained polymers exhibited absorption

115

bands changes with potential. PMOT1 and PMOT2 in the reduced state, the maximum absorption band appeared at about λ_{max} 480 and 485 nm (red colour) and when the polymer film was doped broad absorption peak generated at about centre of maximum wavelength λ_{max} 645 nm and 600 nm (blue colour) for PMOT1 and PMOT2. On the other hand, PMOT-co-PEDOT1 and PMOT-co-PEDOT2 absorption bands changed from 560 nm (blue) during reduction to 795 to 970 nm during oxidation (near infrared region). The modulation of colour by changing voltage in the visible and near infrared region made these material good candidates for application in electrochromic devices.

5.2 Electrochemical studies on 4, 7-dithien-2-yl-2, 1, 3- benzothiadiazole (DTBT) in various media

Oxidation and reduction of DTBT monomer was investigated using cyclic voltammetry in both organic and ionic liquids to generate preliminary electrochemical data about the monomer such as bandgap and oxidation potential. To further understand the kinetics of reduction of DTBT to its anion (DTBT$^-$), electrochemical impedance spectroscopy was used to study DTBT/DTBT$^-$ redox system at equilibrium. The standard heterogeneous rate constant (k^o) is calculated from the charge transfer resistance which was estimated from impedance data. Diffusion coefficient of DTBT, formal potential of DTBT/DTBT$^-$ system was related to the physicochemical properties of the various media employed in this study.

5.2.1 Synthesis and characterization of 4,7-dithien-2-yl-2,1,3- benzothiadiazole

DTBT has been successfully synthesized using Stille coupling reaction according to literature procedure. The product was characterized by employing uv-visible and ATR-FTIR spectroscopy, H^1 NMR and C^{13} NMR spectroscopy.

The purity of DTBT was checked using thin layer chromatography and uv-visible fluorescence, there was no impurity observed in both cases. The melting point of DTBT was found to be in the range of 118 – 122 $^\circ$C, in agreement to that reported by Kitamura *et al* [168]. Uv-visible spectra of DTBT in CHCl$_3$ is shown in (Fig. 5.14) and its wavelength of maximum absorbance occurred at λ_{max} (CHCl$_3$) 446 nm (log ε/dm^3 /mol cm 4.15) which was also consistent with its literature value [168]. ATR-FTIR spectra (Fig. 4.16) stretching frequency around v_{max}/cm 3634 and 1219 (CH) stretching of thiophene and thiophene ring, 1007 (CH) stretching aromatics and 1387 (C=N) shows the presence of thiophene and benzene ring.

The same result as literature consistent with type and number of protons for H^1 NMR and C^{13}NMR were observed for DTBT [168] as depicted from (Fig. 5.16 and 5.17) respectively. H^1 NMR δ 7.21 (dd, J = 3.7, 4.9 Hz, 2H), δ 7.45(dd, J= 0.9, 4.9 Hz, 2H), δ 7.85 (s, 2H), δ 8.10 (dd, J =0.9, 3.7 Hz, 2H) and ^{13}C NMR (δ125.8, 126.0, 126.8, 127.5, 128.0, 139.3, 150.0
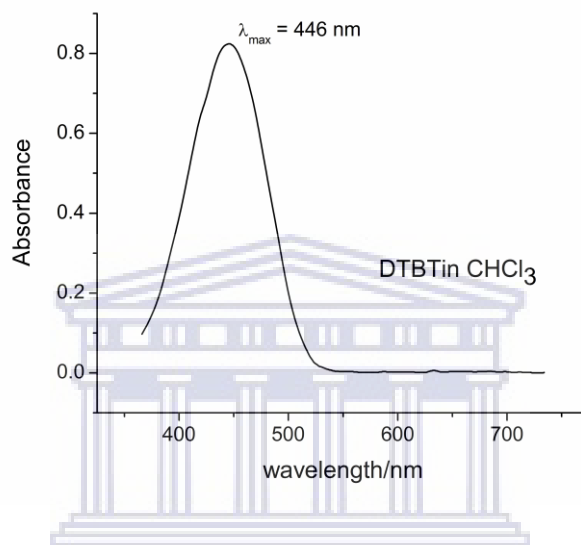
Figure 5.14: Uv-visible spectra of DTBT in CHCl₃.
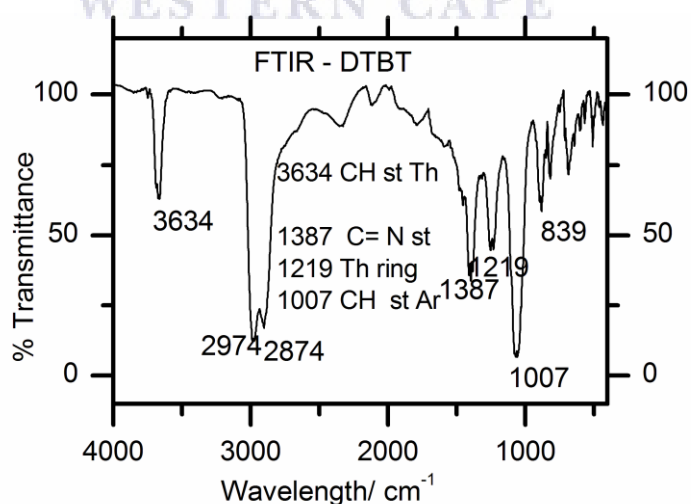
Figure 5.15: ATR - FTIR spectra of DTBT.
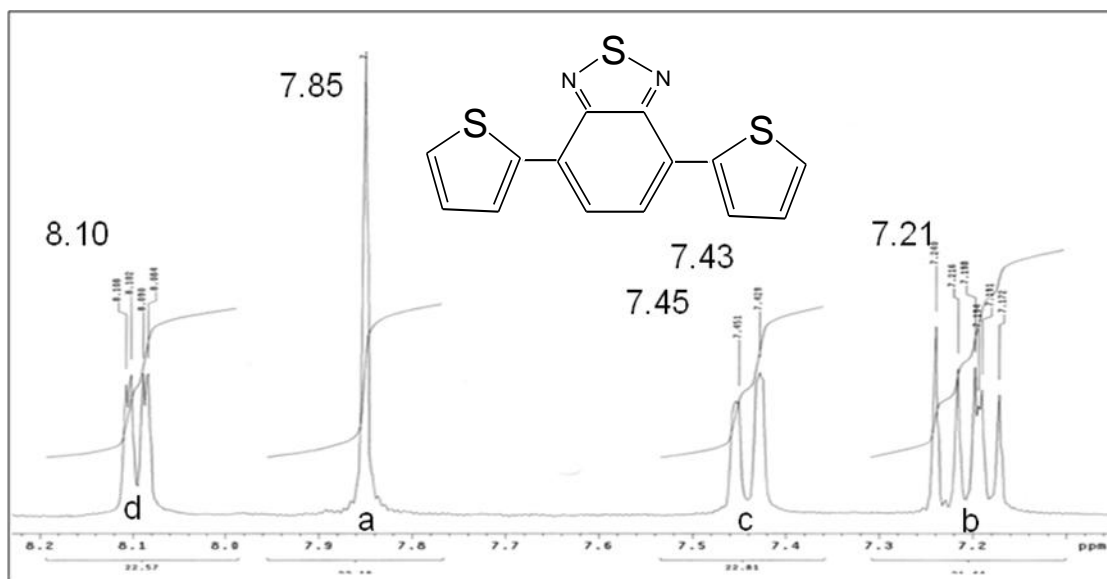
Figure 5.16: H^1 NMR spectra of DTBT.
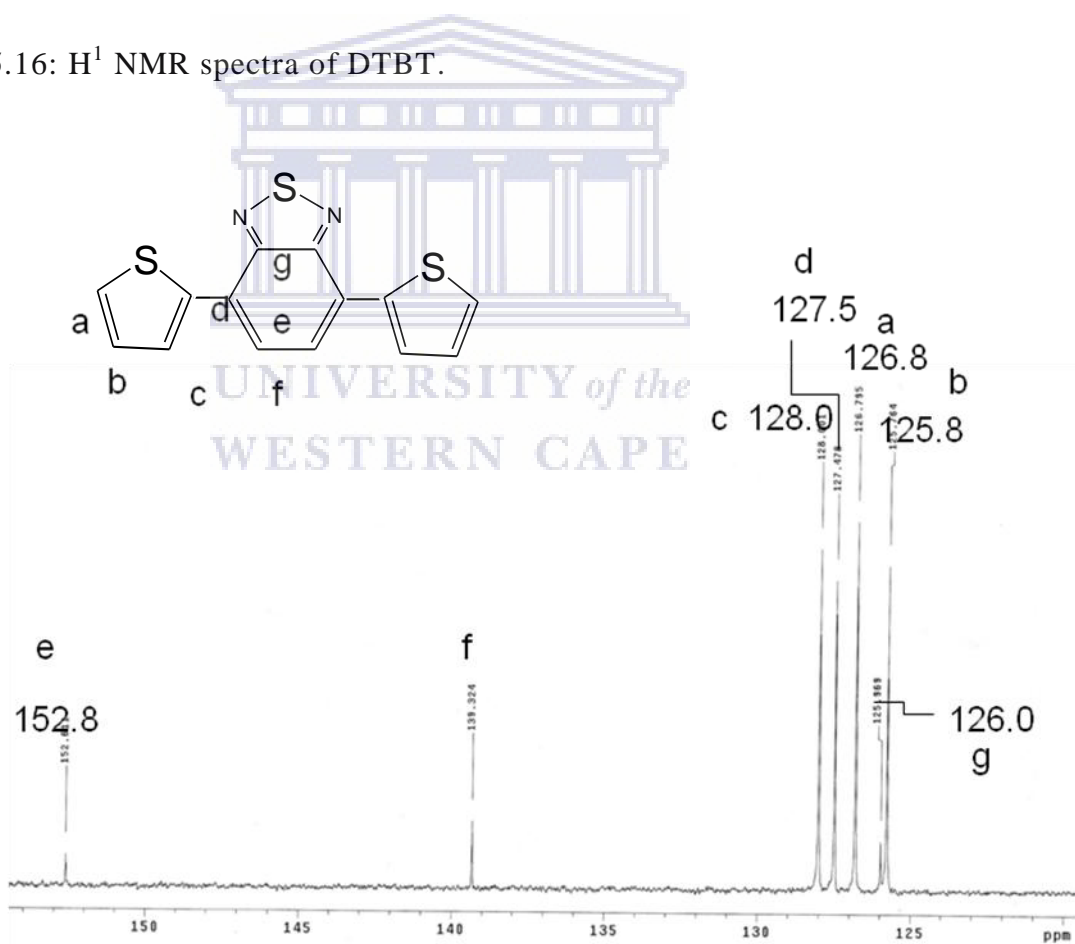
Figure 5.17: C^{13} NMR spectra of DTBT.

5.2.2 Electrochemical profile of DTBT in organic solvents

Electrochemical experiment of 4,7-dithien-2-yl-2,1,3-benzothiadiazole (DTBT) was carried out with a solution of 0.85 mM DTBT in acetonitrile (ACN), dichloromethane (DCM) and mixture of dichloromethane and acetonitrile with a ratio of 2 to 3 (DCM–ACN (2:3 (v/v)) on Au, Pt and GC electrodes using 0.1 M n-tetrabuthylammonium perchlorate (n-Bu$_4$NClO$_4$) as supportive electrolyte. Figure 5.18 shows the cyclic voltammograms of 0.1 M n-tetrabuthylammonium perchlorate supportive electrolytes in acetonitrile, mixture of acetonitlie and dichloromethane and dichloromethane. Cyclic voltammograms of 0.85 mM DTBT in 0.1 M n-Bu$_4$NClO$_4$/acetonitrile, 0.1 M n-Bu$_4$NClO$_4$/acetonitrile – dichloromethane mixture (2:3 v/v) and 0.1M n-Bu$_4$NClO$_4$/ dichloromethane recorded at scan rate of 100 mV/s are presented in Fig. 5.19. 4,7-Dithien-2-yl-2,1,3-benzothiadiazole oxidized at a potential of 1.00 V *versus* Fc/Fc$^+$ on GC electrode. Here after all potentials are reference to ferrocene-ferrocinium redox potential unless stated otherwise, redox couple of Fc/Fc$^+$ was 0.1 V vs. platinum pseudo reference electrode on Au and GC whereas on Pt it was 0.13 V. DTBT showed both an irreversible oxidation and a reversible reduction waves (Fig. 5.19). During anodic scan DTBT oxidized irreversibly and its oxidation peak potential (E$_{pa}$) was around 1.0 V and 0.98 V both at (Pt and Au) and GC electrodes respectively. The type of solvent and electrode used had no significant effect on the oxidation potential of DTBT (Table 5.4). In contrast, during cathodic scan a reversible reduction peak (E$_{pc}$) appeared which was dependent on the type solvent, varied by about 200 mV between acetonitrile and dichloromethane. As shown in the table, reduction peak potential of DTBT were -1.42 V in ACN and -1.62 V in DCM at Au, -1.44 in ACN and -1.57 V in DCM at Pt and -0.95 V in ACN and -1.20 V in DCM at GC electrodes. It is important to notice that DTBT oxidized slightly at lower positive potential and reduced at lower negative potential in acetanilide than in dichloromethane. The result indicates that DTBT exhibited ambipolar (amphoteric) redox

behaviour. A similar finding was reported by Kitamura *et al* [168] from the electrochemical oxidation of DTBT in benzonitrile/0.1 M n-Bu$_4$NClO$_4$ at Pt disk electrode (E_{pa} = 1.23 V and E_{Pc} = -1.22 vs SCE) at the same scan rate of 100 mV/s.

The reduction potential reflects the LUMO levels of the benzothiadiazole heterocyclic acceptor unit whereas the HOMO indicates the donor unit. The difference in redox potential ($\Delta E = E_{pa}–E_{pc}$) approximately corresponds to optical HOMO – LUMO separation calculated
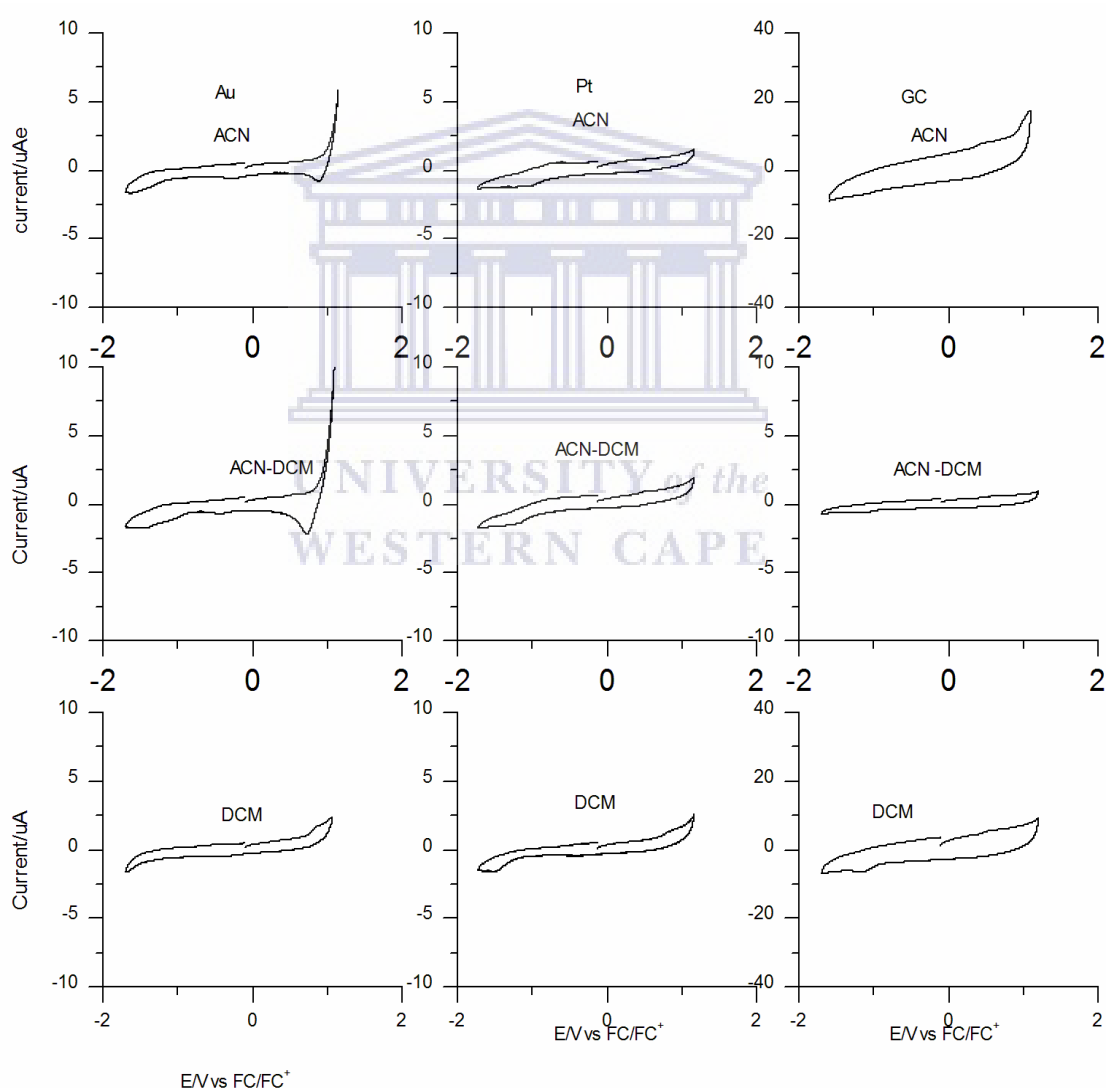
Figure 5.18: Cyclic voltammograms of the supportive electrolyte 0.1 M n-Bu$_4$NClO$_4$ in ACN, 0.1 M n-Bu$_4$NClO$_4$ in DCM-ACN (2:3 v/v) and 0.1 M n-Bu$_4$NClO$_4$ in DCM at Au, Pt and GC electrodes.
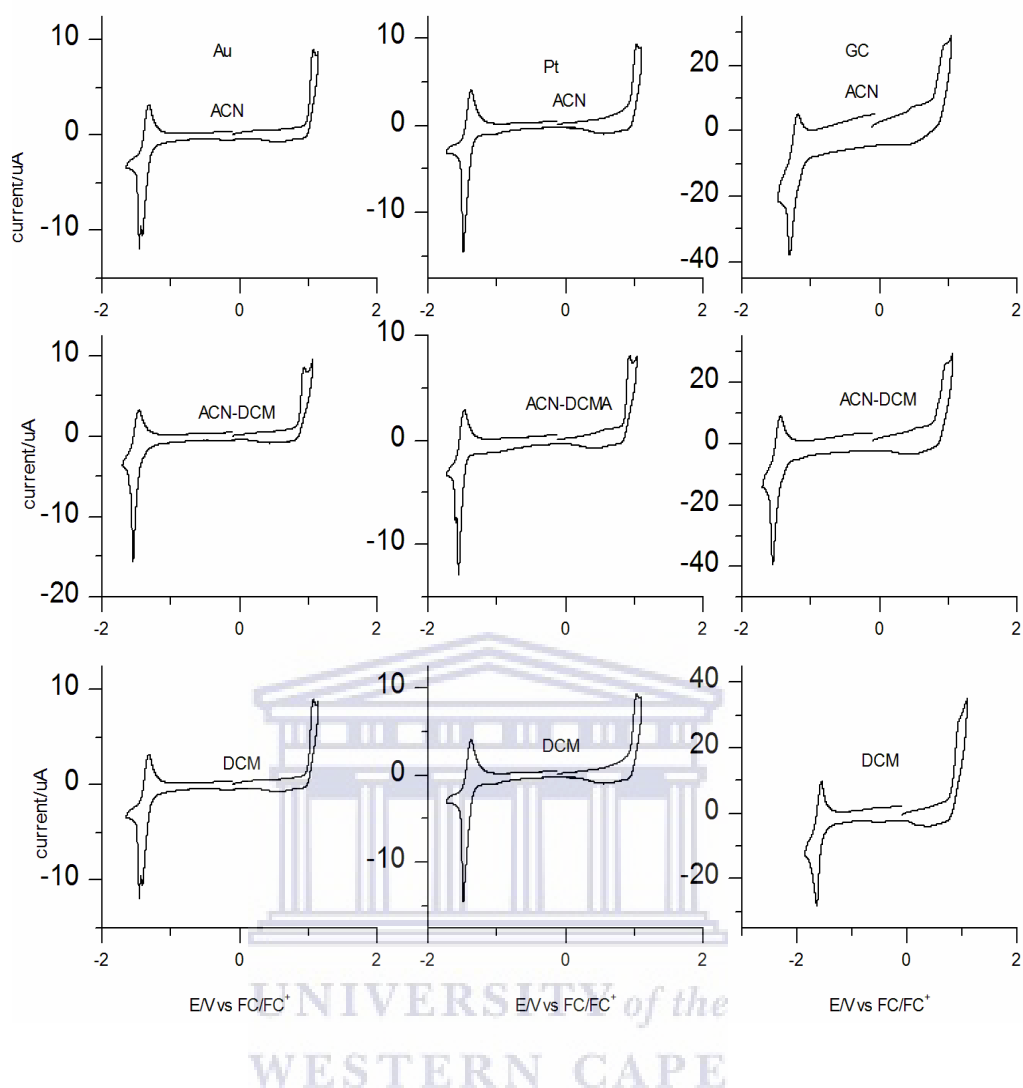
Figure 5.19: Cyclic voltammograms of 0.85 mM DTBT in 0.1 M n-Bu₄NClO₄ + ACN, 0.1 M n-Bu₄NClO₄ + DCM-ACN-(2:3 v/v) and 0.1 M n-Bu₄NClO₄ + DCM/ at Au, Pt and GC electrodes.

Table 5.4: CV parameters of 0.85 mM DTBT oxidation in organic media at scan rate of 100 mV/s.

Electrode	E_{pa}/V			E_{pc}/V			ΔE_p/V		
	ACN	DA	DCM	ACN	DA	DCM	ACN	DA	DCM
Pt	0.90	1.04	0.95	-1.57	-1.44	-1.56	2.33	2.48	2.51
Au	0.94	1.03	0.88	-1.42	-1.46	-1.62	2.36	2.49	2.50
GC	0.98	0.96	0.95	-1.40	-1.54	-1.62	2.28	2.50	2.57

DA represents dichloromethane – acetontrile mixture

Table 5.5: Summary of oxidation of 0.85 mM DTBT in organic media at 100 mV/s, anodic (I) irreversible and (II) cathodic reversible redox pairs.

Electrode	Solvent	E_{pa}^{I}/V	E_{pa}^{II}/V	E_{pa}^{II}/V	E_{g}^{a}/ eV	E_{g}^{b}/eV
Pt	ACN	1.05	-1.48	-1.36	2.53	
	DCM-ACN	0.93	-1.54	-1.46	2.49	
	DCM	0.89	-1.66	-1.61	2.55	
Au	ACN	1.07	-1.43	-1.31	2.50	
	DCM-ACN	0.94	-1.54	-1.45	2.48	
	DCM	0.92	-1.64	-1.58	2.50	2.66
GC	ACN	1.03	-1.34	-1.44	2.48	
	DCM-ACN	1.024	1.00	-1.50	2.49	
	DCM	1.00	0.95	-1.64	2.48	

from maximum absorption wavelength (λ_{max} 466 nm (2.66 eV). As shown in Table 5.4 ΔE_p of DTBT in dichloromethane is slightly wider by about 0.14 to 0.19 eV than in acetonitrile. The result indicates acetonitrile is favourable solvent for reducing HOMO – LUMO separation of DTBT.

5.2.3 Analysis of CV data of DTBT/DTBT⁻ redox system

The reduction of 0.85 mM DTBT to its anion (DTBT⁻) in acetonitrile, dichloromethane and in their mixture in the presence of 0.1 M n-Bu₄NClO₄ as supportive electrolyte were investigated on Pt, Au and GC electrode to study the variation of anodic and cathodic peak potential with subsequent cycles, the dependence of the cathodic and anodic peak potential separations, reversibility of DTBT/DTBT⁻ redox pair and to propose electrode reactions. Representative cyclic voltammograms of DTBT/DTBT⁻ redox couple in acetonitrile,

acetonitrile–dichloromethane (2:3 v/v) and dichloromethane using 0.1 M n-Bu$_4$NClO$_4$ as a supportive electrolyte using various scan rates ranging from 0.075 - 0.5 V/ s are shown in (Figs. 5.20 - 5.22) and the cyclic voltammetric data of 0.85 mM reduction CVs are collected in Table 5.6-5.9. The cyclic voltammograms illustrates that as the voltage becomes more negative during cathodic scan a reduction peak (E$_{pc}$ and i$_{pc}$) appeared and in the reverse scan an anodic peak with a smaller peak current (E$_{pa}$ and i$_{pa}$) formed as a result of oxidation of DTBT$^-$ produced during the first cathodic scan to the neutral DTBT compound. Reduction of DTBT to DTBT$^-$ anion and oxidation of DTBT anion back to DTBT occurred according to the proposed electrode reaction shown in scheme 4.

Scheme 4: Oxidation and reduction of DTBT
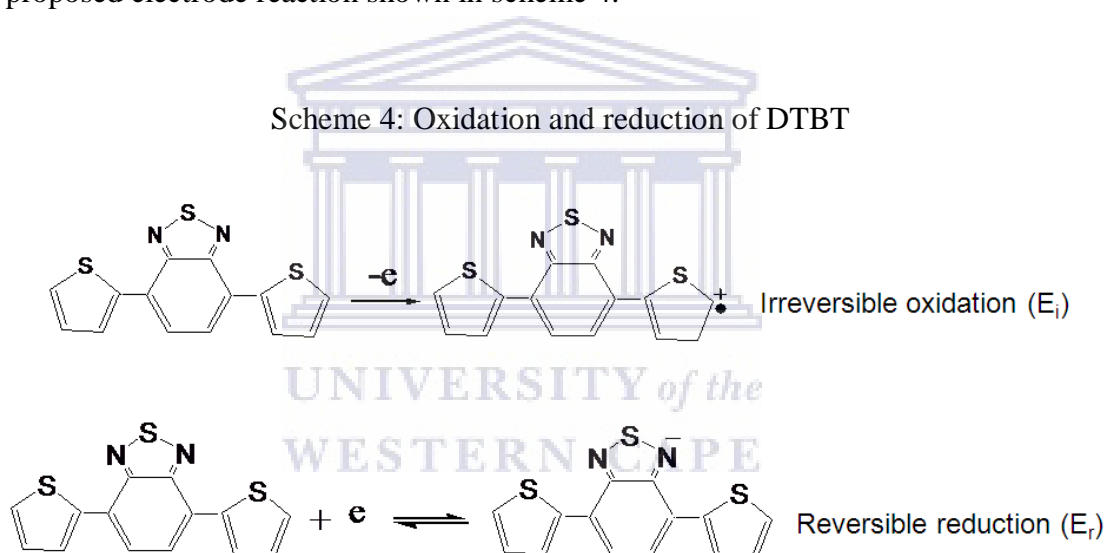
As shown in the Tables, the same redox potential but slightly different peak potentials were recorded with scan rates. The anodic and cathodic peak potentials difference (ΔE_p) was found to be in the range of 0.06 to 0.1 V, reveals reduction of DTBT is a one electron transfer reversible process. A relatively larger value of ΔE_p observed in DCM is due to uncompensated solution resistance.

The anodic peak current (i$_{pa}$) was found to be dependent on the switching potential and the actual baseline for measuring i$_{pa}$ cannot be determined in this case. Therefore the anodic and

cathodic current ratio was calculated using Nicholson expression (Eq.5.1) from the uncorrected anodic peak current $(i_{pa})_o$ with respect to the zero baseline current and the current at switching potential, $(i_{sp})_o$ [192]. It was found that the current ratio was nearly equal to one and remains constant with sweep rate in all of solvents used in the investigation (Table 7-9). Besides, the experimental results presented above the current ration confirmed the reversibility of DTBT/DTBT⁻ redox system with no chemical reactions couple to this one electron transfer process. Furthermore, it illustrates the stability of DTBT anion on the experimental time scale. It was also observed that the cyclic voltammograms recorded at specified scan rate remains constant with successive cycles, indicates the absence of decomposition of reaction product.

$$\frac{i_{pa}}{i_{pc}} = \frac{(i_{pa})_o}{i_{pc}} + \frac{0.485(i_{sp})_o}{i_{pc}} + 0.086 \qquad (5.1)$$

Where $(i_{pa})_o$ uncorrected anodic peak current read at the peak and $(i_{sp})_o$ the current at switching potential.
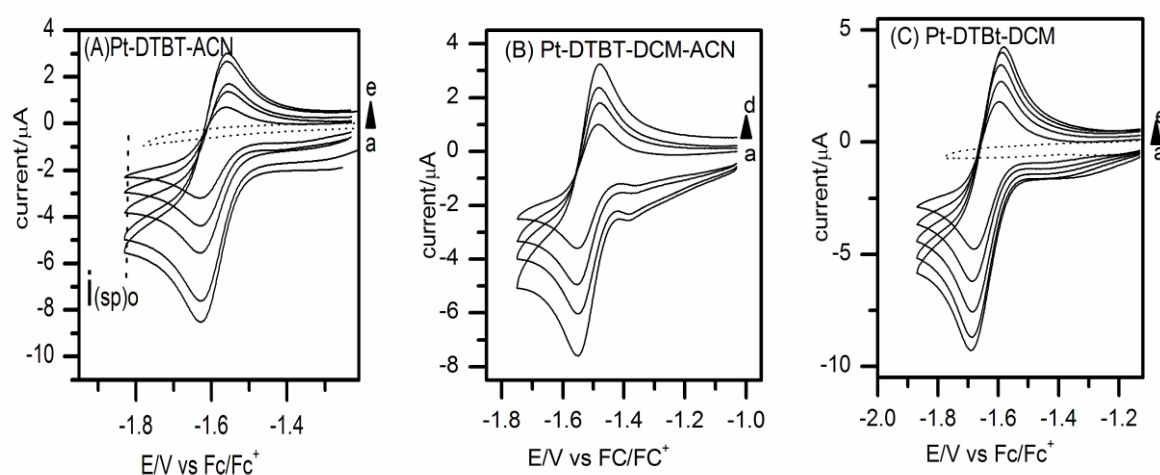
Figure 5.20: Cyclic voltammograms of reduction of 0.85 mM DTBT (A) 0.1 M n-Bu₄NClO₄/ACN, (B) in 0.1 M Bu₄NClO₄/ DCM-ACN (2:3v/v) and (C) in 0.1 M n-Bu₄NClO₄/ DCM at Pt a) 100, b) 200, c) 300, d) 500 mV/s.

125
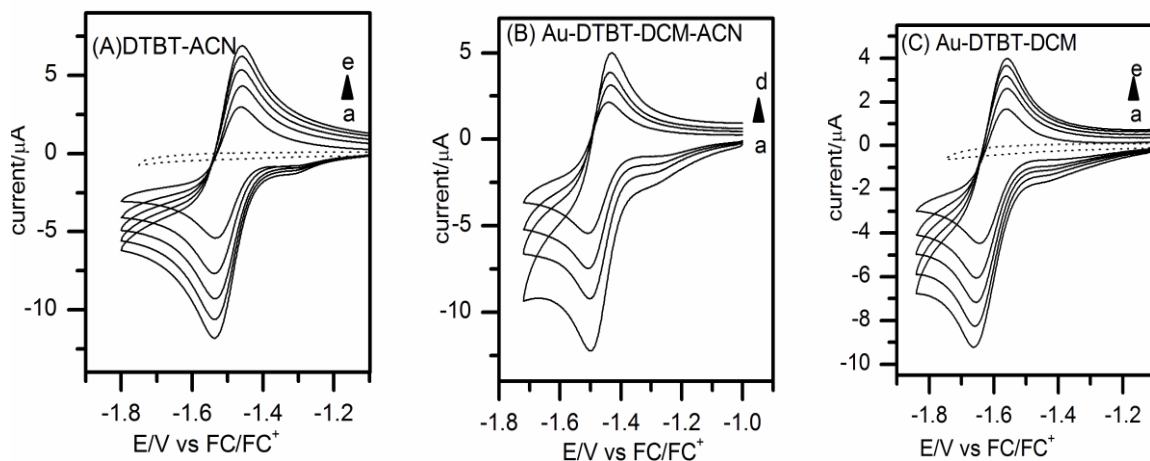
Figure 5.21: Cyclic voltammogram of reduction 0.85 mM DTBT (A) in 0.1 M n-Bu$_4$NClO$_4$/ACN, (B) in 0.1 M Bu$_4$NClO$_4$/ DCM-ACN (2:3 v/v) and (C) in 0.1 M n-Bu$_4$NClO$_4$/ DCM at Au a) 100, b) 200, c) 300 and d) 500 mV/s.
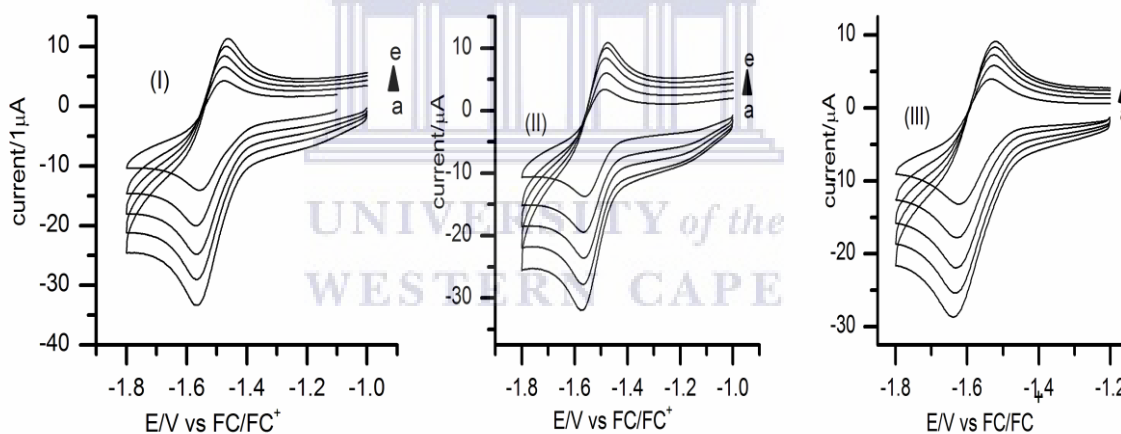
Figure 5.22: Cyclic voltammogram of reduction of 0.85 mM DTBT (I) in 0.1 M n-Bu$_4$NClO$_4$/ACN, (II) 0.1 M n-Bu$_4$NClO$_4$/DCM-ACN (2:3 v/v) and (III) in 0.1 M n-Bu$_4$NClO$_4$/ DCM at GC a) 100, b) 200, c) 300, d) 400 and e) 500 mV/s.
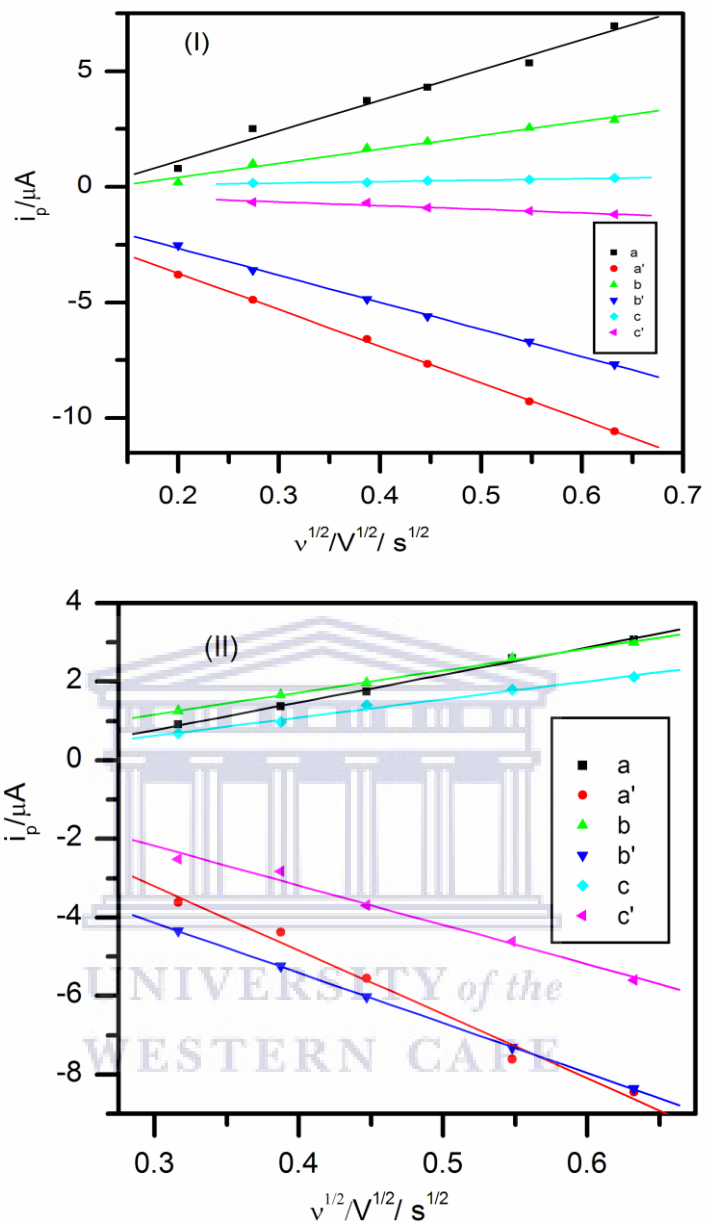
Figure 5.23: "Sevcik plots" of 0.85 mM DTBT (I) at Au electrode a) in ACN: Y = -0.72272 + 11.5186 X (anode), a') Y = -0.47984 -15.95475 X (cathodic), b) in DCM-ACN (2:3 v/v): Y= -0.1132 + 7.21923 X (anodic), b') Y = -0.01826 -16.74338 X (cathodic), c) in DCM Y = -0.4628 + 7.0934 X (anodic), c') Y = 0.79635-12.20623 X (cathodic) and (II) at Pt electrode a) in ACN: Y = -1.16773 + 5.8200 X, (anodic), a') Y = 1.1.20243-13.30874 X (cathodic), b) in DCM-ACN (2:3 v/v): Y = -0.78617 + 5.73788 X (anodic), b') Y = -0.3542 -10.1364 X (cathodic) c) in DCM Y = -0.46281 + 7.09344 X (anodic) and c') Y = 0.79635-12.20623 X (cathodic). In all cases R^2 >0.99.

Summary of scan rate (υ), anodic (E_{pa}) and cathodic (E_{pc}) peak potentials, anodic and cathodic peak current ratios (i_{pa}/i_{pc}), peak potential separation (ΔE_p) from the CV of reduction of 0.85 mM DTBT in ACN, DCM-ACN (2:3 (v/v)) and (DCM) (0.1 M n-Bu$_4$NClO$_4$) are depicted in Table 5.7-5.9.

Table 5.6: Summary of mean CV parameters of 0.85 mM DTBT reduction in organic media (standard deviation 1−3%).

Electrode	Solvent	E_{pa}/V	E_{pc}/V	$E^{o'}$/V	i_{pa}/i_{pc}	ΔE_p/V
Pt	ACN	-1.55	-1.62	-1.56	0.72	0.07
	DCM – ACN	-1.48	-1.54	-1.52	0.78	0.06
	DCM	-1.56	-1.65	-1.62	0.82	0.09
Au	ACN	-1.43	-1.55	-1.50	0.88	0.08
	DCM-ACN	-1.48	-1.56	-1.52	0.85	0.08
	DCM	-1.52	-1.61	-1.56	0.84	0.09
GC	ACN	-1.47	-1.56	-1.51	0.78	0.09
	DCM-ACN	-1.48	-1.56	-1.52	0.75	0.08
	DCM	-1.52	-1.62	-1.58	0.61	0.09

Linear relation was obtained from Randles –Sevcik plot (Fig. 5.23).The result showed the reduction of DTBT was both reversible and diffusion control process in all of the organic solvents and on three of electrodes. DTBT diffusion coefficient was calculated using Randles – Sevcik equation (Eq.4.1) and the values are summarized in Table 5.10. As depicted from the Table, the diffusion coefficient of DTBT was about 10 times larger in ACN

Table 5.7: Parameters from the CV of the reduction of 0.85 mM DTBT in 0.1 M n-Bu$_4$NClO$_4$/organic solvents at Pt electrode.

Acetonitrile

υ/ V/s	E_{pa}/V	E_{pc}/V	i_{pa}/i_{pc}	ΔE_p/V	$E_{1/2}$/V
0.1	-1.560	-1.624	0.66	0.064	-1.592
0.2	-1.554	-1.624	0.73	0.070	-1.589
0.3	-1.554	-1.624	0.74	0.070	-1.589
0.4	-1.554	-1.625	0.77	0.069	-1.589
0.5	-1.554	-1.625	0.77	0.069	-1.589
Dichloromethane-acetonitrile (DCM-ACN (2:3 v/v))					
0.1	-1.487	-1.560	0.70	0.07	-1.549
0.2	-1.482	-1.563	0.77	0.081	-1.523
0.3	-1.478	-1.563	0.80	0.085	-1.520
0.4	-1.478	-1.563	0.83	0.085	-1.520
0.5	-1.478	-1.563	0.83	0.085	-1.520
Dichloromethane (DCM)					
0.1	-1.555	-1.638	0.76	0.073	-1.596
0.2	-1.546	-1.641	0.81	0.095	-1.593
0.3	-1.546	-1.641	0.84	0.095	-1.593
0.4	-1.546	-1.641	0.83	0.095	-1.593
0.5	-1.544	-1.646	0.88	0.102	-1.595

Table 5.8: Parameters from the CV of reduction of 0.85 mM DTBT in 0.1 M n-Bu$_4$NClO$_4$/ organic solvents at Au electrode.

Acetonitrile

υ/V/s	E_{pa}/V	E_{pc}/V	i_{pa}/i_{pc}	ΔE_p/V	$E_{1/2}$/V
0.1	-1.426	-1.498	0.83	0.077	-1.459
0.2	-1.422	-1.498	0.90	0.076	-1.460
0.3	-1.417	-1.498	0.91	0.081	-1.458
0.4	-1.417	-1.498	0.93	0.081	-1.458
0.5	-1.417	-1.498	0.87	0.081	-1.458
Dichloromethane-acetonitrile (2:3 (v/v))					
0.1	- 1.480	-1.553	0.81	0.071	-1.515
0.2	-1.480	-1.558	0.85	0.078	-1.519
0.3	-1.480	-1.562	0.86	0.082	-1.520
0.4	-1.480	-1.562	0.86	0.082	-1.520
0.5	-1.480	-1.562	0.88	0.082	-1.520
Dichloromethane					
0.1	-1.535	-1.601	0.78	0.066	-1.568
0.2	-1.524	-1.608	0.84	0.084	-1.566
0.3	-1.523	-1.608	0.87	0.083	-1.565
0.4	-1.519	-1.608	0.87	0.089	-1.563
0.5	-1.519	-1.608	0.87	0.089	-1.563

Table 5.9: Parameters from the CV of reduction of 0.85 mM DTBT in 0.1 M n-Bu$_4$NClO$_4$/ organic solvents at GCE.

Acetonitrile

υ/V/s	E$_{pa}$/V	E$_{pc}$/V	i$_{pa}$/i$_{pc}$	ΔE$_p$/V
0.1	-1.475	-1.551	0.74	0.076
0.2	-1.472	-1.561	0.85	0.089
0.3	-1.472	-1.561	0.83	0.089
0.4	-1.472	-1.561	0.79	0.089
0.5	-1.469	-1.561	0.91	0.092
Dichloromethane-acetonitrile (2:3 v/v)				
0.1	-1.480	-1.557	0.70	0.077
0.2	-1.475	-1.565	0.78	0.090
0.3	-1.475	-1.565	0.83	0.090
0.4	-1.475	-1.565	0.82	0.090
0.5	-1.472	-1.573	0.81	0.101
Dichloromethane				
0.1	-1.530	-1.618	0.58	0.088
0.2	-1.522	-1.623	0.62	0.101
0.3	-1.522	-1.629	0.63	0.101
0.4	-1.519	-1.629	0.64	0.110
0.5	-1.519	-1.631	0.64	0.112

(1.11 x 10^{-5} cm/s) compare to in DCM (5.75 x 10^{-6} cm/s) whereas in DCM-ACN (2:3 v/v) as expected, the diffusion coefficient falls in the range between the value of DTBT in ACN and DCM. The diffusion coefficient of DTBT increased in the following order DCM < DCM-

ACN < ACN. This is attributed to the progressive decrease of viscosity (η) of the solvent medium as going from DCM to ACN (Table 5.10). The same trend was recorded in all types electrodes.

Table 5.10: Physical properties of acetonitrile and dichloromethane [204].

Solvent	donor number (DN) kJ/mol	density/ ρ g/cm^3	viscosity η/mPa.s	refractive index n
Acetonitrile	59.0	0.78	0.361	1.340
Dichloromethane	4.2	1.316	0.420	1.40

On the other hand, the result presented in Table 5.11, shows a decrease in the diffusion coefficient of DTBT anion (D_{ox}) compare to the neutral DTBT monomer (D_{red}). The diffusion coefficient of DTBT anion was nearly equal to half of the diffusion coefficient of neutral DTBT on Pt and GC electrodes in three of the solvents. When acetonitrile used as a medium at Au electrode the value of D_{ox} of DTBT$^-$ was about one fourth to that of the D_{red} of the neutral species. Explanation to the lower diffusion coefficient of DTBT$^-$ anion could be most likely due to the strong interactions between the anion of DTBT with the solvent molecules (salvation) that can make the hydrodynamic radius of the diffusion species large and hence reduce the mobility. As classically predicted, diffusion coefficient is inversely proportional to viscosity according to Stokes – Einstein equation (Eq.5.2) as shown in literature [205].

$$D = \frac{k_B T}{6\pi c \eta r_h} \qquad (5.4)$$

Where k_B is the Boltzmann's constant, T temperature (K), η viscosity of the solvent medium, r_h hydrodynamic radius and c is a constant.

Table 5.11: Diffusion coefficient of 0.85 mM DTBT in acetonitrile, dichloromethane–acetontrile mixture and dichloromethane (error < 0.08).

Electrode	solvent	D_{red}/cm^2/s	D_{ox}/cm^2/s
Pt	ACN	1.11×10^{-5}	1.63×10^{-6}
	DCM-ACN	5.06×10^{-6}	8.09×10^{-7}
	DCM	7.45×10^{-6}	1.63×10^{-6}
Au	ACN	1.11×10^{-5}	5.51×10^{-6}
	DCM-ACN	6.04×10^{-6}	1.30×10^{-6}
	DCM	5.71×10^{-6}	1.59×10^{-6}
GC	ACN	1.02×10^{-5}	1.25×10^{-6}
	DCM-ACN	7.82×10^{-6}	1.58×10^{-6}
	DCM	5.71×10^{-6}	8.83×10^{-7}

5.2.4 Electrochemical impedance spectroscopy of DTBT/DTBT$^-$ redox couple

Electrochemical impedance spectroscopy (EIS) is a powerful method to determine the electrode kinetics of a redox system. The impedance of a redox couple is measured by applying an ac voltage of a small amplitude 2-10 mV on a system at dc potential commonly at its formal potential in a frequency range of 0.1 mHz to 10^5 Hz. Then the impedance spectra recorded is fitted to an appropriate electrical model to determine circuit elements such as charge transfer resistance. Substituting the charge transfer resistance in (Eq. 4.16), standard exchange current density and charge transfer kinetics (heterogeneous rate constant (k^o)) can be easily calculated using (Eq. 4.15).

EIS was employed to study DTBT/DTBT$^-$ redox couple charge transfer kinetics in organic solvents. Impedance spectra of DTBT/DTBT$^-$ redox couple at Pt and Au electrode in the

presence of 0.1 M n-Bu$_4$NClO$_4$ electrolyte in ACN, DCM-ACN (2:3 v/v) and DCM are shown Nyquist plot (Figs 5.24A & 5.25A) and Bode plot(Figs. 5.24B &5.25B). The impedance spectra of Nyquist plot shows a semi-circle plus a Warburg line (nearly 45°) implies a quasi-reversible process. The presence of a small semi semicircle in higher frequency region shows fast interfacial electron transfer. Spectra of DTBT/DTBT$^-$ was best fitted to a typical Randles cell to find out the electrical parameter. Electrical parameterizes for the redox couple are summarized in Table 5.12 and uncertainties were less than 10% which is considered as an acceptable value.

As depicted in Table 5.12, the charge transfer resistance (Rct) varies with solvent viscosity as expected. It increased in the order of ACN < DCM-ACN < DCM. Similar to Rct, solution resistance (Rs) followed the same trend. Since DCM is more viscous than ACN, higher charge transfer between the electrode and DTBT/DTBT$^-$ interface recorded in comparison to the lower viscous (ACN) solvent. In contrast, a low standard heterogeneous constant (k^o) recorded for DTBT/DTBT$^-$ as evaluated by applying (Eq. 4.15) (Table 5.12), clearly shows relatively a larger magnitude of k^o in acetonitrile than in other solvents. This is attributed to the low viscosity of acetonitrile for the observed DTBT/DTBT$^-$ fast kinetic.

Table 5.12: Electrical parameters of DTBT/DTBT$^-$ from circuit fitting (error < 0.01).

Solvent	Pt				Au			
	R_s/Ω	R_{ct}/Ω	$C_{dl}/\mu F$	$Z_W/k\Omega$	R_s/Ω	R_{ct}/Ω	$C_{dl}/\mu F$	$Z_W/k\Omega$
ACN	381.1	223.7	0.214	47.2	398.3	35.51	0.211	26.2
DCM-ACN	580.7	184.8	1.208	31.1	397.8	64.15	0.226	42.5
DCM	696.4	253.2	0.003	83.8	781.6	214.3	0.182	108.8
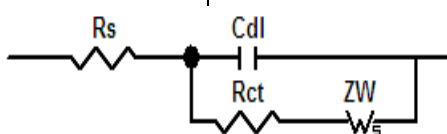
Model: Randles cell

Effect of the type of electrode on charge transfer kinetics was also studied. It is important to notice that, standard heterogeneous constant of DTBT/DTBT⁻ redox system at Au electrode was larger by about three-fold compare to that that of Pt electrode (Table 5.13). Possible explanation to this trend could be the presence of sulphur atoms in benzothiadiazole ring in DTBT molecule. It has been well known that sulfur has a higher affinity towards gold [206], consequently charge transfer kinetics of DTBT/DTBT⁻ at Au is expected to be higher in comparison to Pt electrode.
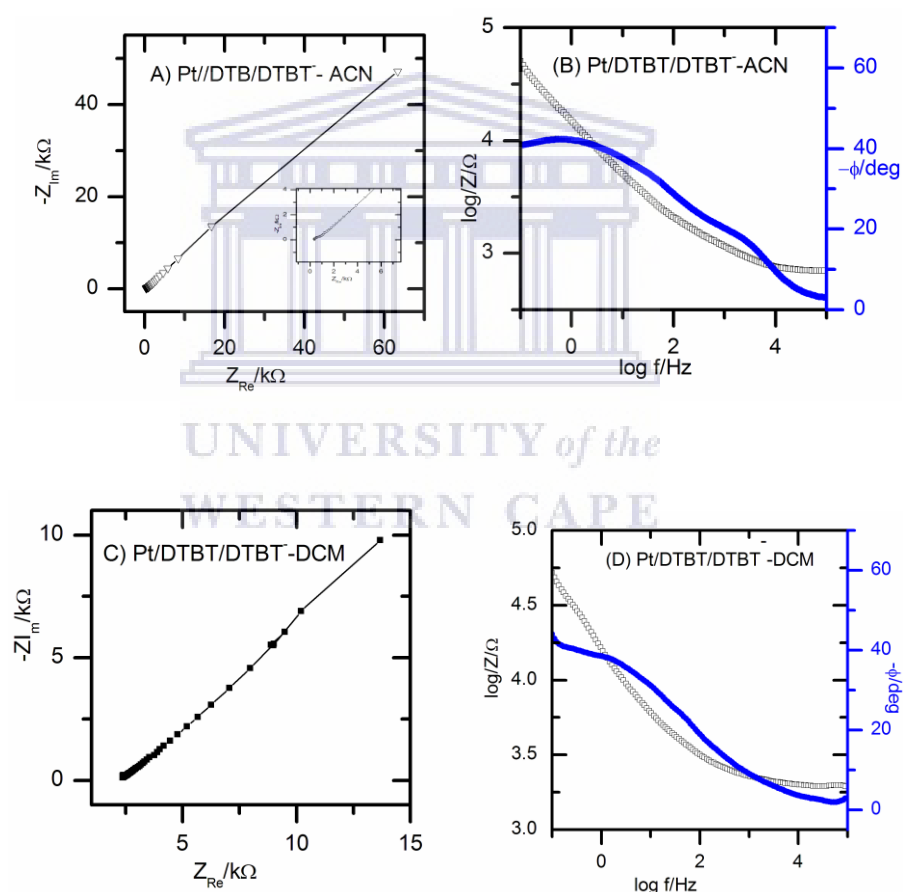
Figure 5.24: EIS spectra of DTBT/DTBT⁻ in 0.1 M n-Bu₄NClO₄ in ACN (A, B) and DCM (C, D) at Pt electrode. (A,C) Nyquist plot and (B,D) Bode plot.
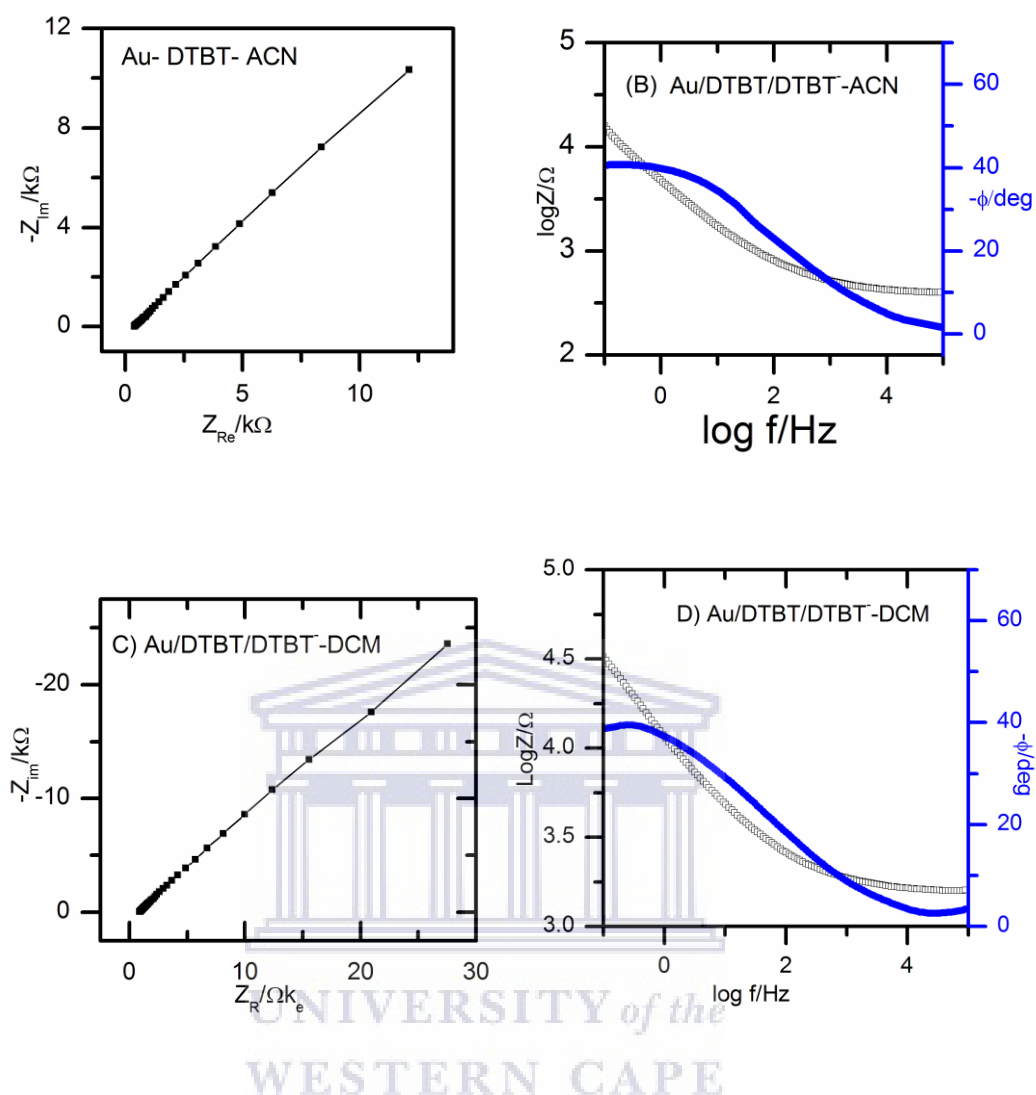
Figure 5.25: EIS spectra of DTBT/DTBT$^-$ 0.1 M n-Bu$_4$NClO$_4$ in ACN (A, B) and DCM (C, B) at Au electrode. (A, C) Nyquist plot and (B, D)) Bode plot.

Table 5.13: Kinetic parameters of DTBT/DTBT$^-$ calculated from charge transfer resistance.

	Pt			Au		
Solvent	R_{ct}/Ω	i_o/A	$k^o/cm/s$	R_{ct}/Ω	i_o/A	$k^o/cm/s$
ACN	223.7	1.13×10^{-4}	0.069	35.5	7.11×10^{-4}	0.434
DCM-ACN	184.8	1.37×10^{-4}	0.083	64.2	3.94×10^{-4}	0.240
DCM	253.2	9.98×10^{-5}	0.061	214.3	1.18×10^{-4}	0.072

Conclusions

DTBT reduction to DTBT$^-$ anion is a reversible one electron transfer process. The redox potential of DTBT/DTBT$^-$ couple was found to be $E^{o'}$ = -1.56 V, The diffusion coefficient of DTBT$^-$ was about half of DTBT in ACN on Au and one tenth in ACN on Pt, one forth in DCM on both electrodes. Higher viscosity of the investigated solvent gives lower diffusion coefficients. More basic solvent medium lower the kinetics of the charge transfer at electrode interface and DTBT/DTBT$^-$ redox couple. About three-fold faster electrode kinetics was estimated for DTBT/DTBT$^-$ system on Au electrode than on Pt.

5.2.5 Electrochemical oxidation of DTBT in ionic liquids

Ionic liquids (ILs) used in this investigation were 1-butyl-3-methylimidazolium tetrafluoroborate (bmimbf$_4$), 1-butyl-3-methylimidazolium hexafluorophosphate (bmimpf$_6$) and 1-butyl-3-methylimidazolium bis(trifuloromethanesulfonyl)imide (bmimtnf$_2$). The physical properties these ionic liquids and their structure are shown in Table 3.1 and 3.2. Two of ILs bmimpf$_6$ and bmimtnf$_2$ are hydrophobic whereas bmimbf$_4$ is a hydrophilic IL. The ionic liquid with tnf$_2^-$ anion have relatively low viscosity and high conductivity and thus ideal for electrochemical polymerization. In our investigation, the solubility of 4,7-dithien-2-yl-2,1,3-benzothiadiazole (DTBT) monomer in ionic liquids was found to be slow compare to organic solvents like acetonitrile and dichloromethane. Therefore, experiments were performed at nearly saturated solution of DTBT in all of the ionic liquids used. Besides, it was noticed that, solubility of DTBT various based on the nature of ionic liquids. It became more soluble as the polarity of the ionic liquid decrease. Preliminary electrochemical properties of DTBT were studied in ILs to generate primary data like oxidation potential and bandgap. These electrochemical properties of DTBT are vital to further understand the interesting material, poly(4,7-dithien-2yl-2,1,3-benzothiadiazole) (section 5.2).

Before electrochemically oxidizing DTBT in ILs, the working potential window of the ionic liquids bmimbf$_4$, bmimpf$_6$ and bmimtnf$_2$ on Au, Pt and GC electrode were determined at scan rate of 100 mV/s. Experimentally values of DTBT are summarized in Table 5.14, As indicated in the table, wider potential window up to 5.3 V achieved for the more viscous bmimbf$_6$ ILs which was quite large compared with that of bmimbf$_4$ (3.30 V) and bmimtnf$_2$ (3.9 V) on Pt electrode. All the potential reported are relative to the redox potential of Fc/Fc$^+$. The redox potential of 5 mM of ferrocene (E$^{o'}$ of Fc/Fc$^+$) are listed in Table 5.15. Formal potential of (E$^{o'}$) Fc/Fc$^+$) was around 0.16 V in bmimbf$_4$, 0.17 V in bmimpf$_6$ and 0.18 V in bmimtnf$_2$ with a standard deviation 0.004 to 0.008.

Table 5.14: Potential window of the ionic liquids.

	bmimbf$_4$	Lit.	bmimpf$_6$	bmimtnf$_2$
Au	3.75		5.28	3.94
Pt	3.30	4.3[a]	5.30	3.04
GC	3.91		5.29	3.49

[a] reference [207]

Table 5.15: Redox potential of (Fc/Fc$^+$) (5 mM ferrocene).

Electrode	ionic liquid		
	E$^{o'}$(bmimbf$_4$)	E$^{o'}$(bmimpf$_6$)	E$^{o'}$ (bmimtnf$_2$)
Au	0.16 ± 0.012	0.17 ± 0.004	0.21 ± 0.004
Pt	0.16 ± 0.012	0.17 ± 0.005	0.21 ± 0.005
GC	0.18 ± 0.025	0.20 ± 0.007	0.18 ± 0.008
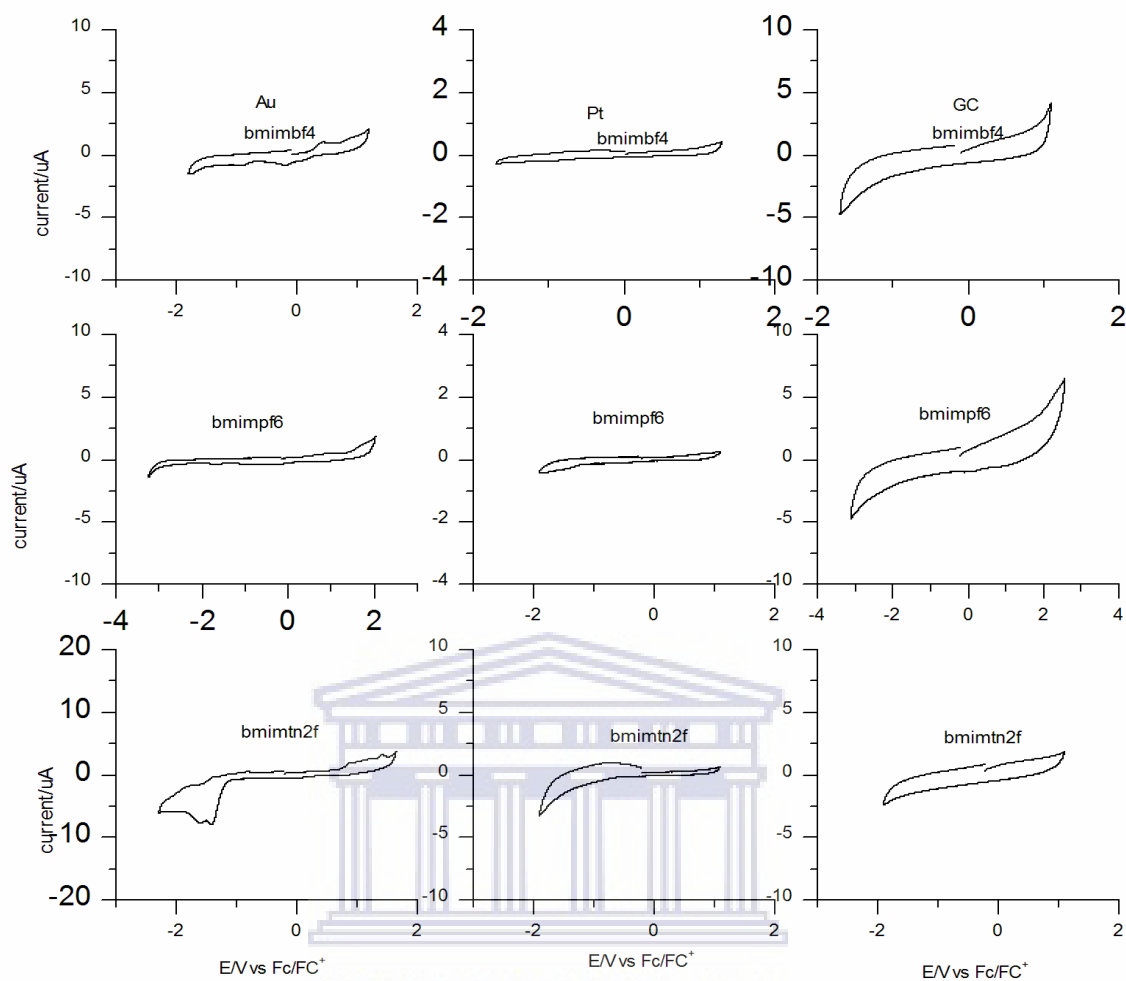
Figure 5.26: Cyclic voltammograms of pure ILs (bmimbf$_4$, bmimpf$_6$ and bmimtnf$_2$) on Au (left), Pt (middle) and GCE (right).

Electrochemical oxidation of 20 mM DTBT was performed in three ILs to compare its oxidation potential of DTBT with the nature of ionic liquids used as well as to its value found in organic media which is presented in section 5.1. Oxidation of DTBT showed amphoteric electrochemical behaviour as reported in organic media. Irreversible oxidation peak (E_{pa}^{I}) at about 0.79 V and a quasi reversible reduction peak (E_{pc}^{II}) appeared in the region of -1.55 to -1.83 V. There was no significance difference across the nature of ILs and types of electrodes on the oxidation and reduction peak potentials (Table 5.16).
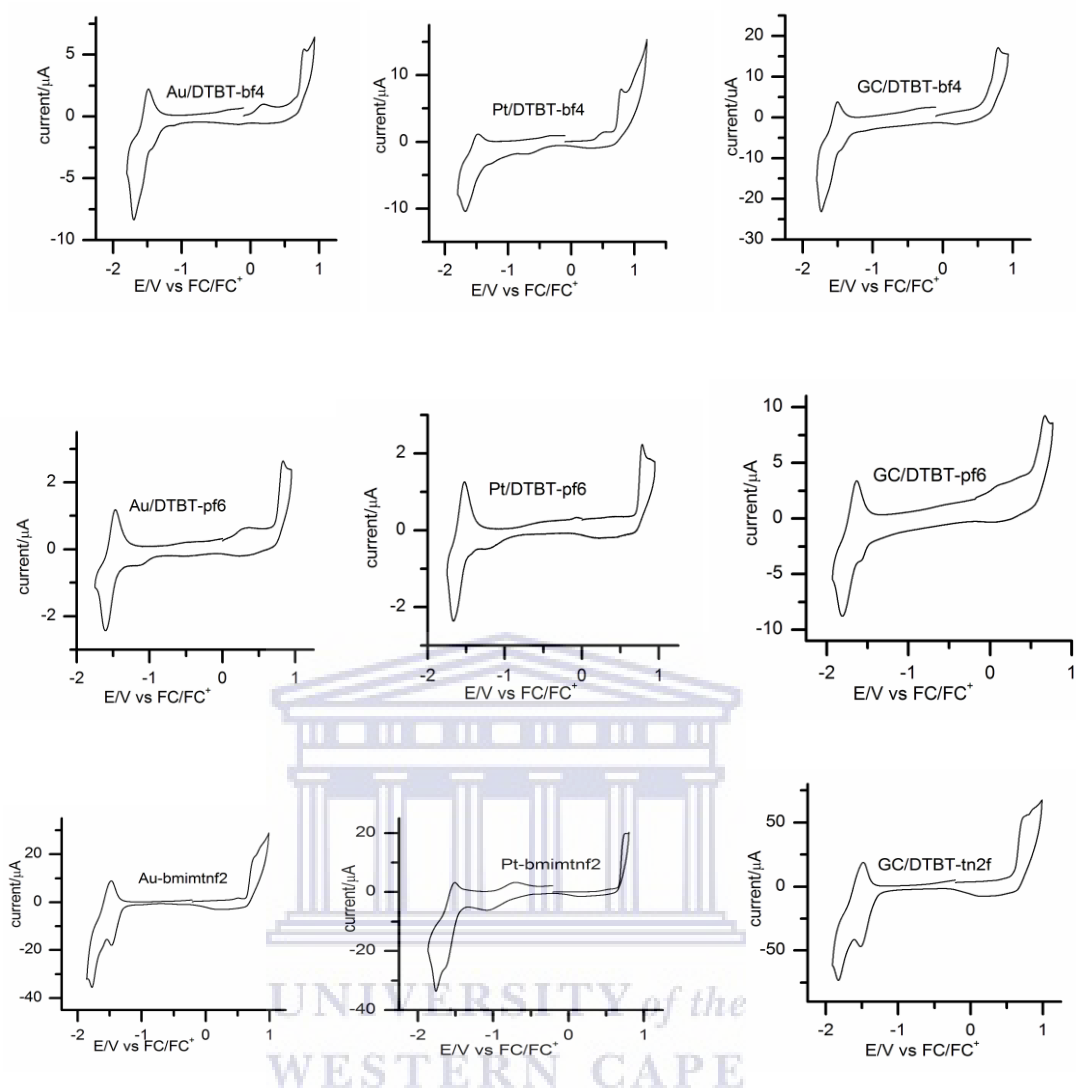
Figure 5.27: Cyclic voltammograms of 20 mM DTBT in bmimbf$_4$, bmimpf$_6$ and bmimtnf$_2$ at Au (left), Pt (middle) and GCE (right). The scan rate was 100 mV/s.

However, DTBT was slightly oxidized at higher potential on Au electrode in bmimpf$_6$ IL because of slower movement of molecules in this viscous media. On the other hand, its reduction potential occurred at a higher negative potential in bmimtnf$_2$ on GC electrode. Peak potentials difference between E_{pa}^{I} and E_{pc}^{II} (ΔE_p) which is equivalent to HOMO and LUMO energy level separation, found to be around 2.5 eV in agreement to its reported value when DTBT electrochemically oxidized in organic media (Table 5.5). This shows that electrochemical bandgap of DTBT monomer was independent of the medium used.

Table 5.16: Summary of peak potentials of 20 mM DTBT in ionic liquids.

Electrode	ILs	E_{pa}^{I}	E_{pa}^{II}	E_{pc}^{II}	ΔE_p
Au	$bmimbf_4$	0.79	-1.49	-1.69	2.48
Au	$bmimbf_6$	0.84	-1.47	-1.61	2.45
Au	$bmimtnf_2$	0.77	-1.46	-1.76	2.53
Pt	$bmimbf_4$	0.79	-1.47	-1.68	2.47
Pt	$bmimpf_6$	0.79	-1.52	-1.67	2.46
Pt	$bmimtnf_2$	0.72	-1.49	-1.76	2.48
GC	$bmimbf_4$	0.79	-1.50	-1.73	2.52
GC	$bmimpf_6$	0.68	-1.67	-1.81	2.49
GC	$bmimtnf_2$	0.73	-1.46	-1.83	2.56

Anodic (I) irreversible and cathodic (II) reversible redox pairs

5.2.6 Analysis of CV data on DTBT/DTBT$^-$ couple in ionic liquids

Reduction of DTBT was also investigated in ionic liquids to evaluate its electrochemical data with the nature of ILs and to that recorded in organic media. In this case 20 mM DTBT is reduced at various scan rates (30 to 500 mV/s). It is important to notice that DTBT at 0.85 mM, no reduction peak formed in $bmimbf_4$, $bmimpf_6$ and $bmimtnf_2$ ILs in contrast to organic solvents at the same concentration. Representative cyclic voltammograms of the reduction of DTBT (20 mM) in $bmimbf_4$, $bmimpf_6$, and $bmimtnf_2$ both as a solvent and supportive electrolyte on Au, Pt and GC electrode are shown in (Figs. 5.28 - 5.30). Electrochemical data from the CVs at different scan rate are collected in Table 5.17-19. Almost invariant anodic and cathodic peak potentials with sweep rate show the reversibility of reduction DTBT to DTBT anion. In addition to this, the formal potential of DTBT/DTBT$^-$ was found to be at

about -1.55 V. The formal potential was independent of scan rates as well as on the nature of ILs, another indication for the reversibility of the process. Furthermore, no significant difference in formal potential difference observed between nonaqueous solvents and Ils. Furthermore, peak potential separation (ΔE_p), falls in the range of 70 to 90 mV and were invariant with scan rates reveals that reduction of DTBT to DTBT anion is a totally one electron transfer reversible redox process.

Figure 5.31 shows the cyclic voltammograms of reduction of DTBT in various media at 100 mV/s. As seen from the CV, the position of the cathodic peak potential occurred at relatively higher negative potential for the more viscous solvents. Cathodic reduction peak (E_{pc}) appeared at higher negative potential in bmimpf$_6$ and it was lowest in ACN. It is important to notice that, the nature of the solvent, on the position of the peak was insignificant compare to its peak currents. As indicated, even, 0.85 mM of DTBT in ACN has higher peak current relative to 20 mM DTBT in Ils.
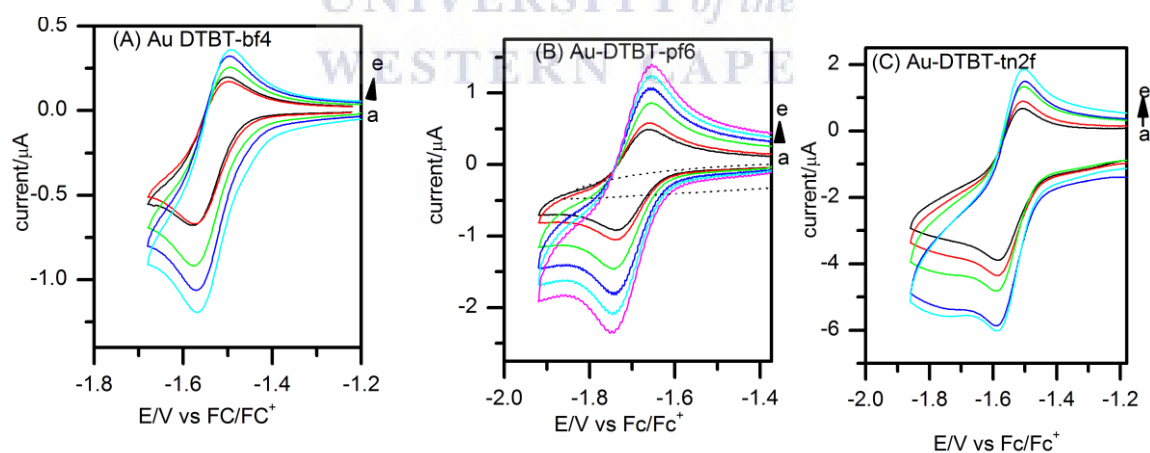
Figure 5:28: Cyclic voltammograms of the reduction of 20 mM DTBT at different scan rates a) 30, b) 50, c) 75, d)100 and e) 150 mV/s at Au electrode (A) in bmimbf$_4$, (B) in bmimpf$_6$ and (C) in bmimtnf$_2$.
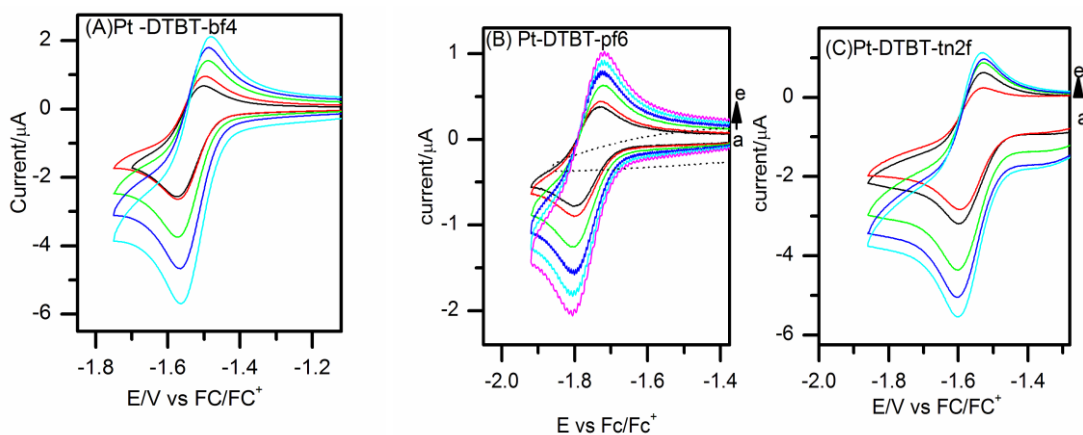
Figure 5.29: Cyclic voltammograms of the reduction of 20 mM DTBT at Pt electrode (A) in bmimbf$_4$ (B) in bmimpf$_6$ and (C) in bmimtnf$_2$ at scan rate of a) 75, b) 100, c) 200, d) 300 and e) 400 mV/s.
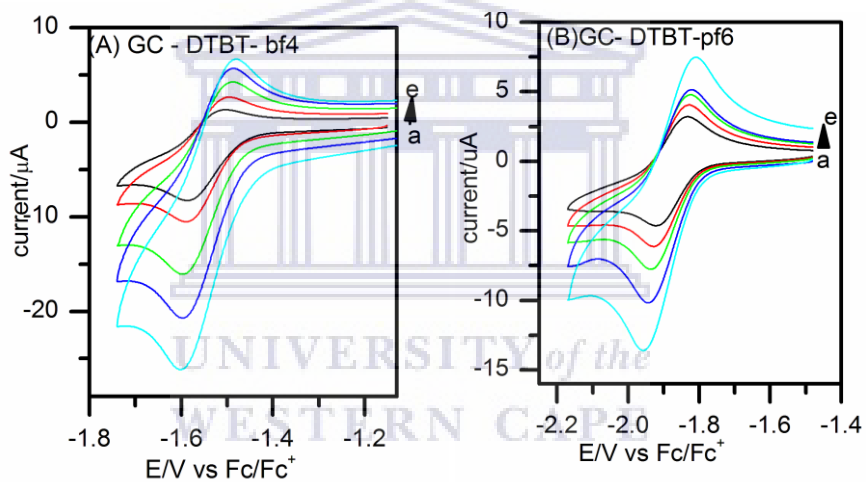
Figure 5.30: Cyclic voltamograms of reduction of 20 mM DTBT at GC electrode (A) in bmimbf$_4$ and (B) bmimpf$_6$ at scan rate of a) 75, b) 100, c) 200, d) 300 and e) 400 mV/s.
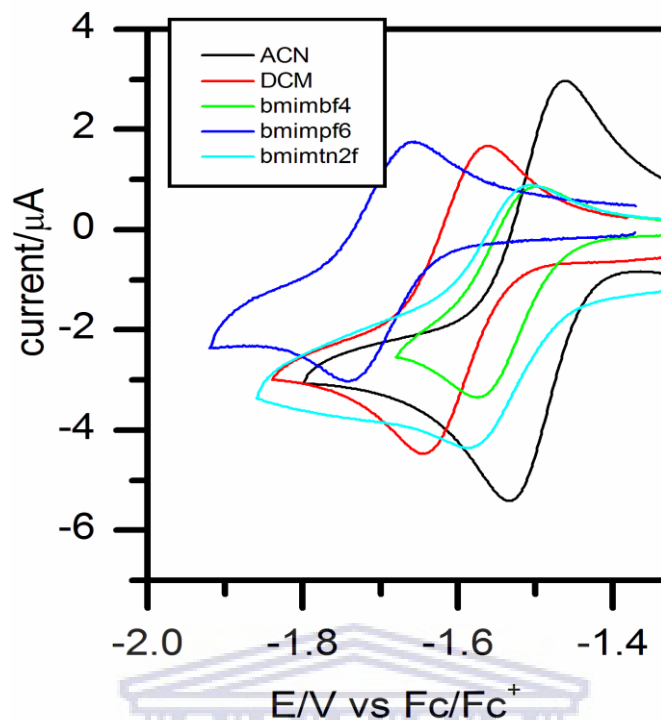
Figure 5.31: Cyclic voltammograms of the reduction of 20 mM DTBT in various media: (black) 0.1M n-Bu$_4$NClO$_4$/ACN, (red) 0.1 M Bu$_4$NClO$_4$/DCM, (light green) bmimbf$_4$, (blue) bmimpf$_6$ and (green) bmimtnf$_2$.

Since the anodic peak current (i$_{pa}$) was dependent on the switching potential, the ratio of anodic to cathodic peak current (i$_{pa}$/i$_{pc}$) was calculated using equation (Eg.5.1) [192]. Ratio of the peak currents was found to be close to one when DTBT reduced in bmimbf$_4$ and bmimpf$_6$ ionic liquids. In contrast to this general trend a ratio about half was obtained when DTBT reduced in bmimtnf$_2$. One possible reason could be DTBT anion diffuses slower because of its interaction with the more nonpolar bmimtnf$_2$ IL hence this could retard its mobility towards the surface of the electrode in the time scale of the experimental conditions. It was also noticed that the ratio of peak currents remains constant with scan rates.

Linear relation was obtained from the plot of peak current (i$_p$) vs. square toot of scan rate ($v^{1/2}$) shown in (Fig. 5.33) indicates diffusion control process. Diffusion coefficient DTBT

calculated using (Eq.4.1) depicted in Table 5.20. As indicated the diffusion coefficient of reduction of DTBT (D_{red}) fall in the range of 9.5 x 10^{-9} to 7.02 x 10^{-10} cm/s in bmimtnf$_2$ and bmimpf$_6$ ionic liquids. On the other hand, diffusion of its anion DTBT$^-$(D)$_{ox}$ decreases by about one tenth in bmimbf$_4$ and one fourth in the other ionic liquids. As expected, the diffusion coefficient of DTBT in ILs was much lower by about $10^{-4.}$ In comparision to its value listed in organic solvents. Clearly, viscosity of Ils played a decisive role in determining the diffusion coefficient of DTBT.

Table 5.17: CV parameters from the reduction of 20 mM DTBT in ionic liquids on Au electrode.

bmimbf$_4$

υ/V/s	E_{pa}/V	i_{pa}/μA	E_{pc}/V	i_{pc}/μA	i_{pa}/i_{pc}
0.075	-1.501	0.68	-1.573	-2.52	0.68
0.1	-1.495	0.95	-1.571	-2.62	0.76
0.2	-1.489	1.40	-1.571	-3.69	0.79
0.3	-1.485	1.79	-1.567	-4.62	0.80
0.4	-1.475	2.12	-1.567	-5.60	0.80

bmimpf$_6$

υ/ V/s	E_{pa}/V	i_{pa}/μA	E_{pc}/V	i_{pc}/μA	i_{pa}/i_{pc}
0.075	-1.66	0.49	-1.73	-0.91	1.00
0.1	-1.66	0.575	-1.74	-1.04	1.02
0.2	-1.66	0.87	-1.74	-1.45	1.06
0.3	-1.66	1.06	-1.74	-1.77	1.08
0.4	-1.66	1.25	-1.74	-2.06	1.08
0.5	-1.65	1.38	-1.75	-2.33	1.07

bmimtnf$_2$

υ/V/s	E_{pa}/V	i_{pa}/μA	E_{pc}/V	i_{pc}/μA	i_{pa}/i_{pc}
0.03	-1.51	0.23	-1.58	-2.65	0.35
0.05	-1.51	0.46	-1.58	-3.26	0.41
0.075	-1.50	0.66	-1.59	-3.82	0.45
0.1	-1.50	0.88	-1.59	-4.32	0.50
0.15	-1.50	1.32	-1.59	-4.83	0.58

Table 5.18: CV parameters from the reduction of 20 mM DTBT in ionic liquids on Pt electrode.

bmimbf$_4$

υ/V/s	E_{pa}/V	i_{pa}/μA	E_{pc}/V	i_{pc}/μA	i_{pa}/i_{pc}
0.075	-1.502	0.17	-1.575	-0.66	0.71
0.1	-1.501	0.20	-1.576	-0.68	0.77
0.2	-1.496	0.26	-1.575	-0.90	0.75
0.3	-1.494	0.32	-1.567	-1.05	0.76
0.4	-1.491	0.39	-1.567	-1.19	0.79

bmimpf$_6$

υ/V/s	E_{pa}/V	i_{pa}/μA	E_{pc}/V	i_{pc}/μA	i_{pa}/i_{pc}
0.075	-1.73	0.39	-1.80	-0.77	0.93
0.1	-1.73	0.45	-1.80	-0.89	0.92
0.2	-1.72	0.63	-1.80	-1.23	0.94
0.3	-1.72	0.78	-1.80	-1.54	0.93
0.4	-1.72	0.89	-1.81	-1.78	0.93
0.5	-1.72	0.99	-1.81	-2.01	0.93

bmimtnf$_2$

υ/V/s	E_{pa}/V	i_{pa}/μA	E_{pc}/V	i_{pc}/μA	i_{pa}/i_{pc}
0.05	-1.53	0.23	-1.60	-2.80	0.5
0.075	-1.53	0.62	-1.60	-3.17	0.61
0.1	-1.53	0.83	-1.60	-4.31	0.61
0.15	-1.53	0.95	-1.60	-5.01	0.61
0.25	-1.525	-1.12	-1.595	-5.58	0.61

Table 5.19: CV parameters from the reduction of 20 mM DTBT in ionic liquids on GC electrode.

bmimbf$_4$

υ/V/s	E_{pa}/V	i_{pa}/μA	E_{pc}/V	i_{pc}/μA	i_{pa}/i_{pc}
0.075	-1.505	1.40	-1.579	-8.08	0.67
0.1	-1.500	2.61	-1.584	-10.30	0.74
0.2	-1.488	4.21	-1.594	-15.84	0.74
0.3	-1.486	5.72	-1.594	-20.48	0.76
0.4	-1.483	6.74	-1.602	-25.83	0.75

bmimpf$_6$

ν/V/s	E_{pa}/V	i_{pa}/μA	E_{pc}/V	i_{pc}/μA	i_{pa}/i_{pc}
0.075	-1.676	1.64	-1.77	-3.50	0.96
0.1	-1.673	1.98	-1.773	-4.01	0.97
0.2	-1.67	3.00	-1.79	-5.72	0.99
0.3	-1.67	3.73	-1.79	-7.18	0.99
0.4	-1.67	4.42	-1.80	-8.33	1.00
0.5	-1.66	4.92	-1.81	-9.23	1.00
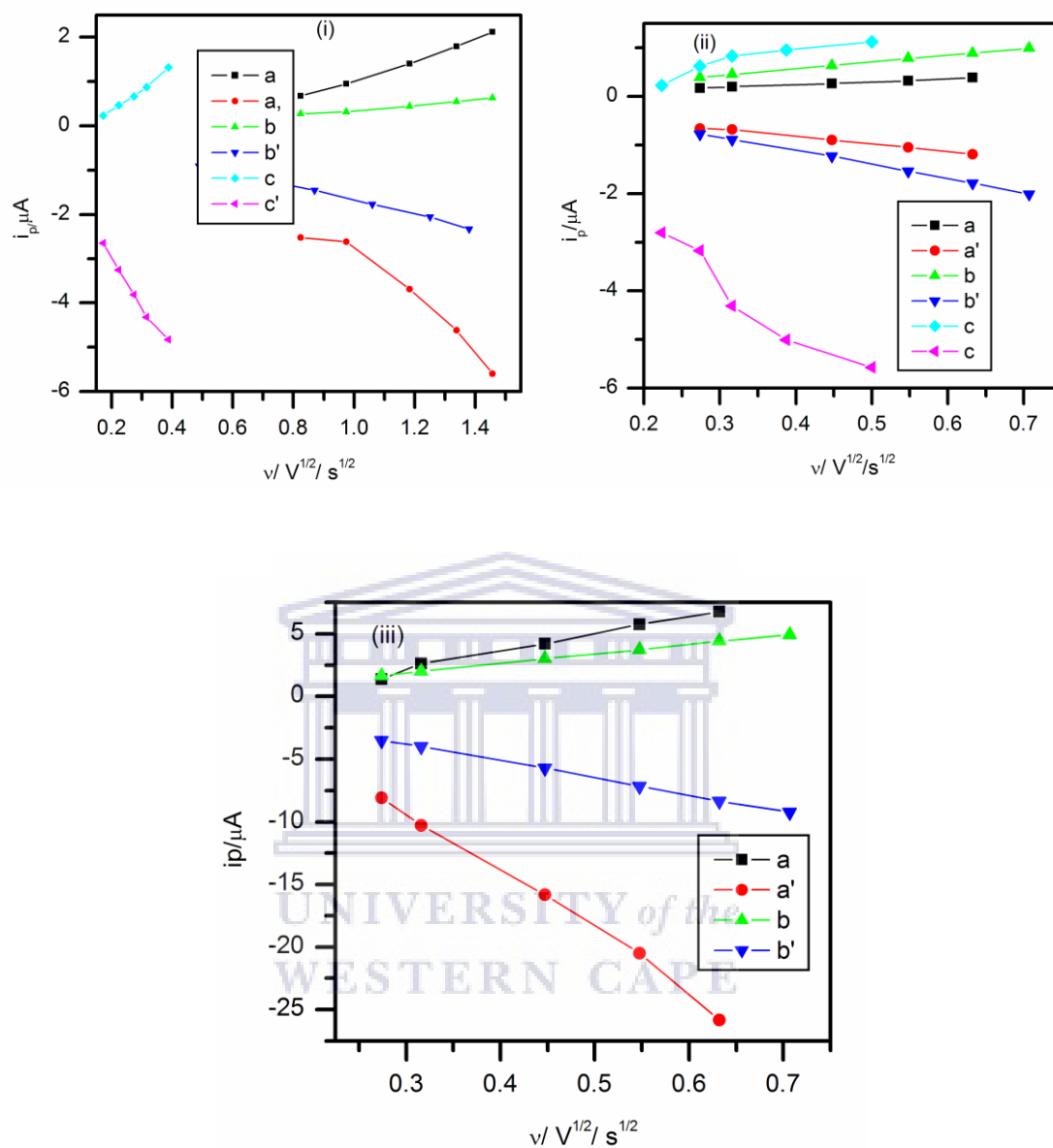
Figure 5.32: "Sevcik plots" for the reduction of 20 mM DTBT (i) at Pt (ii) at Au and (iii) at GC electrode; bmimbf$_4$(a; a'), bmimpf$_6$ (b, b') and bmimtnf$_2$ (c,c'). Anodic (a,b,c) and cathodic (a',b',c').

Table 5.20: Diffusion coefficients of 20 mM DTBT in ionic liquids.

Electrode	Solvent	$D_{red}/cm^2/s$	$D_{ox}/cm^2/s$
Pt	$bmimbf_4$	6.47×10^{-9}	1.31×10^{-9}
	$bmimpf_6$	7.02×10^{-10}	1.67×10^{-10}
	$bmimtnf_2$	9.5×10^{-9}	7.43×10^{-9}
Au	$bmimbf_4$	1.99×10^{-10}	2.97×10^{-11}
	$bmimpf_6$	9.15×10^{-10}	3.72×10^{-10}
	$bmimtnf_2$	9.20×10^{-9}	2.18×10^{-9}
GC	$bmimbf_4$	1.62×10^{-8}	1.46×10^{-9}
	$bmimpf_6$	1.27×10^{-9}	4.07×10^{-10}

Conclusions

The reduction of DTBT in ionic liquids was a reversible one electron transfer process. Its formal potential ($E^{o'}$) was about -1.55 V, the same as its value in organic solvents. The diffusion coefficient of DTBT in ionic liquids was lower by about 10^{-4} compare to its value found in nonaqueos solvents. DTBT anion diffusion coefficient was about one tenth and one fourth of DTBT when it was reduced in $bmimbf_4$ and the other two ionic liquids. In general it was observed that the higher the viscosity of the ionic liquid, the lower the diffusion coefficient of DTBT.

5.3 Electropolymerization and electrochromism of poly(4,7-dithien-2-yl-2,1,3-benzothiadiazole) in 1-butyl-3-methylimidazolium ionic liquids

In this part of the thesis, electrochemical synthesis of poly(4,7-dithen-2-yl-2,1,3-benzothiadiazole) (P(DTBT) and its characterization in ionic liquids which contains the same 1-buthyl-3-methylimidazolium cation and various anions (tetrfluoroborate, hexafluorophosphate and bis(trifluoromethylsulfonyl)imide) are discussed. P(DTBT) oxidation potentials, and its electrochemical bandgab estimated from CV during p-and n-doping process was compared with the monomer 4,7-dithen-2-yl-2,1,3-benzothiadiazole. Influences of the ionic liquids on electrochemical, electrochromic (response time and optical contrast) and on morphology are discussed. Moreover, attempts were made to compare its behaviour with poly(3-methoxythiophene).

5.3.1 Electropolymerization of DTBT in organic media

Electropolymerization of 1.5 mM DTBT in 0.1 M n-Bu_4NClO$_4$/ACN (potential range -0.20 to 1.20 V and scan rate 100 mV/s) was carried out on Pt, Au and GC electrode to compare its electrochemical behaviours to that of P(DTBT) formed in ionic liquids. The cyclic voltammograms during growth is shown in Fig. 5.33. DTBT oxidized irreversibly in the first cycle at around E_{pa} = 0.89 V at Au, 0.82 at Pt and 1.05 V at GC electrode. As the cycle continues an irreversible cathodic redox peak appeared at about 0.41 to 0.57 V at Pt and Au and 0.62 to 0.82 V at GC electrode. Both anodic and cathodic peak current increase with successive cycles indicates the growth of the polymer.

As formed P(DTBT) was rinsed and characterized in monomer free 0.1M n-Bu_4NClO$_4$/ACN in same potential range as polymerization in the range of scan rate 20 − 100 mV/s. It exhibited well defined reversible redox couples with $E_{1/2}$ 0.84 V (Fig. 5.34). The half wave

oxidation potential of the polymer ($E_{1/2}$) appeared around 0.84 V vs Fc/Fc$^+$ at scan rate of 100 mV/s which was close to its reported value (0.78 V vs. Ag/Ag$^+$) [171].
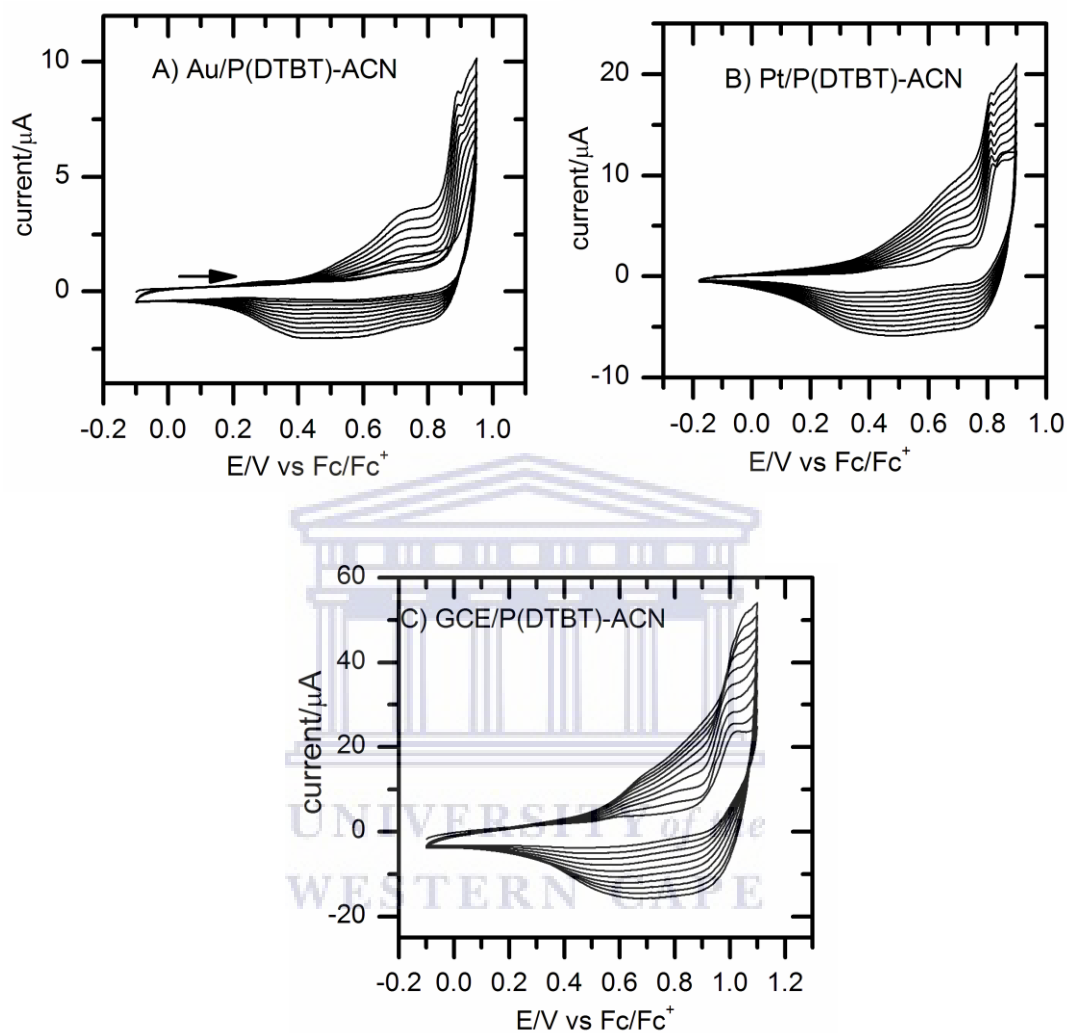
Figure 5.33: Cyclic voltammograms of P(DTBT) grown in 1.5 mM DTBT in 0.1 M n-Bu$_4$NClO$_4$ + ACN (10 cycles) A) Au, B) Pt and C) GC electrode at scan rate of 100 mV/s.
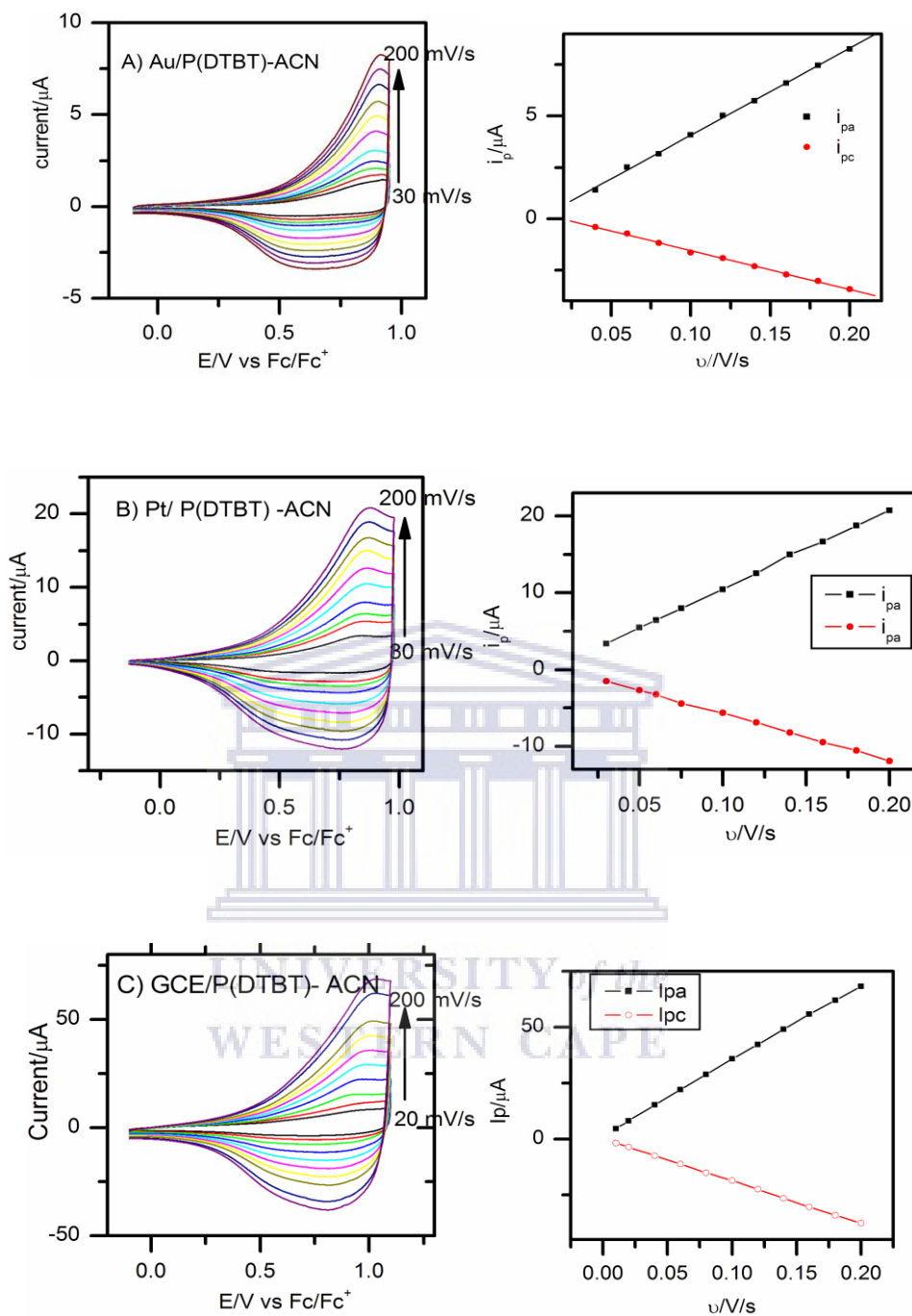
Figure 5.34: Cyclic voltammograms of P(DTBT) grown from 1.5 mM DTBT/0.1 M n-Bu$_4$NClO$_4$ + acetonitrile in monomer free electrolyte at different scan rates 20–200 mV/s and scan rate dependancein of peak current A) Au/P(DTBT) film: Y= 0.16722 + 42 X (anodic) and Y= 0.34296-18.96167X (cathodic); B) Pt/P(DTBT)film: Y = 1.78221 + 335.65378 X (anodic) and Y= 0.1101-189.6468 X (cathodic) and C) GCE/P(DTBT) film:Y = 1.78221 + 335.65378 X (anodic) and Y= 0.1101-189.6468 X (cathodic). In all cases R^2 ≥ 0.999.

Linearity of peak current with scan rate (Fig. 5.34) shows P(DTBT) is electrochemically active and well adherent on the electrode surface. In addition to this, the linearity indicates the redox behaviour is not controlled by mass transport. Furthermore, despite the fact that electron transfer rate is larger than its diffusion rate; the number of electrons in the diffusion layer is constant during the scan but increases as the scan rate increase. The graph reveals that the increment of current density with scan rate is uniform, proving the homogeneity of the film and the uniform polymer growth.

5.3.2 Electrochemical polymerization of DTBT in ionic liquids

Ionic liquids (ILs) used in this investigation was 1-butyl-3-methylimidazolium tetrafluoroborate (bmimbf$_4$), 1-butyl-3-methylimidazolium hexafluorophosphate (bmimpf$_6$) and 1-butyl-3-methylimidazolium bis(trifuloromethanesulfonyl)imide (bmimtnf$_2$).The ionic liquid with tnf$_2^-$ anion bmimtnf$_2$ has relatively a low viscosity and high conductivity make it as ideal medium for electrochemical polymerization[118]. The difference in physical properties of these Ils, would result changes in polymerization rate and poly(4,7-dithien-2-yl-2,1,3-benzothiadiazol (P(DTBT) electrochemical and optical properties when ionic liquids used both as solvent and electrolyte. The solubility of DTBT various based on the nature of ionic liquids used and electropolymerization of DTBT was conducted at nearly saturated condition. It was slightly more soluble in the hydrophobic ionic liquids bmimtnf$_2$ and bmimpf$_6$. However, the fact that bmimpf$_6$ is more viscous than the other two ILs, more likely the rate of polymerization of (DTBT) was reduced in this media. Utilization of imidazolium based ionic liquids for the electropolymerization of poly(4,7-dithien-2-yl-2,1-3-benzothiadiazole) has not been reported previously. For consistence and easy of comparison P(DTBT)1, P(DTBT)2, P(DTBT)3 and P(DTBT)4 used throughout when DTBT electropolymerized and characterized respectively in bmimbf$_4$, bmimpf$_6$, bmimtnf$_2$ ionic

liquids and 0.1 M n-Bu$_4$NClO$_4$ in acetonitrile in the case of CV and dichloromethane in the case of electrochromic properties.

Cyclic voltammograms recorded in the course of potentiodynamically electropolymerization of 20 mM DTBT are shown in Figs. 5.35-37 at GC, Au and Pt electrodes. Potential range for polymerization was between -0.30 to 1.1 V at scan rate of 100 mV/s. Comparison of the electrochemical data recorded for PDTB in the different ionic liquids at GC, Au and Pt electrodes are given in Table 5.21-23. The irreversible peak oxidation potential of 20 mM DTBT was around 0.87 V in bmimbf$_4$, 0.77 V in bmimpf$_6$, and 0.78 V for bmimtnf$_2$ during the first cycle at GCE. The half wave oxidation potential of the polymer (E$_{1/2}$) was estimated to be around 0.75 to 0.85 V versus Fc/Fc$^+$ at scan rate of 100 mV/s a magnitude close to its reported 0.78 V vs. Ag/Ag$^+$ [171]. The half wave potential of the polymer was almost similar to its monomer. As the cycle continues cathodic redox peak (irreversible) appeared as the result of the reduction of the polymer. No second reduction peak observed as that of poly(3-methoxythiophene which have been believed as a result of expulsion of cations trapped during polymerization step [18] or the insertion of anions for charge balance following the change in oxidation state of the polymer upon reduction. Anodic peak potential of the polymer film was independent of the nature of the ionic liquids. The anodic and cathodic peaks as read from the last polymerization cycle appeared for P(DTBT)1 (E$_{pa}$ = 0.77 V, E$_{pc}$ = 0.4 V), for P(DTBT)2 (E$_{pa}$ = 0.84, E$_{pc}$ = 0.27 V) and for P(DTBT)3 (E$_{pa}$ = 0.77, E$_{pc}$ = 0.51 V). Compare to that of DTBT deposited in 0.1 M n-Bu$_4$NClO$_4$/ACN (1.05 V) a lower anodic peak potential recorded in the hydrophobic Ils.

Both anodic and cathodic peak current increase with successive cycles indicates the growth of the polymer. Dark blue polymer film well adhered to the electrode surface was observed in all the Ils used in the investigation. The colour of the film produced was consistent with

previous reports [168]. We have reported the peak polymer oxidation (i_{ox}) and reduction current (i_{red}) from the final growth cycle to enable comparison of the rate polymerization of P(DTBT). We have also reported the total polymerization charge (Q_P) passed during electropolymerization (determined by integration of the cyclic voltammograms of 10 cycles). Magnitude of Q_p has been used as indication of the relative amount of the polymer produced. The rate of polymerization of DTBT in bmimtnf$_2$ to form P(DTBT)3 was slightly faster compare with the formation of P(DTBT)1 and P(DTBT)2. This was informed based on the fact that the anodic polymer growth current (i_{ox}) of the last growth cycle and total polymerization charge passed in the case of bmimtnf$_2$ ($Q_p = 0.805$ mC) was larger compare with that of bmimbf$_4$ ($Q_p = 0.524$ mC) and bmimpf$_6$ ($Q_p = 0.359$ mC) (Table 5.21). This shows that a faster polymer growth rate was observed for the less viscous and more conductive bmimtnf$_2$ than in bmimbf$_4$ and bmimpf$_6$. Lower viscous medium allows faster diffusion of DTBT and the radical cation through the solution to the electrode surface and hence facilitates polymerization. The same trend has been reported for polythiophenes [41].

Electrodeposition of P(DTBT) on Au cyclic voltammograms shown in Fig. 5 36 and Pt electrode its cyclic voltammograms (Fig. 5.37), from 20 mM DTBT in three of the Ils was also studied. The polymer peak potentials occurred at about ($E_{pa} = 0.81$ V; $E_{pc} = 0.69$ V) for P(DTBT)1 and ($E_{pa} = 0.61$ V, $E_{pc} = 0.23$ V) for P(DTBT)2 Table 5.21-22. It is important to notice that there was no significant difference on the anodic and cathodic peak potentials across type of electrodes employed. The same trend was observed for the monomer.
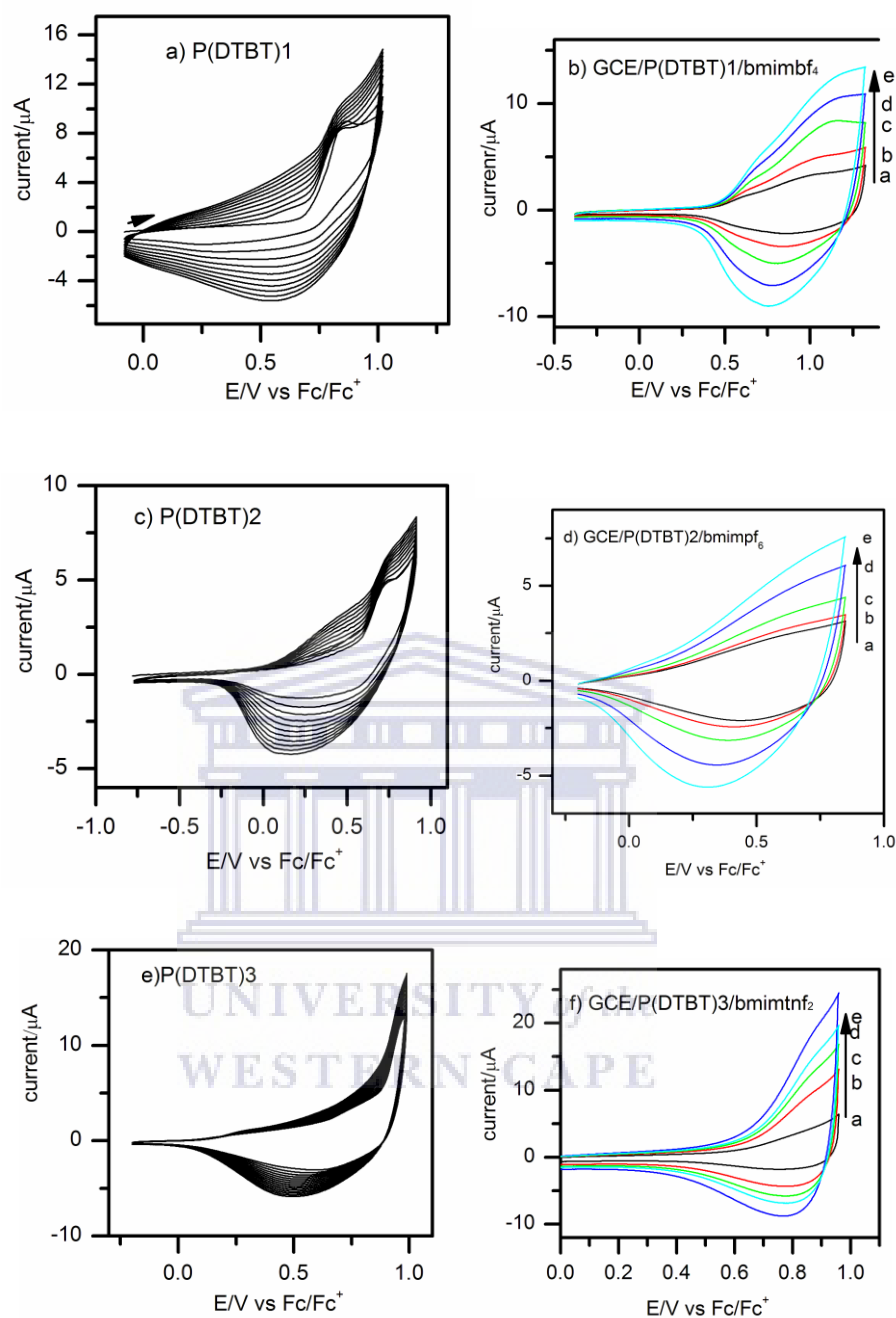
Figure 5.35: Cyclic voltammograms of 20 mM DTBT electropolymerization: a) P(DTBT)1 growth in bmimbf$_4$; b) P(DTBT)1 charcterized in bmimbf$_4$; c) P(DTBT)2 growth in bmimpf$_6$; d) P(DTBT)2 characterized in bmimbf$_6$; e) P(DTBT)3 growth in bmimtnf$_2$ and f) P(DTBT)3 characterized in bmimtnf$_2$ at GC electrode. The scan rate of polymerization was 100 mV/s and for charcterizations a) 30, b) 50, c) 75, d) 100 and e) 150 mV/s.
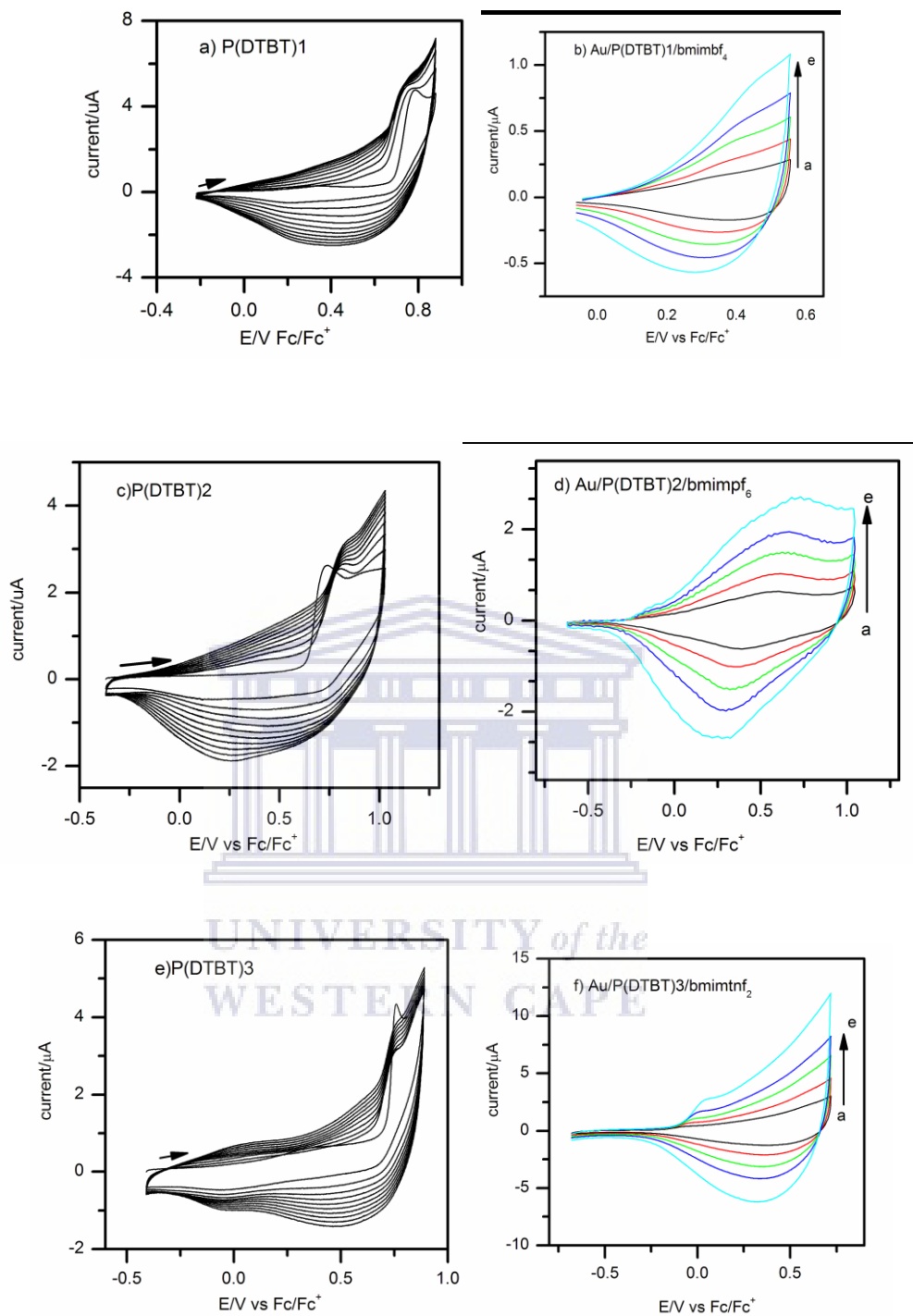
Figure 5.36: Cyclic voltammograms of 20 mM DTBT electroplymerization: a) P(DTBT)1 growth in bmimbf$_4$; b) P(DTBT)1 film characterized in bmimbf$_4$; c) P(DTBT)2 growth in bmimpf$_6$; d) P(DTBT)2 film characterized in bmimbf$_6$; e) P(DTBT)3 growth in bmimtnf$_2$ and f) P(DTBT)3 film characterized in bmimtnf$_2$ at Au electrode. The scan rate of polymerization was 100 mV/s and charctorization a) 30, b) 50, c) 75, d) 100 and e) 150 mV/s.

Table 5.21: Electrochemical parameters evaluated form CV of P(DTBT) at GC electrode.

	P(DTBT)1	P(DTBT)2	P(DTBT)3	P(DTBT)4
Monomer V_{ox}/V	0.69	0.54	0.61	0.89
Polymer i_{ox} /µA	11.6	5.5	14.22	50.48
Polymer V_{ox}/V	0.87	0.77	0.78	1.05
Qp/mC	0.524	0.359	0.805	-
Polymer V_{red}/V	0.58	0.15	0.49	0.63
Polymer i_{red}/µA	-4.6	-3.5	-5.5	-15.70

Table 5.22: Electrochemical parameters evaluated form CV of P(DTBT) at Au electrode.

	P(DTBT)1	P(DTBT)2	P(DTBT)3	P(DTBT)4
Monomer V_{ox}/V	0.69	0.61	0.68	0.84
Polymer i_{ox} /µA	4.2	3.24	4.90	8.35
Polymer V_{ox}/V	0.77	0.84	0.77	0.89
Qp/mC	0.200	0.190	0.204	-
Polymer V_{red}/V	0.35 – 0.49	0.27	0.51	0.41 - 0.57
Polymer i_{red}/µA	-2.40	-1.87	-1.41	-2.00

Table 5.23: Electrochemical parameters evaluated from CV of P(DTBT) at Pt electrode.

	P(DTBT)1	P(DTBT)2	P(DTBT)4
Monomer V_{ox}/V	0.81	0.61	0.74
Polymer i_{ox} /µA	10.0	3.24	18.19
Polymer V_{ox}/V	0.87	0.84	0.82
Polymer V_{red}/V	0.69	0.23	0.43–0.59
Polymer i_{red}/µA	-5.00	-1.25	-5.90
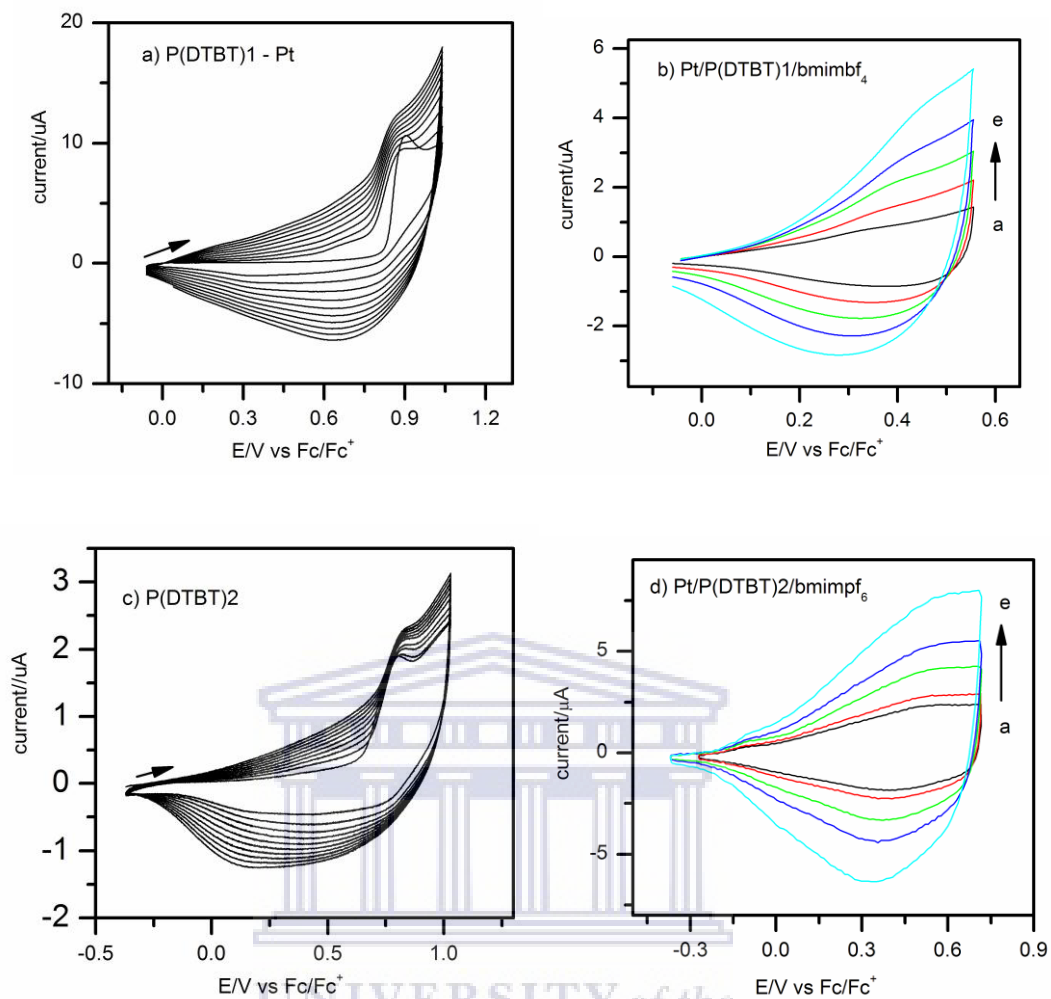
Figure 5.37: Cyclic voltammograms of 20 mM DTBT polymerization: a) P(DTBT)1 groth in bmimbf$_4$; b) P(DTBT)1 film characterized in bmimbf$_4$; C) P(DTBT)2 growth in bmimpf$_6$ and d) P(DTBT)2 characterized in bmimbf$_6$; at Pt electrode. The scan rate of polymerization was 100 mV/s and charcterizations a) 30, b) 50, c) 75, d) 100 and e) 150 mV/s. Arrow indicates the direction of scan.
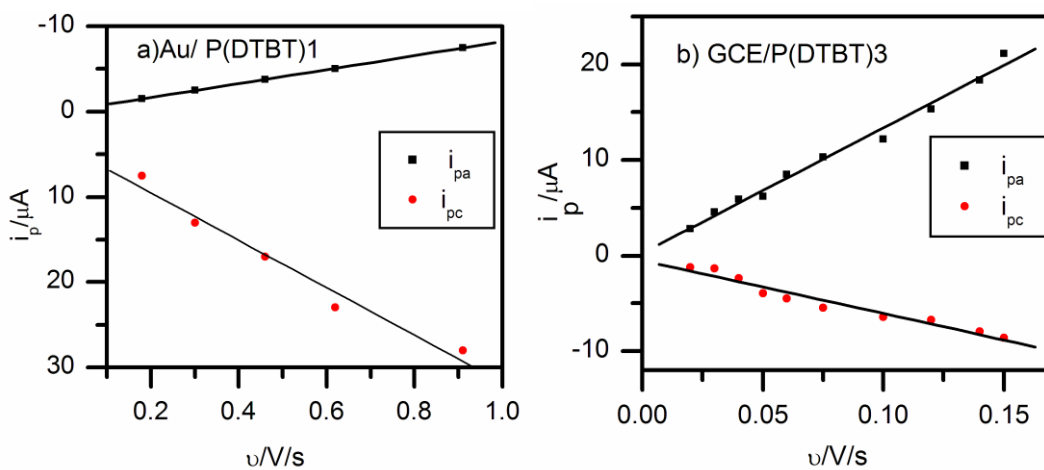
Figure 5.38: Scan rate dependance of peak current for a) Au/P(DTBT)1 in bmimbf$_4$ and b) GCE/P(DTBT)3 film in bmimtnf$_2$.
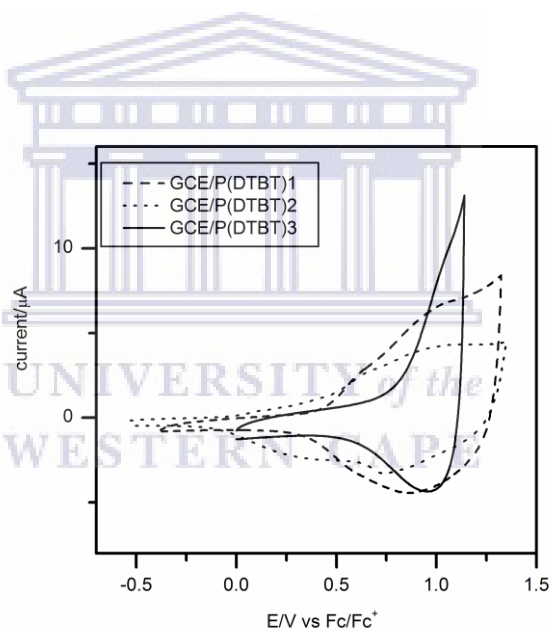
Figure 5.39: Cyclic voltammograms of GCE/P(DTBT)1, GCE/P(DTBT)2 and GCE/P(DTBT)3 film characterized at 50 mV/s in fresh ILs bmimbf$_4$, bmimpf$_6$ and bmimtnf$_2$.

161

5.3.2.1 Characterization of P(DTBT) film in ionic liquids

As formed P(DTBT) on the surface of the electrode was rinsed with a little ionic liquid and placed in monomer free solutions of ionic liquids for characterization by CV at different scan rates 20 to 200 mV/s using the same potential range as polymerization. The cyclic voltammograms depends on the nature of ionic liquids (Figs. 5.35-37). It exhibited well defined irreversible redox couples since peak potential difference was almost greater than 200 mV. This difference was quite large in comparison to P(DTBT) produced and characterized in 0.1 M n-Bu$_4$NClO$_4$/acetonitrile. These CV denotes the polymer is well adhered to the electrode surface. It is important to notice that P(DTBT)2 grown in bmimpf$_6$ showed clear peaks, possibly as a result of slower and more ordered film growth in this viscous ionic liquid.

Linearity of peak current with scan rate shows P(DTBT)s is electrochemically active and well adherent on the electrode surface (Fig. 5.38). The graph reveals that the increment of current density with scan rate is uniform, proving the homogeneity of the film and uniform polymer growth. P(DTBT)3 film was found to be the most electroactive in all electrolytes when comparing peak to charge per peak per unit concentration based on the CV at scan rate of 50 mV/s (Fig. 5.39) followed by P(DTBT)1 and P(DTBT)2. This could be either due to large mass of polymer deposited or increased surface concentration at the same total mass deposited. The same trend was observed as well for the characterization of Au/P(DTBT) film (Fig. 5.37B) and Pt/P(DTBT) (Fig. 5.38B).

Since the polymer has an electron–accepting benzothiadiazole unit, it is also n-dopable polymer. Figure 4.40 (i-iii) shows the cyclic voltammograms of P(DTBT)1, P(DTBT)2 and P(DTBT)3 film deposited on GCE upon p- and n- doping at various scan rates 30, 50, 75 and 100 mV/s. Figure 5.41 shows the cyclic voltammograms of P(DTBT)s upon p- and n- doping

at scan rate of 50 mV/s on GC electrode. P(DTBT)3 film in this case was also the most electroactive. CVs of P(DTBT) show p- doping is an irreversible process whereas n-doping is quasi – reversible. Similar to p-doping behaviour, n- doping is not diffusion limited and was quite stable, unlike poly(3-methoxythiophene) and most of other conducting polymers. The difference between oxidation and reduction onset potentials obtained from p- and n- doping side can be taken as a measure of bandgap (E_g) of the polymer. Bandgap of 1.29 eV was estimated for P(DTBT)1 electrodeposited in bmimbf$_4$ whereas P(DTBT) formed in hydrophobic ionic liquids, narrow bandgap 1.0 to 1.1 eV was obtained. This was in good agreement with the value found by Atwani *et al* [171].

During p- and n- doping process a pre peak emerged, which have not seen when the polymer film characterized in the p–doping potential as well as in the n-doping region. Therefore this peak could be the result of "charge trapping" [208] in the polymer matrices. Charge trapping is caused by conformational changes when the polymer film undergoes doping and dedoping processes [171]. Counter ion inclusion into the misfit free place of the polymer structure during n- doping may be living out during p-doping and vice versa.

Exploiting this n- doping behaviour of P(DTBT), the electron affinity of the polymer can be estimated. Electron affinity of a semi conductor material is defined as the energy required taking away an electron from the conduction band to the next vacuum energy band. In other words, electron affinity is proportional to redox potentials. The oxidation and reduction peak potentials of the polymer appeared at less negative potential compared to DTBT. For example at scan rate of 100 mV/s the reduction peak occurred for P(DTBT)1 (E_{pc} = -1.30 V), P(DTBT)2 (E_{pc} = -1.50 V) and for P(DTBT)3 (E_{pc} = -1.24 V) and formal potential (-1.02 to -1.40 V) as shown in Table 5.18-19 and 5.24, DTBT reduction potential was around -1.77 V

in bmimpf$_6$ and -1.60 V in the other two ionic liquids. The difference between Epc of DTBT

and P(DTBT) is proportional to the electron affinity of P(DTBT) and estimated to be 0.3 eV.
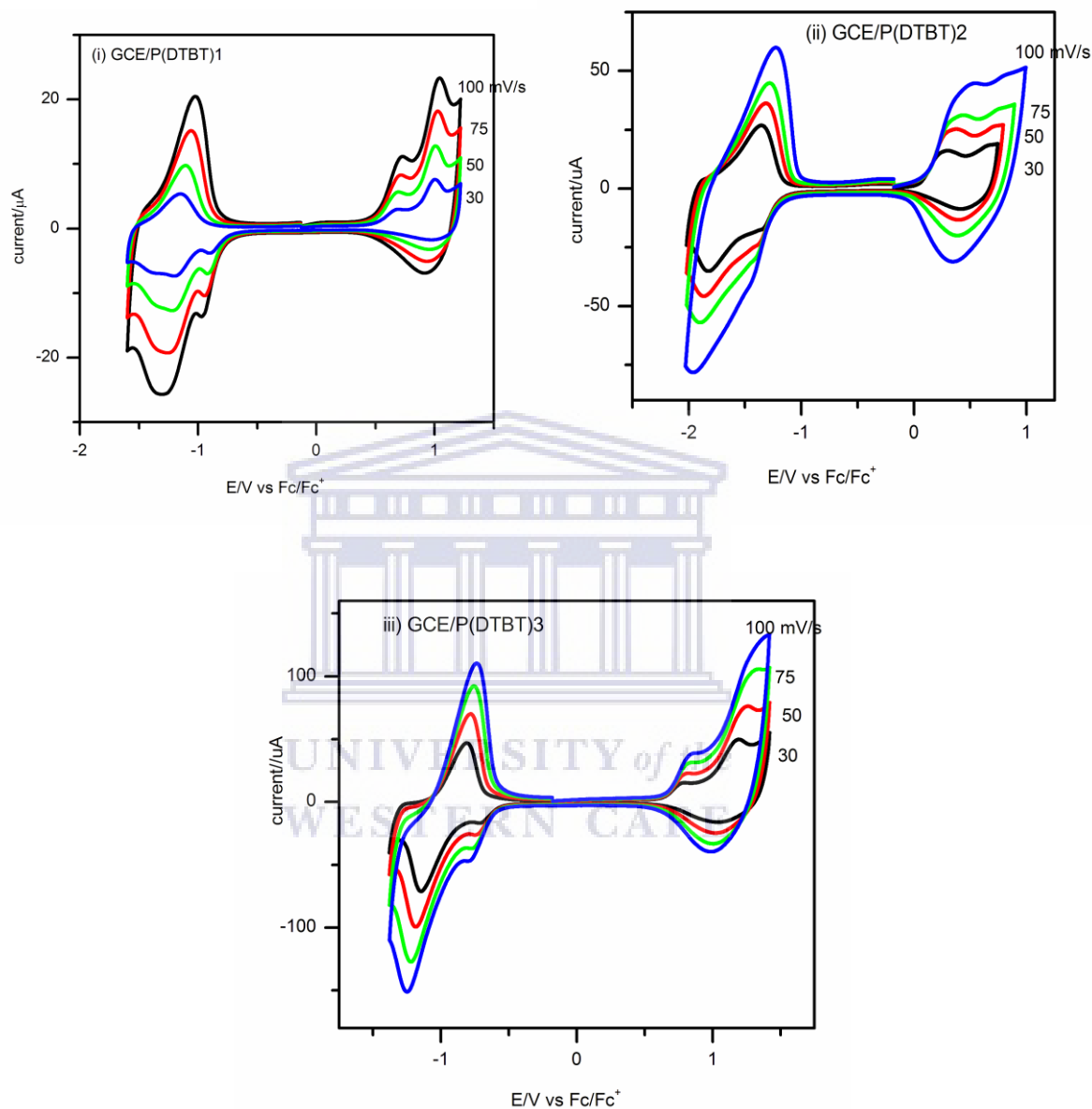
Figure 5.40: Cyclic voltammograms of P(DTBT) during p- and n-doping (i) GCE/P(DTBT)1 polymer film in bmimbf$_4$, (ii) GCE/P(DTBT)2 in bmimpf$_6$ and iii) GCE/P(DTBT)3 in bmimtnf$_2$ at a) 30, b) 50, c) 75, d) 100 and 150 mV/s.

Table 5.24: CV parameters of GCE/P(DTBT) film during n-doping in ionic liquids.

GCE/P(DTBT)1

υ/V/s	E_{pc}/V	i_{pc}/μA	E_{pa}/V	i_{pa}/μA	$E^{o\prime}$/V
0.05	-1.27	-12.10	-1.08	9.74	-1.18
0.075	-1.30	-18.59	-1.06	15.04	-1.18
0.1	-1.30	-25.37	-1.02	20.34	-1.32
GCE/P(DTBT)2					
0.05	-1.86	-43.66	-1.31	33.97	-1.49
0.075	-1.69	-52.86	-1.27	43.16	-1.49
0.1	-1.70	-76.73	-1.25	59.79	-1.48
GCE/P(DTBT)3					
0.05	-1.19	-93.32	-0.81	85.64	-1.01
0.075	-1.24	-119.86	-0.76	87.39	-1.01
0.1	-1.24	-145.13	-0.73	110.74	-1.01
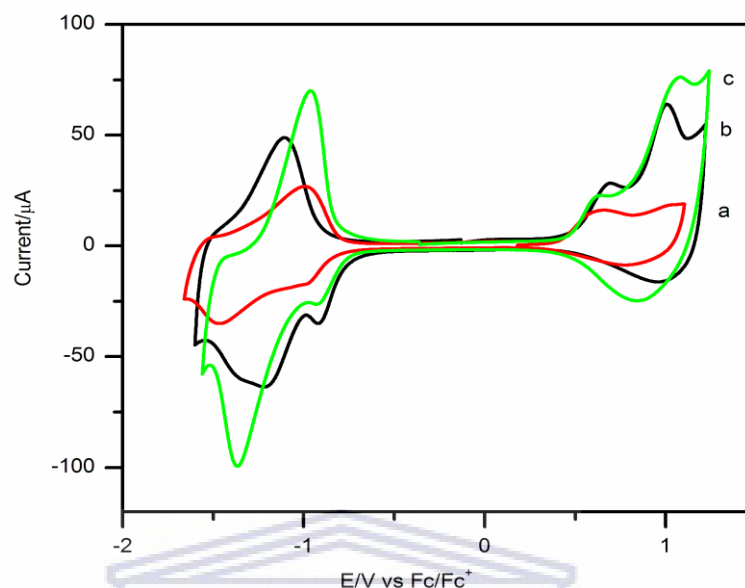
Figure 5.41: Cyclic voltammograms of a) GCE/P(DTBT)1/bmimbf$_4$, b) GCE/P(DTBT)2/bmimpf$_6$ and c) GCE/P(DTBT)3/bmimtnf$_2$ at 50 mV/s.

5.3.2.2 Impedance study of GCE/P(DTBT) film in ionic liquids

Impedance measurement of GCE/P(DTBT)1, GCE/P(DTBT)2 and GCE/P(DTBT)3 polymer film were performed in fresh bmimbf$_4$, bmimpf$_6$ and bmimtnf$_2$ to obtain information about the electrical properties of the GCE/P(DTBT) polymer film/ionic liquid interface. The impedance measurement was carried out by applying 10 mV of ac voltage amplitude in the frequency range 0.01 to 10^5 Hz. As shown in Fig. 5.42, the presence of a semicircle in the higher frequency region for all P(DTBT)s shows the presence of RC parallel circuit. The appearance of Warburg impedance (Z$_w$) line in the lower frequency region is as a result of diffusion of counter ions in the polymer film. It also informed, the redox process is quasi-reversible controlled by both charge transfer (in lower frequency region) and diffusion of counter ions is the rate limiting step in the higher frequency part. Impedance spectra of

P(DTBT) were fitted to the proposed model of an electrical equivalent circuit which contains solution resistance (R_s), double layer capacitance between the polymer film and the electrolyte (C_{dl}), charge transfer resist (R_{ct}) and Warburg diffusion impedance (Z_w) and are summarized in Table 5.25. As an estimation of goodness of the fit, the χ^2 values were about 0.004 – 0.005.

As presented in Table 5.25 GCE/P(DTBT)3/bmimtnf$_2$ system posses relatively a larger double layer capacitance and a lower charge transfer resistance than in bmimpf$_6$ grown film. Double layer capacitance (C_{dl}) difference shows difference in electroactive surface area of PDTBT film. The larger value of C_{dl} in bmimbf$_4$ and bmimtnf$_2$ may be attributed to increased polymer packing density [41] when P(DTBT) formed in less viscous media. Since R_{ct} depend on the viscosity of the ILs it can be related to ion transfer at the polymer – solution interface. Rct increased in the order GCE/P(DTBT)4/ACN <   GCE/P(DTBT)3/bmimtnf$_2$ < GCE/P(DTBT)2/bmimbf$_4$ < GCE/P(DTBT)/bmimpf$_6$. Solution resistance also followed the same order Table 5.25. In contrast, the diffusion impedance (Z_w) at the low frequency part of the impedance spectrum is related to ion diffusion in the polymer film. Diffusion resistance (Z_w) for GCE/P(DTBT) seems dependent on the size of the anion of the electrolyte. GCE/P(DTBT)/bmimtnf$_2$ electrode show the highest Z_w and GCE/P(DTBT)/ACN the lowest.

Table 5.25: Electrical parameters of GCE/P(DTBT)s film % error less 10.

	R_s/Ω	$C_{dl}/\mu C$	R_{ct}/Ω	$Z_w/k\Omega$
P(DTBT)1	1176	8.46×10^{-7}	1534	4.27
P(DTBT)2	1322	1.76×10^{-9}	1896	4.78
P(DTBT)3	689	4.39×10^{-7}	641.1	8.04
P(DTBT)4	236	3.37×10^{-5}	270	0.25
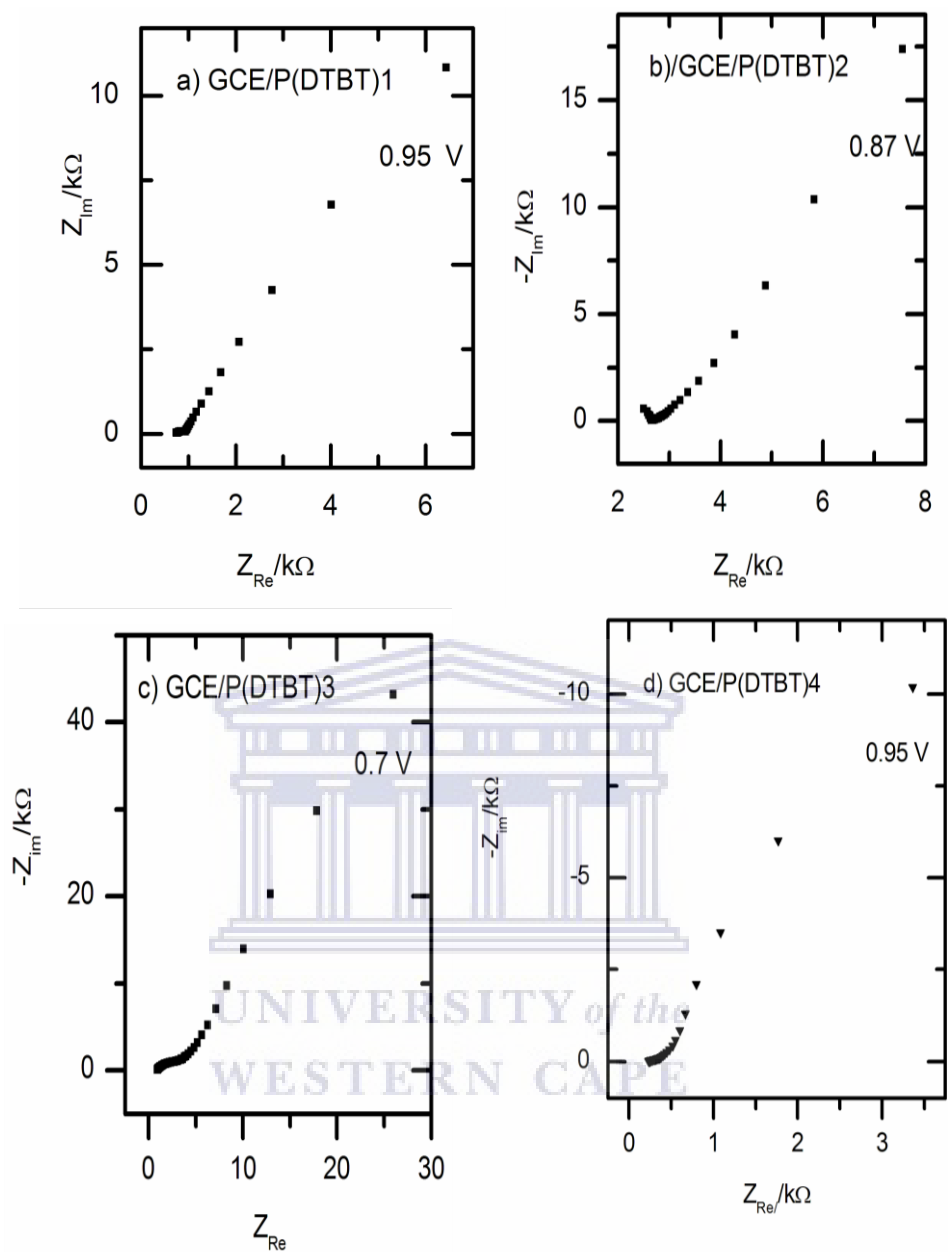
Figure 5.42: Impedance spectra of a) GCE/P(DTBT)1/bmimbf$_4$, b) GCE/P(DTBT)2/bmimpf$_6$, c) GCE/P(DTBT)3/bmimtnf$_2$ and GCE/P(DTBT)4 in 0.1 M n-Bu$_4$NClO$_4$/ acetonitrile.
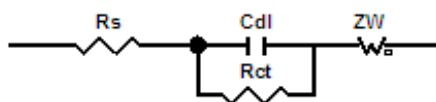
Proposed model for fitting the impedance spectra of P(DTBT)

168

In order to follow the impedance of GCE/P(DTBT)3 and GCE/P(DTBT)4 polymer film variation during the insertion and/or de-insertion of ions from bmimtnf$_2$ and 0.1 M n-Bu$_4$NClO$_4$/ACN, EIS measurement at various potentials was performed. Impedance spectra of P(DTBT) and P(DTBT)4 are shown in Fig. 5.43. As indicated impedance plot consists of a semicircle and Warburg line as explained above due to mixed processes. P(DTBT)s various electrical parameters are listed in Table 5.26-27. A small semicircle which shows a fast electron transfer was observed when the applied potentials approximately approached the formal potential of P(DTBT). Plot of logarithm of charge transfer resistance *versus* applied potential is shown in Fig. 5.44 to estimate the formal potential of P(DTBT)3&4 by extrapolation. P(DTBT)3 grown and characterized in bmimtnf$_2$ its formal potential found to be around 0.75 V, a magnitude nearly the same as the half wave potential predicted from cyclic voltammetry. It was noted that, nearly at this potential the polymer film had a smaller charge transfer resistance.
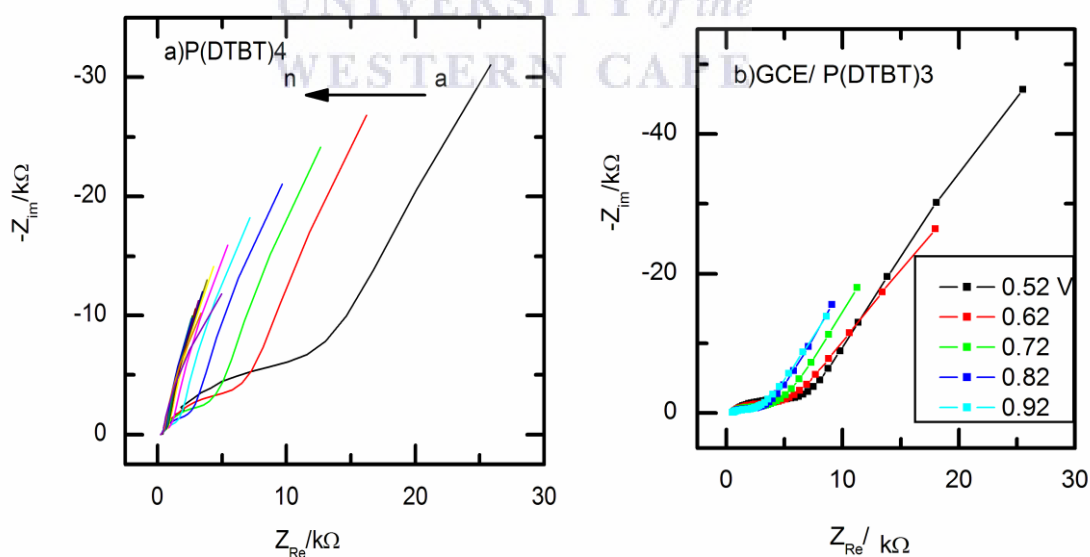
Figure 5.43: Impedance spectra of (a) GCE/P(DTBT)4/0.1 M n-Bu$_4$NClO$_4$ + ACN at various potentials: a) 0.3 V to n) 1.05 V in steps of 0.05 V and b) GCE/P(DTBT)3 at 0.52 to 0.92 V in steps of 0.1 V.
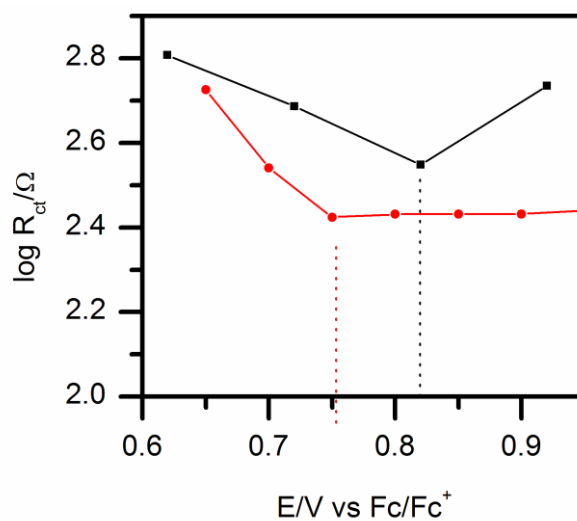
Figure 5.44: Dependance of charge transfer resistnce (R_{ct}) with applied potentials blue points GCE/P(DTBT)3/bmimtnf$_2$ polymer film and red point GCE/P(DTBT)4/0.1 M n-Bu$_4$NClO$_4$ + ACN.

Table 5.26: Elecrical parameters of GCE/P(DTBT)4 polymer film in 0.1 M n-Bu$_4$NClO$_4$/acetonitrile at various potentials.

potential	R_s/Ω	$C_{dl}/\mu C$	R_{ct}/Ω	$Z_w/k\Omega$
0.65	246	11.5	531	0.29
0.7	249	21.0	348	2.28
0.75	238	32.2	266	0.29
0.8	236	36.7	270	0.25
0.85	233	36.7	270	0.25
0.9	236	33.67	270	0.25
0.95	233	32.69	276	2.62

In the case of P(DTBT)4 films electrochemically produced from 1.5 mM n-Bu$_4$NClO$_4$ in acetonitrile, its formal potential found from impedance data was in agreement with that of its half wave potential recorded from cyclic voltammetry (0.82 V).

Table 5.27: Elecrical parameters of GCE/P(DTBT)3/bmimtnf$_2$ polymer film at various potential.

potential	R$_s$/Ω	C$_{dl}$/μC	R$_{ct}$/Ω	Z$_w$/kΩ
0.62	689	0.44	641	8.04
0.72	714	5.63	486	8.57
0.82	834	0.34	353	2.43
0.92	865	0.22	544	3.28

Figure 5.45 shows the impedance spectra of GCE/P(DTBT)3/bmimtnf$_2$ measured during p-doping by applying 0.86 V and n-doping -1.25 V. The same impedance spectra recorded as indicated both form Nyquist and Bode plot. In other words, the electrical parameters have not been significantly changed during p-and n-doping processes.
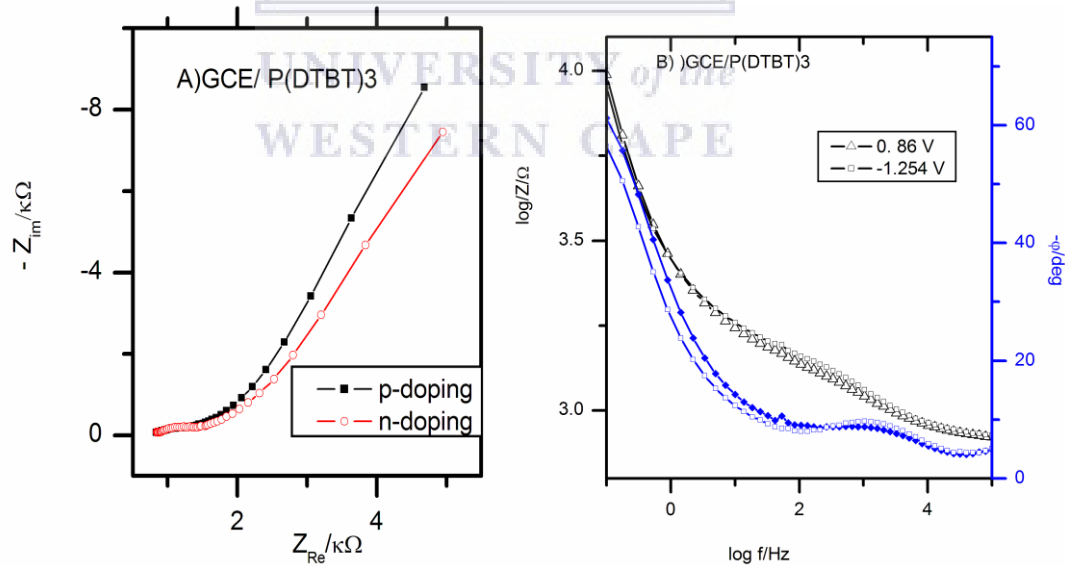
Figure 5.45: A) Nyquist plot of GCE/P(DTBT)3 (p-doping at 0.68 V and n doping at -1.45 V); B) Bode plot P(DTBT)3 (black) total impedance and (blue) phase ange.

5.3.3 Spectroelectrochemistry of P(DTBT)

Thin film of P(DTBT)1, P(DTBT)2, P(DTBT)3 and P(DTBT)4 was electrodeposited potentiodynamically from solution of 20 mM DTBT in fresh bmimbf$_4$, bmimpf$_6$, bmimtnf$_2$ and 0.1 M Bu$_4$NClO$_4$/dichloromethane on indium tin oxide (ITO)-coated glass electrode respectively for uv-vis spectroelectrochemistry study. Uv-vis absorption spectra of P(DTBT)1, of P(DTBT)2, poly(DTB)3 and of P(DTBT)4 is shown in (Fig. 5.46A) for fully reduced state and (Fig. 5.46B) for fully oxidized states. Two absorption bands appeared in the reduced stat appeared both as a result of $\pi - \pi^*$ transitions and the film had dark blue colour. Maximum absorption (λmax) band occurred around 540 nm for P(DTBT)1, 579 nm for P(DTBT)2, 578 nm for P(DTBT)3 and 560 nm for P(DTBT)4 occurred Table 5.28. As illustrated in Fig. 5.46A λ_{max} emerged relatively at longer wavelength (about 25 to 30 nm) when P(DTBT) produced in bmimbf$_6$ and bmimtnf$_2$ ILs compare with of P(DTBT) formed in bmimbf$_4$ due to longer conjugation of the polymer in the hydrophobic ILs. P(DTBT)1 λmax was comparable with that of P(DTNT)4. On the other hand, P(DTBT) polymer electrodeposited in hydrophobic Ils bmimpf$_6$ (1.42 eV) and bmimtnf$_2$ (1.39 eV). In contrast, bandgap of P(DTBT) produced in bmimbf$_4$ (1.58 eV) and dichloromethane/0.1M n-Bu$_4$NClO$_4$ (1.54 eV). About 0.3 eV difference noted from the bandgap calculated from cyclic voltammetry. This kind of variation between optical and electrochemical bandgap for substituted P(DTBT) has been also found [171].

When the film is oxidized, the two $\pi - \pi^*$ transitions bands decreased while a new bands about 766 nm for P(DTBT)1, 802 nm for P(DTBT)2, 800 nm for P(DTBT)3 and 745 nm P(DTBT)4 created in the near infrared region (NIR) corresponding to charge carriers polarons and bipolaron. The colour of the polymer changes to transparent with a red to purple residue colour. Detail uv-vis spectroelectrochemistry of P(DTBT) at different potential are

illustrated in Fig. 5.47, all the absorption spectra have same maximum located at the same wavelength. As a result of this behaviour, the polymer is supposed to have different tons of the same colour which corresponds to the wavelength 560 nm for P(DTBT)4, 578 for P(DTBT)3, 579 for P(DTBT)2 and 542 nm for P(DTBT)1 in the visible region.
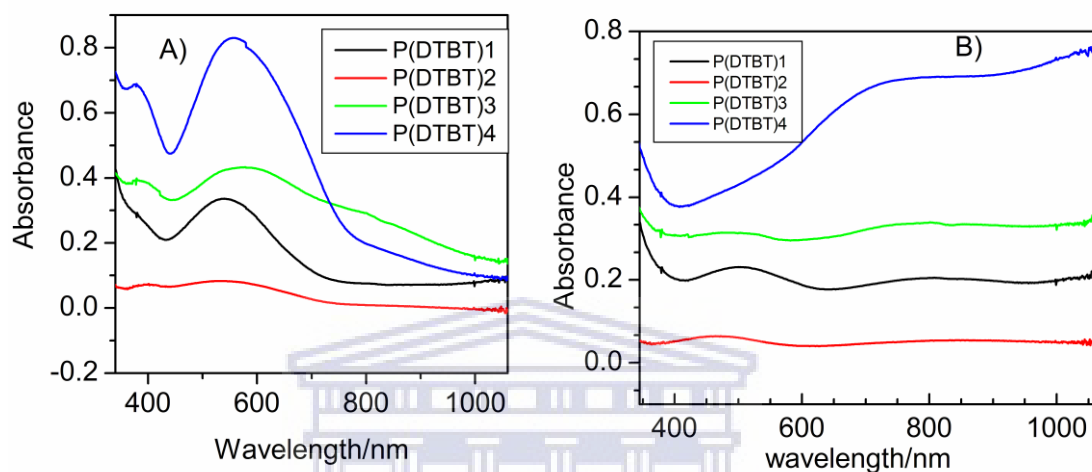
Figure 5.46: Optical spectra of P(DTBT)1 on ITO in bmimbf$_4$, P(DTBT)2 in bmimpf$_6$, P(DTBT)3 in bmimtnf$_2$ and P(DTBT)4 in 0.1 M n-Bu$_4$NClO$_4$/dichloromethane reduced state (-0.6 V) and oxidized state (1.0 V).

Table 5.28: Optical properties of P(DTBT) and maximum of wavelength (λ_{max}/nm).

Polymer	reduced	oxidized	λ(transition)/nm	E$_g$/eV	E$_g^{cv}$/eV
P(DTBT)1	383, 540	766, 1000	654	1.58	1.29
P(DTBT)2	396, 579	802, 1000	702	1.42	1.10
P(DTBT)3	383, 578	800, 1000	724	1.39	1.01
P(DTBT)4	379, 560	700, 1000	654	1.54	-

E$_g^{cv}$ Bandgap estimated from CV and E$_g$ optical bandgap.
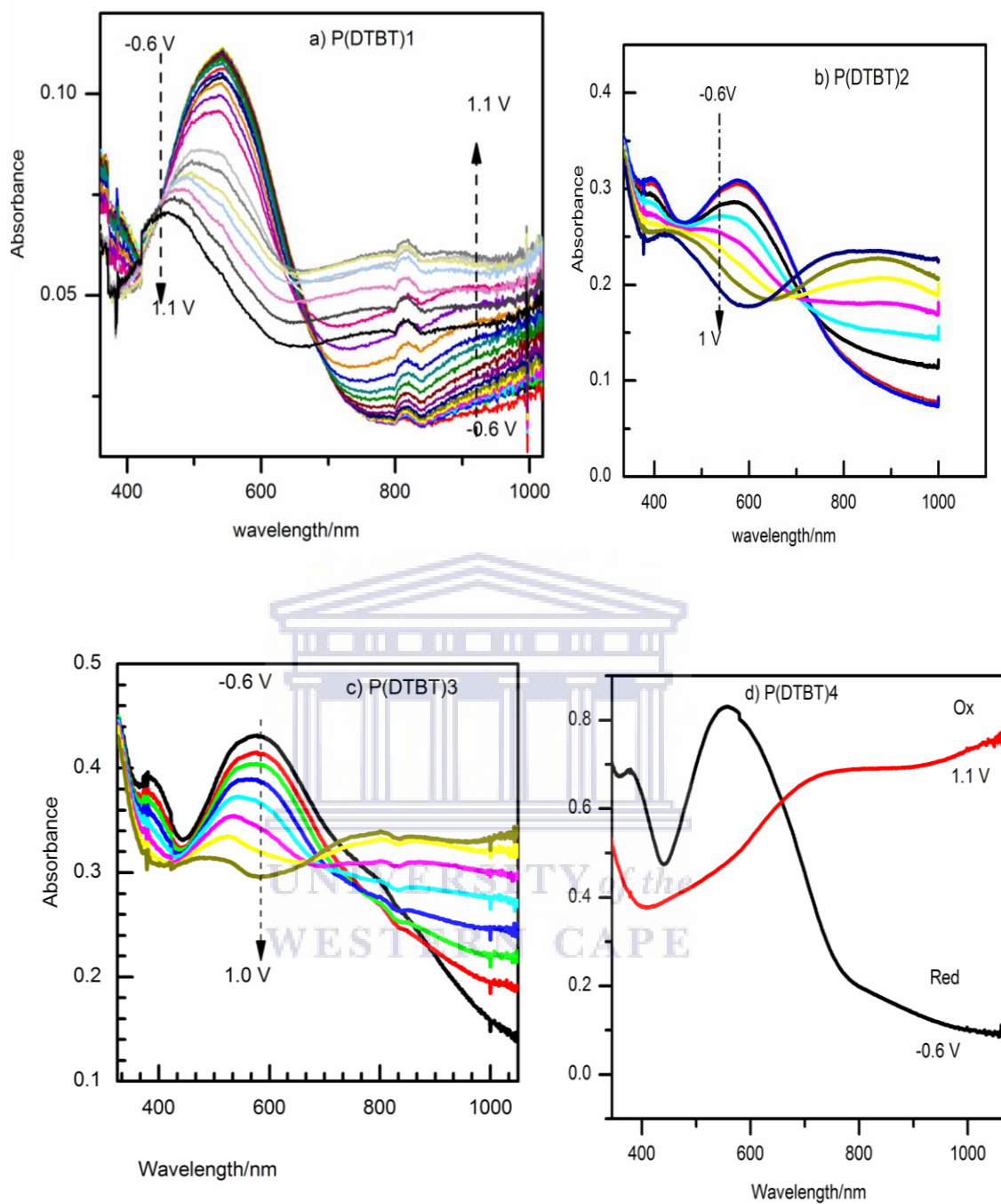
Figure 5.47: Spectroelectrochemistry of a) P(DTBT)1 (from -0.6 to 1.1V) on ITO electrode in bmimbf$_4$, b) P(DTBT)2 (from-0.6 to 1 V) in bmimpf$_6$ and c) P(DTBT)3 (from-0.6 to 1 V)) in bmimtnf$_2$ and d) P(DTBT)4 (from -0.6 to 1.1 V) in 0.1 M n-Bu$_4$NClO$_4$.

5.3.3.1 Switching study of P(DTBT) polymer film

Thin P(DTBT) film prepared on ITO-coated glass as the same condition as spectroelectrochemistry was switched by applying a double potential steps (E_1 = -0.6V, E_2 = 1.1 V) 10 s steps at each potential and transmittance (T) was monitored at constant wavelength (Fig 5.48). Optical contrast ($\Delta T\%$) and response time calculated at 95% of optical change from bleached to coloured state were (11%, 1s) at 800 nm for P(DTBT) electrosynthesized when bmimbf$_4$ used as a medium, (17%, 1.4 s) and (34%, 1.3 s) at 1000 nm for P(DTBT) formed in bmimpf$_6$ and bmimtnf$_2$ ILs.

In contrast, relatively slow response time estimated for P(DTBT) produced in the organic media (39%, 3 s) at 1000 nm. Response time for this polymer film varied in between 3.1 to 5.1 s as the film turned from coloured to bleached state. As noted in the above paragraph, the nature of the ionic liquids affects both optical contrast and response time. A faster response time relative to organic media was evaluated, this possibly could be related to the smoother and homogeneity of P(DTBT) film produced in ionic liquids.

Figure 5.49 shows transmittance and current change vs time for P(DTBT) film as the potential steps several times between -0.6 V to 1 V at fixed wavelength. It was from this plot colouration efficiency (η) of P(DTBT)film calculated. Colouration efficiency can be evaluated using (Eq. 1.3). The charge used in this equation is estimated by integrating chronoamperometry curves shown in Fig. 5.47 during doping and dedoping process. Colouration efficiencies of P(DTBT)s are listed in Table 5.29-230. Depending on the nature of growth medium and as depicted in the Table, colouration efficiency of P(DTBT) falls between 91 o 187 mC/cm^2. It is important to notice that ITO/P(DTBT)3 and ITO/P(DTBT)4 posse's comparable colouration efficiencies 187 and 158 mC/cm^2 respectively. Moreover, the charge consumed during oxidation process was nearly identical to charge consuming during

175

reduction. This result shows the suitability of P(DTBT) film to be used as active layer in electrochromic devices. It was also noticed that P(DTBT)1 film showed a different magnitude of colouration efficiency as switched from bleached to coloured state and from coloured to bleached reverse process. Most likely, this deviation could be due to the variation of charge consumed as a result of difference in kinetics of insertion and exclusion of counter ions in the film during oxidation and reduction.
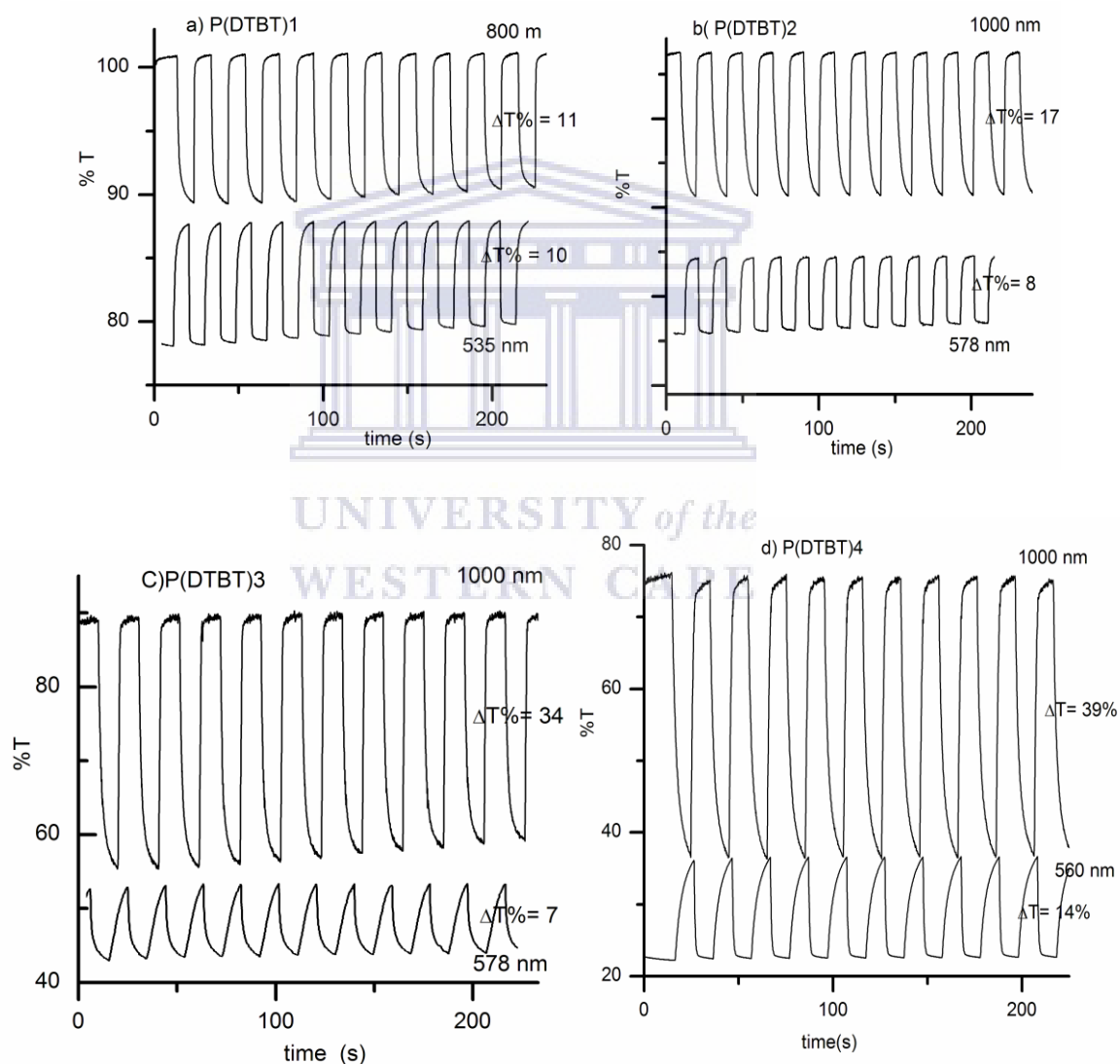
Figure 5.48: Electrochromic switching,optical absorbance for a)ITO/P(DTBT)1 in bmimbf4; b)ITO/P(DTBT)2 in $bmimpf_6$; c)ITO/P(DTBT)3 in $bmimtnf_2$ and d)ITO/P(DTBT)4 in 0.1 M $n-Bu_4NClO_4$/dichloromethane while the polymer was switched between -0.6 and 1.0 V monitored at a) 800 and 535 nm, b) 1000 and 578 nm; c) 1000 and 578 nm; d) 1000 and 560 nm.
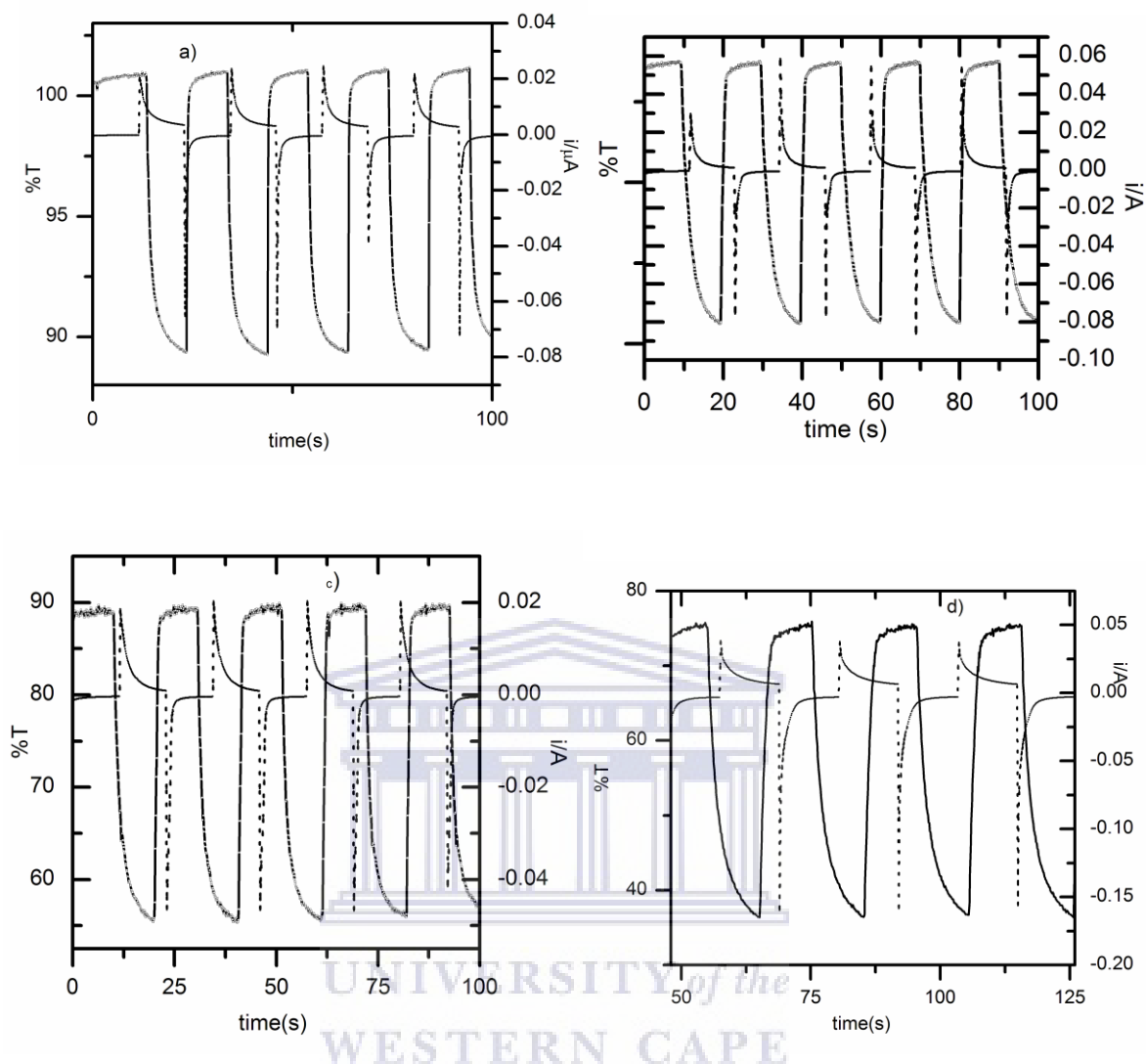
Figure 5.49: Current-time and transmittance-time profiles of a)ITO/P(DTBT)1 in bmimbf$_4$; b)ITO/P(DTBT)2 in bmimpf$_6$; c)ITO/P(DTBT)3 in bmimtnf$_2$ and d)ITO/P(DTBT)4 in 0.1 M n-Bu$_4$NClO$_4$/dichloromethane while the polymer was switched between -0.6 and 1.0 V with a switch time of 10 s monitored at a) 800 nm and (b, c, d) 1000 nm.

Table 5.29: Optical and colouration efficiency data of P(DTBT) at 95 % of full switch (bleached to coloured).

	$\Delta(\%T)$	$\log(T_C/T_b)$	$Q/mC/cm^2$	$\eta/cm^2/C$	t/s
P(DTBT)1	10.5	0.044	0.28	158	1
P(DTBT)2	16.2	0.075	0.82	91	1.4
P(DTBT)3	31.4	0.194	1.04	187	1.3
P(DTBT)4	36.4	0.300	1.7	176	2

Stability of the film has been an important criterion that has to be considered for the practical applications of conducting polymers. As shown Fig. 5.50, upto 500 potential cycling of ITO/P(DTBT)/bmimtnf$_2$ at 200 mV/s, no significant change on electrochemical activity observed as evidenced from the constant anodic and cathodic charge passed with successive cycles (Fig. 5.50A) and from the CV of the 1st and 500th cycle (Fig. 5.50B).

Stability, fast response time, moderate optical contrast and nearly 100 colouration efficiency change during doping and dedoping process demonstrates that P(DTBT) is a potential material to use in colour changing displays.

Table 5.30: Optical and colouration efficiency data of P(DTBT) at 95% of full switch (coloured to bleached)

	$\Delta(\%T)$	$\log(T_c/T_b)$	$Q/mC/cm^2$	$\eta/cm^2/C$	t/s
P(DTBT)1	10.5	0.044	0.45	98	3.3
P(DTBT)2	16.2	0.075	1.04	72	3.7
P(DTBT)3	31.4	0.194	1.05	185	4.2
P(DTBT)4	36.4	0.300	1.68	179	5.1
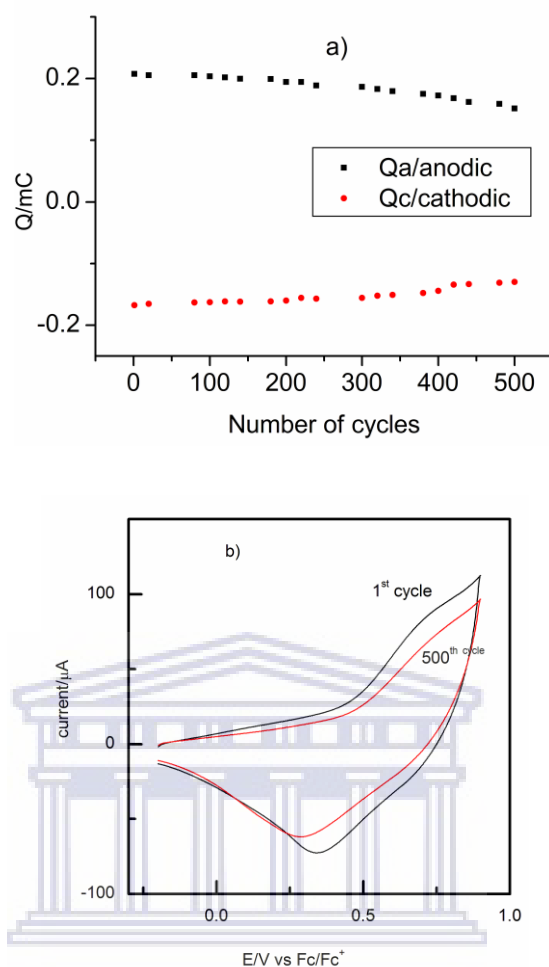
Figure 5.50: Stability of a thin P(DTBT)3 film on ITO electrode cycled 500 times with a scan rate of 200 mV/s in bmimtnf$_2$: a) Anodic charge (black points) and cathodic charge (red points) as a function of cycles; b) Cyclic votammograms of 1st and 500th cycles.

5.3.4 Morphology of P(DTBT)

Scanning electron microscope (SEM) surface image of poly(4,7-dithien-2-yl-2,1,3-benzothiadiazole, P(DTBT) films grown on ITO electrode were acquired to investigate the effect of the nature of ionic liquids has on the morphology of the conducting polymer films (Fig. 5.51A-E). P(DTBT)1 films electrochemically synthesized in ILs bmimbf$_4$ (Fig. 5.51B), P(DTBT)2 in bmimpf$_6$ (Fig. 5.51C), P(DTBT)3 in bmimtnf$_2$ (Fig. 5.51D), and in organic

media 0.1 M Bu$_4$NClO4/DCM P(DTBT)4 (Fig. 5.51E) displays different morphologies. In the case of ILs as medium of electrosynthesis the topography of P(DTBT) looks like a characteristic granular structure bearing more homogeneity with small balls and very similar to that reported by Atwani *et al* [171]. This grain ball shape morphology shows different nucleation and growth mechanism operates at the onset of this film growth. That is the diffusion of radical cations to the electrode surface and start polymerization by 2D and 3D nucleation step before deposited on the surface of the electrode [209]. The mechanism seems initially 2D nucleation dominates as a result of soluble oligomers growth at the ITO substrate. As the process continues on the oligomer deposition on the surface of the electrode, at some critical stage polymer film deposited. The 2D growth mechanism go after by 3D progressive nucleation and growth, most probably gives the formation of branched poly(4,7-dithen-2-yl-2,1,3-benzothiadiazole) affording a cauliflower morphology. This type film growth reported for polythiophens in ionic liquids [41].

It is important to notice that the polymer grown in the hydrophobic bmimtnf$_2$ ionic liquid looks smoother, compact and dense topography compared to the other mediums. Cauliflower morphology was also observed when P(DTBT) is grown in 0.1 M n-Bu$_4$NClO$_4$/dichloromethane. In addition to this, the film looks rough and not bearing small balls as that of P(DTBT) grown in ILs. This shows different mechanism of the polymer film growth between in 0.1 M n-Bu$_4$NClO$_4$/dichloromethane and the ionic liquids. Thus the nature of the ionic liquids caused different morphology as it caused difference electrochemical or optical properties. Homogeneity of P(DTBT) thin film deposited on the ITO-coated glass substrate in ILs indicates the polymer film is a suitable material for electrochromic displays.
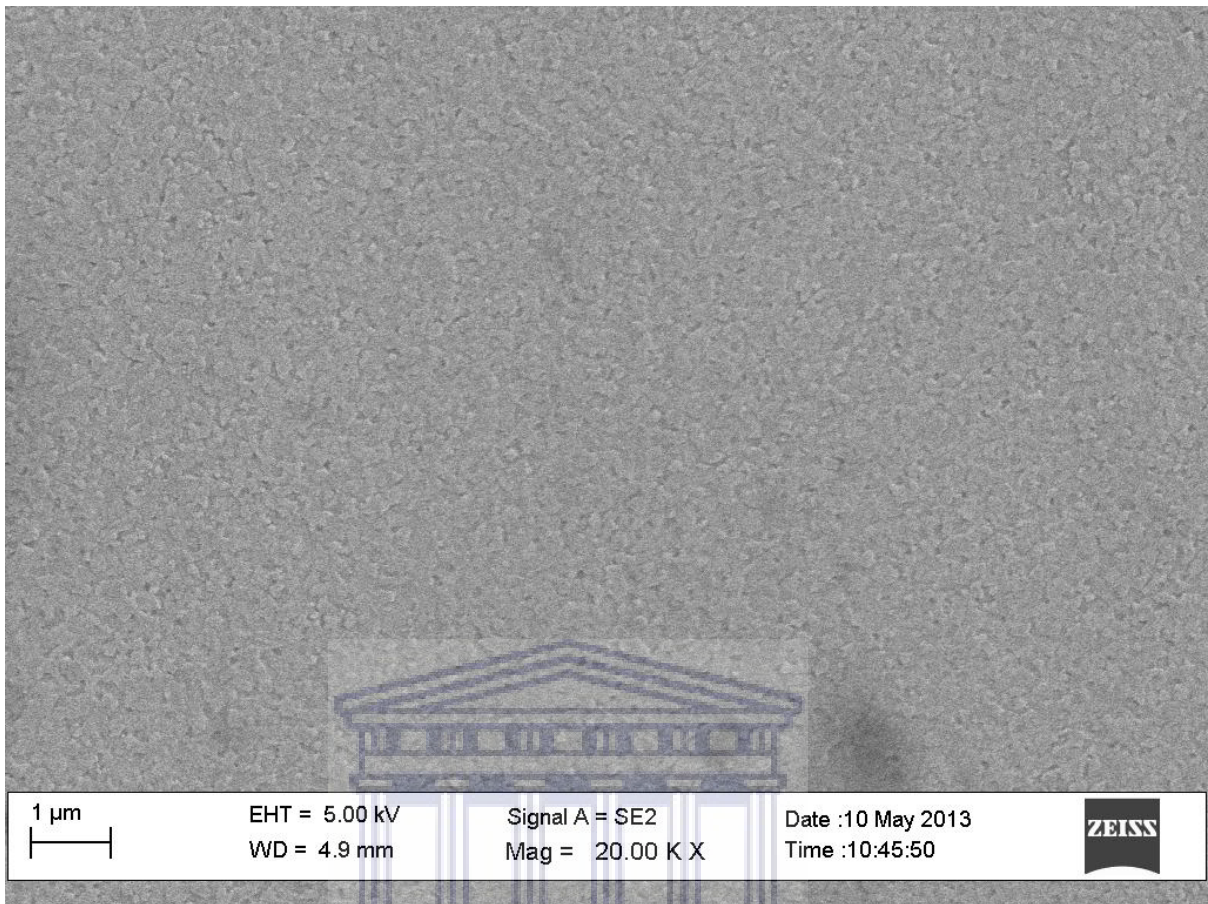
Figure 5.51A: SEM image of ITO-coated glass substrate blank at a magnification of 20,000 K X.
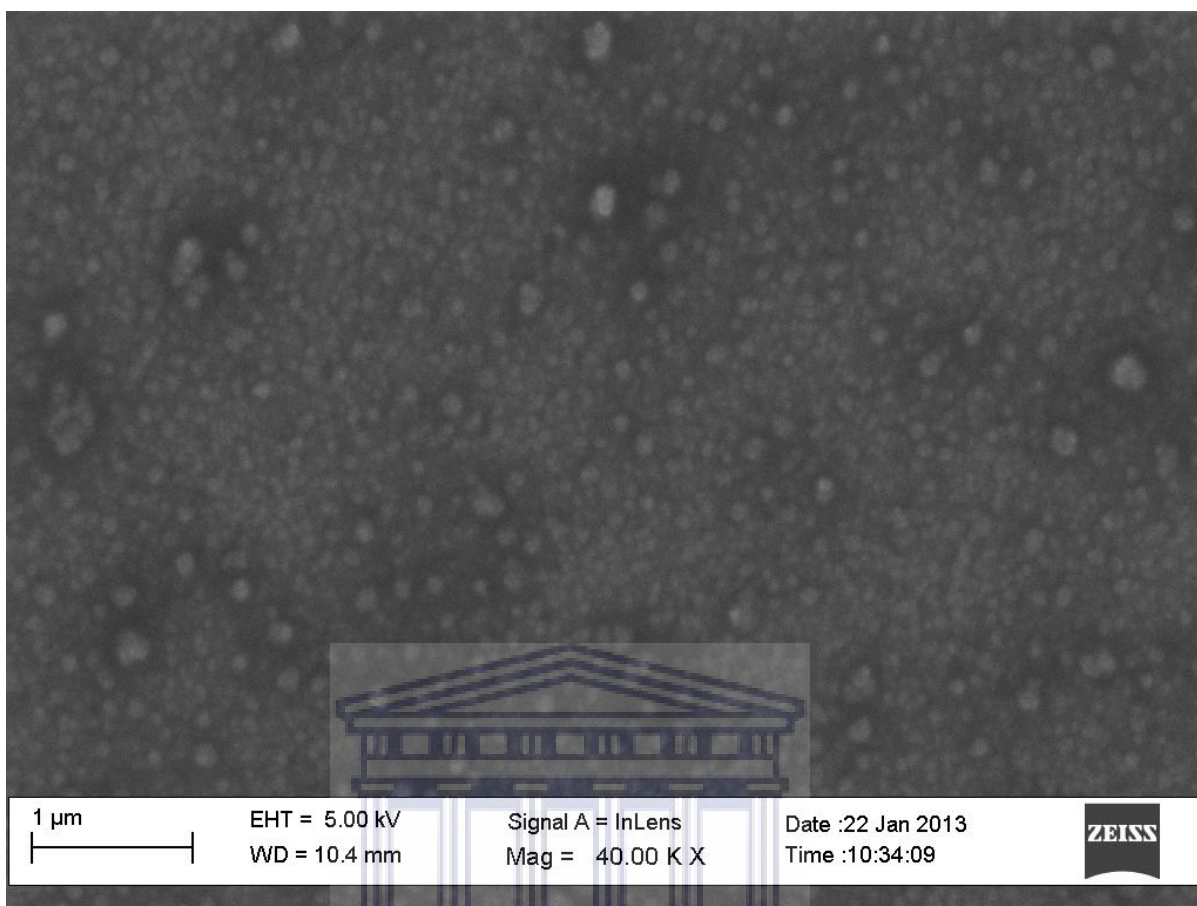
Figure 5.51B: SEM image P(DTBT)1 on ITO electrochemically deposited from 20 mM of DTBT in bmimbf$_4$ at magification of 40,000 K X.
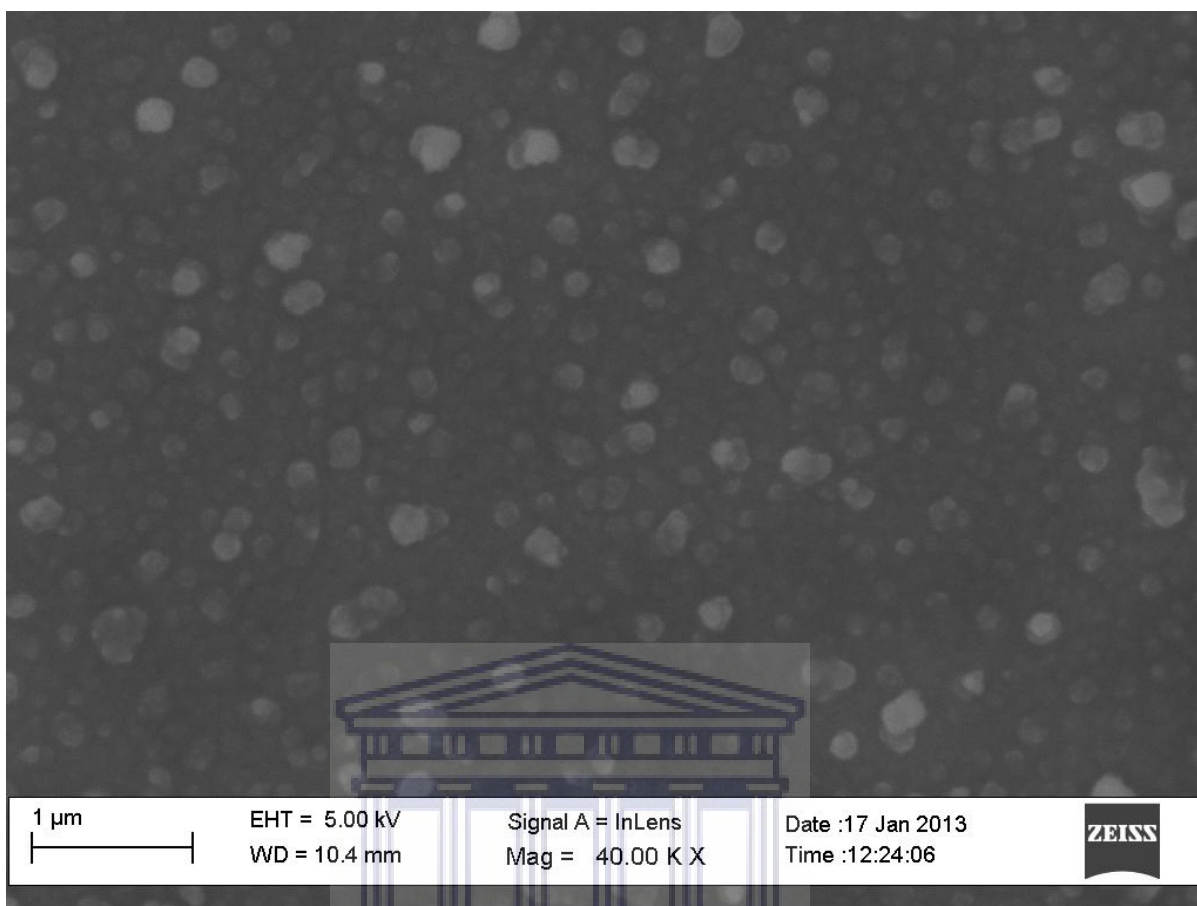
Figure 5.51C:SEM image P(DTBT)2 on ITO electrochemically deposited from 20 mM of DTBT in bmimpf$_6$ at magification of 40,000 K X.
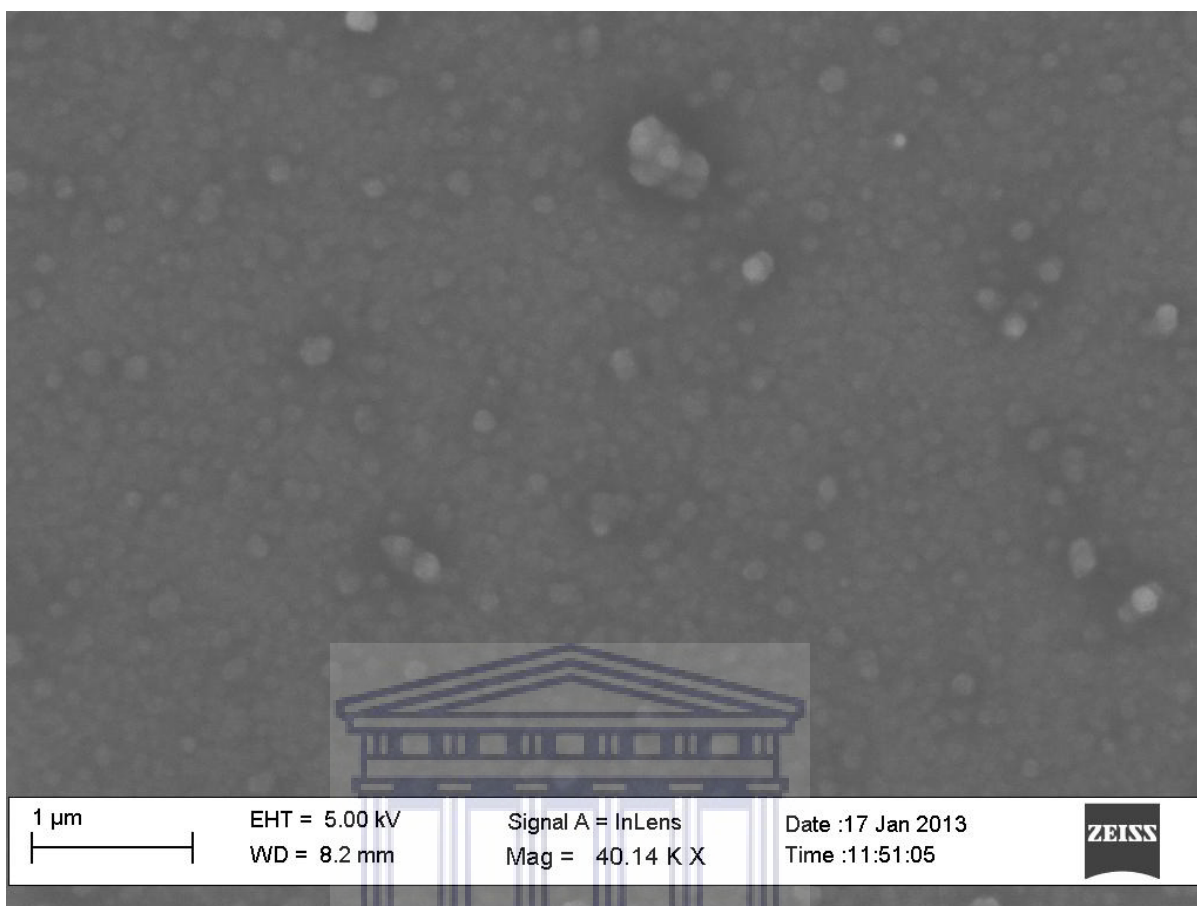
Figure 5.51D: SEM image P(DTBT)3 on ITO electrochemically deposited from 20 mM of DTBT in bmimtnf$_2$ at magification of 40,000 K X.
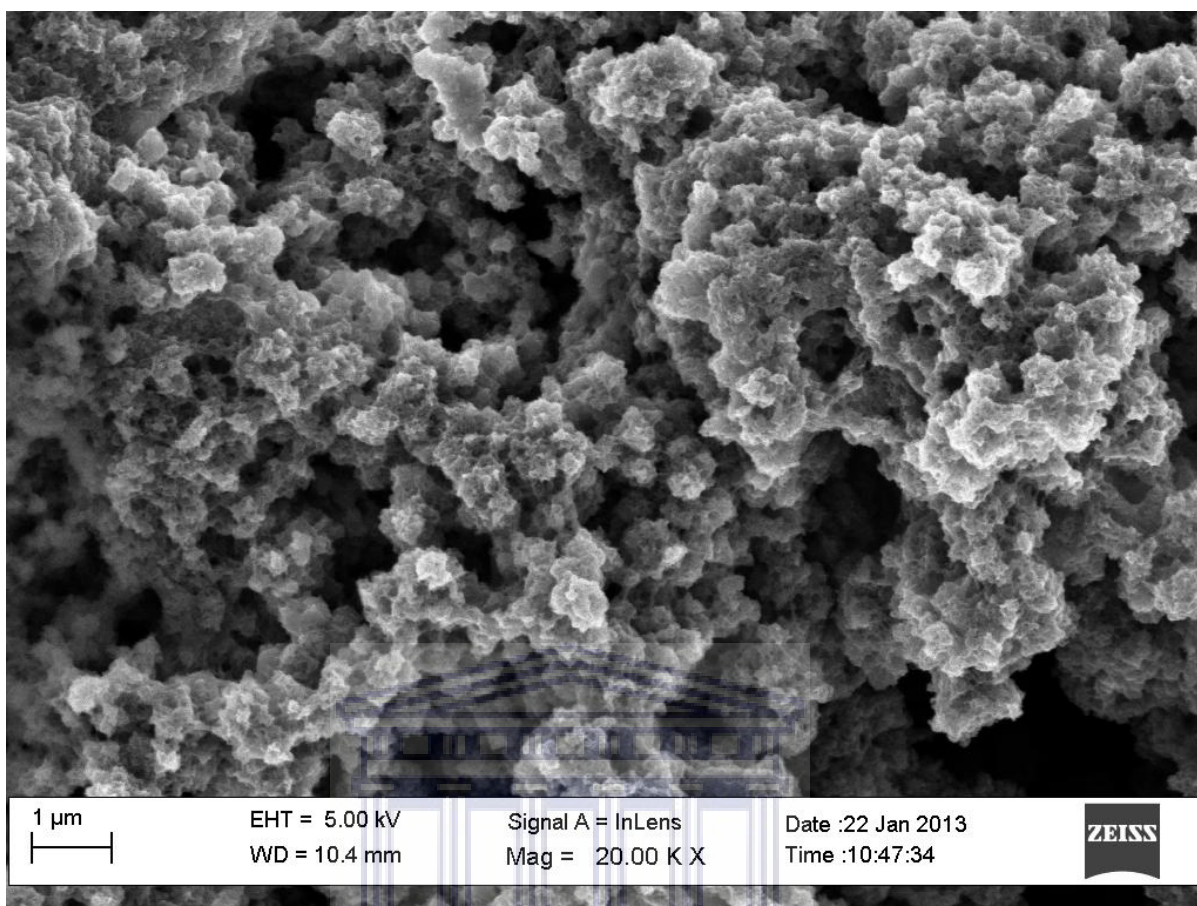
Figure 5.51E: SEM image of P(DTBT)4 on ITO electrochemically deposited from 20 mM of DTBT in 0.1M n-Bu$_4$NClO$_4$/dichloromethane at a magnification of 40,000 K X.

5.4 Copolymerization of DTBT with MOT

In section 5.1 electrodeposition of PMOT and its behaviour in ionic liquids are discussed and in section 5.3 electropolymerization and electrochemical and optical properties of P(DTBT) are presented in detail. In this part of the thesis, a mixture of 4,7-dithien-2-yl-2,1,3-benzothiadiazole (DTBT) and 3-methoxithiophene (MOT) with equal concentration (20 mM each) was copolymerized in two hydrophobic ionic liquids (bmimpf$_6$ and bmimtnf$_2$). Electrochemical and optical properties such as bandgap, colour modulation with potential as well as the morphology of the copolymer film are assessed under this topic.

185

5.4.1 Electrochemical properties of P(DTBT)-co-PMOT

Electrochemical copolymerization of DTBT and MOT (20 mM each) was studied at GC electrode in two hydrophobic ionic liquids namely bmimbf$_6$ and bmimtnf$_2$. Voltammograms recorded during electropolymerizations are indicated in Fig. 5.52. Different from the P(DTBT) and PMOT homopolymers, P(DTBT)2-co-PMOT and P(DTBT)3-PMOT copolymer films grown in ILs bmimpf$_6$ and bmimtnf$_2$ respectively showed two anodic and two cathodic peaks. The onset oxidation potential DTBT and MOT mixture appeared around 0.85 V in bmimbf$_6$ and 0.59 V in bmimtnf$_2$. As expected the onset oxidation potential of the mixture falls between that DTBT and MOT. Anodic peaks around (E_{pa1}= 0.67 V and E_{Pa2} = 1.01V) and cathodic peaks (E_{pc1} = 0.13V, E_{pc2}= 0.71 V) recorded for P(DTBT)2-co-PMOT whereas for P(DTBT)3-co-PMOT anodic peaks were noted at about (E_{pa1}= 0.46 and E_{pa2} = 1.00 V) and reduction peaks (E_{pc1} = -0.20 V and E_{pc2} = 0.31eV). Shift in peak potentials of the copolymer compare to that of the homopolymers indicates the incorporation of both MOT and DTBT in the polymer film. It was also revealed from uv-visible spectroelectrochemistry spectra and their SEM image of P(DTBT)-co-PMOTs.

On the other hand, after the copolymers washed in the respective monomer free ILs, its characterization at different scan rate (5 - 100 mV/s); two anodic and cathodic redox pairs were clearly seen as shown in Fig. 5.52. These peaks were stable at various scan rates reveals that the copolymers are electroactive and well attached on the surface of electrode as similar to their corresponding homopolymers as reported in the previous sections. Linearity of peak current versus scan rate plot shows non diffusion controlled process as well in the case of the copolymers.

Figure 5.53 shows the CV of P(DTBT)3-co-PMOT at various scan rates during p and n-doping. The appearance of redox pairs during n-doping and p doping asserts the presence of

DTBT in the polymer film. As seen from the CV for P(DTBT)3 film, the height of the peak current during n-doping redox pairs were small compare to that p-doping. This could be due to merge of P(DTBT) and PMOT units in p-doping process and hence large current and absence PMOT in n-doping process and therefore smaller current.
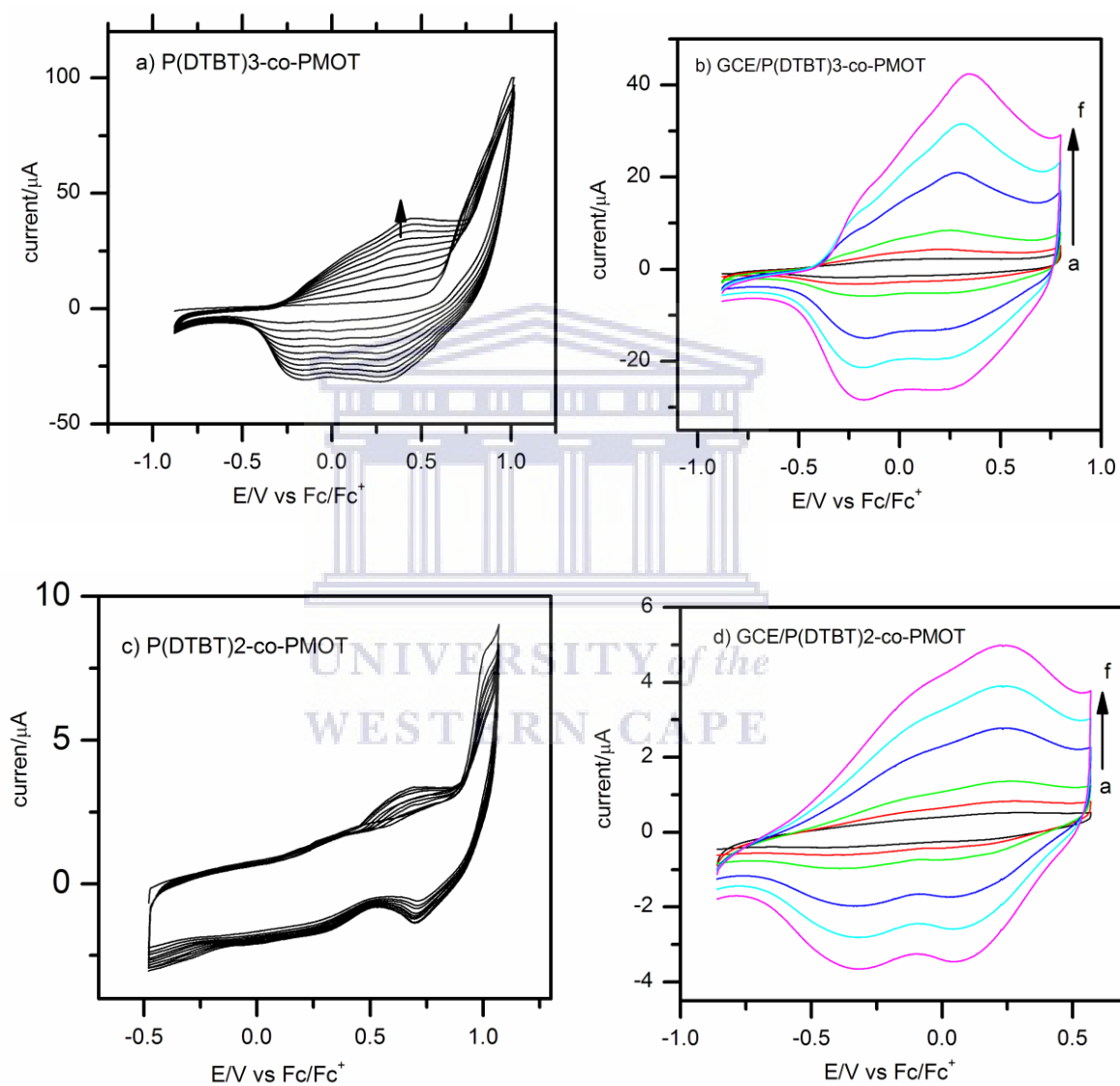
Figure 5.52: a) Cyclic voltammograms of P(DTBT)3-co-PMOT electrodeposited from mixture of 20 mM each DTBT and MOT in bmimtnf$_2$ at scan rate of 100 mV/s and b) GCE/P(DTBT)3-co-PMOT film characterization in monomer free bmimtnf$_2$; c) Cyclic voltammograms of P(DTBT)2-co-PMOT electrodeposited from mixture of 20 mM each DTBT and MOT in bmimpf$_6$ at scan rate of 100 mV/s and d)GCE/P(DTBT)2-co-PMOT film characterization in monomer free bmimpf$_6$ at scan rates of a)5, b) 10, c) 20, d) 50, e) 75 and f) 100 mV/s.

50

0

-50

current/μA

d

a

n-doping

p-doping

-2   -1   0   1

E/V vs Fc/Fc$^+$
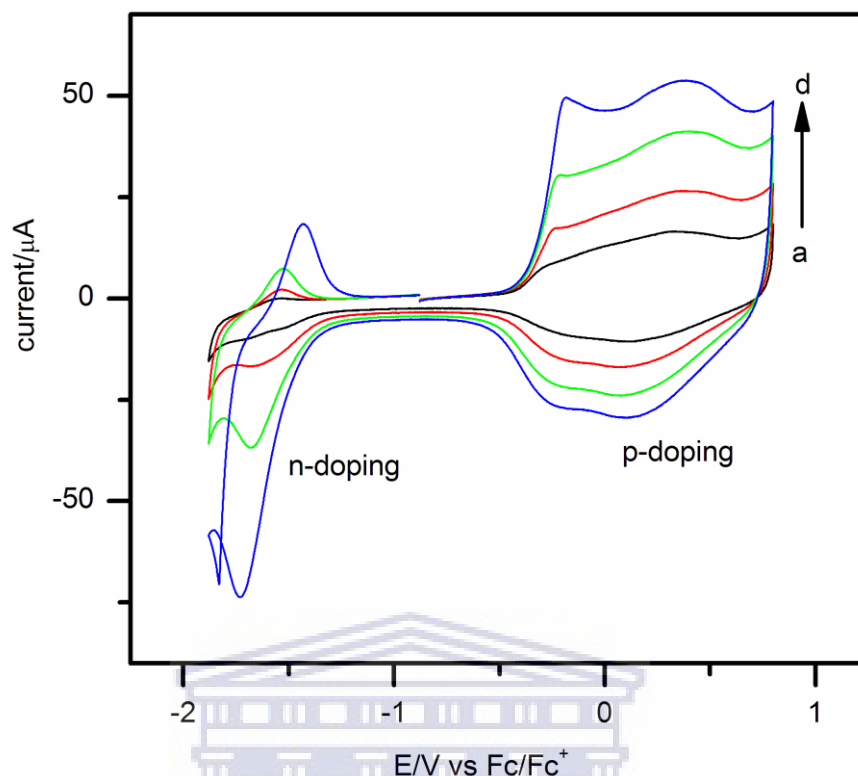
Figure 5.53: Cyclic voltammograms of P(DTBT)3-co-PMOT on GCE in bmimtnf$_2$ during n- and p-doping; a)30, b) 50, c) 75 and d) 100 mV/s.

5.4.2 Spectroelectrochemistry of P(DTBT)-co-PMOT

P(DTBT)-co-PMOT copolymer film electrochemically deposited on ITO glass electrode, uv-vis spectra at various potential are shown in Fig. 5.54 P(DTBT)2-co-PMOT and P(DTBT)3-co-PMOT. Three absorption bands appeared due to $\pi\rightarrow\pi^*$ transitions in the visible region. Maximum absorption bands of the copolymers film are presented in Table 5.31. Three band formation in the neutral state also justified copolymerization of DTBT and MOT.
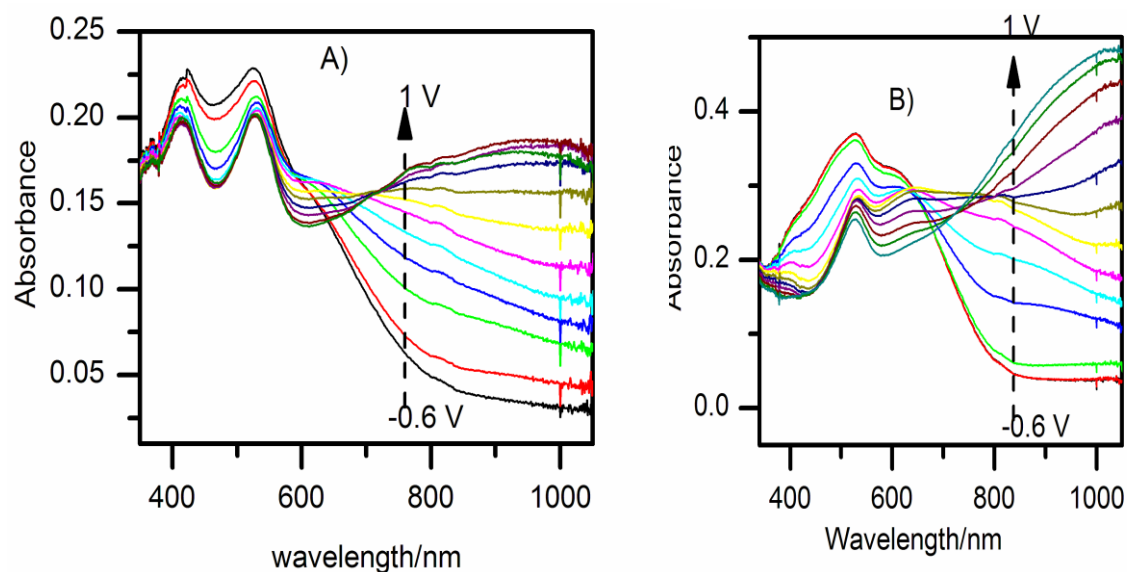
Figure 5.54: Optical spectra of A) P(DTBT)2-co-PMOT on ITO (from -0.6 V to 1 V) in bmimpf$_6$ and B) P(DTBT)3-co-PMOT polymer film on ITO (from -0.6 to 1 V) in bmimtnf$_2$.

Two of the bands emerged are due to P(DTBT) unit whereas the third one is as the result of the presence of PMOT unit. There was no significant maximum absorption as well as optical bandgap (calculated from the onset it was about 1.3 eV) change noted both for P(DTBT)2-coPMOT and P(DTBT)3-co-PMOT deposited in bmimpf$_6$ and bmimtnf$_2$ Ils respectively.

When the copolymer film is completely oxidized, peaks in the visible region decreased in this case not both of them simultaneously depleted as observed for the corresponding homopolymers. The colour of the polymer turns from dark blue colour to blue colour upon oxidation.

Table 5.31: Optical properties of the P(DTBT)-co-PMOT polymer film (λ_{max}/nm).

	reduced	oxidized	E_g/eV
P(DTBT)2-co-PMOT	414, 526, 613	784, 948	1.32
P(DTBT)3-co-PMOT	410, 527, 610	1000	1.31

5.4.2.1 Kinetics study of P(DTBT)-co-PMOT

Double potential step chronoamperometry from -0.6 to 1 V experiment and simultaneously monitoring the percentage transmittance change was performed on ITO/P(DTBT)-co-PMOT thin film at a fixed wavelength of 1000 nm to estimate the switching speed and optical contrast of the copolymers. Compare with the homopolymer P(DTBT)3 its copolymer with PMOT that is P(DTBT)3-co-PMOT showed a maximum optical contrast of 59% in the NIR region. In the case of P(DTBT)2-co-PMOT composite electrosynthesized in bmimpf$_6$ ionic liquids, a smaller optical contrast of about 16 % was recorded (Fig. 5.55).
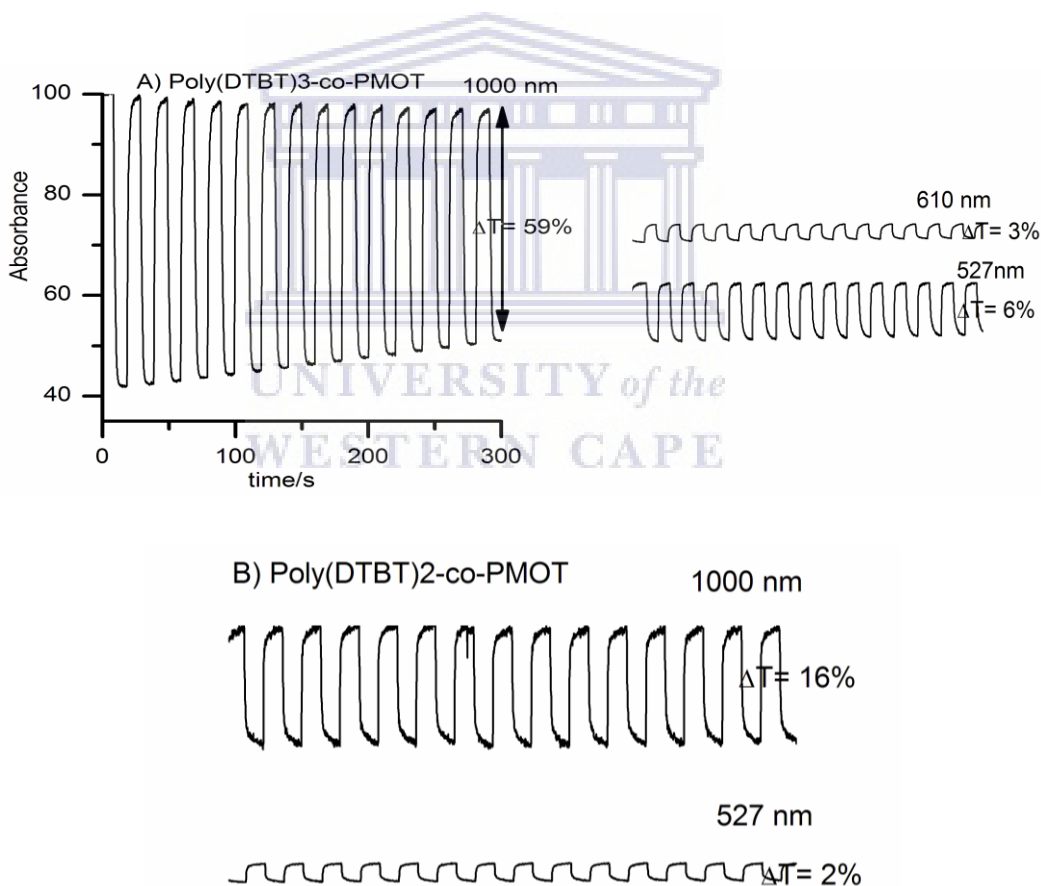
Figure 5.55: Transmittance time profile during double potential step chronoamperometry from -0.6 to 1 V at each potential 10 s for A) P(DTBT)3-co-PMOT on ITO monitored at 1000, 610 and 527 nm and B) P(DTBT)2-co-PMOT on ITO monitored at 1000 and 572 nm.

5.4.3 Morphology of P(DTBT)-co-PMOT copolymer film

SEM images of P(DTBT)-co-PMOT films on ITO electrode were measured to assess the effect of the nature of growth medium and copolymerization on the morphology of the conducting polymer films. P(DTBT)2-co-PMOT films electrochemically synthesized in bmimpf$_6$ (Fig. 5.56A) and P(DTBT)3-co-PMOT in bmimtnf$_2$ (Fig. 5.57A) were found to posses morphologies different from image of P(DTBT)2 and P(DTBT)3 and PMOT respectively. Thus the copolymerization caused different morphology as it caused different electrochemical or optical properties. P(DTBT)2-co-PMOT film formed in bmimpf$_6$ appears to posses characteristic morphologies of P(DTBT)2 granular bearing small grains and globular topography characteristics of PMOT accompanied with significantly incorporating 1-buthyl-3-methyl imidazolium cation [31, 40-41]. The presence granular ball shape grains and globular structure indicates the copolymerization of DTBT and PMOT.
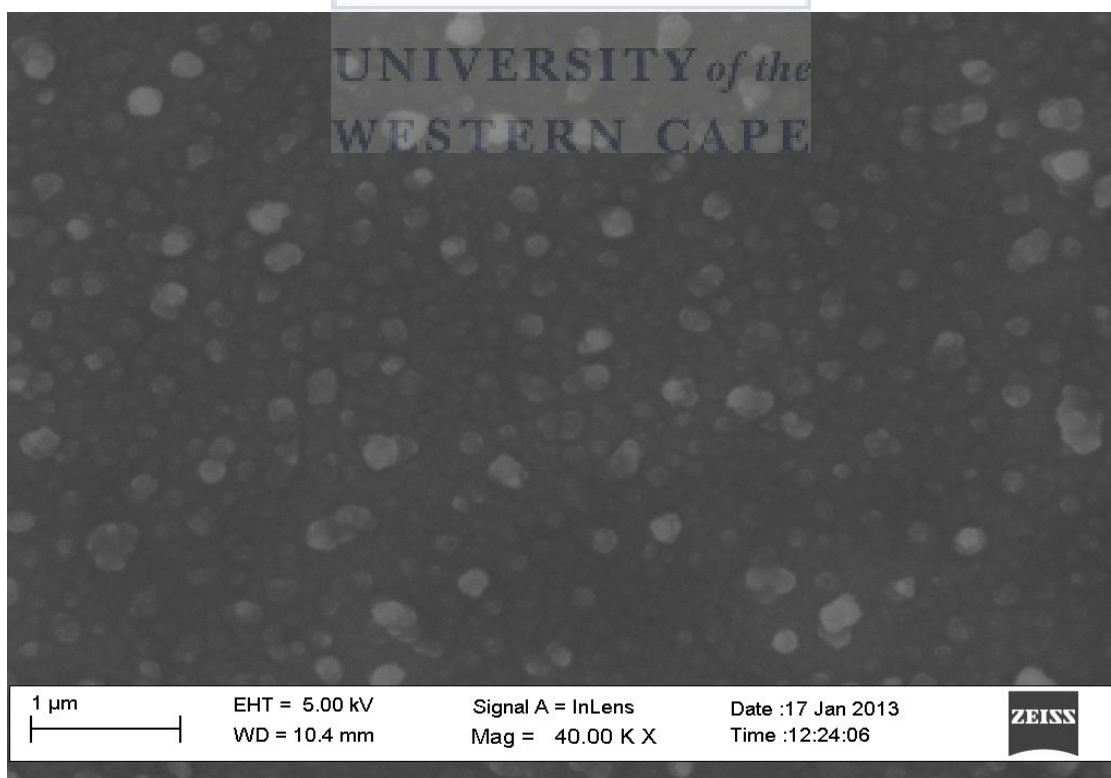
Figure 5.51C
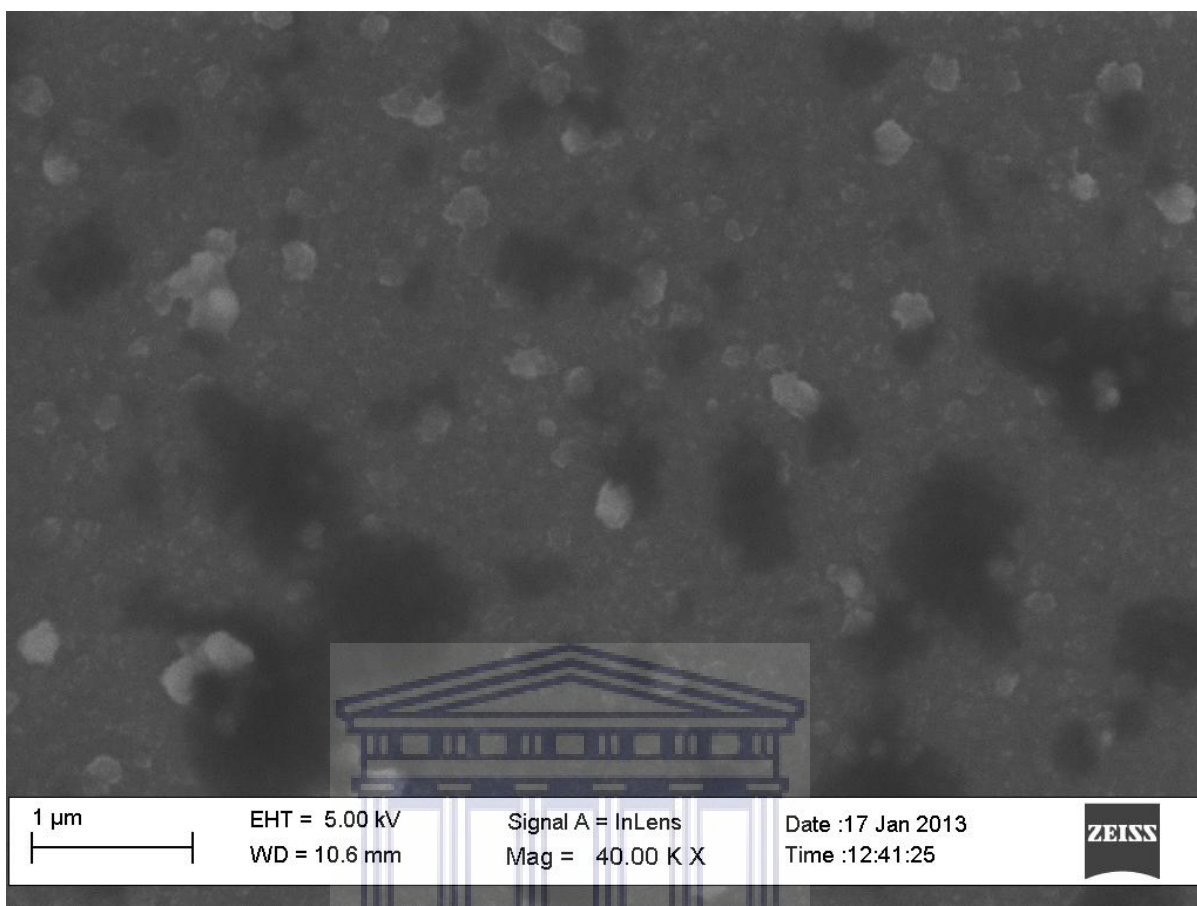
Figure 5.56A: SEM image of P(DTBT)2-co-PMOT on ITO electrochemically deposited from 20 mM of DTBT and MOT in bmimpf$_6$ at a magnification of 40,000 K X.

In contrast, P(DTBT)3-co-PMOT grown in bmimtnf$_2$ its SEM image is smoother, ordered and dense (Fig. 5.57B) compare with that of P(DTBT)2-co-PMOT. Thus the nature of the ionic liquid changes the film morphology.

| 1 μm | EHT = 5.00 kV | Signal A = InLens | Date :10 May 2013 | ZEISS |
| | WD = 4.6 mm | Mag = 40.00 K X | Time :10:36:29 | |
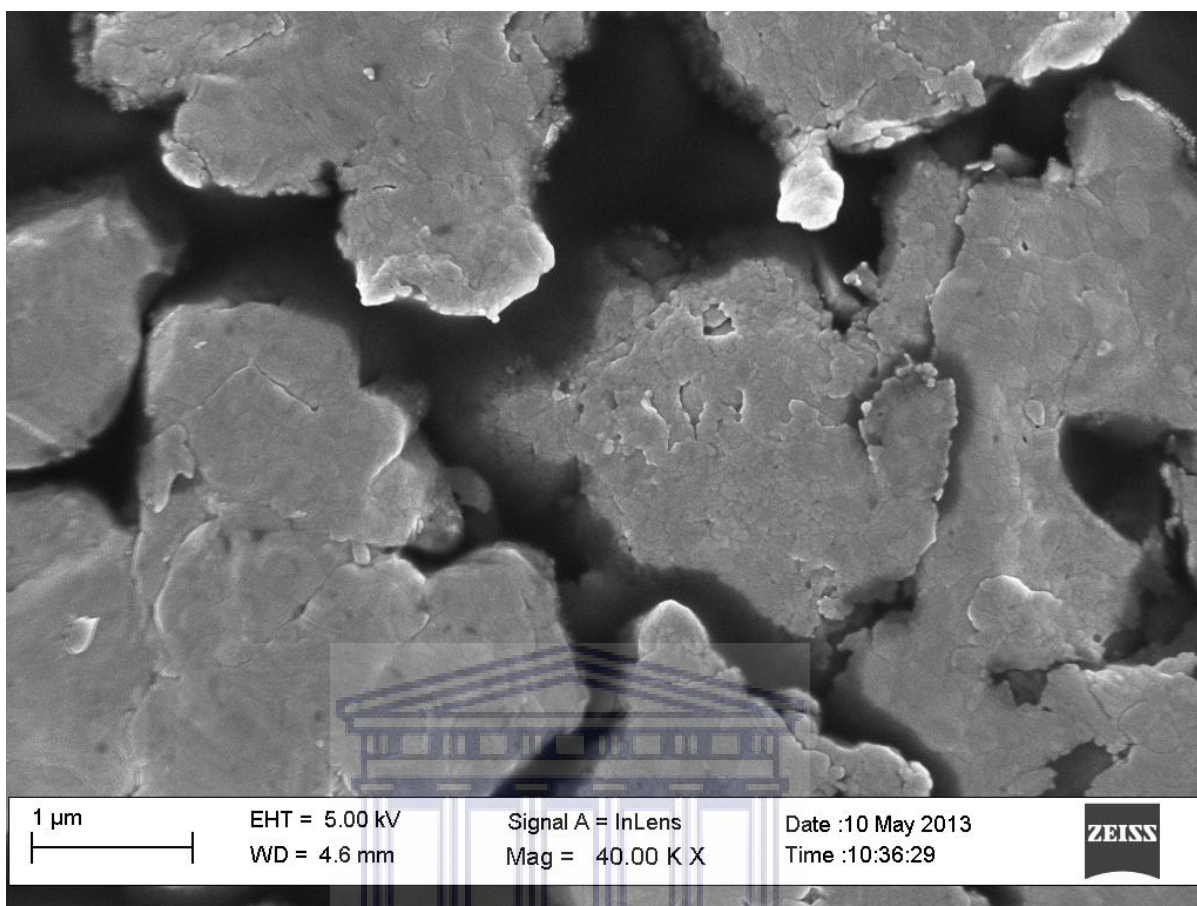
Figure 5.56B: SEM image of PMOT on ITO electrochemically deposited from 20 mM of MOT in bmimpf$_6$ at a magnification of 40,000 K X.
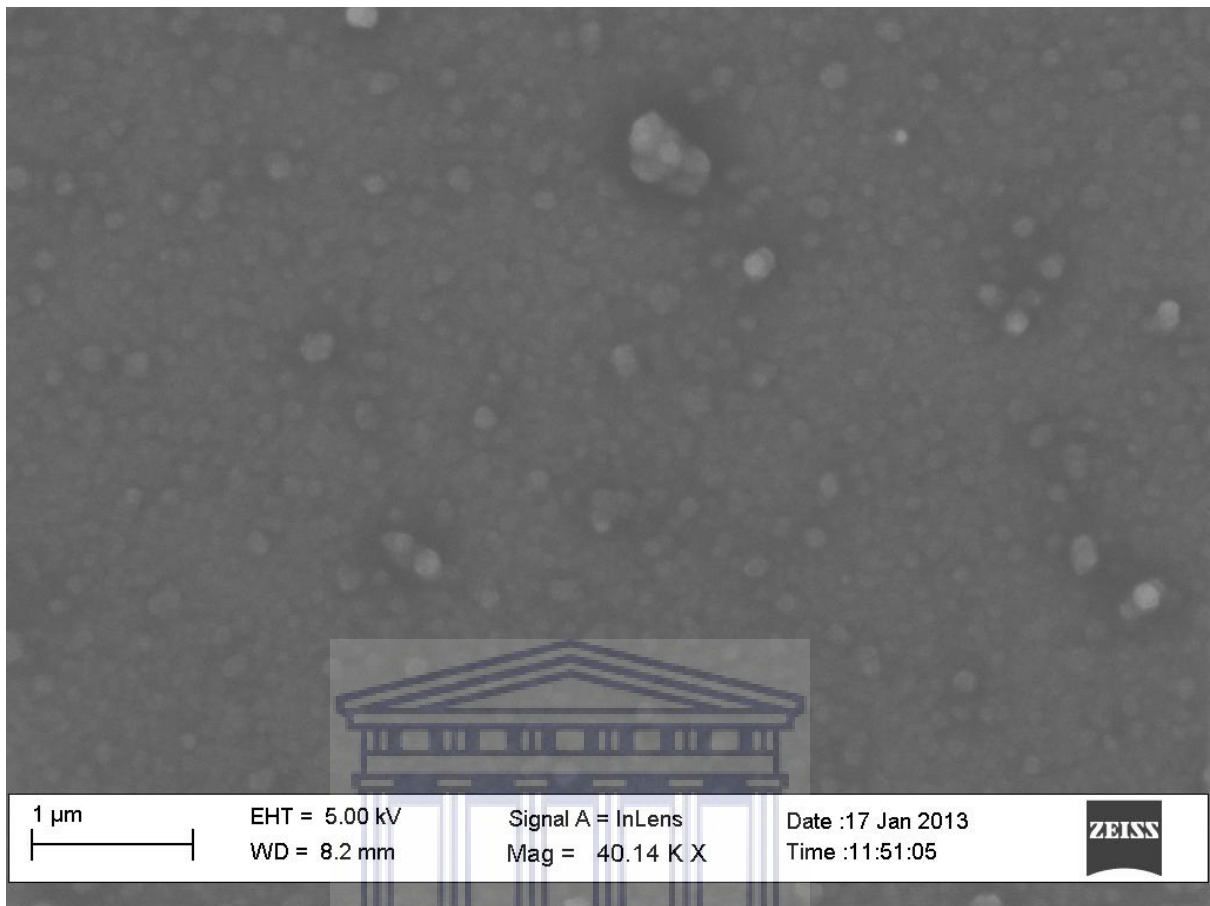
Fig 5.51D
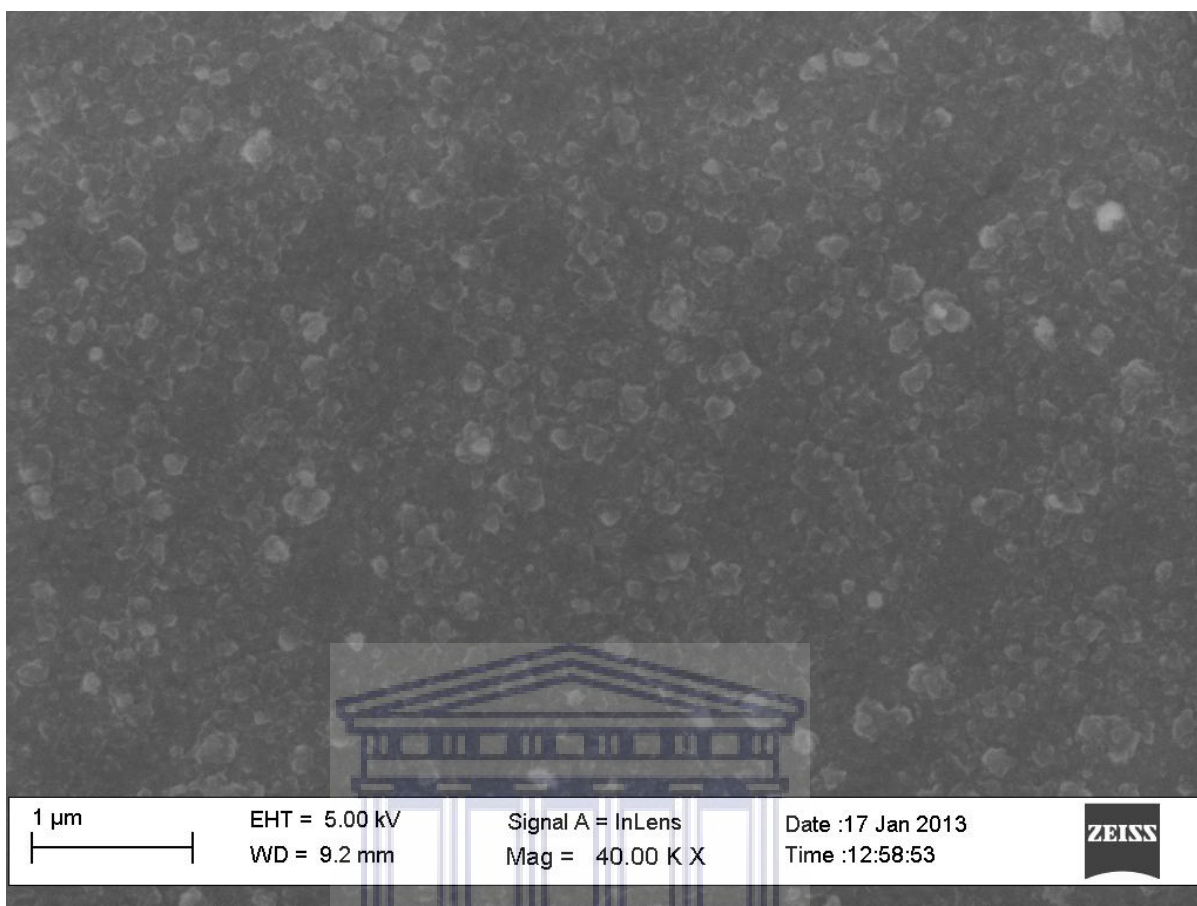
Figure 5.57A: SEM image of P(DTBT)3-co-PMOT on ITO electrochemically deposited from 20 mM of DTBT and MOT in 0.1M bmimtnf$_2$ at a magnification of 40,000 K X.
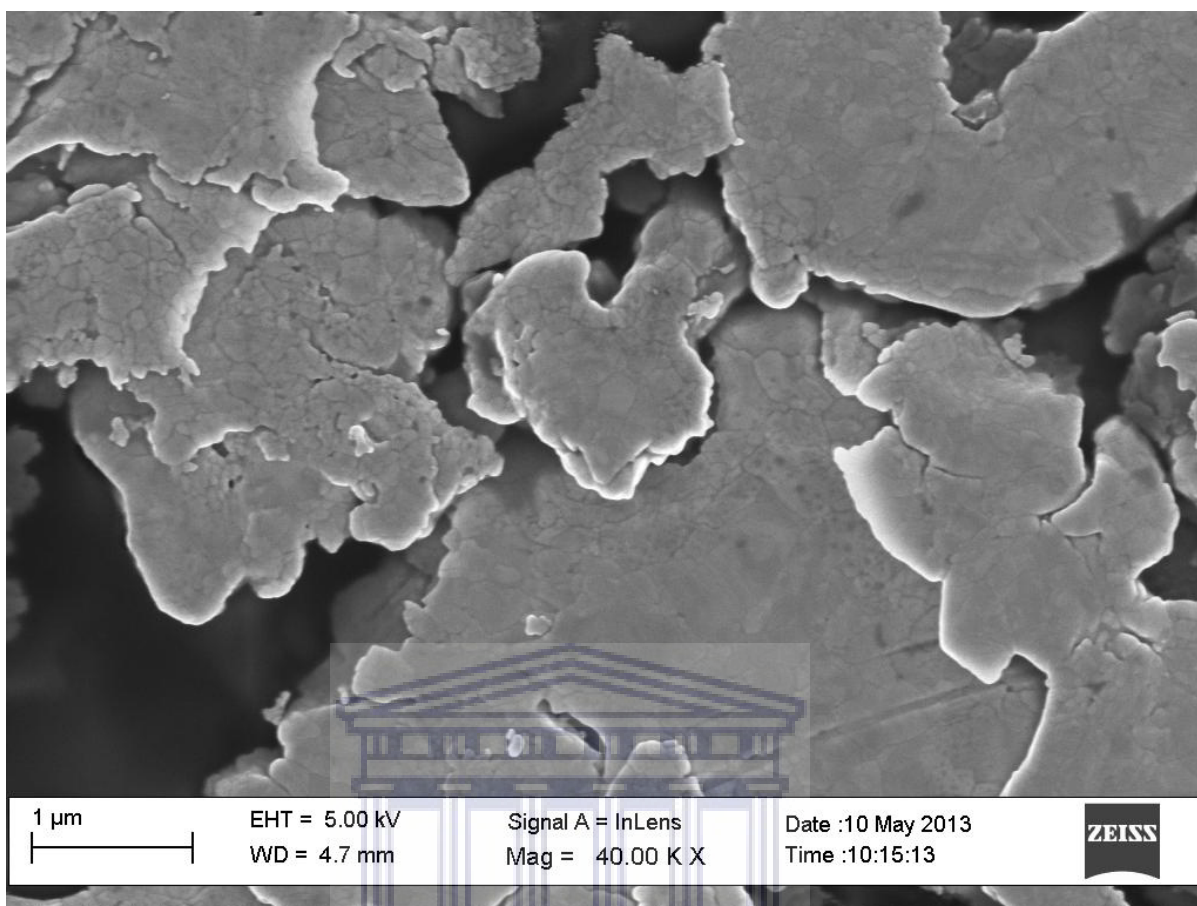
Figure 5.57B: SEM image of PMOT on ITO electrochemically deposited from 20 mM of MOT in bmimtnf$_2$ at a magnification of 40,000 K X.

CHAPTER 6

EXECUTIVE SUMMARY

Electrochemical and electrochromic properties of poly(4,7-dithien-2-yl-2,1-3-benzothiadiazole) P(DTBT) and its copolymer with 3-methoxythiophe (MOT) has been studied in imidazolium based ionic liquids, 1-butyl-3-methylimidazolium compounds of tetrafluroborate (bmimbf$_4$), hexaflurophosphate (bmimpf$_6$), bis(trifluoromethylsulfonyl)imide (bmimtnf$_2$). Effect of the nature of ionic liquid on polymerization rate, stability on the redox processes, morphology, switching times, optical contrast and colouration efficiency were analyzed. Preliminary electrochemical data of 4,7-dithien-2-yl-2,1,3-benzothiadiazole (DTBT) generated to compare and contrast to the polymer P(DTBT) behaviours such as oxidation potential, half wave potential, bandgap and n-doping. Electrosynthesis and characterization of PMOT is presented in the first section of this work to compare its properties with that P(DTBT) as well as to their copolymers.

Electropolymerization of poly(3-methoxythiophene) and its mixture with 3,4-ethylenedioxythiophene (EDOT) have been successfully electropolymerized in four ionic liquids bmimbf$_4$, bmimpf$_6$, bmimtnf$_2$ and 1-octyl-3-methylimidazolium bis(triflu0romethylsulfonyl)imide (octmimtnf$_2$). Deposition of film growth was faster in the less viscous and more conductive octmimtnf$_2$ hydrophobic than bmimbf$_4$ hydrophilic ionic liquids as it was jugged from peak current and total charge of polymerization. Poly(3-methoxythophene) and its copolymer with PEDOT were electrochemically activity both in the growth medium and aqueous LiClO$_4$. Plot of anodic peak current versus scan rate showed a quasi reversible electrochemical profile. PMOT-co-PEDOT1 and PMOT-co-PEDOT2 copolymers CVs, uv-visible spectrum and their morphology were quite different from their

homopolymers PMOT and PEDOT indicating copolymerization. All of the obtained polymers exhibited absorption bands changes with potential. PMOT1 grown in bmimbf$_4$ and PMOT2 grown in octmimtnf$_2$ in the reduced state the maximum absorption band appeared at about λ_{max} 480 and 485 nm (red colour) and when the polymers doped broad absorption peak generated at about centre of maximum wavelength λ_{max} 645 nm and 600 nm (blue colour) for PMOT1 and PMOT2 respectively. On the other hand, PMOT-co-PEDOT1 and PMOT-co-PEDOT2 absorption bands changed from 560 nm (blue) during reduction, 795 to 970 nm during oxidation (near infrared region). The modulation of the colour by changing voltage in the visible and near infrared region made these materials as a good candidate for applications in electrochromic devices.

4,7-dithien-2-yl-benzothiadiazole (DTBT) monomer oxidized at about 1.05 V in 0.1 M n-Bu$_4$NClO$_4$ /acetonitrile and its half wave potential was about 0.87 V in agreement with the literature value whereas in ionic liquids it was slightly lower and appeared around 0.79 V. Electrochemistry of reduction of 4,7-dithien-2-yl-2,1,3-benzothidiazole were investigated using cyclic voltammetry (CV) and electrochemical impedance spectroscopy (EIS) in the presence 0.1 M tetrabuthylammonium perchlorate in acetonitrile (ACN), dichloromethane (DCM) and their mixtures DCM-ACN (2:3 (v/v)) and in three ionic liquids namely 1-butyl-3-methylimidazolium tetrafluoroborate (bmimbf$_4$) hydrophilic and 1-butyl-3-methylimidazolium hexafluorophosphate (bmimpf$_6$) and 1-butyl-3-methylimidazolium bis(trifluoromethylsulfonyl)imide (bmimtnf$_2$) on three electrodes (Pt, Au and GC). Anodic (E_{pa}) and cathodic (E_{pc}) peak potentials as well as their corresponding anodic (i_{pa}) and cathodic (i_{pc}) peak currents acquired at different scan rates between 0.03 to 0.5 V/s. Anodic and cathodic peak potentials as well their differences (ΔE_p) were independent of scan rates, shows the reversibility of DTBT/DTBT$^-$ system. It also confirms one electron is involved in this redox reaction. The formal potential obtained in the various solvents used were in ACN

(-1.56 V) vs. ferrocene/ferrocinium (Fc/Fc$^+$), DCM-ACN (-1.52 V) and DCM (-1.62 V) at Pt electrode and ACN (-1.50 V), DCM-ACN (-1.52 V) and DCM (-1.57 V) at Au electrode. The diffusion coefficient (D) was calculated using Randles – Sevcik equation and found to be in ACN (1.11 x 10^{-5} cm^2/s), DCM-ACN (5.06 x 10^{-6} cm^2/s) and DCM (7.45 x 10^{-6} cm^2/s on Pt electrode and ACN (1.22 x 10^{-5} cm^2/s), DCM-ACN (6.04 x 10^{-6} cm^2) and 6.10 x 10^{-6} cm^2/s) on Au electrode. It was also noted that diffusion coefficient of DTBT was larger by the order of nearly 10 times in the less viscous medium ACN than DCM.

EIS measurement of electrode/DTBT/DTBT$^-$ interface was performed in the frequency range 100 mHz to 100 kHz at amplitude voltage of 10 mV. Standard heterogeneous rate constant (k^o) calculated from impedance data was 0.069 cm/s in ACN, 0.083 cm/s in DCM-ACN and 0.061 cm/s in DCM on Pt electrode while on Au electrode it was 0.434 cm/s in ACN, (0.240 cm/s in DCM-ACN and 0.072 cm/s in DCM. Charge transfer kinetics of DTBT/DTBT$^-$ redox system was faster in acetonitrile on gold compare to that of platinum electrode.

In conclusion, the redox potential of DTBT/DTBT$^-$ couple was found to be E$^{o'}$ = -1.56 V in organic and -1.55 V in ionic liquids, diffusion coefficient of DTBT falls in the range of 1.11 x 10^{-5} to 5.0 x 10^{-6} cm^2/ s in acetonitrile and dichloromethane. Diffusion of the anion (DTBT$^-$) was approximately about one tenth of DTBT and one forth when DTBT reduced in acetonitrile and dichloromethane respectively. On the other hand, DTBT diffusion coefficient in ionic liquids was in the range of 9.0 x 10^{-9} to 7.02 x 10^{-10} cm^2/s when DTBT reduced in the less viscous bmimtnf$_2$ and in the more viscous one bmimpf$_6$ ionic liquids. As expected, because of the higher viscosity of ionic liquids diffusion coefficient of DTBT found to be lower by the order of 10^{-4} in ionic liquids compare to that of its value in organic solvents.

Electrochemical polymerization and characterization P(DTBT) was performed in bmimbf$_4$, bmimpf$_6$, and bmimtnf$_2$ ionic liquids. P(DTBT)1, P(DTBT)2, P(DTBT)3 and P(DTBT)4

represent when P(DTBT) films formed from 20 mM solution of DTBT in bmimbf$_4$, bmimpf$_6$, bmimtfn$_2$, and 0.1 M tetrabutylammonimm perchlorate/ dichloromethane or acetonitrile. Compared to previously reported onset oxidation potentials, the monomer oxidized at a lower potential (0.55 V-0.89 V vs. ferrocene redox potential). A well defined electrochemical activity was observed during p- and n-doping of the polymer. P(DTBT)s polymer film was stable both during p and n -doping with an electrochemical bandgap (1.2 to 1.3 eV) as estimated from CV unlike poly(3-methoxythiphene). n-Doping behaviour resembles its monomer and the redox potentials occurred in lower negative potentials -1.02 to -1.40 V.

Electrochemical impedance spectroscopy experiment was also performed on GCE/P(DTBT)/ionic liquid system. Impedance spectra result showed a semicircle at higher frequency region and Warburg diffusion impedance in the lower frequency region indicating a quasi-reversible redox process. Various electrical parameters estimated by fitting the impedance spectra to the model depend on the nature of the growth medium. For example double layer capacitance was varied as a result of difference in electroactive surface area of P(DTBT) film. P(DTBT) grown in less viscous ionic liquids produce a denser film and because of this a larger double layer capacitance was found for GCE/P(DTBT)/bmimtnf$_2$ system. Besides, this interface posse a lower charge transfer and solution resistance attributed to lower viscosity of bmimtnf$_2$. In contrast, diffusion impedance was large for GCE/P(DTBT)/bmimtnf$_2$ interface. In this case the size of the anions played a vital role in determining diffusion impedance. Since bis(trifluoromethylsulfonyl)imide anion is relatively a larger anion to that of hexafluorophosphate and tetrafluoroborate that possibly limit its movement and hence its diffusion impedance becomes large.

Spectroelectrochemistry spectra of P(DTBT)s film formed on ITO electrode exhibited two absorption bands in the visible range, both attributed to π- π* transitions, and the respective

dominant peaks having λ_{max} = 540 nm, 579 nm, 578 nm, and 560 nm for P(DTBT)1, P(DTBT)2, P(DTBT)3 and P(DTBT)4 respectively. A slight red shift observed for P(DTBT)2 and P(DTBT)3 indicates increased conjugation length of the polymer in the hydrophobic ILs (bmimpf$_6$ and bmimtnf$_2$). P(DTBT)s thin film was blue-black colour in the reduced state and turned to transparent with red-purple residue colour upon complete oxidation. The visible absorption bands disappeared during oxidation and bipolaron bands appeared in the near infrared region around 800 nm for P(DTBT)1, 875 nm and 1000 nm for both P(DTBT)2 and P(DTBT)3 and 1000 nm for P(DTBT)4. Bandgap estimated from uv-vis spectra was found to be 1.58 eV for P(DTBT)1 and 1.54 eV for P(DTBT)4. A lower bandgap for P(DTBT) grown in hydrophobic ionic liquids, 1.42 eV for P(DTBT)2 and 1.39 eV for (PDTBT)3 compare to the film grown in hydrophilic ILs. From simultaneous double potential-step between -0.6 V and 1.0 V) at a period of 10 s for each potential chronoamperometry and fixed-wavelength transmittance (T) measurements, the switching times and maximum optical contrasts (%ΔT) were 14 to 17% and 1 to 1.4 s for P(DTBT)s formed in the ILs at 1000 nm and 39% and 2 s for P(DTBT)4 (λ = 1000 nm), whereas colouration efficiency varied in the range of 91 to 187 mC/cm^2. On the other hand, when the polymer turns from bleached state to coloured state slow response time 3 to 5 s was recorded. Switching ability and stability (no significant lost in electrochemical activity up to 500 cycles at scan rate of 200 mV/s) of P(DTBT) showed its potential applications in colour changing electrochromic devices in the near infrared region. Fast switching ability and moderate optical contrast of the polymer demonstrates its potential for electrochromic device applications.

Narrow bandgap (1.3 eV) copolymer of P(DTBT) and PMOT film was produced by copolymerization showing the incorporation of 3-methyoxythiophene in P(DTBT) chain and

MOT seems act as a π-spacer. As evidenced from the number of peaks from the CV and uv-vis spectra of P(DTBT)-co-PMOT in comparison with the homopolymers P(DTBT) and PMOT indicates copolymerization. A high optical contrast (%ΔT = 56) achieved when DTBT and MOT copolymerized in bmimtnf$_2$ compare to 16 % in bmimpf$_6$. Furthermore, morphology of the film reveals copolymerization as seen consists of globular due to MOT and granular bearing small ball shapes due to P(DTBT). Colour of the film switches from dark blue colour in the reduced state to blue colour when it is oxidized with a switching time of 2.5 to 2.6 s.

A type of donor–acceptor polymer, poly(4,7-dithen-2-yl-2,1,3-benzothiadiazole) which have been electrochemically polymerized from the monomer 4,7-dithien-2-yl-2,1,3-benzothiadiazole (DTBT) is a promising material for electrochromic, solar cell, charge storage and biosensors applications. The same potential application has been reported for PMOT. P(DTBT) polymer electrochemical and optical behaviours in ionic liquids have shown that P(DTBT) and its copolymer with 3-methoxythiophene are potential material for electrochromic device applications.

I believe that the prospect of this investigation on poly(4,7-dithen-2-yl-2,1,3-benzothiadiazole) and its copolymer with 3-methoxythiophene will have its own impact for future research on these materials. Insolubility of P(DTBT) polymer in common organic solvents has been a challenge for practical applications. P(DTBT) solubility can be improved by synthesizing derivatives of DTBT using various strategies. Therefore, the finding in this thesis can be used as a baseline for further research on the electrochromic properties of substituted DTBT or copolymerization with other monomers in ionic liquids or mixture of ionic liquids and organic solvents to reduce the cost implication of ionic liquids are potential areas for future research.

REFERENCES

1. Pron, A. and Rannou, P., *Processible conjugated polymers: from organic semiconductors to organic metals and superconductors.* Progress in Polymer Science, 2001. **27**: p. 135-190.

2. Granstroem, M., Magnus, B., P.Danilo, Olle, I., R., A.M., Thomas, H., and Olof, W., *Self Organizing Polymer film- a route to novel electronic devices based on conjugated polymers.* Supramolecular Science, 1997. **4**: p. 27-34.

3. Das, T.K. and Prusty, S., *Review on Conducting Polymers and Their Applications.* Polymer - Plastics Technology and Engineering, 2012. **51**: p. 1487-1500.

4. De Luca, V., Digiamberardino, P., Di Pasquale, G., Graziani, S., Pollicino, A., Umana, E., and Xibilia, M.G., *Ionic electroactive polymer metal composites: Fabricating, modeling, and applications of postsilicon smart devices.* Journal of Polymer Science, Part B: Polymer Physics, 2013. **51**: p. 699-734.

5. Molapo, K.M., Ndangili, P.M., Ajayi, R.F., Mbambisa, G., Mailu, S.M., Njomo, N., Masikini, M., Baker, P., and Iwuoha, E.I., *Electronics of conjugated polymers (I): Polyaniline.* International Journal of Electrochemical Science, 2012. **7**: p. 11859-11875.

6. Nguyen, T.P., Le Rendu, P., Molinié, P., and Tran, V.H., *Electrical characterization of phenylene-vinylene oligomer based diodes.* Synthetic Metals, 1997. **85**: p. 1357-1358.

7.   Andersson, M.R.O.T., W. Mammo, M. Svenssory, M. Theander and O. Inganas, *Substituted Polythiophenes Designed for Optoelectronic Devices and Conductors.* Journal of Materials Chemistry, 1999. **9**: p. 1933-1940.

8.   Álvarez-Romero, G.A., Ramírez-Silva, M.T., Galán-Vidal, C.A., Páez-Hernández, M.E., and Romero-Romo, M.A., *Development of a chloride ion-selective solid state sensor based on doped polypyrrole-graphite-epoxy composite.* Electroanalysis, 2010. **22**: p. 1650-1654.

9.   Ozyurt, F., Gunbas, E.G., Durmus, A., and Toppare, L., *Processable and multichromic polymer of bis-3-hexylthiophene substituted 4-tert-butylphenyl quinoxaline.* Organic Electronics, 2008. **9**: p. 296-302.

10.   Tarkuc, S., Sahmetlioglu, E., Tanyeli, C., Akhmedov, I.M., and Toppare, L., *Electrochromic properties of poly (1-(phenyl)-2,5-di(2-thienyl)-1H-pyrrole-co-3,4-ethylenedioxy thiophene) and its application in electrochromic devices.* Optical Materials, 2008. **30**: p. 1489-1494.

11.   Johansson, T., Mammo, W., Svensson, M., Andersson, M.R., and Inganaes, O., *Electrochemical bandgaps of substituted polythiophenes.* Journal of Materials Chemistry, 2003. **13**: p. 1316-1323.

12.   Hapiot, P. and Lagrost, C., *Electrochemical Reactivity in Room-Temperature Ionic Liquids.* Chemical Reviews, 2008. **108**: p. 2238-2264.

13.   Fikus, A., Rammelt, U., and Plieth, W., *Characterization of semiconductor properties of polybithiophene film electrodes in contact with aqueous electrolytes.* Electrochimica Acta, 1999. **44**: p. 2025-2035.

14. Inganäs, O., Svensson, M., Zhang, F., Gadisa, A., Persson, N.K., Wang, X., and Andersson, M.R., *Low bandgap alternating polyfluorene copolymers in plastic photodiodes and solar cells.* Applied Physics A: Materials Science & Processing, 2004. **79**: p. 31-35.

15. Dong, B., Xu, J., Zheng, L., and Hou, J., *Electrodeposition of conductive poly(3-methoxythiophene) in ionic liquid microemulsions.* Journal of Electroanalytical Chemistry, 2009. **628**: p. 60-66.

16. Thémans, B., André, J.M., and Brédas, J.L., *Electronic structure of the alkyl, benzyl and methoxy derivatives of polythiophene.* Synthetic Metals, 1987. **21**: p. 149-156.

17. Chang, A.-C., Blankespoor, R.L., and Miller, L.L., *Characterization and spectroelectrochemical studies of soluble polymerized 3-methoxythiophene.* Journal of Electroanalytical Chemistry and Interfacial Electrochemistry, 1987. **236**: p. 239-252.

18. Fall, M., Aaron, J.J., Sakmeche, N., Dieng, M.M., Jouini, M., Aeiyach, S., Lacroix, J.C., and Lacaze, P.C., *Electrochemical and spectroscopic properties of poly(3-methoxythiophene) electrosynthesized in an aqueous micellar medium.* Synthetic Metals, 1998. **93**: p. 175-179.

19. Fall, M., Dieng, M.M., Aaron, J.J., Aeiyach, S., and Lacaze, P.C., *Role of surfactants in the electrosynthesis and the electrochemical and spectroscopic characteristics of poly(3-methoxythiophene) films in aqueous micellar media.* Synthetic Metals, 2001. **118**: p. 149-155.

20.   Alves, M.R.A., Calado, H.D.R., Donnici, C.L., and Matencio, T., *Electrochemical polymerization and characterization of new copolymers of 3-substituted thiophenes.* Synthetic Metals, 2010. **160**: p. 22-27.

21.   Yohannes, T., Carlberg, J.C., Inganaes, O., and Solomon, T., *Electrochemical and spectroscopic characteristics of copolymers electrochemically synthesized from 3-methylthiophene and 3,4-ethylenedioxythiophene.* Synthetic Metals., 1997. **88**: p. 15-21.

22.   Catellani, M., Arbizzani, C., Mastragostino, M., and Zanelli, A., *Poly(3-buthyl-co-3,4-dibuthylthiophene)s: synthesis and electrochromic characterization.* Synthetic Metals, 1995. **69**: p. 373-374.

23.   Pang, Y., Xu, H., Li, X., Ding, H., Cheng, Y., Shi, G., and Jin, L., *Electrochemical synthesis, characterization, and electrochromic properties of poly(3-chlorothiophene) and its copolymer with 3-methylthiophene in a room temperature ionic liquid.* Electrochemistry Communications, 2006. **8**: p. 1757-1763.

24.   Nie, G., Qu, L., Xu, J., and Zhang, S., *Electrosyntheses and characterizations of a new soluble conducting copolymer of 5-cyanoindole and 3,4-ethylenedioxythiophene.* Electrochimica Acta, 2008. **53**: p. 8351-8358.

25.   Fall, M., Diagne, A.A., Dieng, M.M., Deflorian, F., Rossi, S., Bonora, P.L., Volpe, C.D., and Aaron, J.J., *Electrochemical impedance spectroscopy of poly(3-methoxythiophene) thin films in aqueous LiClO4 solutions.* Synthetic Metals, 2005. **155**: p. 569-575.

26.   Han, Z., Zhang, J., Yang, X., Zhu, H., and Cao, W., *Synthesis and photoelectric property of poly (3-methoxythiophene)/titanium dioxide complexes.* Solar Energy Materials and Solar Cells, 2010. **94**: p. 755-760.

27.   Atta, N.F., Galal, A., Ersin Karagözler, A., Russell, G.C., Zimmer, H., and Mark Jr, H.B., *Electrochemistry and detection of some organic and biological molecules at conducting poly(3-methylthiophene) electrodes.* Biosensors and Bioelectronics, 1991. **6**: p. 333-341.

28.   Ates, M. and Sarac, A.S., *Electrochemical Impedance Spectroscopic Study of Polythiophenes on Carbon Materials.* Polymer-Plastics Technology and Engineering, 2011. **50**: p. 1130-1148.

29.   Shu, D., Zhang, J., He, C., Meng, Y., Chen, H., Zhang, Y., and Zheng, M., *Improved electrochemical redox performance of 2,5-dimercapto-1,3,4-thiadiazole by poly(3-methoxythiophene).* Journal of Applied Electrochemistry, 2006. **36**: p. 1427-1431.

30.   Schneider, O., Bund, A., Ispas, A., Borissenko, N., Zein El Abedin, S., and Endres, F., *An EQCM Study of the Electropolymerization of Benzene in an Ionic Liquid and Ion Exchange Characteristics of the Resulting Polymer Film.* The Journal of Physical Chemistry B, 2005. **109**: p. 7159-7168.

31.   Wagner, K., Pringle, J.M., Hall, S.B., Forsyth, M., MacFarlane, D.R., and Officer, D.L., *Investigation of the electropolymerisation of EDOT in ionic liquids.* Synthetic Metals, 2005. **153**: p. 257-260.

32. Murray, P.S., Ralph, S.F., Too, C.O., and Wallace, G.G., *Electrosynthesis of novel photochemically active inherently conducting polymers using an ionic liquid electrolyte.* Electrochimica Acta, 2006. **51**: p. 2471-2476.

33. Kubisa, P., *Ionic liquids as solvents for polymerization processes-Progress and challenges.* Progress in Polymer Science, 2009. **34**: p. 1333-1347.

34. Sekiguchi, K., Atobe, M., and Fuchigami, T., *Electropolymerization of pyrrole in 1-ethyl-3-methylimidazolium trifluoromethanesulfonate room temperature ionic liquid.* Electrochemistry Communications, 2002. **4**: p. 881-885.

35. Naudin, E., Ho, H.A., Branchaud, S., Breau, L., and Bélanger, D., *Electrochemical Polymerization and Characterization of Poly(3-(4-fluorophenyl)thiophene) in Pure Ionic Liquids.* The Journal of Physical Chemistry B, 2002. **106**: p. 10585-10593.

36. Lu, W., Fadeev, A.G., Qi, B., and Mattes, B.R., *Stable Conducting Polymer Electrochemical Devices Incorporating Ionic Liquids.* Synthetic Metals, 2003. **135-136**: p. 139-140.

37. Randriamahazaka, H., Plesse, C., Teyssié, D., and Chevrot, C., *Electrochemical behaviour of poly(3,4-ethylenedioxythiophene) in a room-temperature ionic liquid.* Electrochemistry Communications, 2003. **5**: p. 613-617.

38. Damlin, P., Kvarnström, C., and Ivaska, A., *Electrochemical synthesis and in situ spectroelectrochemical characterization of poly(3,4-ethylenedioxythiophene) (PEDOT) in room temperature ionic liquids.* Journal of Electroanalytical Chemistry, 2004. **570**: p. 113-122.

39. Carstens, T., El, A.S.Z., and Endres, F., *Electrosynthesis of poly(para)phenylene in an ionic liquid: cyclic voltammetry and in situ STM/tunnelling spectroscopy studies.* A European Journal of Chemical Physics and Physical Chemistry, 2008. **9**: p. 439-444.

40. Pang, Y., Xu, H., Li, X., Ding, H., Cheng, Y., Shi, G., and Jin, L., *Electrochemical synthesis, characterization, and electrochromic properties of poly(3-chlorothiophene) and its copolymer with 3-methylthiophene in a room temperature ionic liquid.* Electrochemistry Communications, 2006. **8**: p. 1757-1763.

41. Pringle, J.M., Forsyth, M., MacFarlane, D.R., Wagner, K., Hall, S.B., and Officer, D.L., *The influence of the monomer and the ionic liquid on the electrochemical preparation of polythiophene.* Polymer, 2005. **46**: p. 2047-2058.

42. Sekiguchi, K., Atobe, M., and Fuchigami, T., *Electropolymerization of pyrrole in 1-ethyl-3-methylimidazolium trifluoromethanesulfonate room temperature ionic liquid.* Electrochemistry Communications, 2002. **4**: p. 881-885.

43. Monk, P.S.M., Mortimer, R.J., and Rosseinsky, D.R., *Electrochromism Fundamentals and Applications*. 1995, VCH Verlagsgesellschaft mbH: Weinheim (GermanY). p. 243.

44. Monk, P.S.M., Mortimer, R.J., and Rosseinsky, D.R., *Electrochromism and Electrochromic Devices*. 2007, Cambridge University press: New York. p. 512.

45. Sonmez, G., Shen, C.K.F., Rubin, Y., and Wudl, F., *A Red, Green, and Blue (RGB) Polymeric Electrochromic Device (PECD): The Dawning of the PECD Era.* Angewandte Chemie International Edition, 2004. **43**: p. 1498-1502.

46.   Sonmez, G., Sonmez, H.B., Shen, C.K.F., Jost, R.W., Rubin, Y., and Wudl, F., *A Processable Green Polymeric Electrochromic.* Macromolecules, 2005. **38**: p. 669-675.

47.   Kattouf, B., Ein-Eli, Y., Siegmann, A., and Frey, G.L., *Hybrid mesostructured electrodes for fast-switching proton-based solid state electrochromic devices.* Journal of Materials Chemistry C, 2013. **1**: p. 151-159.

48.   Lin, C.K., Tseng, S.C., Cheng, C.H., Chen, C.Y., and Chen, C.C., *Electrochromic performance of hybrid tungsten oxide films with multiwalled-CNT additions.* Thin Solid Films, 2011. **520**: p. 1375-1378.

49.   Zhang, J., Tu, J.P., Zhang, D., Qiao, Y.Q., Xia, X.H., Wang, X.L., and Gu, C.D., *Multicolor electrochromic polyaniline-WO 3 hybrid thin films: One-pot molecular assembling synthesis.* Journal of Materials Chemistry, 2011. **21**: p. 17316-17324.

50.   Wang, K., Zeng, P., Zhai, J., and Liu, Q., *Electrochromic films with a stacked structure of WO 3 nanosheets.* Electrochemistry Communications, 2013. **26**: p. 5-9.

51.   Xie, Z., Gao, L., Liang, B., Wang, X., Chen, G., Liu, Z., Chao, J., Chen, D., and Shen, G., *Fast fabrication of a WO 3·2H 2O thin film with improved electrochromic properties.* Journal of Materials Chemistry, 2012. **22**: p. 19904-19910.

52.   Welsh, D.M., Kumar, A., Morvant, M.C., and Reynolds, J.R., *Fast electrochromic polymers based on new poly(3,4-alkylenedioxythiophene) derivatives.* Synthetic Metals, 1999. **102**: p. 967-968.

53.   Cai, G.F., Gu, C.D., Zhang, J., Liu, P.C., Wang, X.L., You, Y.H., and Tu, J.P., *Ultra fast electrochromic switching of nanostructured NiO films electrodeposited from choline chloride-based ionic liquid.* Electrochimica Acta, 2013. **87**: p. 341-347.

54.   Havinga, E.E., ten Hoeve, W., and Wynberg, H., *Alternate donor-acceptor small-band-gap semiconducting polymers; Polysquaraines and polycroconaines.* Synthetic Metals, 1993. **55**: p. 299-306.

55.   Koyuncu, F.B., Koyuncu, S., and Ozdemir, E., *A novel donor-acceptor polymeric electrochromic material containing carbazole and 1,8-naphtalimide as subunit.* Electrochimica Acta, 2010. **55**: p. 4935-4941.

56.   Hu, B., Lv, X., Sun, J., Bian, G., Ouyang, M., Fu, Z., Wang, P., and Zhang, C., *Effects on the electrochemical and electrochromic properties of 3,6 linked polycarbazole derivative by the introduction of different acceptor groups and copolymerization.* Organic Electronics: physics, materials, applications, 2013. **14**: p. 1521-1530.

57.   Cevher, S.C., Unlu, N.A., Ozelcaglayan, A.C., Apaydin, D.H., Udum, Y.A., Toppare, L., and Cirpan, A., *Fused structures in the polymer backbone to investigate the photovoltaic and electrochromic properties of donor-acceptor-type conjugated polymers.* Journal of Polymer Science, Part A: Polymer Chemistry, 2013. **51**: p. 1933-1941.

58.   Güneş, A., Cihaner, A., and Önal, A.M., *Synthesis and electro-optical properties of new conjugated hybrid polymers based on furan and fluorene units.* Electrochimica Acta, 2013. **89**: p. 339-345.

59.   Xu, C., Zhao, J., Wang, M., Cui, C., and Liu, R., *Electrosynthesis and characterization of a donor-acceptor type electrochromic material from poly(4,7-dicarbazol-9-yl-2,1,3-benzothiadia-zole) and its application in electrochromic devices.* Thin Solid Films, 2013. **527**: p. 232-238.

60.   Nurioglu, A.G., Akpinar, H., Sendur, M., and Toppare, L., *Multichromic benzimidazole-containing polymers: Comparison of donor and acceptor unit effects.* Journal of Polymer Science, Part A: Polymer Chemistry, 2012. **50**: p. 3499-3506.

61.   Wu, C.-G., M.-I. Lu and P.-F. Tsai, *Full - color processible electrocromic polymers based on 4,4-Dioctyl-cyclopentadithiophene.* Molecular Chemistry and Physics, 2009. **210**: p. 1851 - 1855.

62.   Argun, A.A., Aubert, P.-H., Thompson, B.C., Schwendeman, I., Gaupp, C.L., Hwang, J., Pinto, N.J., Tanner, D.B., MacDiarmid, A.G., and Reynolds, J.R., *Multicolored Electrochromism in Polymers: Structures and Devices.* Chemistry of Materials, 2004. **16**: p. 4401-4412.

63.   Koyuncu, S., Zafer, C., Koyuncu, F.B., Aydin, B., Can, M., Sefer, E., Ozdemir, E., and Icli, S., *A new donor–acceptor double-cable carbazole polymer with perylene bisimide pendant group: Synthesis, electrochemical, and photovoltaic properties.* Journal of Polymer Science Part A: Polymer Chemistry, 2009. **47**: p. 6280-6291.

64.   Idzik, K.R., Rapta, P., Cywinski, P.J., Beckert, R., and Dunsch, L., *Synthesis and electrochemical characterization of new optoelectronic materials based on conjugated donor-acceptor system containing oligo-tri(heteroaryl)-1,3,5-triazines.* Electrochimica Acta, 2010. **55**: p. 4858-4864.

65. Yigitsoy, B., Karim, S.M.A., Balan, A., Baran, D., and Toppare, L., *Benzyl substituted benzotriazole containing conjugated polymers: Effect of position of the substituent on electrochromic properties.* Synthetic Metals, 2010. **160**: p. 2534-2539.

66. Camurlu, P., Durak, T., and Toppare, L., *Solution processable donor acceptor type dibenzothiophen-S,S-dioxide derivatives for electrochromic applications.* Journal of Electroanalytical Chemistry, 2011. **661**: p. 359-366.

67. Byun, Y.S., Kim, J.H., Park, J.B., Kang, I.N., Jin, S.H., and Hwang, D.H., *Full donor-type conjugated polymers consisting of alkoxy- or alkylselenophene-substituted benzodithiophene and thiophene units for organic photovoltaic devices.* Synthetic Metals, 2013. **168**: p. 23-30.

68. Wang, T., Chen, Y., Bao, X., Du, Z., Guo, J., Wang, N., Sun, M., and Yang, R., *A new isoindigo-based molecule with ideal energy levels for solution-processable organic solar cells.* Dyes and Pigments, 2013. **98**: p. 11-16.

69. Casado, A.L. and Espinet, P., *On the Configuration Resulting from Oxidative Addition of RX to Pd(PPh3)4 and the Mechanism of the cis-to-trans Isomerization of [PdRX(PPh3)2] Complexes (R = Aryl, X = Halide).* Organometallics, 1998. **17**: p. 954-959.

70. Casado, A.L. and Espinet, P., *Mechanism of the Stille Reaction. 1. The Transmetalation Step. Coupling of R1I and R2SnBu3 Catalyzed by trans-[PdR1IL2] (R1 = C6Cl2F3; R2 = Vinyl, 4-Methoxyphenyl; L = AsPh3).* Journal of the American Chemical Society, 1998. **120**: p. 8978-8985.

71.   Hong, J.-A., Kim, R., Yun, H.-J., Park, J.-M., Shin, S.C., and Kim, Y.-H., *A benzodithiophene-based semiconducting polymer for organic thin film transistor.* Bulletin of the Korean Chemical Society, 2013. **34**: p. 1170-1174.

72.   Kitamura, C., Tanaka, S., and Yamashita, Y., *Design of Narrow-Bandgap Polymers. Syntheses and Properties of Monomers and Polymers Containing Aromatic-Donor and o-Quinoid-Acceptor Units.* Chemistry of Materials, 1996. **8**: p. 570-578.

73.   Akoudad, S. and Roncali, J., *Electrogenerated poly(thiophenes) with extremely narrow bandgap and high stability under n-doping cycling.* Chemical Communications, 1998: p. 2081-2082.

74.   Roncali, J., *Synthetic principles for bandgap control in linear π-conjugated systems.* Chemical Reviews, 1997. **97**: p. 173-205.

75.   Bundgaard, E. and Krebs, F.C., *Low bandgap polymers for organic photovoltaics.* Solar Energy Materials and Solar Cells, 2007. **91**: p. 954-985.

76.   Blouin, N., Michaud, A., and Leclerc, M., *A low-bandgap poly(2,7-carbazole) derivative for use in high-performance solar cells.* Advaced Materials, 2007. **19**: p. 2295-2300.

77.   Waltman, R.J., Bargon, J., and Diaz, A.F., *Electrochemical studies of some conducting polythiophene films.* Journal of Physical Chemistry, 1983. **87**: p. 1459-1463.

78.   Unemoto, A., Ogawa, H., Ito, S., and Honma, I., *Electrical conductivity, self-diffusivity and electrolyte performance of a quasi-solid-state pseudo-ternary system,*

bis(trifluoromethanesulfonyl) imide-based room temperature ionic liquid-lithium bis (trifluoromethanesulfonyl) imide-fumed silica nanoparticles. Journal of the Electrochemical Society, 2013. **160**: p. A138-A147.

79. Azaceta, E., Tuyen, N.T., Pickup, D.F., Rogero, C., Ortega, J.E., Miguel, O., Grande, H.J., and Tena-Zaera, R., *One-step wet chemical deposition of NiO from the electrochemical reduction of nitrates in ionic liquid based electrolytes.* Electrochimica Acta, 2013. **96**: p. 261-267.

80. Garnier, F., Tourillon, G., Gazard, M., and Dubois, J.C., *Organic conducting polymers derived from substituted thiophenes as electrochromic material.* Journal of Electroanalytical Chemistry and Interfacial Electrochemistry, 1983. **148**: p. 299-303.

81. Evans, G.P., ed. *The Electrochemistry of Conducting Polymers, in Advances in Electrochemical Science and Engineering.* Vol. 1. 1990, VCH: New York. p. 51-56.

82. Linford, R.G. and Editor, *Electrochemical Science and Technology of Polymers, Vol. 2.* 1990: Elsevier Appl. Sci. p. 1-419.

83. Downard, A.J. and Pletcher, D., *A study of the conditions for the electrodeposition of polythiophene in acetonitrile.* Journal of Electroanalytical Chemistry and Interfacial Electrochemistry, 1986. **206**: p. 147-52.

84. Hillman, A.R. and Mallen, E.F., *Nucleation and growth of polythiophene films on gold electrodes.* Journal of Electroanalytical Chemistry and Interfacial Electrochemistry, 1987. **220**: p. 351-67.

85. Hillman, A.R. and Mallen, E.F., *A spectroelectrochemical study of the electrodeposition of polythiophene films.* Journal of Electroanalytical Chemistry and Interfacial Electrochemistry, 1988. **243**: p. 403-17.

86. Hamnett, A. and Hillman, A.R., *An ellipsometric study of the nucleation and growth of polythiophene films.* Journal of the Electrochemical Society, 1988. **135**: p. 2517-24.

87. Schrebler, R., Grez, P., Cury, P., Veas, C., Merino, M., Gomez, H., Cordova, R., and del, V.M.A., *Nucleation and growth mechanisms of poly(thiophene). Part 1. Effect of electrolyte and monomer concentration in dichloromethane.* Journal of Electroanalytical Chemistry, 1997. **430**: p. 77-90.

88. Atkins, P., *Physical Chemistry*, ed. 9. 2010, New york: W.H. Freeman and Company. p. 1-972.

89. Laidlaw, W.G., *Introduction to Quantum Concepts in Spectroscopy (McGraw-Hill Series in Undergraduate Chemistry)*. 1970: McGraw-Hill. p. 1-240.

90. Workalemahu, B., *Electronic Properties of Junctions Between Aluminium and Doped Polyheterocycles*, in *Physics and Measurment Technology*. 1996, Linköping University: Linköping. p. 123.

91. Inganäs, O. and Lundström, I., *Electronic properties of metal/polypyrrole junctions.* Synthetic Metals, 1984. **10**: p. 5-12.

92. van Mullekom, H.A.M., Vekemans, J.A.J.M., Havinga, E.E., and Meijer, E.W., *Developments in the chemistry and bandgap engineering of donor–acceptor*

substituted conjugated polymers. Materials Science and Engineering: R: Reports, 2001. **32**: p. 1-40.

93. Brocks, G. and Tol, A., *Small Bandgap Semiconducting Polymers Made from Dye Molecules: Polysquaraines.* The Journal of Physical Chemistry, 1996. **100**: p. 1838-46.

94. Brocks, G. and Tol, A., *A theoretical study of polysquaraines.* Synthetic Metals, 1996. **76**: p. 213-16.

95. Li, J.C. and Liu, Z., *Progress in the theory studies of CIECAM02.* Imaging Science and Photochemistry, 2009. **27**: p. 391-398.

96. Logvinenko, A.D., *A theory of unique hues and colour categories in the human colour vision.* Color Research and Application, 2012. **37**: p. 109-116.

97. Fredlake, C.P., Crosthwaite, J.M., Hert, D.G., Aki, S.N.V.K., and Brennecke, J.F., *Thermophysical properties of imidazolium-based ionic liquids.* Journal of Chemical and Engineering Data, 2004. **49**: p. 954-964.

98. Li, H., Bhadury, P.S., Song, B., and Yang, S., *Immobilized functional ionic liquids: Efficient, green, and reusable catalysts.* RSC Advances, 2012. **2**: p. 12525-12551.

99. Seddon, K.R., *Ionic liquids for clean technology.* Journal of Chemical Technology and Biotechnology, 1997. **68**: p. 351-356.

100. Cai, Q.H., Hou, Y.W., Shi, S.Y., Lu, B., and Shan, Y.K., *A novel ionic liquid based on small size cation.* Chinese Chemical Letters, 2009. **20**: p. 62-65.

101. Barrer, R.M., *Viscosity of pure liquids. II. Polymerized ionic melts.* Transactions of the Faraday Society, 1943. **39**: p. 59-67.

102. Wilkes, J.S. and Zaworotko, M.J., *Air and water stable 1-ethyl-3-methylimidazolium based ionic liquids.* Journal of the Chemical Society, Chemical Communications, 1992: p. 965-7.

103. Jin, H., O'Hare, B., Dong, J., Arzhantsev, S., Baker, G.A., Wishart, J.F., Benesi, A.J., and Maroncelli, M., *Physical properties of ionic liquids consisting of the 1-butyl-3-methylimidazolium cation with various anions and the bis(trifluoromethylsulfonyl)imide anion with various cations.* The Journal of Physical Chemistry, 2008. **112**: p. 81-92.

104. Li, D., Zang, H., Wu, C., and Yu, N., *1-Methylimidazolium hydrogen sulfate catalyzed convenient synthesis of 2,5-dimethyl-N-substituted pyrroles under ultrasonic irradiation.* Ultrasonics Sonochemistry, 2013. **20**: p. 1144-1148.

105. Natrajan, A. and Wen, D., *A green synthesis of chemiluminescent N-sulfopropyl acridinium esters in ionic liquids without using the carcinogen 1,3-propane sultone.* Green Chemistry Letters and Reviews, 2013. **6**: p. 237-248.

106. Fuller, J., Carlin, R.T., and Osteryoung, R.A., *The room-temperature ionic liquid 1-ethyl-3-methylimidazolium tetrafluoroborate: electrochemical couples and physical properties.* Journal of the Electrochemical Society, 1997. **144**: p. 3881-3886.

107. Niedermeyer, H., Hallett, J.P., Villar-Garcia, I.J., Hunt, P.A., and Welton, T., *Mixtures of ionic liquids.* Chemical Society Reviews, 2012. **41**: p. 7780-7802.

108. Sydam, R., Deepa, M., and Joshi, A.G., *A novel 1,1'-bis[4-(5,6-dimethyl-1H-benzimidazole-1-yl)butyl]-4, 4'-bipyridinium dibromide (viologen) for a high contrast electrochromic device.* Organic Electronics: physics, materials, applications, 2013. **14**: p. 1027-1036.

109. Hayyan, M., Mjalli, F.S., Hashim, M.A., AlNashef, I.M., and Mei, T.X., *Investigating the electrochemical windows of ionic liquids.* Journal of Industrial and Engineering Chemistry, 2013. **19**: p. 106-112.

110. Costa, R.D., Werner, F., Wang, X., Groenninger, P., Feihl, S., Kohler, F.T.U., Wasserscheid, P., Hibler, S., Beranek, R., Meyer, K., and Guldi, D.M., *Beneficial effects of liquid crystalline phases in solid-state dye-sensitized solar cells.* Advanced Energy Materials, 2013. **3**: p. 657-665.

111. Wang, Y., Luo, J., and Liu, Z., *Synthesis of a novel 8-hydroxyquinoline functionalized poly (ethylene glycol) bridged dicationic ionic liquid and its application in palladium-catalyzed Heck reaction under solvent-free conditions.* Journal of Organometallic Chemistry, 2013. **739**: p. 1-5.

112. Wu, J.W., Wang, C.H., Wang, Y.C., and Chang, J.K., *Ionic-liquid-enhanced glucose sensing ability of non-enzymatic Au/graphene electrodes fabricated using supercritical CO2 fluid.* Biosensors and Bioelectronics, 2013. **46**: p. 30-36.

113. Chaban, V.V. and Prezhdo, O.V., *Ionic and molecular liquids: Working together for robust engineering.* Journal of Physical Chemistry Letters, 2013. **4**: p. 1423-1431.

114. Fannin, A.A., Jr., Floreani, D.A., King, L.A., Landers, J.S., Piersma, B.J., Stech, D.J., Vaughn, R.L., Wilkes, J.S., and Williams, J.L., *Properties of 1,3-dialkylimidazolium*

chloride-aluminum chloride ionic liquids. 2. Phase transitions, densities, electrical conductivities, and viscosities. The Journal of Physical Chemistry, 1984. **88**: p. 2614-21.

115. Suarez, P.A.Z., Einloft, S., Dullius, J.E.L., De, S.R.F., and Dupont, J., *Synthesis and physical-chemical properties of ionic liquids based on 1-n-butyl-3-methylimidazolium cation.* The Journal of Chemical Physics, 1998. **95**: p. 1626-1639.

116. Zhang, S., Sun, N., He, X., Lu, X., and Zhang, X., *Physical properties of ionic liquids: database and evaluation.* Journal of Physical and Chemical Reference Data, 2006. **35**: p. 1475-1517.

117. Noda, A., Hayamizu, K., and Watanabe, M., *Pulsed-Gradient Spin-Echo 1H and 19F NMR Ionic Diffusion Coefficient, Viscosity, and Ionic Conductivity of Non-Chloroaluminate Room-Temperature Ionic Liquids.* The Journal of Physical Chemistry B, 2001. **105**: p. 4603-4610.

118. Bonhote, P., Dias, A.-P., Papageorgiou, N., Kalyanasundaram, K., and Graetzel, M., *Hydrophobic, Highly Conductive Ambient-Temperature Molten Salts.* Inorganic Chemistry, 1996. **35**: p. 1168-78.

119. Pereiro, A.B., Legido, J.L., and Rodrı´guez, A., *Physical properties of ionic liquids based on 1-alkyl-3-methylimidazolium cation and hexafluorophosphate as anion and temperature dependence.* The Journal of Chemical Thermodynamics, 2007. **39**: p. 1168-1175.

120. Zhao, H., *Current studies on some physical properties of ionic liquids.* Physics and Chemistry of Liquids, 2003. **41**: p. 545-557.

121. Ab, R.M.A., Brant, A., Crowhurst, L., Dolan, A., Lui, M., Hassan, N.H., Hallett, J.P., Hunt, P.A., Niedermeyer, H., Perez-Arlandis, J.M., Schrems, M., Welton, T., and Wilding, R., *Understanding the polarity of ionic liquids.* Physical Chemistry Chemical Physics, 2011. **13**: p. 16831-16840.

122. Tokuda, H., Tsuzuki, S., Susan, M.A.B.H., Hayamizu, K., and Watanabe, M., *How Ionic Are Room-Temperature Ionic Liquids? An Indicator of the Physicochemical Properties.* The Journal of Physical Chemistry B, 2006. **110**: p. 19593-19600.

123. Galiński, M., Lewandowski, A., and Stępniak, I., *Ionic liquids as electrolytes.* Electrochimica Acta, 2006. **51**: p. 5567-5580.

124. Okoturo, O.O. and VanderNoot, T.J., *Temperature dependence of viscosity for room temperature ionic liquids.* Journal of Electroanalytical Chemistry, 2004. **568**: p. 167-181.

125. Fitchett, B.D., Knepp, T.N., and Conboy, J.C., *1-Alkyl-3-methylimidazolium bis(perfluoroalkylsulfonyl)imide water-immiscible ionic liquids. The effect of water on electrochemical and physical properties.* Journal of the Electrochemical Society, 2004. **151**: p. E219-E225.

126. Buzzeo, M.C., Evans, R.G., and Compton, R.G., *Non-haloaluminate room-temperature ionic liquids in electrochemistry-a review.* A European Journal of Chemical Physics and Physical Chemistry, 2004. **5**: p. 1106-1120.

127. Jacquemin, J., Husson, P., Padua, A.A.H., and Majer, V., *Density and viscosity of several pure and water-saturated ionic liquids.* Green Chemistry, 2006. **8**: p. 172-180.

128. Noda, A. and Watanabe, M., *Electrochemistry using ionic liquid. 4. Ionic transport in ionic liquids.* Electrochemistry (Tokyo, Japan.), 2002. **70**: p. 140-144.

129. McEwen, A.B., Ngo, E.L., LeCompte, K., and Goldman, J.L., *Electrochemical properties of imidazolium salt electrolytes for electrochemical capacitor applications.* Journal of the Electrochemical Society, 1999. **146**: p. 1687-1695.

130. Suarez, P.A.Z., Consorti, C.S., De, S.R.F., Dupont, J., and Goncalves, R.S., *Electrochemical behavior of vitreous glass carbon and platinum electrodes in the ionic liquid 1-n-butyl-3-methylimidazolium trifluoroacetate.* Journal of the Brazilian Chemical Society, 2002. **13**: p. 106-109.

131. Huddleston, J.G., Visser, A.E., Reichert, W.M., Willauer, H.D., Broker, G.A., and Rogers, R.D., *Characterization and comparison of hydrophilic and hydrophobic room temperature ionic liquids incorporating the imidazolium cation.* Green Chemistry, 2001. **3**: p. 156-164.

132. Kroon, M.C., Buijs, W., Peters, C.J., and Witkamp, G.-J., *Quantum chemical aided prediction of the thermal decomposition mechanisms and temperatures of ionic liquids.* Thermochimica Acta, 2007. **465**: p. 40-47.

133. Johansson, T., Mammo, W., Andersson, M.R., and Inganäs, O., *Light-Emitting Electrochemical Cells from Oligo(ethylene oxide)-Substituted Polythiophenes: Evidence for in Situ Doping.* Chemistry of Materials, 1999. **11**: p. 3133-3139.

134. Diaz, A., *Electrochemical preparation and characterization of conducting polymers.* Chemica Scripta, 1981. **17**: p. 145-8.

135. Kaneto, K., Kohno, Y., Yoshino, K., and Inuishi, Y., *Electrochemical preparation of a metallic polythiophene film.* Journal of the Chemical Society, Chemical Communications, 1983: p. 382-3.

136. Aeiyach, S., Bazzaoui, E.A., and Lacaze, P.-C., *Electropolymerization of thiophene on oxidizable metals in organic media.* Journal of Electroanalytical Chemistry, 1997. **434**: p. 153-162.

137. Waltman, R.J., Diaz, A.F., and Bargon, J., *Substituent effects in the electropolymerization of aromatic heterocyclic compounds.* The Journal of Physical Chemistry, 1984. **88**: p. 4343-6.

138. Kobel, W., Kiess, H., Egli, M., and Keller, R., *Characterization of poly(3-methylthiophene) films by IR, elemental analysis, thermogravimetry and mass spectrometry.* Molecular Crystals and Liquid Crystals, 1986. **137**: p. 141-50.

139. Johansson, T., W. Mammo, M. Svensson, M.R. Andersson and O. Inganas, *Electrochemical bandgab of substituted polythiophenes.* Journal of Materials Chemistry, 2003. **13**.

140. Danielsson, P., Bobacka, J., and Ivaska, A., *Electrochemical synthesis and characterization of poly(3,4-ethylenedioxythiophene) in ionic liquids with bulky organic anions.* Journal of Solid State Electrochemistry, 2004. **8**: p. 809-817.

141. Randriamahazaka, H., Plesse, C., Teyssié, D., and Chevrot, C., *Ions transfer mechanisms during the electrochemical oxidation of poly(3,4-ethylenedioxythiophene) in 1-ethyl-3-methylimidazolium*

bis((trifluoromethyl)sulfonyl)imide ionic liquid. Electrochemistry Communications, 2004. **6**: p. 299-305.

142. Cho, M., Seo, H., Nam, J., Choi, H., Koo, J., and Lee, Y., *High ionic conductivity and mechanical strength of solid polymer electrolytes based on NBR/ionic liquid and its application to an electrochemical actuator.* Sensors and Actuators, B: Chemical, 2007. **128**: p. 70-74.

143. Ramdin, M., De Loos, T.W., and Vlugt, T.J.H., *State-of-the-art of CO 2 capture with ionic liquids.* Industrial and Engineering Chemistry Research, 2012. **51**: p. 8149-8177.

144. Beaujuge, P.M. and Reynolds, J.R., *Color control in π-conjugated organic polymers for use in electrochromic devices.* Chemical Reviews, 2010. **110**: p. 268-320.

145. Garnier, F., Tourillon, G., Gazard, M., and Dubois, J.C., *Organic conducting polymers derived from substituted thiophenes as electrochromic material.* Journal of Electroanalytical Chemistry and Interfacial Electrochemistry, 1983. **148**: p. 299-303.

146. Gazard, M., Dubois, J.C., Champagne, M., Garnier, F., and Tourillon, G., *Electrooptical properties of thin films on polyheterocycles.* Journal de Physique. Colloques, 1983: p. 537-42.

147. Druy, M.A. and Seymour, R.J., *Poly(2,2'-bithiophene): an electrochromic conducting polymer.* Journal of Applied Polymer Science, 1983. **48**: p. 561-5.

148. Aizawa, M., Watanabe, S., Shinohara, H., and Shirakawa, H., *Electrochemical cation doping of a polythienylene film.* Journal of the Chemical Society, Chemical Communications, 1985: p. 264-5.

149.	Cecchet, F., Bignozzi, C.A., Paolucci, F., and Marcaccio, M., *Electrochemical and electrochromic investigation of polybithiophene films on a mesoporous TiO2 surface.* Synthetic Metals, 2006. **156**: p. 27-31.

150.	Pang, Y., Li, X., Ding, H., Shi, G., and Jin, L., *Electropolymerization of high quality electrochromic poly(3-alkyl-thiophene)s via a room temperature ionic liquid.* Electrochimica Acta, 2007. **52**: p. 6172-6177.

151.	Roncali, J., *Conjugated poly(thiophenes): synthesis, functionalization, and applications.* Chemical Reviews, 1992. **92**: p. 711-38.

152.	Song, X.C., Wang, X., Zheng, Y.F., and Yin, H.Y., *Electrochemical synthesis and electrochromic properties of nano-poly(3-methoxy-thiophene) in a room temperature ionic liquid.* Current Nanoscience, 2012. **8**: p. 410-413.

153.	Wu, C.-G., M.-I. Lu and P.-F. Tsai, *Full -color processible electrochromic polymers based on 4,4-dioctyl-cyclopentadithiophene.* Molecular Chemistry and Physics, 2009. **210**: p. 1851 -1855.

154.	Thompson, B.C., Kim, Y.-G., McCarley, T.D., and Reynolds, J.R., *Soluble Narrow Bandgap and Blue Propylenedioxythiophene-Cyanovinylene Polymers as Multifunctional Materials for Photovoltaic and Electrochromic Applications.* Journal of the American Chemical Society, 2006. **128**: p. 12714-12725.

155.	Tsami, A., Buennagel, T.W., Farrell, T., Scharber, M., Choulis, S.A., Brabec, C.J., and Scherf, U., *Alternating quinoxaline/oligothiophene copolymers-synthesis and unexpected absorption properties.* Journal of Materials Chemistry, 2007. **17**: p. 1353-1355.

156. Baran, D., Balan, A., Celebi, S., Meana, E.B., Neugebauer, H., Sariciftci, N.S., and Toppare, L., *Processable Multipurpose Conjugated Polymer for Electrochromic and Photovoltaic Applications.* Chemistry of Materials, 2010. **22**: p. 2978-2987.

157. DuBois, C.J. and Reynolds, J.R., *3,4-ethylenedioxythiophene-pyridine-based polymers: redox or n-type electronic conductivity?* Advanced Materials, 2002. **14**: p. 1844-1846.

158. Beaujuge, P.M., Ellinger, S., and Reynolds, J.R., *Spray processable green to highly transmissive electrochromics via chemically polymerizable donor-acceptor heterocyclic pentamers.* Advanced Materials, 2008. **20**: p. 2772-2776.

159. Lee, B.-L. and Yamamoto, T., *Syntheses of New Alternating CT-Type Copolymers of Thiophene and Pyrido[3,4-b]pyrazine Units: Their Optical and Electrochemical Properties in Comparison with Similar CT Copolymers of Thiophene with Pyridine and Quinoxaline.* Macromolecules, 1999. **32**: p. 1375-1382.

160. Amb, C.M., Dyer, A.L., and Reynolds, J.R., *Navigating the Color Palette of Solution-Processable Electrochromic Polymers†.* Chemistry of Materials, 2010. **23**: p. 397-415.

161. Prieto, I., Teetsov, J., Fox, M.A., Vanden Bout, D.A., and Bard, A.J., *A Study of Excimer Emission in Solutions of Poly(9,9-dioctylfluorene) Using Electrogenerated Chemiluminescence.* The Journal of Physical Chemistry A, 2000. **105**: p. 520-523.

162. Hellström, S., Henriksson, P., Kroon, R., Wang, E., and Andersson, M.R., *Blue-to-transmissive electrochromic switching of solution processable donor–acceptor polymers.* Organic Electronics, 2011. **12**: p. 1406-1413.

163. Colaneri, N., Kobayashi, M., Heeger, A.J., and Wudl, F., *Electrochemical and opto-electrochemical properties of poly(isothianaphthene).* Synthetic Metals, 1986. **14**: p. 45-52.

164. Kobayashi, M., Colaneri, N., Boysel, M., Wudl, F., and Heeger, A.J., *The electronic and electrochemical properties of poly(isothianaphthene).* The Journal of Physical Chemistry, 1985. **82**: p. 5717-23.

165. Ferraris, J.P., Bravo, A., Kim, W., and Hrncir, D.C., *Reduction of steric interactions in thiophene-pyridino[c]thiophene copolymers.* Journal of the Chemical Society, Chemical Communications, 1994: p. 991-2.

166. Tanaka, S. and Yamashita, Y., *Synthesis of a narrow bandgap heterocyclic polymer: poly[4,6-di(2-thienyl)thieno[3,4-c][1,2,5]thiadiazole].* Synthetic Metals, 1993. **55**: p. 1251-4.

167. Nayak, K. and Marynick, D.S., *The interplay between geometric and electronic structures in polyisothianaphthene, polyisonaphthothiophene, polythieno(3,4-b)pyrazine, and polythieno(3,4-b)quinoxaline.* Macromolecules, 1990. **23**: p. 2237-45.

168. Kitamura, C., Tanaka, S., and Yamashita, Y., *Design of Narrow-Bandgap Polymers. Syntheses and Properties of Monomers and Polymers Containing Aromatic-Donor and o-Quinoid-Acceptor Units.* Chemistry of Materials, 1996. **8**: p. 570-578.

169. Van, M.H.A.M., Vekemans, J.A.J.M., and Meijer, E.W., *Band-gap engineering of donor-acceptor conjugated polymers.* The Journal of American Chemical Society, 1998. **39**: p. 1002-1003.

170. Van, M.H.A.M., Vekemans, J.A.J.M., and Meijer, E.W., *Band-gap engineering of donor-acceptor-substituted π-conjugated polymers.* Chemistry of A European Journal, 1998. **4**: p. 1235-1243.

171. Atwani, O., Baristiran, C., Erden, A., and Sonmez, G., *A stable, low bandgap electroactive polymer: Poly(4,7-dithien-2-yl-2,1,3-benzothiadiazole).* Synthetic Metals, 2008. **158**: p. 83-89.

172. Niu, Q., Zhao, L., Zhang, Y., Li, X., and Wang, Y., *Highly efficient white polymer light-emitting diodes with a conjugated polyelectrolyte as host polymer.* Advanced Material Research, 2012. **516-517**: p. 1881-1884.

173. Wang, C., Fang, Y., Cao, Z., Huang, H., Zhao, B., Li, H., Liu, Y., and Tan, S., *Synthesis and photovoltaic properties of new branchlike organic dyes containing benzothiadiazole or triphenylamine-linked consecutive vinylenes units.* Dyes and Pigments, 2013. **97**: p. 405-411.

174. Lim, S.L., Chen, E.C., Chen, C.Y., Ong, K.H., Chen, Z.K., and Meng, H.F., *High performance organic photovoltaic cells with blade-coated active layers.* Solar Energy Materials and Solar Cells, 2012. **107**: p. 292-297.

175. Guo, X., Zhang, M., Huo, L., Xu, F., Wu, Y., and Hou, J., *Design, synthesis and photovoltaic properties of a new D-π-A polymer with extended π-bridge units.* Journal of Materials Chemistry, 2012. **22**: p. 21024-21031.

176. Gu, Z., Tang, P., Zhao, B., Luo, H., Guo, X., Chen, H., Yu, G., Liu, X., Shen, P., and Tan, S., *Synthesis and photovoltaic properties of copolymers based on benzo[1,2-*

b:4,5- b ']dithiophene and thiophene with different conjugated side groups. Macromolecules, 2012. **45**: p. 2359-2366.

177. Kim, J., Heo, M., Jin, Y., Kim, J., Shim, J.Y., Song, S., Kim, I., Kim, J.Y., and Suh, H., *Novel 4,7-dithien-2-yl-2,1,3-benzothiadiazole-based conjugated copolymers with cyano group in vinylene unit for photovoltaic applications.* Bulletin of the Korean Chemical Society, 2012. **33**: p. 629-635.

178. Tanriverdi, S., Tuncagil, S., and Toppare, L., *A New Amperometric Alcohol Oxidase Biosensor Based on Conducting Polymer of (4,7-Dithien-2-yl-2, 1,3-benzothiadiazole).* Journal of Macromolecular Science Part A Pure and Applied Chemistry, 2012. **49**: p. 185-190.

179. Raimundo, J.-M., Blanchard, P., Brisset, H., Akoudad, S., and Roncali, J., *Proquinoid acceptors as building blocks for the design of efficient π-conjugated fluorophores with high electron affinity.* Chemical Communications, 2000: p. 939-940.

180. Jayakannan, M., Van, H.P.A., and Janssen, R.A.J., *Synthesis and structure-property relationship of new donor-acceptor-type conjugated monomers and polymers on the basis of thiophene and benzothiadiazole.* Journal of Polymer Science Part A: Polymer Chemistry, 2001. **40**: p. 251-261.

181. Svensson, M., Zhang, F., Veenstra, S.C., Verhees, W.J.H., Hummelen, J.C., Kroon, J.M., Inganaes, O., and Andersson, M.R., *High-performance polymer solar cells of an alternating polyfluorene copolymer and a fullerene derivative.* Advanced Materials, 2003. **15**: p. 988-991.

182. Boudreault, P.-L.T., Michaud, A., and Leclerc, M., *A new poly(2,7-dibenzosilole) derivative in polymer solar cells.* Macromolecular Rapid Communications, 2007. **28**: p. 2176-2179.

183. Liao, L., Dai, L., Smith, A., Durstock, M., Lu, J., Ding, J., and Tao, Y., *Photovoltaic-Active Dithienosilole-Containing Polymers.* Macromolecules, 2007. **40**: p. 9406-9412.

184. Hou, Q., Hong, W., Zhang, Y., Liu, J., Chen, Y., and Shi, G., *Synthesis and photovoltaic properties of dithienosilole-based copolymers.* Journal of Materials Science: Materials in Electronics, 2013. **24**: p. 536-541.

185. Hou, Q., Hong, W., Zhang, Y., Liu, J., Chen, Y., and Shi, G., *Synthesis and photovoltaic properties of dithienosilole-based copolymers.* Journal of Materials Science: Materials in Electronics, 2012: p. 1-6.

186. Wen, S., Pei, J., Li, P., Zhou, Y., Cheng, W., Dong, Q., Li, Z., and Tian, W., *Synthesis and photovoltaic properties of low-bandgap 4,7-dithien-2-yl-2,1,3-benzothiadiazole-based poly(heteroarylenevinylene)s.* Journal of Polymer Science Part A: Polymer Chemistry, 2011. **49**: p. 2715-2724.

187. Jiang, S., Shen, P., Jiang, P., Zhou, W., Zhao, B., Liu, Y., and Tan, S., *Synthesis and photovoltaic properties of a phenylenevinylene copolymer with dithienylbenzothiadiazole and bis(di(p-tolyl)phenylamino)phenylene units.* European Polymer Journal, 2011. **47**: p. 2424-2431.

188. Moule, A.J., Tsami, A., Buennagel, T.W., Forster, M., Kronenberg, N.M., Scharber, M., Koppe, M., Morana, M., Brabec, C.J., Meerholz, K., and Scherf, U., *Two Novel Cyclopentadithiophene-Based Alternating Copolymers as Potential Donor*

Components for High-Efficiency Bulk-Heterojunction-Type Solar Cells. Chemistry of Materials, 2008. **20**: p. 4045-4050.

189. Li, H., Luo, H., Cao, Z., Gu, Z., Shen, P., Zhao, B., Chen, H., Yu, G., and Tan, S., *Synthesis and photovoltaic performances of conjugated copolymers with 4,7-dithien-5-yl-2,1,3-benzothiadiazole and di(p-tolyl)phenylamine side groups.* Journal of Materials Chemistry, 2012. **22**: p. 22913-22921.

190. Tien, H.T., *Cyclic voltammetry of bilayer lipid membranes.* The Journal of Physical Chemistry, 1984. **88**: p. 3172-4.

191. Gosser, D.K., *Cyclic Voltammetry: Simulation and Analysis of Reaction Mechanisms.* 1993: VCH. p. 1-154.

192. Bard, A.J. and Faulkner, L.R., *Electrochemical Methods: Fundamentals and Applications.* 1980: Wiley. p. 1-718.

193. Barsoukov, E. and MacDonald, R., *Impedance Spectroscopy: Theory, Experiment, and Applications, 2nd Edition.* 2005: John Wiley & Sons. p. 1- 608.

194. Kaim, W. and Fiedler, J., *Spectroelectrochemistry: The best of two worlds.* Chemical Society Reviews, 2009. **38**(12): p. 3373-3382.

195. Yassar, A., Roncali, J., and Garnier, F., *Conductivity and conjugation length in poly(3-methylthiophene) thin films.* Macromolecules, 1989. **22**: p. 804-9.

196. Fitchett, B.D.K., Travis N.; Conboy, John C., *1-Alkyl-3-methylimidazolium bis(perfluoroalkyl)imide water immiscible ionic liquid. The effect of water on*

electrochemical and physical properties. Journal of Electrochemical Society, 2004. **151**: p. E219 - E225.

197.   Marque, P. and Roncali, J., *Structural effect on the redox thermodynamics of poly(thiophenes).* The Journal of Physical Chemistry, 1990. **94**: p. 8614-8617.

198.   Pickup, P.G.a.O., *Electrochemical polymerization of Pyrrole and Electrochemistry of Polypyrrole Films in Ambient Temperature Molten Salts* Journal of the American Chemical Society, 1984. **106**: p. 2294.

199.   Zhang, L., *Attachment of Gold Nanoparticles to Glassy Carbon Electrode and its Application for the Direct Electrochemistry and Eectrocatalytic Behavior of Hemoglobin.* Biosensors and Bioelectronics, 2005. **21**: p. 337 - 347.

200.   Greef, R., R., P., L.M., P., and D., P., *Instrumental Methods in Electrochemistry.* 1990, London: Ellis Harwood limited. p. 1-442.

201.   Cornil, J., Beljonne, D., and Brédas, J.L., *Nature of optical transitions in conjugated oligomers. II. Theoretical characterization of neutral and doped oligothiophenes.* Journal of Chemical Physics, 1995. **103**: p. 842.

202.   Cornil, J., Beljonne, D., and Brédas, J.L., *Nature of optical transitions in conjugated oligomers. I. Theoretical characterization of neutral and doped oligo(phenylenevinylene)s.* Journal of Chemical Physics, 1995. **103**: p. 834.

203.   Louarn, G., Trznadel, M., Buisson, J.P., Laska, J., Pron, A., Lapkowski, M., and Lefrant, S., *Raman Spectroscopic Studies of Regioregular Poly(3-alkylthiophenes).* The Journal of Physical Chemistry, 1996. **100**: p. 12532-12539.

204.   Tsierkezos, N., *Cyclic Voltammetric Studies of Ferrocene in Nonaqueous Solvents in the Temperature Range from 248.15 to 298.15 K.* Journal of Solution Chemistry, 2007. **36**: p. 289-302.

205.   Tokuda, H., Hayamizu, K., Ishii, K., Susan, M.A.B.H., and Watanabe, M., *Physicochemical Properties and Structures of Room Temperature Ionic Liquids. 1. Variation of Anionic Species.* The Journal of Physical Chemistry, 2004. **108**: p. 16593-16600.

206.   Borsari, M., Cannio, M., Gavioli, G., and Ranieri, A., *S-containing molecules films: characterization and use in direct electrochemistry of redox proteins.* Current Topics in Electrochemistry, 2001. **8**: p. 57-65.

207.   Min, G.-H., Yim, T., Lee, H.Y., Huh, D.H., Lee, E., Mun, J., Oh, S.M., and Kim, Y.G., *Synthesis and properties of ionic liquids: imidazolium tetrafluoroborates with unsaturated side chains.* The Bulletin of the Korean Chemical Society, 2006. **27**: p. 847-852.

208.   Zotti, G., Schiavon, G., and Zecchin, S., *Irreversible processes in the electrochemical reduction of polythiophenes. Chemical modifications of the polymer and charge-trapping phenomena.* Synthetic Metals, 1995. **72**: p. 275-81.

209.   Li, F.B. and Albery, W.J., *Electrochemical deposition of a conducting polymer, poly(thiophene-3-acetic acid): the first observation of individual events of polymer nucleation and two-dimensional layer-by-layer growth.* Langmuir, 1992. **8**: p. 1645-53.